Characterisation of keratinocyte-derived epidermal signals in the initiation of contact hypersensitivity to chemicals

A thesis submitted by
Vicki Louise Summerfield
For the degree of
Doctor of Philosophy
University College London
2015

Division of Infection and Immunity
University College London

Declaration

I, Vicki Louise Summerfield confirm that the work presented in this thesis is my own. Where information has been derived from other sources, I confirm that this has been indicated in the thesis.

……..…….

Vicki Summerfield B.Sc, M.Sc

Abstract

Contact hypersensitivity reactions result from an adaptive immune response following topical exposure to chemical allergen. The initiation of this response requires the production of an inflammatory micro-environment, however the contribution of epidermal keratinocytes in creating this environment is not well-characterised. In particular, the molecular processes that regulate inflammatory mediator release in response to chemical allergen, and the function of keratinocyte-derived mediators in dendritic cell migration and maturation, have not been fully explored.

Keratinocytes (HaCaT cell line) and three-dimensional reconstructed human epidermis were evaluated as possible models for investigating these questions. We have found that, in response to chemical allergen, keratinocytes transcribe and release inflammatory mediators (interleukin-6 (IL-6) and IL-8), and a cytokine known to induce dendritic cell migration (IL-1β). Furthermore, the production of these mediators was greater than that induced by a simple chemical irritant, and different to lipopolysaccharide/interferon-γ stimulation. Transcriptomic analysis was performed to investigate the molecular mechanisms behind the inflammatory mediator release. Principal component analysis of the data showed distinct clustering of gene expression profiles associated with different doses of 2,4-dinitrochlorobenzene (DNCB, allergen) and sodium dodecyl sulfate (SDS, irritant) exposed keratinocytes. Many of the differentially expressed genes that were found in response to DNCB map to components of stress-induced pathways such as nuclear factor κ-light-chain-enhancer of activated B cells (NF-κB) and nuclear factor erythroid 2-related factor 2 (Nrf2). Investigation of the upstream signal transduction cascades revealed activation of mitogen-activated protein kinase (MAPK) pathways, specifically phosphorylation of p38MAPK and c-Jun N-terminal kinase (JNK), with a simultaneous decrease in the phosphorylation level of extracellular-signal-regulated kinase (ERK). There was also evidence of partial activation of the NF-κB pathway. The mechanism by which chemical allergens initiate these responses is unknown, however we have identified two possible triggers: production of reactive oxygen species, and activation of a receptor tyrosine kinase.

Acknowledgements

There are a number of people I would like to thank. Firstly, my supervisor Prof. Benny Chain for his guidance, support and for being an inspiring role model. Theres Matjeka for her continued support and teaching in the lab. The other amazing scientists in the lab at UCL from whom I learnt a tremendous amount during my placement.

Unilever colleagues: Dan Scott and Sam Fletcher for encouraging me to attempt this in the first place! Andrew White for sharing his expertise in transcriptomics and bioinformatics and Gavin Maxwell for many interesting discussions on skin immunology.

I am also grateful to Unilever for providing me with financial support and time to carry out experimental studies, and to the Unilever personal care team; in particular Andrew Mayes for giving me the space to finish.

My Mum and Dad, and Lee, Victoria and Eppie for their love and for never providing any pressure. Katherine, Steve and Thomas Phillips (aged 2 ¾) for showing me what strength really is.

And most importantly, Michael Davies, a brilliant scientist of many disciplines and a wonderful and supportive fiancé, who believed in me enough to help me to find confidence in myself.

Table of Contents

List of Figures

List of Tables

Abbreviations

3D	3-dimentional
ACD	Allergic contact dermatitis
AD	Atopic dermatitis
AMP	Antimicrobial peptide
AP-1	Activator protein 1
APC	Antigen-presenting cell
ARE	Antioxidant response element
ASC	Apoptosis-associated speck-like protein containing a CARD
ASK	Apoptosis signal-regulating kinase
ATF	Activating transcription factor
ATP	Adenosine triphosphate
BAFF	B cell activating factor
Bcl2	B-cell lymphoma 2
b-FGF	Basic fibroblast growth factor
BKC	Benzalkonium chloride
BM	Basement membrane
BSA	Bovine serum albumin
CARD	Caspase recruitment domain
CCL	Chemokine (C-C motif) ligand
CCR	Chemokine (C-C motif) receptor
CD	Cluster of differentiation
C/EBP	CCAAT-enhancer-binding protein
CHS	Contact hypersensitivity
CLA	Cutaneous lymphocyte-associated antigen
CLR	C-type lectin receptors
CREB	cAMP response element-binding 1
cRNA	Complementary RNA
cSMAC	Central SMAC
CTLA	Cytotoxic T-lymphocyte-associated protein
CX3CL	Chemokine (C-X3-C motif) ligand
CXCL	Chemokine (C-X-C motif) ligand

CXCR	Chemokine (C-X-C motif) receptor
Cy	Cyanine
DAMP	Damage-associated molecular pattern
DAVID	Database for Annotation, Visualization and Integrated Discovery
DC	Dendritic cell
DCNB	1,2-Dichloro-4-nitrobenzene
DC-SIGN	DC-specific intracellular adhesion molecule-3-grabbing non-integrin
DNTB	Dinitrothiocyanobenzene
dDC	Dermal dendritic cell
DEJ	Dermal-epidermal junction
DMEM	Dulbecco's Modified Eagle's Medium
DMSO	Dimethylsulfoxide
DNA	Deoxyribonucleic acid
DNAJB	DnaJ (Hsp40) homolog, subfamily B
DNBS	2,4 Dinitrobenzene sulfonic acid
DNCB	2,4-Dinitrochlorobenzene
DNFB	1-Fluoro-2,4-dinitrobenzene
DNP	Dinitrophenol
DPRA	Direct peptide reactivity assay
DTH	Delayed type hypersensitivity
EC3	Estimated concentration for 3-fold stimulation (LLNA)
E-cadherin	Epithelial cadherin
ECM	Extra-cellular matrix
ECVAM	European centre for the validation of alternative methods
EE	Epidermal equivalent
EGF	Epidermal growth factor
EGFR	Epidermal growth factor receptor
ELISA	Enzyme-linked Immunosorbent Assay
ELK1	E twenty-six (ETS)-like transcription factor 1
ERK	Extracellular signal-regulated kinase
FasL	Fas ligand
FBS	Fetal bovine serum
FGF	Fibroblast growth factor

Fos	FBJ murine osteosarcoma viral oncogene homolog
FoxP3	Forkhead box P3
FSC	Forward scatter
GCLC	Glutamate-cysteine ligase, catalytic subunit
GCLM	Glutamate-cysteine ligase, modifier subunit
G-CSF	Granulocyte colony-stimulating factor
GM-CSF	Granulocyte-macrophage colony-stimulating factor
GO	Gene ontology
gp	Glycoprotein
GPMT	Guinea pig maximisation test
GRO	Growth-regulated protein
HBSS	Hank's buffered saline solution
HBD	Human β defensin
hCLAT	Human cell line activation test
H&E	Haematoxylin and Eosin
HEV	High endothelial venules
HLA	Human leukocyte antigen
HMGB1	High-mobility group protein box 1
HMOX	Heme oxygenase (decycling)
HSA	Human serum albumin
Hsp/HSP	Heat-shock protein (protein/gene)
HSV	Herpes simplex virus
hTCPA	Human T cell priming assay
ICAM-1	Intercellular adhesion molecule-1
ICD	Irritant contact dermatitis
Ic	Intracellular
ICE	IL-1β converting enzyme
ICOS	Inducible T cell costimulator
IFN	Interferon
IGF	Insulin growth factor
Ig	Immunoglobulin
IκB	NF-κB inhibitor
IKK	IκB kinase

IL	Interleukin
IL-18R	Interleukin 18 receptor
IL-1ra	Interleukin-1 receptor antagonist
IL-1RAcP	Interleukin-1 receptor accessory protein
IL-1R	IL-1 receptor
IL-1R1	Type 1 IL-1 receptor
IL-1R2	Type 2 IL-1 receptor
IL-1RL1	Interleukin-1 receptor-like 1
IL-1ra	Interleukin-1 receptor antagonist
IP-10	Interferon-γ inducible protein 10 (CXCL10)
IRAK	IL-1R-associated kinase
IRF	Interferon regulatory factor
JAK	Janus kinase
JNK	c-Jun N-terminal kinase
KGF	Keratinocyte growth factor
K	Keratin
LC	Langerhans cell
LCSA	Loose fit co-culture based sensitisation assay
LFA	Leukocyte function associated antigen
LICOS	ICOS ligand
LLNA	Local lymph node assay
LN	Lymph node
LPS	Lipopolysaccharide
LSE	Living skin equivalent
LTB_4	Leukotriene B 4
MAL	MyD88 adaptor-like
MAP3K	MAPK kinase
MAPK	Mitogen-activated protein kinase
MAPKK	MAPK kinase
MAPKKK	MAPKK kinase
MAX	Myc associated factor X
MCP	Monocyte chemoattractant protein (CCL2)
MEF	Myocyte enhancer factor

MEK	MAPK/ERK kinase
MEKK	MEK kinase
MHC	Major histocompatibility complex
MIG	Monokine induced by Interferon-γ (CXCL9)
MIP	Macrophage Inflammatory Protein
MKK	MAPK kinase
MMP	Matrix metalloproteinase
mRNA	Messenger RNA
MTT	3-(4,5-dimethylthiazol-2-yl)-2,5-diphenyltetrazolium bromide
Myc	Avian myelocytomatosis viral oncogene homolog
MyD88	Myeloid differentiation primary response gene 88
NALP3	NACHT, LRR and PYD domains-containing protein 3
NEMO	NF-kB essential modulator
NFAT	Nuclear factor of activated T-cells
NF-κB	Nuclear factor kappa-light-chain-enhancer of activated B cells
NHK	Normal human keratinocytes
NK cells	Natural killer cells
NKT cells	Natural killer T cells
NLK	Nemo-like kinase
NLR	NOD-like receptors
NO	Nitric oxide
NOD	Nucleotide-binding oligomerisation domain-containing protein 1
NQO	NAD(P)H dehydrogenase, quinone
Nrf2	Nuclear factor (erythroid-derived 2)-like 2
P2X7	Purinergic receptor P2X, ligand-gated ion channel, 7
PAGE	Polyacrylamide-gel ectrophoresis
PAMP	Pathogen-associated molecular pattern
PBMC	Peripheral blood mononuclear cells
PBS	Phosphate buffered saline
PCA	Principal component analysis
PD	Programmed cell death
pDC	Plasmacytoid DC
PDL	PD ligand

PGE_1	Prostaglandin E1
PI	Propidium iodide
Poly I:C	Polyinosine-polycytidylic acid
PPD	Para-phenylenediamine
PPRA	Peroxidase peptide reactivity assay
PRR	Pattern-recognition receptors
pSMAC	Peripheral SMAC
RAGE	Receptor for advanced glycation end products
RANTES	Regulated on activation, normal T expressed and secreted
RHD	Rel homology domain
RHE	Reconstructed human epidermis
RIG-I	Retinoic acid-inducible gene 1
RLR	RIG-like receptors
RIN	RNA integrity number
RLH	RIG-I-like helicases
RNA	Ribonucleic acid
ROS	Reactive oxygen species
RPMI	Roswell Park Memorial Institute
RSK	Ribosomal S6 kinase
S100p	S100 calcium binding protein
SARM	Selective androgen receptor modulator
SDS	Sodium dodecyl sulphate
SLS	Sodium lauryl sulphate
SMAC	Supramolecular activation cluster
SOD	Superoxide dismutase
SP1	Specificity Protein 1
SSC	Side scatter
STAT	Signal transducer and activators of transcription
T cells	T lymphocytes
TBS	Tris-buffered saline
Tc	Cytotoxic T cell
TCR	T cell receptor
TF	Transcription factor

TGF	Transforming growth factor
Th	T helper cell
TIR	Toll/IL-1 receptor
TIRAP	Toll-Interleukin-1 receptor domain-containing adaptor protein
TLR	Toll-like receptor
TNBS	2,4,6 Trinitrobenzene sulfonic acid
TNCB	2,4,6-Trinitrochlorobenzene
TNF	Tumour necrosis factor
TNFAIP	TNFα induced protein
TNFR	Tumour necrosis factor receptor
TNFRSF	Tumor necrosis factor receptor superfamily, member
TRAF	TNF-receptor-associated factor
TRAM	TRIF-related adaptor molecule
Treg	Regulatory T cells
TRIF	TIR-domain-contatining adapter-inducing interferon-beta
TSLP	Thymic stromal lymphopoietin
TxA_2	Thromboxane
TXNRD	Thioredoxin reductase
UV	Ultraviolet
VEGF	Vascular epidermal growth factor

1 INTRODUCTION

1.1 Human skin

Human skin is an effective physical barrier that restricts the penetration of harmful chemicals and pathogens into the body, and prevents water loss. It is comprised of three general layers (Figure 1-1): the epidermis, the dermis and the hypodermis (Montagna and Parakkal, 1974).

The epidermis is a stratified epithelium, largely consisting of a continuously self-regenerating population of terminally differentiating keratinocytes, which make up >90% of the total epidermal cell mass (Montagna and Lobitz, 1964). Resident cell types with specialised functions, such as melanocytes (pigmentation), Langerhans cells (antigen presentation) and Merkel cells (sensory perception) occupy the majority of the remaining cell mass (Marzulli and Maibach, Dermatotoxicology, 1996; Urmacher, 1990).

The dermal compartment provides tensile strength and elasticity to the skin and supports appendages such as nerves, hair follicles, sweat glands and lymphatic and blood vessels (Urmacher, 1990). The dermis largely consists of fibroblasts, which secrete extra-ceullular matrix (ECM) components such as collagen, elastin, glycosaminoglycans and hyaluronic acid. In addition to fibroblasts, the dermis also contains other resident cell types, such as mast cells, macrophages, dermal dendritic cells (Urmacher, 1990) and a small number of T lymphocytes. The tissue of the dermis and epidermis are linked via a basement membrane containing types IV and VII collagen and laminin, which are secreted by both fibroblasts and keratinocytes (Lee and Cho, 2005).

The hypodermis is a sub-cutaneous layer consisting mainly of adipocytes, which have cytoplasms packed with lipids such as triglycerides and fatty acids. These lipids provide insulation and thermoregulation, and act as a major store of energy.

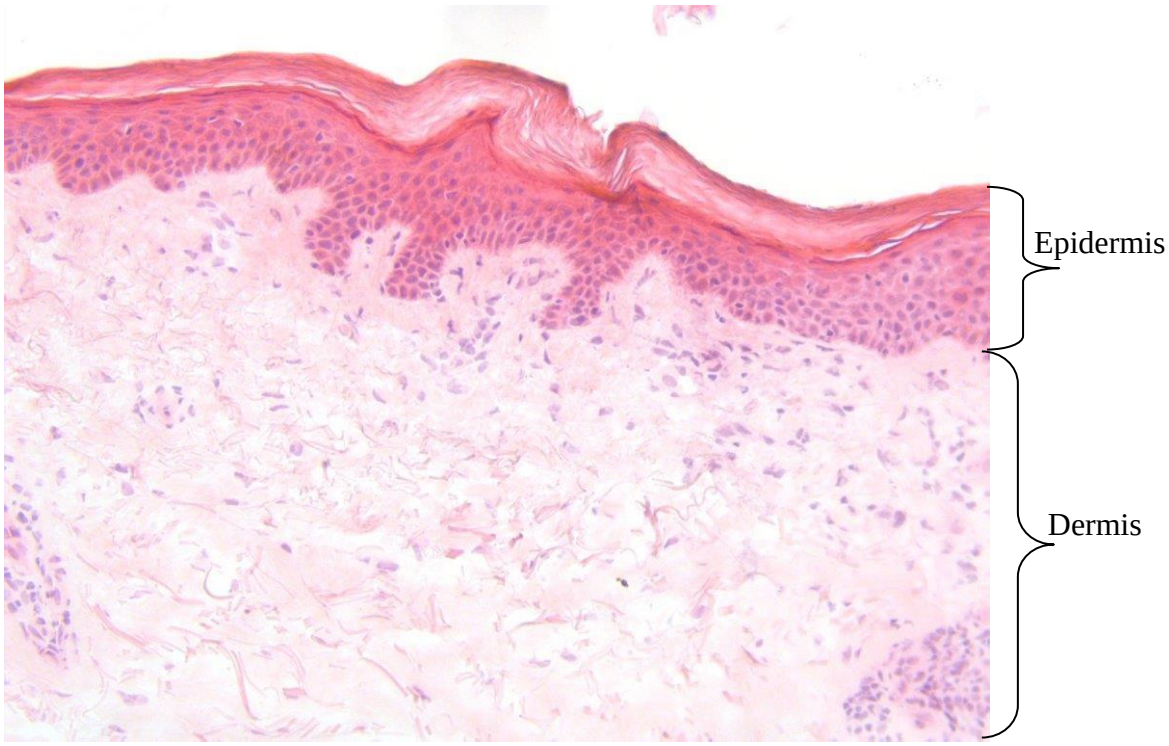

Figure 1-1 Haematoxylin and Eosin (H&E) stained human skin (sun protected), reproduced with permission from Nikki Hudson

1.2 Epidermal keratinocytes

Epidermal keratinocytes continually migrate from the basement membrane to the skin apical surface (over 5-30 days), where they undergo a cell shedding process termed desquamation. As they migrate, they differentiate to form 4 distinct layers or strata (keratinisation) (Smith and Hotchkiss, 2001). From the dermal-epidermal junction (DEJ) outwards, these are: stratum basale, stratum spinosum, stratum granulosum and stratum corneum. Each well-defined stratum can be identified by a particular keratinocyte morphology and pattern of protein and lipid expression. The stratum basale is a single cell layer of epidermal stem cells and transit-amplifying cells that proliferate to continuously regenerate the epidermis (Watt, 2001). They can be distinguished by their expression of keratins 5 and 14, in contrast to suprabasal keratinocytes, which express keratins 1 and 10 (Fuchs and Green, 1980). Basal keratinocytes are attached, via α and β integrins, to the basement membrane. As they proliferate by asymmetric mitosis, their daughter keratinocytes enter the stratum spinosum, where they grow and develop strong cellular interactions through the formation of desmosomes. As the cells migrate into the stratum granulosum, they develop tight junctions (Morita and Miyachi, 2003). They also produce intracellular keratohyalin granules containing filaggrin (Lavker and Matoltsy, 1971), and smaller lamellar granules or Odland bodies (Odland, 1991), which contain lipid to contribute towards the permeability barrier. Finally, the keratinocytes of the stratum corneum (termed corneocytes) lack intracellular organelles following the action of lysosomal enzymes. These dead, keratinised cells contain relatively little water and have insoluble, cornified plasma membranes, which are formed by cross-linking of proteins such as involucrin and loricrin (Rice and Green, 1977; Candi et al, 2005). The intercellular space in the stratum corneum is packed with lipid, such as free fatty acids, cholesterol and ceramides, which make up the lipid lamellae (Coderch et al, 2003).

The homeostatic process of basement to apical turnover of epidermis is regulated by a complex balance between proliferation, differentiation and cell death. Growth and proliferation are mediated via the epidermal growth factor receptor (EGFR) in response to EGF, transforming growth factor-alpha (TGF-α) (Coffey et al, 1987) and amphiregulin (Plowman et al, 1990; Piepkorn et al, 1994). Keratinocyte growth is also tightly regulated by fibroblast growth factor (FGF) and keratinocyte growth factor

(KGF) secreted by dermal fibroblasts (reviewed in Basilico et al, 1992). The rate of programmed cell death (cornification) is closely balanced with the basal cell proliferation rate to maintain homeostasis.

1.3 The skin immune system

It is essential that any perturbation of epidermal barrier homeostasis by wounding, pathogenic infection or exposure to harmful chemicals is controlled by the skin immune system. Cutaneous immune responses occur in the dermal and epidermal layers (Kupper and Fuhlbridge, 2004). Resident immune cells in the epidermis include Langerhans cells (LC) and T lymphocytes (T cells), and in the dermis include dermal (dDC) and plasmacytoid dendritic cells (pDC), T cells, natural killer T (NKT) cells, mast cells and macrophages (Nestle et al, 2009). The T cell population in human skin (epidermis and dermis) is mostly comprised of cutaneous lymphocyte-associated antigen $(CLA)^+$ cluster of differentiation 4 positive ($CD4^+$) T helper 1 (Th1) effector memory cells, with minority populations of central memory, Th2 and regulatory T cells (Treg) (Clark et al, 2006). Human epidermis contains both $CD4^+$ and $CD8^+$ T cells, mostly memory or effector phenotype (Spetz et al, 1996). Long-lived resident memory $CD8^+$ T cells that have potent effector function have been found following skin infection to vaccinia virus in mice (Jiang et al, 2012). Following herpes simplex virus infection in mice, $CD8^+$ skin resident T cells were confined largely to the original site of infection, while $CD4^+$ T cells migrated rapidly through the skin (Gebhardt et al, 2011). In addition to circulating T cells, other immune cells infiltrate into dermal and epidermal tissue during inflammation, such as monocytes (which differentiate into macrophages and dendritic cells), granulocytes (neutrophils, basophils and eosinophils) and natural killer (NK) cells (Kupper and Fuhlbridge, 2004). Co-ordination of this diverse set of immune cells occurs by communication involving a complex network of endogenous mediators, such as cytokines, chemokines and growth factors, expressed by immune and skin resident cells.

Innate lymphoid cells (ILCs) have also recently been shown to be present in human skin, and their important role in inflammatory skin disease is becoming apparent. ILCs are of lymphoid lineage, but do not express antigen specific B cell or T cell receptors (BCR or TCR), therefore although some of their cytokine responses are analogous to

those produced by helper T cells, ILCs are not adaptive immune cells and respond to innate stimuli. ILCs are categorised into three subsets based on their transcription factor profile and cytokine production.

Group 1 ILCs include natural killer (NK) cells and ILC1 cells. Both of these cell types produce IFNγ in response to IL-12 and IL-15 (via their expression of CD161) and are dependent on the transcription factor T-bet. ILC1 differ from NK cells in that they do not express granzyme B or perforin and therefore are not cytolytic. ILC1s are present in skin but infrequent (Teunissen et al, 2014), and their role has not been well characterised. However, due to expression of IFNγ, they have the potential to be involved in skin inflammation and Th1-associated pathologies such as allergic contact dermatitis (Kim, 2015).

Group 2 ILCs (ILC2) produce the type 2 cytokines IL-4, IL-5 and IL-13 in response to IL-25, IL-33, thymic stromal lymphopoietin (TSLP) and prostaglandin D_2 (PGD_2) and are dependent on the transcription factors RORα and GATA-3. ILC2 obtained from blood express skin homing markers CLA, CCR4 and CCR10 (Salimi et al, 2013). ILC2s are found to be resident in healthy skin and significantly enriched in atopic dermatitis lesions (Salimi et al, 2013). In addition to driving innate responses, ILC2s express MHCII and co-stimulatory molecules (CD80, CD86) (Oliphant et al, 2014) and are capable of direct interaction with T cells, skewing naïve T cells towards a Th2 phenotype (Mirchandani et al, 2014).

Group 3 ILCs (ILC3) produce cytokines IL-17 and IL-22 in response to IL-1β and IL-23 and are dependent on the transcription factor RORγt. Group 3 ILCs include three subtypes. The first type identified were the lymphoid tissue inducers (LTi), which are essential for the development of lymphoid organs. Another subtype have the potential to induce cytotoxicity due to expression of the natural cytotoxicity triggering receptor (NCR), and hence are termed NCR^+ ILC3. Finally, the NCR^- ILC3 population express large amounts of MHCII and can process and present antigen, but do not express co-stimulatory molecules. Therefore, they are unable to trigger T cell differentiation and may instead act as regulators to reduce T cell responses (Salimi and Ogg, 2014). Recent studies have linked ILC3s with psoriasis. Th17 cells were previously considered to be

the dominant source of IL-17 and IL-22 driving inflammation in psoriatic skin. However, it is now thought that NCR^+ ILC3 also contribute to production of these cytokines, and furthermore NCR^+ ILC3 levels were found to be elevated in blood and skin from psoriasis patients compared to healthy controls (Villanova et al, 2014; Dyring-Anderson et al, 2014). The role of ILCs in inflammatory skin disease will become better understood as they are further studied.

1.4 Molecular pattern recognition

Diverse immune responses to viral, fungal, bacterial and parasitic pathogens are possible due to cellular expression of evolutionarily conserved innate pattern recognition receptors (PRRs), which allow cells to sense the environment and signal appropriately to the immune system. Once stimulated, these receptors are able to trigger phagocytosis and/or intracellular signalling cascades.

PRRs that lead to phagocytosis include: Fc receptors, C-type lectin receptors (CLR), which recognise carbohydrate patterns, such as dectin-1, and the mannose receptor. In addition to phagocytic PRRs, there are other PRRs that cause activation of intracellular signalling cascades, such as: cytoplasmic nod-like receptors (NLRs); RIG-1 (retinoic acid-inducible gene 1) like receptors (RLRs); and membrane-associated toll-like receptors (TLRs) (Iwasaki and Medzhitov, 2004). TLRs broadly recognise molecules commonly expressed by pathogens, termed pathogen associated molecular patterns (PAMPs). There are 10 distinct membranous TLRs in humans (TLR 1-10), some of which reside on endosomal membranes (TLR 3, 7, 8 and 9).

In addition to PAMPs, endogenous danger signals released by stressed, damaged or necrotic cells (Galluci and Matzinger, 2001), termed damage associated molecular patterns (DAMPs), can also trigger cell activation through binding to innate pattern recognition receptors (reviewed in Palm and Medzhitov, 2009). DAMPs include: heat shock proteins (Hsp), uric acid, high-mobility group protein box 1 (HMGB1), adenosine triphosphate (ATP), S100 proteins, cathelicidins, defensins (Kono and Rock 2008), nucleotides, reactive oxygen species (ROS), neuromediators and ECM breakdown products (such as hyaluronic acid, heparan sulphate and fibrinogen) (reviewed in Gallucci and Matzinger 2001).

In addition to recognising PAMPs, TLRs are also thought to be able to sense DAMPs. TLR 2 and/or TLR 4 can sense endogenous molecules produced through tissue damage, such as fibronectin (Okamura et al, 2001), Hsp60 (Ohashi et al 2000), Hsp70 (Asea et al, 2002), HspGp96 (Vabulas et al, 2002), Hsp22 (B8), αA crystallin (Roelofs et al, 2006), fibrinogen (Smiley et al, 2001), surfactant protein A (Guillot et al, 2002), heparan sulphate (Johnson et al, 2002), β-defensin (Biragyn et al, 2002; Funderburg et al, 2007), HMGB1 (Park et al, 2004; Yu et al 2006), hyaluronic acid (Termeer et al, 2002) and uric acid (Liu-Bryan et al, 2005). Nucleic acids are also endogenous ligands for TLR 7 and 9 (Barrat et al, 2005). The identification of endogenous ligands for TLRs, in particular the heat shock proteins, remains controversial due to the potential for microbial contamination, which has not been well characterised in a number of these studies (Bausinger et al, 2002).

NLRs are also known to detect both PAMPs and DAMPs. There are many different subtypes of NLRs, including nucleotide-binding oligomerization domain-containing protein 1 (NOD1) and NOD2. Many NLRs are directly involved in mediating inflammation, and hence the complexes they form are termed inflammasomes (Martinon et al, 2009). The NACHT, LRR and PYD domains-containing protein 3 (NALP3) inflammasome has a direct role in mediating adaptive immune responses (Watanabe et al, 2006). It is activated by adjuvant signals (such as alum) (Li et al, 2008; Franchi and Nunez, 2008; Eisenbarth et al, 2008) and can also be activated by DAMPs such as ATP or uric acid (Mariathasan et al 2006; Giamarellos-Bourboulis et al 2009; Martinon et al, 2006), or ROS generated by mitochondria from damaged cells (Iyer et al, 2009, Zhou et al 2011). Recent literature suggests that the apoptosis-associated speck-like protein containing a CARD (ASC) component of the NALP3 inflammasome can be released from macrophages as a danger signal to amplify the inflammatory response (Baroja-Mazo et al, 2014) and may function extracellularly (Franklin et al, 2014).

Intracellular signalling in response to PRR activation

Stimulation of most of these receptors results in activation of the transcription factor nuclear factor kappa-light-chain-enhancer of activated B cells (NF-κB) (Kawai and Akira, 2007), which up-regulates production of pro-inflammatory cytokines and chemokines. For example, following TLR activation, signalling is initiated through a family of five adaptor proteins: myeloid differentiation primary response gene 88 (MyD88), TIR-domain-contatining adapter-inducing interferon-beta (TRIF), TRIF-related adaptor molecule (TRAM), Selective androgen receptor modulator (SARM) and Toll-Interleukin-1 receptor domain-containing adaptor protein (TIRAP) (also known as MyD88 adaptor-like or Mal). All of these adaptor proteins contain a Toll-interleukin-1 receptor (TIR) domain (reviewed in O'Neill and Bowie, 2007), which can interact with the cytosolic face of the TLR. All of the TLRs (except for TLR3, which uses TRIF) signal via MyD88, and activate downstream protein kinase cascades that culminate in the activation of the transcription factors NF-κB, activator protein-1 (AP1) and cAMP response element-binding 1 (CREB) (via MAPK), leading to the transcription of pro-inflammatory cytokines. The transcription factors of the interferon regulatory factor (IRF) family (IRF3 and IRF7) are also activated leading to transcription of type 1 interferons, such as IFNα and IFNβ (reviewed in O'Neill and Bowie, 2007).

Activation of dendritic cells by DAMPs and PAMPs

DC maturation can be achieved via recognition of DAMPs from the microenvironment at the site of infection, as well as PAMP recognition. This concept, that the immune system is activated by substances that cause tissue damage (or cellular stress), rather than to those which are simply foreign, was independently proposed by Matzinger (1994) and Ibrahim et al (1995). It allows an explanation for scenarios that do not fit the self vs. non-self hypothesis, such as the ability of tumorigenic protein to evade the immune system and the requirement of adjuvant for immunisation with purified protein antigen. It is hypothesised that LCs and DCs act as sentinels that receive both immunogenic protein and danger signals and convey the information to the adaptive immune system. Dendritic cells mature in response to PAMPs or DAMPs through binding to innate PRRs (reviewed in Palm and Medzhitov, 2009). The resultant DC

maturation state depends on the type, combination, duration and timing of stimuli received (reviewed in Macagno et al, 2007).

The response of the DC to dangerous environments differs depending on the mode of cell death by bystander cells. In the presence of apoptosis, DC engulf apoptotic cells and induce tolerance due to a lack of full maturation (Steinman et al, 2000, Lutz and Schuler, 2002). In response to necrotic cells, but not apoptotic cells, DC are triggered to fully mature (Galllucci et al 1999, Sauter et al, 2000). However, in situations where bystander apoptosis is prolonged or at high level, end stage/secondary necrosis occurs and full DC maturation is also triggered (Rovere et al, 1998; Ip and Lau, 2004). In this situation, DCs are able to present both apoptotic cells debris (via MHCI and MHCII) (Rovere et al, 1998) and co-stimulatory molecules to T-cells to initiate immunity.
DAMPs that have been shown to directly stimulate expression of co-stimulatory molecules on DCs include; IL-1α (Matjeka et al, 2012), Hsps (Basu et al, 2000), HMGB1 (Messmer et al, 2004) and ATP (Schnurr et al, 2000).

1.5 Inflammation

Cutaneous trauma following exposure to ultraviolet (UV) radiation, toxic/corrosive/ irritant chemicals, foreign organisms and/or mechanical wounding all provoke a reaction from the innate immune system to clear infection and repair damaged tissue. The resultant cutaneous inflammation is largely co-ordinated by inflammatory cytokine cascades and lipid mediators released within the epidermis, arising from many different cell types. The kinin and arachidonic acid systems become activated and trigger a cascade of proteins and lipids that produce pro-inflammatory mediators. Arachidonic acid released from membrane phospholipid can be metabolised via a series of enzymes (Leslie et al, 1987) to produce prostaglandins, prostacylins, thromboxanes and leukotrienes. These lipid mediators are pro-inflammatory (Goldyne et al, 1975) and cause direct effects on the hypothalamus (affecting body temperature via prostaglandin E1 (PGE_1) and PGE_2) (Nistico et al, 1979) and on local pain receptors (PGE_2) (Ferreira et al, 1979). Lipid mediators also affect local blood vessels, causing vasoconstriction and vasodilation (thromboxane, TxA_2; and PGE_2) (Feigen et al, 1981) and alteration in endothelial permeability (leukotriene LTB_4) (Dahlen et al, 1981), allowing recruitment of innate cell types (Janeway, 2004). These processes correspond to the characteristic

clinical signs of inflammation: heat, pain, redness and oedema. The initial cellular infiltrate recruited during inflammation is largely made up of neutrophils and monocytes (which differentiate into macrophages). In addition to removing cellular debris, both neutrophils and macrophages are able and recognise and phagocytose common pathogens and destroy them by acidification, lysosomal activity (antimicrobial enzymes, proteins and peptides) or production of respiratory burst (consisting of nitric oxide (NO), superoxide ($O2^-$) and hydrogen peroxide (H_2O_2) (Babior et al, 1984).

Pro-inflammatory cytokines

The pro-inflammatory cytokines that control inflammation are: interleukin-1 alpha (IL-1α), IL-1β, IL-18, IL-6, IL-8 and tumour necrosis factor-alpha (TNF-α). IL-1α, IL-1β, IL-18 and TNFα are termed primary cytokines (Williams and Kupper, 1996) as they are capable of inducing processes that directly result in rapid, local inflammation. Primary cytokines (IL-1 and TNF-α) are able to induce the release of secondary mediators (such as IL-6 and IL-8) in an autocrine or a paracrine manner from other cell types to amplify and assist the inflammatory response (Larsen et al, 1989). In order to regulate this process, there exist anti-inflammatory counterparts to these, namely IL-10 and interleukin-1 receptor antagonist (IL-1ra).

1.6 Proinflammatory cytokines & chemokines produced by keratinocytes

Human keratinocytes have been shown to express these key pro- and anti-inflammatory cytokines, along with many others cytokines, chemokines and growth factors that contribute to the inflammatory response (summarised in Table 1-1).

IL-1 family (IL-1α, IL-1β, IL-18, IL-33)

Human keratinocytes are capable of producing IL-1α, IL-1β and structurally related IL-18 and IL-33, which are all synthesised as pro-cytokines lacking a signal sequence. The predominant IL-1 species produced by keratinocytes is IL-1α (Kupper et al, 1986), which is active in its precursor form (Mosley et al, 1987) and is pre-stored in epidermis (Hauser et al, 1986). Upon cellular damage, IL1-α is instantly (within 10 minutes)

released from pre-made intracellular stores in murine epidermis (Wood et al, 1996). Keratinocyte IL1-α release has been shown to occur following exposure to mitogens, UV, LPS, irritants and allergens both *in vitro* and *in vivo* (Luger and Schwarz, 1990; Coquette et al, 2003; Van Och et al, 2005). IL-1β and IL-18 are produced in an inactive form (Mizutani et al, 1991; Companjen et al, 2000) and must be cleaved into a fully bioactive form by caspase-1 (Thornberry et al, 1992, Ghayur et al, 1997; Gu et al, 1997), which is itself regulated by the inflammasome (Martinon et al, 2002). In contrast, IL-1α and IL-33 are cleaved by calcium-activated calpain to produce mature forms (Kobayashi et al, 1990; Meephanson et al, 2012).

IL-1α and IL-1β compete to signal through the IL-1 receptor (IL-1R) on target cells. This receptor contains a cytoplasmic Toll/IL1R (TIR) domain and shares some homology with MyD88 TLR signalling domains (Medzhitov et al, 1998). IL-1 signalling triggers production of numerous pro-inflammatory cytokines, for example IL-6 (Kupper et al, 1989) and IL-8 (Larsen et al, 1989; Andrew et al, 1999). It is also able to cause systemic effects, such as fever or stimulation of the acute phase response, as well as augmented lymphocyte responses (Dinarello, 1996), maturation of antigen presenting cells (Ozawa et al, 1996) and up-regulation of adhesion molecules (Groves et al, 1992). In addition to extracellular function, IL-1α has nuclear function, causing activation of pro-inflammatory genes, potentially via NF-κB and AP-1 (Werman et al, 2004). IL-33 also has dual functionality in the nucleus as a suppressor of transcription (Carriere et al, 2007) and as an extracellular ligand for IL-1RL1 (Schmitz et al, 2005). IL-33 signalling induces pro-inflammatory and Th2 cytokines (Schmitz et al, 2005) and $CD8^+$ responses (Bonilla et al, 2012). IL-18, in combination with IL-12, stimulates T cells and NK cells to produce IFNγ (Okamura et al, 1995), drives the development of type 1 $CD8^+$ effector T cells (Okamoto et al, 1999) and triggers DC maturation (Li et al, 2004).

IL-1α	Luger et al, 1981; Ansel et al, 1983; Kupper et al, 1986; Phillips et al, 1995
IL-1β	Kupper et al, 1986; Zepter et al, 1997
IL-1RA	Haskill et al, 1991; Phillips et al, 1995; Bigler et al, 1992
IL-6	Kupper et al, 1989; Khan et al, 1993; Ishimaru et al, 2013
IL-7	Heufler et al, 1993; Ariizumi et al, 1995
IL-8 (CXCL8)	Larsen et al, 1989; Li et al, 1996; Barker et al, 1990; Andrew et al, 1999
IL-10	Rivas and Ullrich, 1992
IL-12	Aragane et al, 1994; Yawalkar et al, 1996
IL-15	Blauvelt et al, 1996
IL-18	Stoll et al, 1997; Naik et al, 1999
IL-23	Larsen, 2009
IL-33	Meephansan et al, 2012; Taniguchi et al, 2013
IFNα/β	Fujisawa et al, 1997
TNF-α	Kock et al, 1990
MCP-1 (CCL2)	Barker et al, 1990, 1991
RANTES (CCL5)	Li et al, 1996
TGFα	Coffey et al, 1987
TGFβ	Bascom et al, 1989
GM-CSF	Kupper et al, 1988; Pastore et al, 1997
VEGF	Trompezinski et al, 2004

Table 1-1 Cytokines and chemokines produced by keratinocytes

TNF-α

In addition to the IL-1 family of cytokines, TNF-α is a primary cytokine that is able to activate effector mechanisms to trigger cutaneous inflammation (Barker, 1991). TNF-α has been shown to be released from both primary keratinocytes and epidermoid carcinoma cells in response to LPS, UV light (Kock et al, 1990; Trefzer et al, 1993) and contact sensitisers (Piguet et al, 1991). TNF-α is pro-inflammatory and modulates pro-inflammatory cytokines such as IL-1, IL-6 and IL-8 (Larsen et al, 1989; Partridge et al, 1991), and cutaneous adhesion molecule expression including ICAM-1 (Groves et al, 1995; Trefzer et al, 1991). TNF-α also induces apoptosis (reviewed in Smith et al, 2003).

IL-6

IL-6 is not produced in abundance in either normal epidermis or un-induced keratinocytes *in vitro,* but is significantly increased in keratinocytes in response to primary cytokines such as IL-1α and TNFα, mitogens, LPS and UVB radiation (Kupper et al, 1989; Luger and Schwarz, 1990). An increase in IL-6 production is induced in dermal fibroblasts in response to keratinocyte derived IL-1α (Boxman et al, 1996). IL-6 is involved in local lymphocyte activation, and has systemic effects on both the hypothalamus (Mastorakos et al, 1993) as an endogenous pyrogen to increase body temperature (Helle et al, 1988), and on the liver to induce acute phase response (Gauldie et al, 1990; reviewed in Heinrich et al, 1990). IL-6 signals through the IL-6R and gp130 signalling receptor subunits to trigger JAK/STAT and MAPK cascades (Heinrich et al, 2003). IL-6 has been shown to enhance B cell growth and differentiation (Van Damme et al, 1987) and more recently to promote differentiation of Th17 cells and alter the Th17/Treg balance (Goodman et al, 2009).

IL-8

IL-8 (CXCL8) is a secondary mediator essential for acute inflammation. Primary human keratinocytes have low background levels of IL-8, both at the protein and transcript level, but its release is stimulated in response to primary cytokines such as IL-1α, TNF-α and IFN-γ (Baggiolini et al, 1989; Li et al, 1996). IL-8 is a potent activator

and chemokine for neutrophils (Harada et al, 1994). Its production is responsible for targeting immune cell traffic out of the bloodstream into the epidermis (Esche et al, 2005) and it also activates respiratory burst (by superoxide generation) in neutrophils to aid pathogen destruction (Peveri et al, 1988).

Anti-inflammatory cytokines

Anti-inflammatory cytokines have immunosuppressive properties in that they inhibit the function of, or antagonise pro-inflammatory cytokines. IL-10, for example, inhibits T cell proliferation and suppresses the synthesis of IL-2, IL-3, GM-CSF and TNF-α (Feliciani, 1996). IL-1 receptor antagonist (IL-1ra) antagonises the effect of IL-1 by competing with the active forms of IL-1α and IL-1β for binding to the IL-1 membrane receptor 1 (IL-1R1). In normal skin, this binding occurs at a ratio of approximately 100:1 (IL-1ra:IL-1, Arend, 1990), although the relative levels of IL-1ra, IL-1α and IL-1β are different in differentiated vs. non-differentiated keratinocytes (Gruaz-Chatellard et al, 1991). Production of the antagonist (IL-1ra) must be significantly greater than that of the pro-inflammatory mediator IL-1 to competitively inhibit IL-1α activity and reduce inflammation (Kong et al, 2006).

1.7 Inflammatory signalling cascades

The transcription of many pro-inflammatory cytokines is controlled by the NF-κB and MAPK signalling cascades. IL-1β, IL-6, IL-8 and have promoter binding sites for NF-κB (Kunsch and Rosen, 1993; Libermann and Baltimore, 1990; Hiscott et al, 1993) and transcription factors downstream of MAPK, such as c-Jun and Fos /AP-1 (Faggioli et al, 2004; Cucinotta et al, 2008; Roman et al, 2000). Both signalling cascades are triggered by receptor tyrosine kinases.

NF-κB

There are 5 proteins in the NF-κB family of transcription factors that share N-terminal Rel homology domains (RHD) these are; RelA (p65), RelB, c-Rel, NF-κB1 (p105 cleaved to p50) and NF-κB2 (p100 cleaved to p52). Rel A, Rel B and c-Rel have

transactivation domains that drive transcription. The 5 proteins form homo- or hetero-dimers, for example one of the most common is RelA/p50. Two main pathways for NF-κB activation exist; the classical (canonical) and the alternative (non-canonical) pathway (Figure 1-2). Cytokines (e.g via IL-1R, TNFR), PAMPs (e.g. via TLRs) and cellular stress (UV or ROS) trigger the classical pathway, in which receptor activated IKK (complex of IKKα and IKKβ and NEMO) phosphorylates IκB allowing ubiquitination and targeting it for proteasomal degradation. As IκB inhibits NF-κB (RelA/p50) function by sequestering it in the cytosol, its degradation allows NF-κB (RelA/p50) to translocate to the nucleus and initiate transcription. The alternative pathway is triggered by BAFF (B-cell activating factor) or lymphotoxin β receptors, leading to IKKα phosphorylation, which in turn phosphorylates p100 dimerised to RelB, this enables cleavage of p100 to p52 and subsequent nuclear translocation of RelB/p52 which binds to NF-κB promoter sites.

In general, NF-κB signalling is involved in maintaining the balance of keratinocyte cell proliferation, differentiation and death required for epidermal homeostasis. Keratinocytes in the basal layer have been shown to express NF-κB (p50) in the cytoplasm, whereas suprabasal keratinocytes demonstrate only nuclear expression (Seitz et al, 1998). NF-κB has been shown to prevent premature apoptosis in suprabasal epidermal keratinocytes committed to terminal differentiation (Qin et al, 1999; Seitz et al, 2000). Mutations in NEMO (IKKγ) cause the genetic disorder incontinentia pigmenti, with symptoms including skin lesions and abnormal pigmentation. Also, epidermis-specific deletion of IKKβ leads to the development of severe inflammatory skin disease (Pasparakis et al, 2002), suggesting NF-κB is required for normal immune homeostasis in skin.

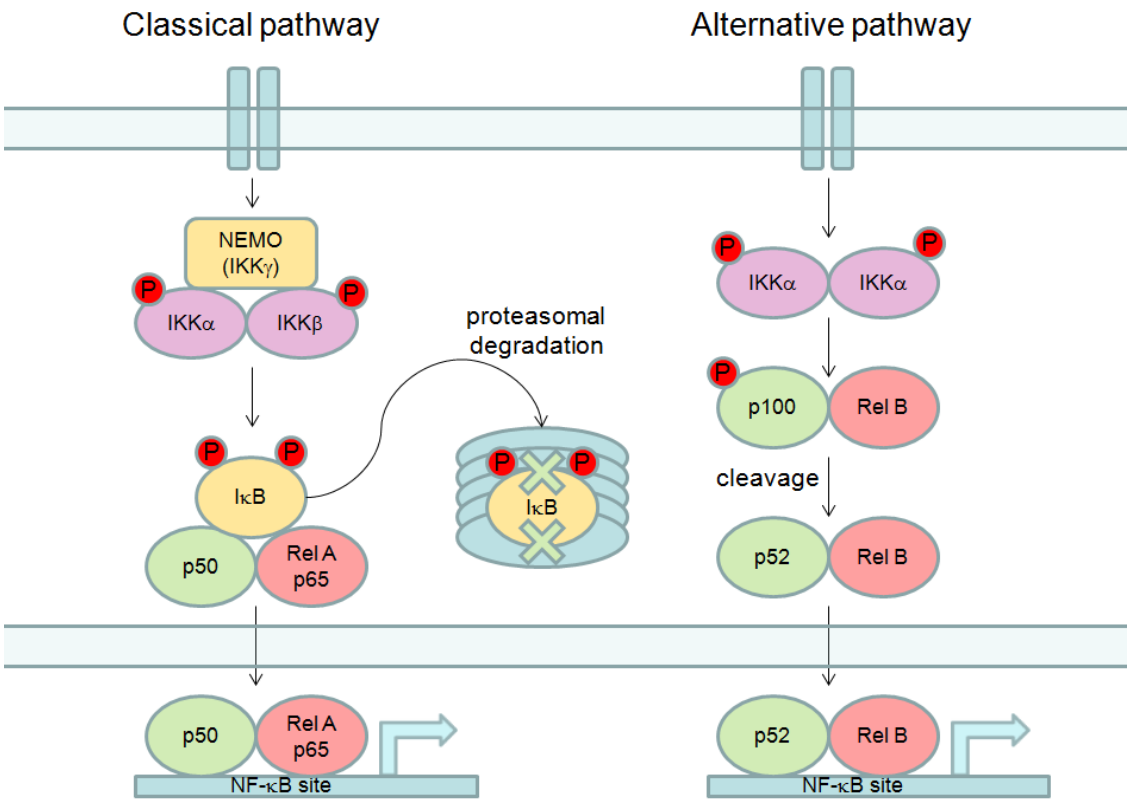

Figure 1-2 NF-κB signalling cascades (classical and alternative pathways)

Mitogen activated protein kinase (MAPK)

The MAPK signalling cascades are evolutionarily conserved pathways that regulate inflammation, cell survival, proliferation and differentiation, allowing extracellular signals (e.g. from EGFR or PRR) to be transduced to target gene transcription. There are 14 known MAPKs in mammalian cells: ERK1-2; JNK1-3; p38MAPKα, β, γ and δ; ERK3-5, 7 and NLK. MAPK signalling is predominantly stimulated by mitogens, growth factors, stress or inflammatory stimuli. All of the MAPK pathways feature a 3-tier kinase cascade (Figure 1-3), beginning with a serine/threonine MAPKKK that can phosphorylate a serine/threonine/tyrosine MAPKK, which in turn phosphorylates the target threonine/tyrosine MAPK (e.g. ERK, JNK, p38MAPK). The action of the kinases is counteracted by dual specificity phosphatases (DUSP), also called MAP kinase phosphatases (MKP), which help regulate MAPK signalling via complex feedback loops. ERK1 and 2 are p44 and p42 proteins, respectively, and are phosphorylated by MEK1/2 (MAPKK), which are activated by Raf (MAPKKK). For JNK (p46 and p54) and p38MAPK, the MAPKK are MKK4/7 and MKK3/6 respectively. Downstream of ERK, JNK and p38MAPK are common transcription factors ELK1, c-Fos, c-Jun, ATF2, AP-1, STAT1, MEF2, c-Myc, CREB and C/EBPα. Specifically in epidermis, ERK has a role in keratinocyte proliferation and survival, while p38MAPK affects differentiation and apoptosis (Efimova et al, 1998). The MAPKKK ASK1, upstream of p38MAPK, has also been shown to be important in keratinocyte differentiation (Sayama et al, 2001).

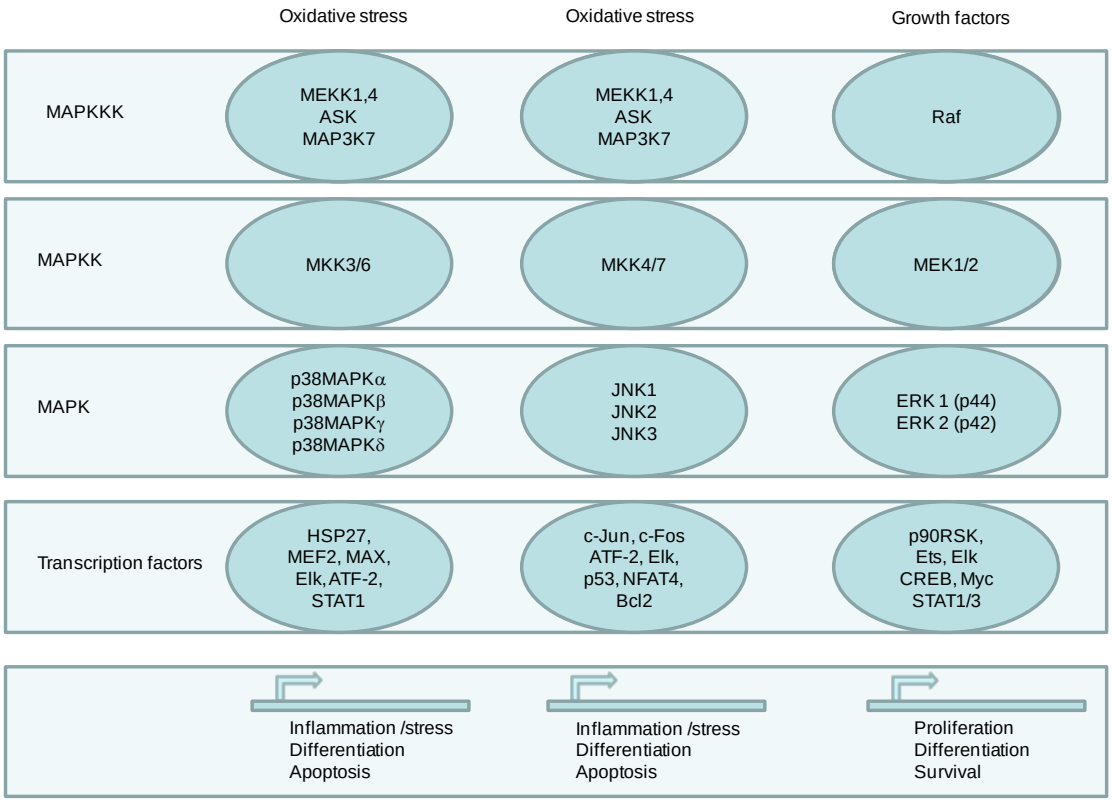

Figure 1-3 MAPK signalling cascades

MAPK pathways have three tiers of sequential kinases and activate a wide range of target transcription factors to produce diverse functional effects.

1.8 Skin diseases

Dermatitis (inflammatory) skin diseases include atopic, allergic, irritant and seborrhoeic dermatitis. Contact dermatitis is the clinical term given to an inflammatory reaction in the skin resulting from direct contact with exogenous chemicals. There are two forms of contact dermatitis; irritant contact dermatitis (ICD) and allergic contact dermatitis (ACD). Both of these conditions present in the clinic as epidermal erythema and oedema, which may progress to development of vesicles or blisters. The clinical signs of ICD are difficult to distinguish from ACD as very little difference exists in the responding cell types and sequence of cellular events during elicitation (Brasch et al, 1992). ACD reactions are, however, predominantly eczematous whereas ICD pathologies vary between chemicals, concentration, type and duration of exposure (Burns et al, 2004). Under histological examination, these pathologies are characterised by spongiosis, intracellular vacuolation and nuclear pyknosis of keratinocytes (Brasch et al, 1992; Willis et al, 1986). This is followed by infiltration of macrophages and T-lymphocytes ($CD4^+$ and $CD8^+$) and $CD1a^+$ cells (Carr et al, 1984; Lipkow et al, 1991; Scheynius et al, 1984; Willis et al, 1993). Both acute and chronic exposure to surfactants such as sodium dodecyl sulphate (SDS) and other chemical irritants, such as lactic acid and benzalkonium chloride, can result in ICD (Basketter et al, 2004). ACD develops following contact exposure to metal allergens, such as nickel (Cavelier et al, 1985), and chemical allergens, such as 1-chloro-2, 4-dinitrobenzene (DNCB) (Friedmann et al, 1983) and *p*-phenylenediamine (PPD) (McFadden et al, 1998). ACD is one of the most prevalent occupational skin diseases (Cherry et al, 2000).

Clinically, ICD and ACD are very similar, however, they do differ in the kinetics of their response. ACD is a delayed reaction that occurs 24-72 hours post initial exposure. This delayed response can be explained by the differing cellular mechanisms controlling these two immunological responses.

ICD is the result of a local inflammatory reaction, caused by direct damage to epidermal cells and release of pro-inflammatory mediators, which involves cells of the innate immune system. Whereas for ACD, in addition to elements of inflammation, the final elicitation is the result of a delayed (type IV) contact hypersensitivity (CHS) reaction which causes an adaptation of immunological memory.

1.9 Allergic contact dermatitis (ACD)

ACD is an adaptive immune response that involves not only cells required for innate responses and inflammation but also cells involved in adaptive immune processes. The mechanism driving ACD involves two distinct phases; the asymptomatic sensitisation phase, where the immune system first encounters the antigen, and the elicitation phase which generates the ACD clinical response (Figure 1-4).

Sensitisation phase

Sensitisation is the process by which exposure to non-self antigen (e.g. from invading pathogen) results in an 'immunological memory' of the encounter. Following epidermal penetration, chemical allergens (sensitisers) cannot directly stimulate an immunogenic response. The most well-studied hypothesis for CHS responses to chemical allergen is the hapten hypothesis, in which a chemical must first covalently modify self protein to produce an immunogenic entity (a process termed haptenation) (Landsteiner and Jacobs, 1936; Eisen et al, 1952). Chemical allergens tend to be highly reactive electrophiles, and protein haptenation is hypothesised to be achieved through nucleophilic substitution mechanisms (Aleksic et al, 2007). It is not yet clear which proteins in the epidermis are specifically targeted for haptenation. Following modification, the resultant immunogenic protein is engulfed by resident immature antigen presenting cells (APCs), such as epidermal Langerhans cells (LCs) or dermal dendritic cells (DCs), due to their capacity for endocytosis (Levine and Chain, 1992). Both DCs and LCs are able to phagocytose particulates (Reis e Sousa et al, 1993; Inaba et al, 1993) and capture antigen by macropinocytosis or via endocytic receptors (e.g. mannose receptor) (Sallusto et al 1995). It is not known which of these mechanisms is responsible for the association of chemical allergen (such as DNCB) with APCs (Carr et al, 1984). In addition to the hapten hypothesis, there are alternative hypotheses from the delayed-drug hypersensitivity field, which could be relevant to ACD and should be investigated further. The pharmacological interaction with immune receptors hypothesis (p-i hypothesis) proposes that reversible, high affinity binding of a drug directly to MHC and/or the TCR can trigger T cell proliferation and cytokine release (e.g sulfamethoxazole, carbamazepine) (Adam et al, 2011; Pichler, 2008). The altered-self repertoire hypothesis suggests that drug binding to empty MHC allows peptides that

normally have low affinity for MHC to bind and be presented to T cells (e.g abacavir) (Illing et al, 2012; Ostrov et al, 2012).

DC subsets involved in CHS

There are three main skin resident DC subtypes in the skin: epidermal (basal and supra-basal) LCs which express $CD1a^{++}$, $langerin^{+}$ (CD207), $CD36^{-}$ and $CD103^{-}$, dermal DCs (dDC), which are $CD1a^{+}$, $langerin^{-}$ and $CD36^{+}$ (Lenz et al, 1993) and $langerin^{+}$ dermal DC that are $CD103^{+}$ (Bursch et al, 2007). Most types of DC are derived from haematopoietic precursors in blood, whereas LCs have a distinct origin. LCs are seeded from precursors during mid-embryogenesis (Ginhoux and Merad, 2010; Schuster et al, 2014), following which TGFβ1 and M-CSFR ligands are key for their development in the epidermis (Ginhoux and Merad, 2010; Schuster et al, 2009). LCs are therefore able to self-renew from resident haematopoietic precursors in skin (Merad et al, 2002). However, in situations where there is substantial tissue inflammation, LCs can also be repopulated from monocyte precursors (Merad et al, 2002). In adult skin, LCs express CD45, HLA-DR, CD1a and Langerin, which forms their characteristic Birbeck granules (Schuster et al, 2009). There is some evidence to suggest that LCs might promote tolerance by activation of regulatory T cells and limited capacity to present bacterial antigen (van der Aar et al, 2013; Kautz-Neu et al, 2011), in contrast dermal DCs can induce a strong effector response (Shklovskaya et al, 2011). However, a recent study has shown that LCs may be capable of activating effector cells during infection, whilst also maintaining tolerance by activating Treg cells during homeostasis (Seneschal et al, 2012). It is not clear whether LCs or dermal DCs are responsible for driving CHS reactions, as the literature surrounding the relative roles for LC, dDC and $langerin^{+}$ dDC in the initiation of CHS remains contradictory. LC deficient mice have been shown to develop enhanced (Kaplan et al, 2005) or normal (Streilein, 1989) CHS reactions, and dDC have been shown to play a dominant role (Funkunaga et al, 2008). The antigen/hapten concentration is a critical factor in determining which subset is activated in vivo (Bacci et al, 1997).

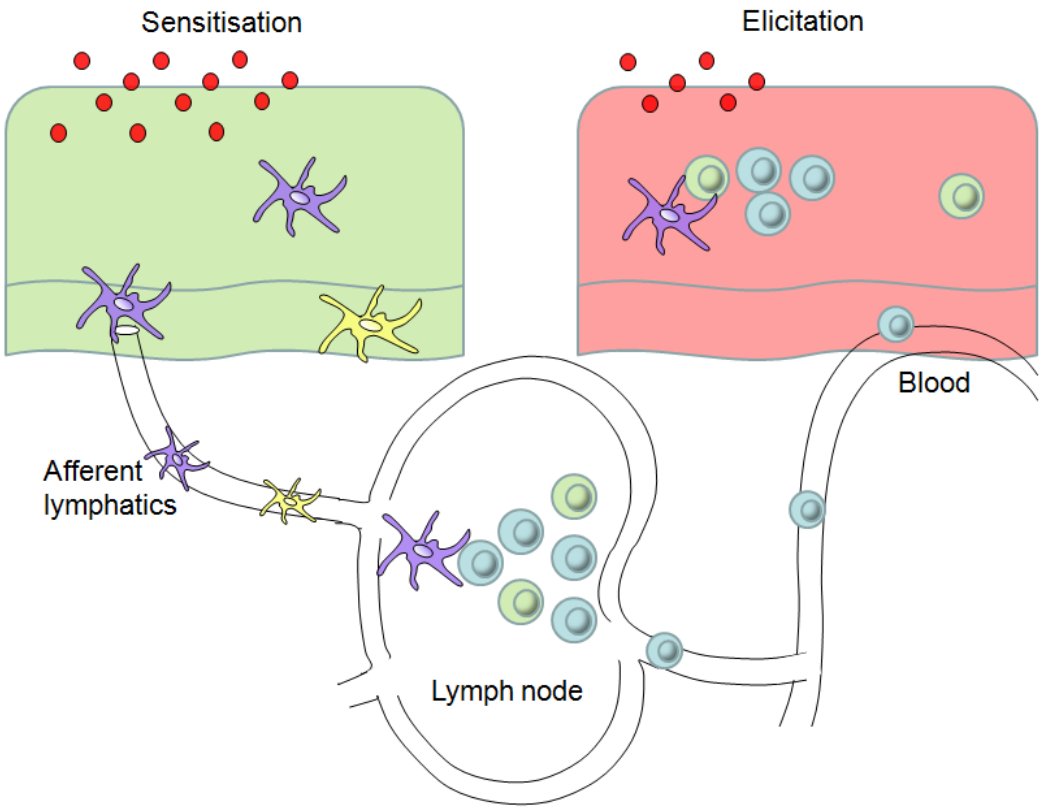

Figure 1-4 Sensitisation and elicitation phases of ACD.

During the sensitisation phase, chemical allergen (red circles) penetrates the skin and haptenates epidermal proteins. Langerhans cells (purple) and dermal dendritic cells (yellow) are triggered to migrate to the local draining lymph node, where they present antigen to T cells (blue, green). Antigen-specific T cells undergo proliferation and differentiation to generate a memory T cell population. T cells enter the circulation and distribute to tissues, including skin. Following sensitisation, re-exposure to a low amount of chemical allergen triggers elicitation involving cutaneous antigen presenting cells and memory T cells.

DC migration

In order to initiate naïve T-cell proliferation and differentiation, skin-resident Langerhans cells (LC) and dendritic cells (DC) migrate out of the epidermis and dermis, and travel through the afferent lymphatic system (Silberberg et al, 1976; Frey and Wenk, 1956) to the paracortex of the local draining lymph node. The migration of antigen presenting cells from the skin occurs in response to chemical sensitisers (Silberberg et al, 1976) and irritants (Willis et al, 1990; Brand et al, 1993; Jacobs et al, 2006), as well as pathogens, mechanical stress and UV exposure. The process of migration is controlled by a number of molecular factors. It is initiated primarily by inflammatory cytokines: TNF-α,; IL-1β; and IL-18 (Cumberbatch and Kimber, 1992; Cumberbatch et al, 1995, 1997, 2001; Shornick et al, 2001), and the danger signal HMGB1 (Dumitriu et al, 2007), and can be inhibited by IL-10 (Wang et al, 1999) and IL-4 (Takayama et al, 1999). The combined effect of these signals causes down-regulation of E-cadherin (Jakob and Udey, 1998), and hence dissociation of LC from neighbouring keratinocytes (however the cells do not move) (Jakob and Udey, 1998). A down-regulation in E-cadherin has been seen in skin in response to contact allergen (Schwarzenberger and Udey, 1996). Following detachment, migration out of the epidermis is driven by a CXCL12 chemokine gradient originating from dermal fibroblasts (in response to CXCR4 on LC) (Ouwehand et al, 2008). For epidermal LC to move along this CXCL12 gradient into the dermis, they must cross the basement membrane (BM). In order to do this they express α6-integrin, which allows interaction with laminin in the BM (Price et al, 1997); and produce matrix-metalloproteinases (MMP2 and MMP9) to facilitate movement through the BM by enzymatic degradation (Ratzinger et al, 2002; Saalbach et al, 2010).

Once in the dermis, LC and dDC follow the same route to the lymph node. Movement though the dermis is facilitated by up-regulation (in response to TNF-α) of CD44, which binds hyaluronic acid in the ECM (Haegel-kronenberger et al, 1998). Integrins CD54 (ICAM-1) and β2-integrin (in response to CCL21) (Johnson and Jackson, 2010) are also upregulated allowing LC and dDC to cross the endothelium of the afferent lymphatic vessel. The chemokine receptor CCR7 is up-regulated upon LC/DC maturation (Saeki et al, 1999; Forster et al, 1999), allowing movement (Ohl et al, 2004) towards CCL19 (produced in stromal cells in the paracortex), and towards CCL21

(Saeki et al, 1999; Gunn et al, 1999; Haessler et al, 2011), which originates from lymph node HEV and fibroblastic reticular cells, and lymphatic vessels (Gunn et al, 1998). The production of CCL21 is increased by oncostatin M (IL-6 family cytokine) (Sugaya et al, 2006) and TNF-α (Martin-Fontecha et al, 2003), which may represent systemically acting inflammatory initiators of DC migration.

In humans, chemical allergens stimulate LC migration out of the epidermis with a mean epidermal reduction of LC of ~18% (DNCB) and 29.4% (diphencyprone), when assessed 17-18 hours following exposure (Pickard et al, 2009; Griffiths et al, 2001). In these studies, migration was not observed at 4 hours post exposure, indicating that the time-course of this response is between 4 and 18 hours. Whilst total LC migration is consistently 20-30% following trauma (Griffiths et al, 2005), the kinetics of migration vary upon stimulus, for example in response to intradermal injection of tumour necrosis factor alpha (TNF-α) there is a mean epidermal LC reduction of 24.2% in just 2 hours (in mice this response occurs in 30 min with concurrent arrival in the lymph node within 2 hours) (Cumberbatch 1999). In mice, the arrival of hapten-loaded DC in the LN peaks 2 days after exposure and LN proliferation peaks 4 days after exposure (Macatonia et al, 1987). Murine dDC have been observed to arrive in the LN first, and colonise distinct areas, compared to the slower migrating LC (Kissenpfennig et al, 2005), however, this has not yet been shown in humans.

DC maturation

As immature LCs/DCs migrate, they differentiate into mature antigen presenting cells (Schuler and Steinman, 1985; Larsen et al, 1990; Aiba and Katz, 1990). The maturation status of the DC is critical to driving a proliferative T cell response.

DC maturation is recognised by a loss of expression of molecules and receptors involved in antigen capture, and an up-regulation of molecules and receptors involved in antigen presentation (MHC) (Aiba and Katz, 1990) and co-stimulation (CD40, CD80 and CD86) (reviewed in Cella et al, 1997; Merad et al, 2008). Chemokine receptor expression is also altered, with up-regulation of CCR7 and a concurrent down-regulation of CCR5, CCR1 and CCR6. To enable migration from neighbouring keratinocytes, e-cadherin is also down-regulated and ICAM-1 up-regulated. CD83 and DC-SIGN are also often used as markers of mature DCs. IL-1, IL-18 and GM-CSF

have been shown to promote DC maturation (Witmer-Pack et al, 1987; Heufler et al, 1988; Ozawa et al, 1996; Li et al, 2004). Although it is not clear by which mechanism, chemical haptens have been shown to cause up-regulation of these markers in human PBMC-DC *in vitro* (Aiba et al. 1997; Tuschl et al.2000; Arrighi et al. 2001; Aiba et al. 2003; De Smedt et al. 2005).

TLR/ NLR activation in DC during CHS

The involvement of skin-derived DAMPs in CHS is beginning to be investigated. In the absence of PAMPs, in response to chemical allergens, it is hypothesised that endogenous DAMPs provide the necessary adjuvant for activation of LC and dDC. TLR 2 and 4 deficient mice have been shown to have reduced CHS responses (Martin et al, 2008). The activation of TLR 2 and 4 is likely to be through DAMPs, although direct activation of TLR4 cannot be ruled out, as is the case for Nickel and Cobalt metal allergy (Raghavan et al, 2012; Schmidt et al, 2010). Further evidence for the involvement of DAMPs in CHS includes the finding that P2X7 deficient mice have reduced CHS responses (Weber et al, 2010) and the DAMP that signals via P2X7, ATP, is released in response to sensitisers (Onami et al, 2014; Weber et al, 2010). Hyaluronic acid, which signals via TLR2/4 is also found to be associated with ACD (Esser et al, 2012; Termeer et al, 2002).

NLRs have also been demonstrated to be involved in CHS. Inflammasome component knock-out mice display impaired CHS responses (Watanabe et al, 2006; Sutterwala et al 2006), and the degree of danger signalling to the inflammasome can be modulated to turn tolerizers into sensitisers and sensitisers into tolerizers (Watanabe et al, 2008). The inflammasome also controls IL-1β activation (Thornberry et al, 1992), hence its role in CHS is beginning to be explored. IL-1R and IL-18R/MyD88 pathways are also required during the sensitisation phase of CHS, but only appear to be required in certain cell types (Klekotka et al, 2010).

To drive a response to chemical-derived antigen, haptenated protein must be processed and loaded onto cell surface major histocompatibility complex (MHC) molecules. There is, however, no direct evidence of the contribution of MHCI, MHCII or cross-presentation antigen processing in response to chemical hapten. In the lymph node,

mature DCs present processed antigen on MHC (Macatonia et al, 1987) to naive, antigen-specific T lymphocytes (T-cells).

DC:T cell synapse and initiation of T cell signalling

During an immune response, the recognition of a dendritic cell (DC) presenting antigen by a T cell with a cognate T-cell receptor (TCR) results in the formation of the immunological synapse. This association between cells can last from minutes to hours, however 2-4 hours of contact is required for naïve $CD8^+$ (van Stipdonk et al, 2001) and at least 6 hours for naïve $CD4^+$ T cell clonal expansion (Celli et al, 2007). Contact at the immunological synapse consists of a number of specific molecular interactions.

Initially, as T cells move through the lymph node, they transiently interact with DC via adhesion molecules (CD58 (LFA-3), ICAM-1 (CD54), ICAM-2 (CD102) and DC-SIGN (CD209)) associating with their T cell counterparts (CD2, LFA-1 ($\alpha\beta$ integrin CD11a:CD18), LFA-1 and ICAM-3 (CD50) respectively). This brief encounter with a DC is enough to stall further migration of the T cell, which provides time to sample the complementarity of the TCR (CD3) for the large number of diverse peptide MHC (pMHC) on the DC. Where there is a positive encounter (~1 in 2 $x10^5$ T cells; Blattman et al, 2002), signalling through the TCR induces a conformational change in the LFA-1 molecule, increasing its affinity for ICAM-1/2 and stabilising the interaction. Binding of the TCR to pMHC also requires co-receptor association (for MHCI presentation this needs CD8 and for MHCII, CD4). In addition to antigen presentation (signal 1), there must be interaction of co-stimulatory molecules on DC (CD80 (B7.1) and CD86 (B7.2)) with CD28 on T cells. This co-stimulation (signal 2) is fundamentally required to produce antigen-specific clonal expansion, and without it the T cell becomes anergic. In response to activation, the T cell up-regulates CD40L to the synapse, which binds to CD40 on DC and triggers further DC co-stimulatory molecule expression to further potentiate the signal. 4-1BB (CD137) on T cells and its DC ligand 4-1BBL perform a similar role to CD40. Activated T cells also express ICOS, which interacts with its DC ligand LICOS to induce IL-10 production, which inhibits Th1 differentiation (Janeway et al, 2004, unless specified).

The initial interaction of the TCR with cognate pMHC triggers the formation of TCR microclusters; these then rearrange to form defined concentric rings termed supramolecular activation clusters (SMAC) (Monks et al, 1998). The central cluster (cSMAC) contains the TCR, CD4/CD8, CD28 and CD2. Blocking of CD28 interactions have been shown to result in a lack of defined cSMAC (reviewed in Thauland et al, 2010). The next ring domain of molecules is termed the peripheral SMAC (pSMAC) which consists of adhesion molecule interactions such as LFA-1 (Monks et al, 1998).

In order to terminate the interaction, activated T cells up-regulate CTLA4 (CD152), which binds to CD80 and CD86 on DC with a higher affinity than CD28, and hence negatively blocks the signal (Walunas et al, 1994). Like CTLA4, PD-1 is also a negative regulator of the response and binds PDL-1 and PDL-2 on DC to suppress T-cell activation (Butte et al, 2007). Cellular apoptosis can be signalled by the interaction of Fas and FasL on both T cells and DCs. TCRs are also constitutively internalised and recycled, but are internalised and targeted for degradation once triggered by pMHC (Bachmann et al, 1997); this serves as a potential mechanism to protect against excessive signalling.

T cell populations involved in ACD

Both $CD4^+$ Th1 and $CD8^+$ type 1 cytotoxic T cells have been shown to be involved in developing CHS to chemical allergens (Wang et al, 2000). However, the response is thought to be predominantly CD8-driven (Kalish et al, 1994, Gocinski and Tigelaar, 1990; Martin et al, 2000, 2003), which indicates that MHCI might be the dominant antigen processing pathway in DC in response to contact allergens. IL-4/IL-10 producing $CD4^+$ (Th2) T-cells are also induced in CHS, which are thought to negatively regulate the response (Xu et al, 1996).

Activated T-cells increase their expression of cutaneous lymphocyte associated antigen (CLA) and CCR10, which interacts with basal keratinocyte-derived CCL27 to direct the T-cells back to the skin (Homey et al, 2002).

When an antigen specific memory T-cell population is produced, the host is said to be sensitised to that particular antigen. Upon subsequent exposure to the same allergen, the host already has antigen-specific memory T-cells available to respond, which allows rapid elicitation of ACD.

Elicitation

Re-exposure to antigen results in recruitment of antigen specific T-cells to the site of contact. These are initially $CD8^+$ T-cells followed by an infiltration of $CD4^+$ T-cells (Okazaki et al, 2002). Th17/Tc17 cells (Zhao et al, 2009) and activated NK T-cells (Gober et al, 2008) have also been shown to be present during elicitation of CHS, although their roles remain to be fully characterised. The responding T-cells produce cytokines (such as IFNγ and IL-17), which drive production of pro-inflammatory cytokines, and chemokines (Barker et al, 1990; Albanesi et al, 2000) that promote infiltration of innate immune cells. This cellular infiltrate, together with cytotoxic T-cell-induced keratinocyte apoptosis (Trautmann et al, 2000), drive the clinical signs of allergic contact dermatitis. It is possible that naturally occurring $CD4^+CD25^+$ regulatory T-cells (Tregs) are able to suppress CHS reactions by production of IL-10 (Ring et al, 2006).

1.10 The role of keratinocytes in immune responses and CHS

In addition to providing the structural and barrier properties of the skin, keratinocytes have been shown to be capable of influencing skin immune responses. Their role in the initiation of innate and adaptive responses (including CHS) is driven by their ability to signal to immune cells, and sense and take up antigen.

During T cell-mediated adaptive immune responses, keratinocytes are also able to present antigen on major histocompatibility complex I (MHCI) and on interferon-gamma (IFNγ) induced MHC II (Black et al, 2007). In addition to MHCII, IFNγ also induces intercellular adhesion molecule-1 (ICAM-1) expression on keratinocytes (Griffiths et al, 1989; Basham et al, 1984), assisting interactions between basal keratinocytes and T cells (Barker et al, 1989).

Keratinocytes express phagocytic PRRs that lead to endocytosis of pathogen or protein including: Fc receptors (Livden et al, 1988; Bjerke et al, 1994); CLRs, such as dectin-1 (Lee et al, 2009), and the mannose receptor (Cerdan et al, 1991; Szolnoky et al, 2001). Complement receptors and regulatory proteins are also produced by keratinocytes, which may aid endocytosis of opsonised particles (Dovezenski et al, 1992).

There is some debate in the literature as to which TLRs can be expressed by human keratinocytes. Some authors have reported that human keratinocytes express TLR 1-6, 9 and 10 (Song et al, 2002; Kollisch et al, 2005; Lebre et al, 2007), whereas Mempel et al (2003) state that TLRs 4, 6, 7, 8 and 10 cannot be detected in primary human keratinocytes. It is possible that the differentiation state of the keratinocytes *in vitro* might account for some of these differences in TLR detection, as TLR 5 and TLR 9 have been shown to exist in different strata of the epidermis (TLR 5 in basal keratinocytes, and TLR 9 more diffuse throughout the epidermis, but concentrated in the stratum granulosum) (Miller et al, 2005). Keratinocytes are also able to up-regulate TLRs in response to pathogen. TLR 4 has been shown to be up-regulated in response to lipopolysaccharide (LPS) (Song 2002). TGFα can increase levels of TLR 5 and TLR 9 (Miller et al, 2005), and IFNα increases TLR 3 expression (Prens et al, 2008). NLRs are also expressed by keratinocytes, such as NOD1 and NOD2 (Harder and Nunez, 2009; Voss et al, 2006; Kobayashi et al., 2009). The NALP3 inflammasome has a direct role in mediating adaptive immune responses and is expressed by keratinocytes (Watanabe et al, 2006).

NF-κB signalling in keratinocytes has been shown to be driven by TLRs. For example, in response to TLR activation in keratinocytes, NF-κB RelA translocated into the nucleus, and intereukin-8 (IL-8) was secreted (Kollisch et al, 2005). Both Staphylococccus aureus and its purified cell wall components (lipoteichoic acid and peptidoglycan) cause NF-κB activation via TLR2 in keratinocytes (Mempel et al, 2003).

DAMPs produced by keratinocytes

Keratinocytes are able to produce DAMPs such as Hsps (Wang et al, 2011), hyaluronic acid (by expression of hyaluronidase, Kurdykowski et al, 2011; Malaisse et al, 2014),

ATP (Inoue et al, 2014) and HMGB1 in response to erythema toxicum (Marchini et al, 2007). Pre-stored cytokines in keratinocytes, such as IL-1α and IL-33 (Luthi et al, 2009) may also be considered DAMPs. Keratinocytes also produce potent anti-microbial peptides, which act as DAMPs, as part of the epithelial innate defence mechanism, for example human β defensin (HBD) 1 and 2 (Harder et al, 1997; Ali et al, 2001), HBD 3 (Sørensen et al, 2006), and cathelicidin (LL-37, Frohm et al, 1997).

Cytokines and chemokines produced in skin in response to chemical sensitiser

At an early time-point in the skin following exposure to chemical allergens, detectable levels of cytokines and chemokines are stimulated in the epidermis (summarised in Table 1-2). However, in many studies it is difficult to identify which skin cell type is responsible for the production of each cytokine.

In mouse skin, in response to chemical allergens (oxazolone/urushiol/TNCB/DNFB), epidermal keratinocytes have been shown to transcribe or release IL-1α, IL-1β, IL-6, IL-10, IL-12, IL-18, IFNγ, TNFa, IP-10, MIP-2, and GM-CSF (referenced in Table 1-2). IL-1α mRNA increases in mouse skin following exposure to TNCB at 2 hours and remains elevated until 18 hours (Enk and Katz, 1992a), and also following 4 hour exposure to TNCB, DNFB and DNCB, but not non-sensitiser analogues DCNB or DNTB (Enk and Katz, 1992c). IL-1α mRNA was also up-regulated following 6 hour stimulation with oxazolone, DNFB or urushiol (Haas et al, 1992).

Up-regulation of IL-1β mRNA expression was faster than IL-1α in mouse skin following exposure to TNCB. It was elevated after just 15 minutes and continued to rise until 2 hours where it remained constant for 24 hours (Enk and Katz, 1992a). Like IL-1α, IL-1β expression was also seen following a 4 hour exposure to TNCB, DNFB and DNCB, but not non-sensitiser analogues DCNB or DNTB (Enk and Katz, 1992c). Another sensitiser, oxazolone, also caused a rapid and transient increase (5 to 90 minutes) in IL-1β mRNA in mouse skin (Kermani et al, 2000). Impaired CHS responses have been seen to TNCB in IL-1β deficient mice (Shornick et al, 1996).

IL-6 protein was detected in mouse skin following topical exposure to oxazolone, which peaks at 4 to 8 hours, and is dose dependent (Holliday et al, 1996; Flint et al, 1998). IL-6 expression is reported to be mostly attributable to epidermal DCs (Cumberbatch et al, 1996). T cell responses to DNP-HSA have been shown to be dependent on IL-6 (supplementary data, Palm and Medzhitov, 2009).

IL-10 mRNA increases in response to TNCB at 4-12 hours, peaking at 12 hours and appears to be specific to sensitiser and not irritants (Enk and Katz, 1992b). In contrast, IL-10 was not seen to be released in mouse skin up to 24 hours following exposure to oxazolone (Holliday et al, 1996).

IL-18 mRNA was increased in mouse skin in response to TNCB at 2 hours, peaking at 6 hours; this was also seen following exposure to DNFB but not irritants SDS and BKC (Stoll et al, 1997).

The expression of TNFα (mRNA and protein) in mouse skin following exposure to oxazolone was found to be under tight temporal constraints. A transient and localised transcriptional expression peaked and dropped within 20 minutes, and protein expression was found to be maximal at 2 hours, returning to normal by 4 hours (Flint et al, 1998). TNFα mRNA was up-regulated following 6 hour stimulation with oxazolone, DNFB, urushiol (Haas et al, 1992).

Cytokines produced by keratinocytes in response to chemical sensitiser

In response to chemical allergens, keratinocytes (primary, 3D models or cell lines) specifically have been shown to transcribe or release IL-1α, IL-1β, IL-8, IL-12, IL-18, IL-23 and TNF-α (referenced in Table 1-3).

IL-1α expression, in response to sensitisers and irritants has been well studied. In the mouse keratinocyte cell line, HEL30, cell-associated (and to a much lesser extent released) IL-1α was found to be induced by allergens (DNCB, oxazolone, eugenol and Ni) (Corsini et al, 1998). In reconstructed epidermal models, IL-1α release was very

low in response to allergens, but much higher in response to irritant exposure (Coquette et al, 2003).

IL-1β was found to be constitutively expressed in normal human keratinocytes and the mature form was seen in response to urushiol (Zepter et al, 1997). In this study, keratinocytes were also found to synthesize ICE (caspase-1) which could be induced to process IL-1β into mature form by urushiol (Zepter et al, 1997).

IL-8 was released following exposure of normal human keratinocytes, and the HaCaT cell line, in response to 6-24 hours exposure to DNFB (Mohamadzadeh et al, 1994). IL-8 was also strongly expressed in reconstructed epidermal models in response to allergens, but to a much lesser degree in response to irritants (Coquette et al, 2003).

IL-12p35 was found to be constitutively produced by human epidermal cells. IL-12p40, however, was only detected in epidermis treated with Nickel (Larsen et al, 2009). IL-12p40 was also shown to be stimulated in human skin following exposure to TNCB at 6 and 12 hours, and could be induced in keratinocyte cells by TNBS or IL-1β (Muller et al, 1994).

IL-18 was found to be expressed constitutively (stored intracellularly) by keratinocytes in the inactive unprocessed form (24kDa) and in the epidermis (Companjen et al, 2000). The active form of IL-18 was found to be expressed and secreted following exposure to DNCB (Naik et al, 1999). Intracellular IL-18 was found to increase in response to a number of sensitisers, but not irritants (Corsini et al, 2009; van Och et al, 2005)

A very low level release of TNF-α from keratinocytes was detected in response to phenol and resorcinol (Newby et al, 2000). These low levels (<50 pg/ml) are consistent with TNFα release from keratinocytes in other studies (Kock et al, 1990).

IL-1α	Enk and Katz 1992a/c; Haas et al, 1992
IL-1β	Enk and Katz 1992a/c; Kermani et al, 2000
IL-6	Cumberbatch et al, 1996; Holliday et al, 1996; Flint et al, 1998
IL-10	Enk and Katz 1992b; Nickoloff et al, 1994
IL-12	Muller et al, 1994
IL-18	Stoll et al 1997
IFNγ	Enk and Katz 1992a; Howie et al, 1996
TNF-α	Piguet et al,1991., Haas et al, 1992; Flint 1998; Enk and Katz 1992a/c
IP-10	Enk and Katz 1992a/c
MIP-2	Enk and Katz 1992a/c
GM-CSF	Enk and Katz 1992a/c

Table 1-2 Cytokines and chemokines produced in response to sensitisers in skin

IL-1α	Corsini 1998, Curtis et al, 2007; Coquette et al, 2003; Newby et al, 2000
IL-1β	Zepter, 1997
IL-8 (CXCL8)	Newby et al, 2000, Coquette et al, 2003; Mohamadzadeh, 1994
IL-12	Larsen et al, 2009
IL-18	Stoll et al 1997; Naik et al, 1999
IL-23	Larsen et al, 2009
TNF-α	Newby et al, 2000

Table 1-3 Cytokines and chemokines produced in response to sensitisers in keratinocytes

1.11 Risk assessment for skin sensitisation

To ensure consumer safety, risk assessments are produced on novel chemical ingredients for cosmetic, home and personal care (HPC) products. Risk assessments involve the consideration of both hazard and exposure scenario information, in order to evaluate the likelihood of adverse ACD reactions in consumer populations. Historically, to identify a chemical as an irritant (causing ICD) or as a sensitiser (causing ACD), animal tests such as the mouse local lymph node assay (LLNA) (Kimber et al, 1994) or the guinea pig maximisation test (GPMT; Magnusson and Kligman, 1969) have been used. However, due to a desire to base risk assessments on human rather than animal biology, and ethical considerations, the cosmetics and HPC industries are committed to invest in the development of alternatives to animal testing. The 7th Amendment to the EU cosmetics directive, which bans the marketing in Europe of products containing chemicals tested on animals, came into effect in 2013. The industry has had success in replacing many of the acute toxicity endpoints. For example, the Draize animal test (Draize et al, 1944) was used for many years to identify irritancy potential, but was replaced by an *in vitro* assay that measures cell death in a human artificial skin model (Spielmann et al, 2007). This assay is now ECVAM validated and serves as a direct replacement of animal tests for irritancy. The repeat exposure toxicity endpoints such as allergy, cancer and reproductive toxicity are more challenging as they involve co-ordinated responses between many different cell types and/or organs. There has been substantial research into the development of *in vitro* assays to predict the potential of chemicals to induce ACD.

Historically, the identification of chemicals with sensitisation potential was assessed using the LLNA (Kimber et al, 2001). This assay involves three consecutive applications of chemical to the mouse ear, and the measurement of cell proliferation in the lymph nodes using tritiated thymidine incorporation. The proliferation is assumed to correlate with the generation of a chemical-derived antigen specific memory T cell population. A chemical is identified as positive if the proliferation reaches 3-fold higher than control. The concentration at which the chemical-induced proliferation reaches this threshold (termed EC3) is used to assign potency classes for sensitisers as: weak, moderate, strong or extreme (Gerberick et al, 2004).

1.12 *In vitro* assays for skin sensitisation potential

The development of *in vitro* assays to predict sensitiser potential and potency fall into four main themes: the ability of chemicals to modify protein; stress responses of keratinocytes to chemical; the ability of chemical to activate/mature dendritic cells; and the simulation of DC-induced T cell proliferation.

Peptide reactivity assays

The direct peptide reactivity assay (DPRA) measures the binding of chemicals to synthetic cysteine and lysine peptides (by depletion) and is motivated by the electrophilic nature of sensitisers (Gerberick et al, 2004). A similar assay uses additional peptides, and the detection of chemical adducts by mass spectroscopy (Aleksic et al, 2009). The DPRA was extended by the addition of a peroxidase step to oxidise chemicals that are metabolised into haptens (pro-haptens), termed the peroxidase peptide reactivity assay (PPRA) (Troutman et al, 2011). Surface plasmon resonance has also been used to screen allergen binding to nucleophilic amino acids (Achilleos et al, 2009).

Keratinocyte assays

Several assays have been developed that measure different aspects of keratinocyte or skin model responses to chemicals: cytokine release; gene expression; and signalling pathway activation. In many of these studies, cell death is not controlled to be comparable between test chemicals and is a confounding factor.

Assays have been proposed involving measurement of intracellular IL-1α (Corsini 1998; Van Och et al, 2005), or IL-18 (Corsini et al, 2009; Van Och et al, 2005; Galbiati et al, 2011), in primary keratinocytes or keratinocyte cell lines. The release of cytokines from 3D skin models has also been investigated as a possible predictor of skin sensitisation potential. Examples include: IL-1α (dos Santos et al, 2011); and IL-1α and IL-8 in combination (Coquette et al, 2003; Poumay et al, 2004; Spiekstra et al, 2009).

Sensitiser-induced transcriptome changes in keratinocytes have also been investigated to find predicative subsets of genes that discriminate sensitisers from non-sensitisers. In general, these genes are transcription factors (ATF3, cFOS); heat shock proteins (HSPA1B, HSPA6, HSPH1, DNAJB1, DNAJB4); cytokines and related proteins (IL-1β, IL-8, TNFAIP3); or genes associated with oxidative stress response/Nrf2 (HMOX1, NQO1, TXNRD1, GCLC, GCLM) (Yoshikawa et al, 2010; Saito et al, 2013; Vandebriel et al, 2010; Van der Veen et al, 2013). Other assays are based on a small number of genes from these studies in keratinocytes (Emter et al, 2013; McKim et al, 2010) or skin models (McKim et al, 2012).

Attempts are also being made to predict sensitisation potential based on activation of intracellular signalling cascades in keratinocytes in response to sensitiser. KeratinoSens is an assay based on nuclear factor (erythroid derived 2)-like 2 (Nrf-2) activation, which utilises a luciferase reporter gene under the control of the ARE in HaCaT cells, and has been extensively evaluated (Natsch et al, 2011; Emter et al, 2010). In a small study, Koeper et al (2007) proposed the use of MAPK signalling for discriminating between sensitisers and irritants in skin models.

Dendritic cell assays

PBMC-derived dendritic cell and dendritic-like (monocytic) cells, such as THP-1, U937 and MUTZ3, are also being explored for the prediction of sensitisation potential. Predictive biomarkers include: cell surface molecule expression (as a measure of DC activation); cytokine release; gene expression; signalling pathway activation; and generation of ROS.

The activation status of the DC or DC-like cell line is often measured as a possible predictor of the sensitisation potential of chemicals. Co-stimulatory molecules such as HLA-DR, CD80, CD83, CD86, ICAM-1 and CD40, DC-SIGN and the chemokine receptor CCR7 are used as indicators of DC activation. The human cell line activation test (hCLAT) (Ashikaga et al, 2005; Sakaguchi et al, 2006, 2009) aims to predict allergens from irritants based on expression of CD86 and CD54 on THP-1 cells following chemical exposure. The myeloid U937 skin sensitisation test (MUSST) is a similar assay measuring CD86 in U937 cells (Python et al, 2007; Ade et al, 2006).

CD86 also features in a PBMC-DC assay by Reuter et al (2011), and was found to be the most reliable biomarker in a comparison of 8 markers across 6 DC cell lines (Azam et al, 2006). In many of these studies cell death is a confounding factor, given that, in the cell surface expression studies in particular, the cells are often up to 50% dead. To circumvent this, the loose fit co-culture based sensitisation assay (LCSA) was developed measuring CD86 and cytokines from a co-culture of monocytes with keratinocytes (Schreiner et al, 2007, 2008). In another co-culture assay, containing HaCaT and THP-1 cells, CD86 CD40 and CD54 on THP-1 were measured (Hennen et al, 2011). Other DC-based assays measured IL-8 release from monocyte-derived DCs or THP-1 cells instead of cell surface markers (Toebak et al, 2006; Mitjans et al 2008; Nukada et al, 2008).

Transcriptional changes in response to sensitising chemicals have been explored in dendritic or dendritic-like cells (Ryan et al, 2004; Johansson et al, 2011; Miyazawa and Takashima, 2012; Yoshikawa et al, 2010; Schoeters et al, 2007; Python et al, 2009; Szameit et al, 2009), with the objective of finding a small number of genes to predict sensitisation potential (Gildea et al, 2006; Hooyberghs et al, 2008; Lambrechts et al, 2010; Johansson et al, 2013).

Other groups have investigated activation of intracellular signalling pathways in DC in response to sensitisers. Two studies have focused on transcription of genes associated with Nrf2 signalling (HMOX, NQO1) in THP-1 and $CD34^+$ DCs or MoDCs (Ade et al, 2009; Migdal et al, 2013). MAPK signalling in MoDCs was evaluated as a possible sensitiser screening tool (Trompezinski et al, 2008), and p38MAPK phosphorylation in THP-1 cells was a positive signal for sensitisers (Suzuki et al, 2009; Mitjans et al 2008). ROS generated in XS106 or THP-1 DC-like cells was used as a biomarker in response to sensitisers (Miyazawa et al, 2012; Saito et al, 2013).

Proliferation and IFNγ secretion from T cells in response to DC exposed to haptenated peptide (Martin et al, 2010) led to development of the human T cell priming assay (hTCPA). In this assay, MoDC are pulsed with test chemical or chemical protein conjugates, and co-cultured with T cells, and the IFNγ/TNFα positive $CD4^+$ or $CD8^+$ T

cells are measured (Richter et al, 2013). This assay has been improved by the depletion of Tregs (Vocanson et al, 2014).

Developments of *in vitro* assays in all of these areas are continuing, in particular many authors are now attempting to extend their assays to predict sensitisation potency in addition to potential.

1.13 HaCaT cell line

The HaCaT cell line is widely used to study human keratinocyte behaviour. HaCaT cells are a spontaneously immortalised cell line, originally derived from the distant periphery of an adult human skin melanoma (Boukamp et al, 1988). They are cytogenetically abnormal, and have mutations in both alleles of the p53 gene, which results in mutant p53 protein with an extended half life (Lehman et al, 1993), however, they are non-tumorigenic (Boukamp et al, 1988, 1997).

HaCaT cells are thought to represent basal keratinocytes, expressing keratins 5 and 14 (Boukamp et al, 1988). However, they can be induced to differentiate by culture at high concentrations of calcium, or at confluency > 85%, leading to increased expression of differentiation markers keratin 1 and involucrin (Deyroeux and Wilson, 2007). As HaCaT cells retain the ability to differentiate, they can provide stratified epidermal tissue when grafted onto mice (Boukamp et al, 1988). However, attempts to produce 3D skin models with HaCaT cells were not successful, due to a lack of terminal differentiation (Boelsma et al, 1999).

1.14 3D skin models

3D skin models, also known as reconstructed human epidermis (RHE), living skin equivalents (LSE), or epidermal equivalents (EE), were first developed to provide skin grafts from *in vitro* culture (Bell et al, 1983). They are models of stratified epidermal keratinocytes, layered on a collagen or polycarbonate matrix, or a matrix containing dermal fibroblasts. The inclusion of fibroblasts in the dermal compartment assists keratinocyte attachment, growth and differentiation (Krejci et al, 1991). The models are cultured at the air:liquid interface, which causes differentiation of the keratinocytes,

resulting in stratification that resembles the physiology of human skin *in vivo* (Asselineau et al, 1985). Due to the formation of a stratum corneum layer, 3D skin models have some barrier function to water permeation, which can be altered by varying the culturing conditions: humidity, vitamin D and the support matrix composition (Mak et al, 1991). However, the barrier is not as effective as normal human skin, as permeation rates through 3D skin models are up to 10-fold greater (Regnier et al, 1993). RHE models have been shown to express suprabasal keratins 1 and 10, similar to human skin, however, they over-express keratin 6 and express suprabasal involucrin, transglutaminase and filaggrin which are all markers of hyper- proliferative epidermis (Ponec et al, 1991).

Due to their physiological approximation to human skin and the ability to dose topically with test chemicals, these models have been adopted for use in *in vitro* toxicology assays for irritancy, by measurement of cytotoxicity and IL-1α release (Spielmann et al, 2007). Skin models have also been investigated as possible *in vitro* tools to develop assays to predict skin sensitisation potential (dos Santos et al, 2011; Coquette et al, 2003; Poumay et al, 2004; Spiekstra et al, 2009; Spiekstra et al, 2005; McKim et al, 2012). However, repeat application testing is not possible, due to the lack of desquamation in the models (Ponec et al, 2002). There are two main commercially available skin models: EpiDerm™ (MatTek Corporation) and EpiSkin (SkinEthic), which have been demonstrated to be representative of normal human skin (Monteiro-Riviere et al, 1997; Rosdy et al, 1993). Ponec et al (2000) performed a comparision of the EpiDerm, EpiSkin and SkinEthic models to human skin, and found them to have similar lipid content. Ceramide 7 was, however, not present in the skin models, and ceramides 5 and 6, and free fatty acids were much lower than those detected in human skin. A comprehensive comparison of the commercially available skin models is summarised in Ponec et al (2002).

EpiDerm is also available as a full thickness version, EpiDermFT™, with a dermal compartment containing human fibroblasts. Further developments of skin models are in progress, to attempt to incorporate immune cells, such as $CD34^+$ LC-like cells (Facy et al, 2005), MUTZ derived-LCs (Ouwehand 2011) and $CD4^+$ T cells (van den Bogaard et al, 2014).

1.15 Aims

CHS is an extensively studied immune response, however, investigations into the roles of different cell types during CHS have focused mainly on LCs, DCs and T cells. Keratinocytes are the most numerous cells in skin and the first cell type to encounter chemical allergen following topical exposure, and are known to be capable of influencing cutaneous immune responses, but their contributions to CHS responses are not well understood. For example, previous *in vitro* studies have focused on the response of DCs following direct exposure to chemical allergen, however, few have looked at the crosstalk between keratinocytes and DCs or at the molecular response of the keratinocyte to chemical allergen. A commonly expressed hypothesis is that danger signals produced by keratinocytes induce the co-stimulatory signal expression on DCs required to generate an adaptive immune response. However, keratinocytes may also regulate cutaneous immune responses in other ways, for example by influencing/attracting other cell types (T cells, macrophages, granulocytes, fibroblasts) through their mediator release. Investigation of which cytokines, chemokines and growth factors are generated by keratinocytes may provide clues about which other cells are most likely to respond as a result of keratinocyte signalling.

The objective of this project is to characterise keratinocyte-derived epidermal signals in the initiation of contact hypersensitivity to chemicals. We also intend to investigate the molecular mechanisms involved in generating intercellular mediator signals in response to chemical allergen, to understand how chemicals may interact with keratinocytes to trigger CHS responses. We will first establish which cellular communication mediators (such as cytokines, chemokines and growth factors) are released by different *in vitro* keratinocyte models, specifically in response to chemical allergen and distinct from a cytotoxic response. Our next aim is to identify candidate molecular mechanisms for the cytokine/chemokine release through a comprehensive analysis of modulation of the transcriptome. Finally, we will ascertain which intracellular signal transduction cascades are responsible for sensitiser-specific mediator expression using functional assays.

2 MATERIALS AND METHODS

2.1 Cell culture

HaCaT cell line

The spontaneously immortalised human keratinocyte cell line, HaCaT (supplied by Professor N. Fusenig, Heidelberg, Germany) was used for comparison with the 3-dimensional keratinocyte models. HaCaT cells (passage 48-52) were cultured in high glucose Dulbecco's modified Eagle medium (DMEM) containing 0.37% sodium bicarbonate, 10% heat inactivated foetal calf serum, 2mM L-glutamine, 1mM sodium pyruvate, 100U/ml penicillin and 100μg/ml streptomycin (solution prepared in normal saline) (all Gibco). Cells were maintained at 37°C in an atmosphere of 5% CO_2 and passaged (or dosed) when approximately 80% confluent. To subculture, HaCaT cells were washed with phosphate buffered saline (PBS) and detached by 10 minute incubation at 37°C in 1mM trypsin (0.25%)/ethylenediaminetetraacetic acid (EDTA) (Sigma). Cells were harvested and pelleted by centrifugation at 160 x g for 10 minutes and re-suspended in fresh media.

EpiDerm and EpiDermFT models

Two types of human artificial skin models were used; a keratinocyte only model and a keratinocyte and fibroblast model (models and media supplied by MatTek; Ashland, MA, USA). The keratinocyte only models (EpiDerm^{TM}) are stratified cultures derived from normal human epidermal keratinocytes (NHEK) from neo-natal foreskin (single donor). To form stratified layers, keratinocytes were grown on collagen coated tissue culture plate inserts (Millicell™, Millipore) at the air liquid interface. The keratinocyte and fibroblast models (EpiDermFT^{TM}) are stratified cultures of NHEK from neo-natal foreskin tissue layered on top of normal human dermal fibroblasts (NHDF) also from neo-natal foreskin (multiple donors). The full thickness (FT) models were produced by culturing on tissue culture plate inserts (Millicell, Millipore) at the air liquid interface. The culturing conditions for production are proprietary to MatTek. Upon arrival, both models were cultured at 37^{o}C in 5% CO_2 in serum free Dulbecco's modified Eagle medium (DMEM) containing 5μg/ml gentamicin, 0.25μg/ml amphotericin B, phenol red, insulin, epidermal growth factor (EGF) and lipid precursors (MatTek proprietary).

The EpiDerm media contained additional stimulators of epidermal differentiation (MatTek proprietary). All tissues and media were requested to be hydrocortisone-free (removed 3 days prior to shipment) to enable inflammatory signalling to be studied. The media were also requested to contain the minimum amount of epidermal growth factor required for viability and to be free from all other cytokines present on the Luminex 30-plex panel (see section on Luminex). Models derived from three different donors were obtained to address inter-individual variability; the same three keratinocyte donors were used to prepare the EpiDerm and the EpiDermFT cultures.

2.2 Chemical exposure

1-Chloro-2,4-dinitrobenzene (DNCB) was selected as an extreme skin sensitiser based on its classification in the Local Lymph Node Assay (LLNA) (Loveless et al, 1996). Sodium dodecyl sulphate (SDS) was chosen as a representative irritant based on human patch test classification (Basketter et al, 2004). Interestingly, this irritant gives a false positive result in the LLNA (Loveless et al, 1996). Lipopolysaccharide (LPS) and Interferon-gamma (IFNγ) were chosen as positive controls as they are known to activate the immune system and hence have the potential to stimulate cytokine release (Pastore et al, 1998) (all chemicals, Sigma).

HaCaT cell line

HaCaT cells (passage 49-52) were harvested by incubation with 1mM trypsin (0.25%)/EDTA (Sigma) and seeded into 6-well plates (2ml per well of $4x10^5$cells/ml). Following overnight culture, maintenance media was removed and the cells exposed to DNCB (between 2.5μM and 40μM), or SDS (between 1μM and 500μM) diluted in 0.2% dimethyl sulfoxide (DMSO) (Sigma) in culture media (see section on cell culture). HaCaT cells were also exposed to LPS/IFNγ (1μg of each in 1ml culture media) to act as a positive control; and culture media, or 0.2% DMSO in culture media to act as negative/vehicle controls. Following 1, 4 or 24 hour exposure, supernatants were removed and stored at -80ºC (for cytokine analysis). The cells were assessed for viability using the MTT assay (see section on MTT assay below).

EpiDerm and EpiDermFT models

Following overnight incubation in culture media (see section on cell culture), the models were transferred into 6-well plates containing 2ml of fresh, pre-warmed, culture media. Models were dosed topically with 700µl (large models) or 100µl (small models) of culture media; 0.2%, 0.5% or 1% DMSO in culture media; DNCB (between 62.5µM and 1000µM diluted in 0.2%, 0.5% or 1% DMSO in culture media); SDS (between 1mM and 40mM) or LPS/IFNγ (1µg of each in 1ml culture media). The models were then incubated at 37°C in 5% CO_2 and saturated humidity for 1 hour, 4 hours or 24 hours. Following incubation with chemical, supernatants were removed and stored at -80ºC (for cytokine analysis/ lactate dehydrogenase (LDH) assay). Cultures were then washed thoroughly with PBS and punched from their housings using a biopsy punch. Tissues were divided into three equal parts. For the histological analysis, sections were immersed in 10% (v/v) neutral buffered formalin (NBF) (Sigma). For mRNA analysis tissues were immersed in 'RNA-Later' (Applied Biosystems). The remaining tissue sections were lysed in RIPA protein lysis buffer (Sigma). This procedure was repeated for 3 different donors of EpiDerm and EpiDermFT. All tissue and supernatant samples were stored at –80ºC.

2.3 Cytotoxicity

MTT assay

The MTT (3-(4, 5-Dimethylthiazol-2-yl)-2, 5-diphenyltetrazolium bromide) assay was used to assess the cytotoxicity of chemicals in the HaCaT cells and the skin models. Following treatment, HaCaT cells or skin models were washed with PBS and exposed to 0.5mg/ml of MTT (Sigma). Cultures were incubated in MTT in the dark at 37°C in 5% CO_2 for 3 hours. Following this incubation, HaCaT cells or EpiDerm models were washed twice with PBS and incubated (with shaking) in isopropanol for 10 minutes (HaCaTs) or 2 hours (models) at room temperature. The epidermis and dermis of the full thickness models were separated (using tweezers) at this stage and analysed separately. The absorbance of the isopropanol at a wavelength of 570nm was read using a spectrophotometer (Spectramax, Molecular Diagnostics). Cell viability (%) was assessed by comparing the absorbance (at 570nm) of treated cells to the untreated/vehicle controls.

LDH assay

The LDH cytotoxicity assay was used in place of the MTT assay to estimate cell viability in some of the skin models (so that the tissue could be utilised in other endpoints). The TOX-7 assay kit (Sigma) was used for this assay. The LDH assay mix was prepared by mixing equal amounts of LDH assay Substrate, LDH assay Cofactor (re-hydrated in tissue culture grade water) and LDH assay Dye Solution. Supernatant samples (100µl) generated from EpiDerm models were aliquoted into a 96 well flat-bottom plate. LDH assay mix was added to each well at twice the volume of sample. The plate was covered with foil and incubated at room temperature for 30 minutes. The reaction was terminated by the addition of 30µl of 1N HCl (Sigma) to each well. The absorbance of each well was measured using a spectrophotometer (Spectramax, Molecular Diagnostics) at a wavelength of 490nm. The background absorbance at 690nm was also measured and subtracted from the primary (490nm) wavelength measurement. Model viability (%) was assessed by comparing the absorbance of treated models to the vehicle controls.

2.4 Histology

Changes in the morphology of the skin models in response to chemical exposure were visualised using histology.

Tissue Processing

Following 3 hour incubation in 10% (v/v) neutral buffered formalin (NBF), the cultures were placed into processing cassettes to maintain the tissue structure. Tissue processing was performed using the Leica TP1020 tissue processor according to the following procedure (IMS: Industrial Methylated Spirit):

Station	Reagent	Temperature	Time
1	70% IMS	Ambient	30 minutes
2	80% IMS	Ambient	90 minutes
3	90% IMS	Ambient	90 minutes
4	100% IMS	Ambient	90 minutes
5	100% IMS	Ambient	90 minutes

6	100% IMS	Ambient	90 minutes
7	Xylene	Ambient	30 minutes
8	Xylene	Ambient	60 minutes
9	Xylene	Ambient	90 minutes
10	Wax	60^{o}C	90 minutes
11	Wax	60 ^{o}C	90 minutes
12	Wax	60 ^{o}C	90 minutes

Tissue embedding and sectioning

Wax infiltrated tissues were embedded in paraffin wax blocks for sectioning using the Leica EG1140 HC tissue embedding centre. Processing cassettes were removed from the tissue processor and bathed in molten wax and tissues were then removed from the cassette and cut in half to create a flat surface. Molten wax was poured into a metal mould and the tissues were orientated in the wax so that the flat edge lay at the bottom of the mould. Once in position the mould was placed on a cold plate and the wax containing the tissue set to give a hardened wax block containing EpiDerm/ EpiDermFT tissue. The wax blocks were trimmed to remove excess wax from around the tissue. The block was then placed in a microtome (Leica rotary microtome 2035) and the wax shaved until the tissue was exposed. Sections were cut at 4μm and floated in warm water onto a clean microscope slide. The sections were covered with a cover-slip and placed in an incubator at 56^{o}C to dry overnight.

H&E staining

Haematoxylin and Eosin (H&E) staining was carried out using the Leica Autostainer according to the following procedure:

Station	Method	Time
1	Immerse in Xylene	1 minute
2	Immerse in Xylene	1 minute
3	Immerse in 100% ethanol	1 minute
4	Immerse in 100% ethanol	1 minute

5	Immerse in 95% ethanol	1 minute
6	Immerse in 95% ethanol	1 minute
7	Rinse in water	
8	Haematoxylin	5 minutes
9	Rinse in water	
10	Differentiate in 1% acid ethanol	
11	Blue in water	10 minutes
12	Eosin	5 minutes
13	Rinse in water	
14	Immerse in 95% ethanol	1 minute
15	Immerse in 95% ethanol	1 minute
16	Immerse in absolute ethanol	1 minute
17	Place in fresh absolute ethanol	1 minute
18	Immerse in Xylene	1 minute
19	Place in fresh Xylene	1 minute
20	Mount in DPX	

The slides were examined under the microscope for histological changes and photographed with both the x10 and x40 zoom using a photomicroscope (Leica DM5500).

2.5 Luminex

Culture supernatants from HaCaT cells, EpiDerm and EpiDermFT models exposed to DNCB, SDS and LPS/IFNγ were analysed for the presence of cytokines, chemokines and growth factors using the Luminex 200IS platform (Luminex). The human 30-plex cytokine/chemokine kit or the human inflammatory 5-plex and the IL-1α single plex kit were used to analyse the supernatants (IL1-α was analysed separately to IL1-β as the antibodies for these cytokines cannot be analysed together). Kits contained all reagents unless otherwise stated (Invitrogen).

Cytokine/chemokine detection

Lyophilised standards for 30 cytokines (IL-1RA, IL-1β, IL-2, IL-2R, IL-4, IL-5, IL-6, IL-7, IL-8, IL-10, IL-12, IL-14, IL-15, IL-17, IP-10, MCP-1, MIG, MIP-1α, MIP-1β, RANTES, TNFα, VEGF, EGF, EOTAXIN, FGF-basic, GCSF, GM-CSF, HGF, IFNα, IFNγ) or 5 cytokines (IL-1β, IL-6, IL-8, GM-CSF, TNFα) and a separate batch for IL-1α were reconstituted in 50% assay diluent and 50% of the relevant culture media. A standard curve was prepared for each cytokine by serially diluting (1:3) the reconstituted standard in 50% assay diluent plus 50% culture medium. Following this, a 96-well filter plate was hydrated with diluted wash solution and aspirated from the wells using a vacuum manifold (< 5 inches Hg). Diluted bead solution containing beads coated with antibodies for each cytokine was added to each well (25µl) and the plate shielded from light, using a foil coated lid. The beads were washed by addition of 0.2ml wash solution to each of the wells. After 30 seconds the wash solution was removed from the wells by aspiration with the vacuum manifold. This step was repeated and the filter plate blotted to remove residual liquid. Incubation buffer (50µl) was then added into each well. 100µl of appropriate standard dilution was added to the wells designated for the standard curve. Assay diluent (50µl) followed by sample (50µl) was added to the wells designated for samples. The plate was incubated for 2 hours at room temperature on an orbital shaker to keep the beads suspended during the incubation (~550 rpm). Following the 2 hour incubation the liquid was aspirated and the wells washed twice with wash solution. The filter plate was blotted to remove residual liquid and 100µl of the diluted biotinylated detector antibody added to each well. The plate was then incubated for 1 hour at room temperature on an orbital shaker (~550 rpm). Following the 1 hour incubation the liquid was aspirated and the wells washed twice with wash solution. The filter plate was blotted to remove residual liquid and 100µl diluted Streptavidin-RPE added to each well. The plate was then incubated for a further 30 minutes at room temperature on an orbital shaker. After 30 minutes, the liquid was removed from the wells by aspiration with the vacuum manifold. The wells were washed 3 times in wash solution and the filters blotted to remove residual liquid. Wash solution (100µl) was then added to each well and the beads re-suspended by shaking on an orbital shaker (500-600 rpm) for 2-3 minutes. Plates were analysed using the Luminex 200IS platform. The software was set to read 100 events per bead region with a doublet discriminator gate set at 7800-15200. Data were collected as

median relative fluorescence units (RFU) and the concentration of each cytokine was determined using the standard curves.

Cytokines and chemokines IL-8, IL-6 and MCP-1 released into the supernatant by the EpiDermFT models had concentrations that exceeded the standard curve and so were diluted (1:80 for IL-6 and IL-8 or 1:5 for MCP-1) in the corresponding culture medium and reanalysed.

2.6 Ribonucleic acid (RNA) extraction: TRIzol method

Total RNA from HaCaT cells and 3D skin models was extracted using a combination of TRIzol (Invitrogen) extraction and column purification using the RNeasy mini kit (Qiagen).

HaCaT cells were lysed directly in 1ml of TRIzol reagent (Invitrogen) and transferred into centrifuge tubes. For the 3D skin models, 50mg of tissue was taken out of RNA later and placed in a FastPrep F-matrix tube containing 2 ceramic beads and 1ml of TRIzol reagent (Invitrogen). The tissue was homogenised using the FastPrep-24 (MP Biomedicals) 3 times for 20 seconds at 4 macerations/ second each time with 3 min on ice between each cycle. The FastPrep matrix were pelleted by centrifugation at 9,300 x g for 2.5 minutes and the TRIzol containing lysed tissue transferred into fresh centrifuge tubes.

For both, Chloroform:Isoamyl alcohol mixture (0.2ml) (BioUltra, Sigma) was added (into TRIzol lysate) and shaken vigorously to ensure complete mixing. Following 3 minutes incubation at room temperature the samples were centrifuged at 10,000 x g for 15 minutes at 4^{o}C. The upper aqueous phase of the solution (containing RNA) was transferred to a fresh eppendorf tube to which 0.53x volumes of absolute ethanol were added. The aqueous/ethanol mix was added to an RNeasy mini column (Qiagen) and centrifuged for 1 minute at 15,700 x g in a bench top centrifuge. The column was washed with 700µl of buffer RW1 (Qiagen) and centrifuged for 1 minute at 9,300 x g, then rinsed with 500µl buffer RPE (Qiagen) and re-centrifuged for 1 minute at 9,300 x g. The rinse with 500µl buffer RPE was repeated and the column centrifuged at 9,300 x

g for 2 minutes. RNase free water (50µl) was added to the column and incubated for 2 minutes. Following this, total RNA was eluted off the column into a fresh RNase free eppendorf tube by centrifugation at 15,700 x g for 1 minute. RNA was stored at -80^{o}C.

2.7 Analysis of RNA quality

The concentration and purity of the RNA samples were determined using the Agilent 2100 Bioanalyser. The RNA 6000 Nano kit (Agilent) was used for this assessment. The chip priming station was prepared by attaching a new syringe and adjusting the syringe clip and base plate to RNA chip specific positions. The gel-dye mix was prepared by adding RNA 6000 Nano gel matrix to a spin filter and centrifuging at 1500 x g for 10 minutes at room temperature. Filtered gel matrix (65µl) was transferred to a fresh micro-centrifuge tube and 1µl of Nano dye concentrate added. The solution was vortexed and centrifuged at 13,000 x g for 10 minutes at room temperature. The gel-dye mix (9µl) was then loaded onto the RNA 6000 Nano chip and driven through using the syringe. Two additional 9µl aliquots of gel-dye mix were also loaded onto the chip (see manufactures instructions for loading positions). RNA 6000 Nano marker (5µl) was added into each of the remaining wells, to which either 1µl RNA ladder or 1µl of sample RNA was added. The chip was vortexed for 1 minute and then analysed using the Agilent 2100 Bioanalyser.

2.8 cDNA synthesis from total RNA

Single stranded complementary deoxyribonucleic acid (cDNA) was synthesised from total RNA using the High Capacity RNA-to-cDNA kit (Applied Biosystems). RNA (2µg total) was added (on ice) to reverse transcription (RT) buffer and RT enzyme mix (both Applied Biosystems) and made up to 20µl with nuclease free water (Applied Biosystems). The reverse transcription was performed using a thermal cycler (Perkin Elmer) by heating to 37^{o}C for 60 minutes followed by 95^{o}C for 5 minutes. The cDNA was stored at -20 ^{o}C and analysed for quality and concentration before use in qRT-PCR measurements using a NanoDrop ND-1000 spectrophotometer (Labtech International Ltd).

2.9 Quantitative real time polymerase chain reaction

TaqMan gene expression master-mix (Applied Biosystems) and gene specific TaqMan gene expression assays for IL-1β (hs01555410), IL-6 (hs00985641), IL-8 (hs99999034), glyceraldehyde-3-phosphate dehydrogenase (GAPDH) (hs99999905) and hypoxanthine phosphoribosyltransferase 1 (HPRT) (hs99999909) containing unlabeled primers (final concentration 900nM per primer) and FAM™ dye-labelled TaqMan minor groove binder (MGB) probe (final concentration 250nM) (all Applied Biosystems) were combined as per manufactures instructions:

Gene	Assay ID	Context Sequence
IL-1β	Hs01555410_m1	AGATGAAGTGCTCCTTCCAGGACCT
IL-6	Hs00985641_m1	TGCAGAAAAAGGCAAAGAATCTAGA
IL-8	Hs99999034_m1	GCAGCTCTGTGTGAAGGTGCAGTTT
GAPDH	Hs99999905_m1	GGGCGCCTGGTCACCAGGGCTGCTT
HPRT1	Hs99999909_m1	ATGGTCAAGGTCGCAAGCTTGCTGG

TaqMan gene expression master-mix and gene specific TaqMan gene expression assays were added to 50ng cDNA diluted in nuclease free water (to total volume 20μl) in a fast MicroAmp™ optical 96-well reaction plate (Applied Biosystems). The plate was loaded into a 7500 fast real-time PCR machine (Applied Biosystems) and run in standard mode under the following conditions:

Step	**Temperature (°C)**	**Duration**	**Cycles**
UDG incubation	50	2 min	HOLD
AmpliTaqGoldUP enzyme activation	95	10 min	HOLD
Denature	95	15 sec	40
Anneal/Extend	60	1 min	40

Data were collected for IL-1β, IL-6, IL-8, and housekeeping genes GAPDH and HPRT for normalisation.

2.10 Transcriptomics

Cell culture and dosing

HaCaT cells, as previously described (in the section on cell culture), were harvested by incubation with 1mM Trypsin (0.25%)/EDTA (Sigma) and seeded into 6-well plates (2ml per well of $4x10^5$cells/ml). Following overnight culture, maintenance media was removed and the cells exposed to DNCB (20μM, 27.5μM or 30μM), or SDS (250μM); both chemicals were diluted in 0.2% Dimethyl Sulfoxide (DMSO) (Sigma) in culture media (see section on cell culture). HaCaT cells were also cultured in 0.2% DMSO in culture media to act as a vehicle control. Following 4 hour exposure, supernatants were removed and stored at -80ºC (for cytokine/LDH analysis). Total RNA was immediately extracted from the cells using the methods previously described (see Ribonucleic acid (RNA) extraction: TRIzol method and Analysis of RNA quality sections).

Preparation and Labelling of cRNA

The transcriptomic analysis was performed using the Agilent human genome CGH microarray system (4x44k).

Sample RNA diluted in nuclease free water (400ng) was added (6.25ml of 64ng/ml) to T7 promoter primer (1.2μl) along with one colour spike mix (3.5μl of a diluted stock solution at 1:2500 in dilution buffer) (Agilent RNA spike-in kit). The RNA:primer:spike mix was heated to 65ºC for 10 minutes in a thermocycler to denature both sample and spike-in RNA allowing binding of the promoter primer. Following this, samples were incubated on ice for 5 minutes. A cDNA master mix was prepared containing first strand buffer (pre-warmed to 80ºC for 4 minutes), dithiothreitol (DTT), deoxynucleotide (dNTP) mix, moloney murine leukemia virus (MMLV) reverse transcriptase and RNase-out. The cDNA master mix was added to the primed RNA samples and incubated at 40ºC for 2 hours, followed by 15 minutes at 65ºC and then 5 minutes on ice. During this incubation a transcription mastermix was prepared containing; nuclease free water, transcription buffer, DTT, NTP mix, polyethylene glycol (PEG; pre-warmed to 40ºC for 1 minute), RNaseOUT, Inorganic pyrophosphatase, T7 RNA polymerase and Cyanine-3 CTP (all Agilent). Transcription

master mix was added to the cDNA samples and incubated at 40^{o}C for 2 hours. The resultant labelled cRNA was purified using a Qiagen RNeasy mini spin column.

Purification and quantification of cRNA (Qiagen mini kit)

RLT buffer (350µl) and ethanol (>96%) (250µl) were added to cRNA samples (previously made up to 100µl in nuclease free water). The resultant samples were added to RNeasy mini columns in a collection tube (Qiagen) and centrifuged for 30 seconds at 15,700 x g in a bench top centrifuge. In a new collection tube, the column was rinsed with 500µl buffer RPE (containing ethanol) and re-centrifuged for 30 seconds at 15,700 x g. The rinse with 500µl buffer RPE was repeated and the column centrifuged at 30 seconds at 15,700 x g. The dry column was then re-centrifuged at 15,700 x g for 1 minute to remove all traces of RPE. cRNA was eluted off the column into a fresh RNase-free eppendorf tube by the addition of 50µl RNase-free water. This column was incubated with RNase-free water for 1 minute and then centrifuged at 15,700 x g for 30 seconds. The resultant labelled-cRNA was stored in the dark at -80^{o}C.

cRNA was quantified using a UV-VIS spectrophotometer (measuring at 260 nm and 550 nm) in an Implen cuvette with a factor 10 LP 1mm cap. The spectrophotometer was blanked using nuclease free water until a constant zero reading could be achieved. The RNA absorbance at 260nm and the cyanine-3 dye absorbance at 550nm for each eluted cRNA sample were measured. From these values the cRNA concentrations (ng/µl) (=A_{260nm} x dilution factor (10) x optical density of RNA (40 ng/µl)) and hence yields in µg (in 50µl total volume) were calculated. The concentration of Cy3 dye was also calculated in each sample (pmol/µl) (=A_{550nm} x dilution factor (10) x pmol factor (1000) / absorbance co-efficient of Cy3 (0.15)). The specific activity of the Cy3 dye in each sample was calculated as [Cy3 (pmol/µl)]/ [cRNA (ng/µl) x (1000)]. The values were assessed for use in hybridisation reactions.

Preparation of hybridization reaction mixtures

For each array, a 2µg Cy3-labelled cRNA sample was brought to a final volume of 20µl in nuclease-free water. To this, blocking agent (11µl), fragmentation buffer (2.2µl) and

nuclease free water (21.8µl) were added and the tube placed in a thermocycler for 30 minutes at 60ºC. The fragmentation process was stopped by the addition of 55µl of 2x GEx hybridisation buffer HI-RPM. The sample was placed on ice until loading onto the array.

Loading and hybridization

The hybridisation chamber was assembled and the samples dispensed into the guides (gaskets) on the SureHyb gasket slide (Agilent). The active array was aligned and lowered onto the gasket slide and the slides clamped together. The assembled slide chambers were placed into a rotisserie in a hybridisation oven at 65ºC. Slides were rotated at 10rpm at 65ºC for 17 hours.

Washing of array slides

Following incubation the hybridisation camber was disassembled and the array-gasket sandwich prised apart whilst submerged in wash buffer 1 (Agilent). The microarray was placed in a slide rack and submerged in a beaker containing wash buffer 1 for 1 min at room temperature with constant stirring. Following this, the array was transferred to a beaker containing wash buffer 2 (Agilent) for 1 min at 37ºC with constant stirring. Following this wash, the array was transferred to a beaker containing acetonitrile at room temperature for 30 seconds. The slide was then transferred to a 50ml tube containing stabilization and drying solution (Agilent) for 30 seconds with gentle rocking. The array was removed from this solution very slowly, placed on tissue and scanned immediately.

Array scanning and analysis

Arrays were scanned using the Agilent microarray scanner, at both a high (100) and a low (10) PMT setting to maximise data from both low and high end signals. A 5µm resolution was used, at which each 50µm spot was comprised of approximately 100 pixels. The array images were visually checked for any obvious artefacts and the data was checked for quality using the QC software on the scanner. Numerical expression

data from each image was obtained using the feature extraction software and this data was loaded into GeneSpringGx v12.6 software (Agilent) for further analysis.

2.11 Western blotting

Electrophoresis

Protein lysates were added to NuPAGE LDS sample buffer (Invitrogen, proprietary) and NuPAGE reducing agent (Invitrogen, proprietary), in deionised water. Samples were heated to 70^{o}C for 10 minutes in a block heater and then loaded (10 or 20µl/lane of the gel) onto duplicate NuPAGE Novex 4-12% or 12% Bis-Tris gels (Invitrogen) in an XCell surelock mini cell filled with MOPS NuPAGE SDS running buffer (Invitrogen). NuPAGE antioxidant (500µl) was added to the upper chamber. Proteins were separated by electrophoresis at 200V constant for 50 minutes with a current of 100-125mA/gel. For larger proteins, heated samples were loaded (10 or 20µl/lane of the gel) onto duplicate NuPAGE Novex 3-8% Tris-Acetate gels (Invitrogen) in an XCell surelock mini cell filled with Tris-Acetate SDS running buffer (Invitrogen). NuPAGE antioxidant (500µl) was added to the upper chamber. Proteins were separated by electrophoresis at 150V constant for 1 hour with a current of 40-55mA/gel.

Total protein loading control

Following electrophoresis, one gel was stained for total protein to act as a loading control. The gel was extracted from the casing, micro-waved in ultrapure water for 1 minute (750watts) and cooled on a shaker for 1 minute. The water was discarded and the process repeated twice. Simply Blue total protein gel stain (25ml) (Invitrogen) was added to the gel and micro-waved for 1 minute (750watts). The stain was left to develop on a shaker for 5 minutes and then discarded. The gel was then washed in ultrapure water for 10 minutes on an orbital shaker and the background removed by washing with 20ml of 20% NaCl (Sigma) in ultrapure water for 5 minutes. The gel was left to soak in ultrapure water for 1 hour to clear excess background staining.

Blot

The non-loading control gel was transferred by western blotting to a PVDF membrane. The Xcell II blot module was constructed to contain the electrophoresed gel and the PVDF membrane. The blotting module was placed in the XCell sure lock mini cell tank (Invitrogen). The upper chamber (covering the gel and membrane) was filled with NuPAGE transfer buffer (Invitrogen proprietary recipe) supplemented with 10% methanol and 0.1% NuPAGE antioxidant and the outer chamber was filled with deionised water. The transfer was performed using 30V constant for 1 hour.

Protein visualisation

To visualise proteins, the PVDF membrane was first immersed in blocking buffer containing 0.1% TWEEN (Sigma) and 3% dried milk (Marvel) in PBS for 1 hour at room temperature. The membrane was then incubated overnight with primary antibody diluted in antibody dilution buffer (0.03% TWEEN and 1% dried milk (Marvel) in PBS):

- anti-human IL-18, mouse (1.0 mg/ml) (R&D systems) diluted 1:1000
- anti-phospho p38 MAPK, mouse (2.1mg/ml) (Sigma) diluted 1:10000
- anti-phospho ERK 1&2 MAPK, mouse (2.0mg/ml) (Sigma) diluted 1:10000
- anti-phospho JNK MAPK, rabbit (cell signalling) diluted 1:1000
- anti-phospho HSP27, rabbit (cell signalling) diluted 1:1000
- anti-IκB, mouse (cell signalling) diluted 1:1000
- anti-phospho tyrosine, mouse (cell signalling) diluted 1:2000
- anti-phospho EGFR, rabbit (R&D systems) diluted 1:2000
- anti-β–actin, mouse (2.0mg/ml) (sigma) diluted 1:10000

Following overnight incubation the membrane was washed three times for 5 minutes in PBS containing 0.1% Tween (Sigma). The membrane was then incubated for 1 hour in secondary antibody diluted in antibody dilution buffer (0.03% TWEEN and 1% dried milk (Marvel) in PBS):

- anti-mouse IgG HRP-conjugate (cell signalling) diluted 1:3000
- anti-rabbit IgG HRP-conjugate (cell signalling) diluted 1:2000

- anti-rabbit IgG HRP-conjugate (Invitrogen) diluted 1:3000
- anti-mouse IgG HRP-conjugate (Dako) diluted 1:1000

Following this, the membrane was washed 3 times for 5 minutes in PBS with 0.1% tween and rinsed in deionised water for 2 minutes. Antibody probed bands were visualised using the Sigma-Fast 3,3'-Diaminobenzidine tetrahydrochloride (DAB) and urea hydrogen peroxide tablets (Sigma) solubilised in ultrapure water. Membranes were agitated in this solution until the bands became visible (approximately 6 minutes). The membrane was then rinsed in sterile water and left to dry.

2.12 Inhibition experiments

HaCaT cells were plated out at $4x10^5$cells/ml in 6 well plates (2ml/well). Following 1.5 days in culture (or when reached 80% confluency) culture media was removed and the cells dosed with 2ml of the required concentration of inhibitor or culture media for 1 hour:

- SB203580 (p38 Inhibitor, Calbiochem) 1μM - 25μM
- BAY 11-7082 (NF-κB inhibitor, Calbiochem) 1μM - 25μM

Following 1 hour in culture with inhibitor, 30μM DNCB (in 0.15% DMSO) or 0.15% DMSO (as vehicle control) were added and cultured for an additional 4 hours. As positive controls, 20ng/ml TNFα (for NF-κB) or 20ng/ml IL-1α (for p38MAPK) were added for 4 hours or 30 minutes respectively. After incubation the supernatant was removed and frozen at -80^{o}C (for cytokine analysis) and the RNA extracted (see section on RNA extraction).

2.13 Detection of phosphorylated kinases

HaCaT cells were plated out at $4x10^5$cells/ml in 6 well plates (2ml/well). Following 2 days in culture (or when reached 80% confluency) culture media was removed and the cells dosed with 2ml of 20μM - 32.5μM DNCB, 200μM - 500μM SDS or vehicle control (0.2% DMSO) in culture media, LPS or IFNγ and incubated for 30 min, 1, 4,

8 or 24hrs. Following incubation, the supernatant was removed for cytokine analysis. The cells and reagents were kept on ice during lysis. Cells were washed in ice cold wash buffer (2ml) (Bio-Rad), then lysed in 0.7ml/well lysis solution containing 9.9ml cell lysis buffer (BioRad), 40µl factor 1, 20µl factor 2 and 40µl of 500mM PMSF (from frozen). Cells were scraped on ice in lysis buffer using a cell scraper, then agitated at 300rpm for 20mins at 4°C. Cell lysates were collected and centrifuged at 4500 x g for 20 mins at at 4°C. The supernatants were collected and the protein concentration determined using the Bio-Rad DC protein assay. A standard curve was created using BSA (2mg/ml) serially diluted in lysis buffer (described previously). Samples were also prepared neat and diluted 1:2. 5µl of standards or samples were aliquoted into a 96 well plate, to which 25µl of reagent A' (containing 20µl of reagent S to each ml of reagent A) was added. Following this, 200µl of reagent B were added into each well. After 15 minutes, absorbance was read at 750 nm and lysate protein concentration determined using the standard curve.

Phosphorylated signalling protein assay

The following proteins from the Bio-Plex phosphoproteins and total target assay (Bio-Rad) were analysed using the Luminex 200IS (Luminex):

Total protein (10):	**Phosphorylated protein (17):**
Akt	Akt
c-Jun	c-Jun
CREB	CREB
ERK1/2	ERK1/2
HSP27	HSP27
IκB	IκB
JNK	JNK
MEK-1	MEK-1
p38 MAPK	p38 MAPK
p90 RSK	p90RSK
	p70
	Histone H3

	Src
	STAT3 (Tyr 705)
	STAT6
	TrkA
	Tyk2

The following control lysates were used:

Lysate	**Phospho-specific targets**
EGF-treated HEK293	Akt (Ser473), ERK1(Thr202/Tyr204), ERK2 (Thr185/Tyr187), ERK1/2 (Thr202/Tyr204, Thr185/Tyr187), GSK-3α/β (Ser21/Ser9), MEK1 (Ser217/Ser221)
EGF-treated HeLa	EGFR (Tyr), HSP27 (Ser78), S6 ribosomal protein (Ser235/Ser236)
IFN-α-treated HeLa	STAT2 (Tyr689), STAT3 (Tyr705), STAT3 (Ser727)
IL-4-treated HeLa	STAT6 (Tyr641)
NGFβ-treated PC12	IRS-1 (Ser636/Ser639), p70 S6 kinase (Thr421/Ser424), p90RSK (Thr359/Ser363), TrkA(Tyr490)
TNF-α-treated HeLa	IκB-α (Ser32/Ser36), NF-κB p65 (Ser536)
UV-treated HEK293	ATF-2 (Thr71), c-Jun (Ser63), CREB (Ser133), JNK (Thr183/Tyr185), p38MAPK (Thr180/Tyr182), p53(Ser15)
Phosphotase-treated HeLa	Background control for all phosphoprotein assays
Untreated HeLa	Positive control for all total target assays except p53 and Bcr-Abl

Experimental and control lysates were thawed from –20ºC storage and an equal volume of assay buffer added to the experimental lysates. The 96-well filter plate was washed by adding 100µl wash buffer to each well. The buffer was then removed by vacuum filtration and the bottom of the plate blotted dry. Coupled beads (premixed) were prepared by vortexing and diluting 1:50 in wash buffer. 50µl of diluted beads were

added to each well and immediately vacuum filtered. The beads were then washed twice using 100µl wash buffer. The lysates were the vortexed and added (50µl each) to the specified well. The lysates were incubated with the beads overnight (approximately 18hrs) at room temperature in the dark on a microplate shaker at 300rpm. Following incubation, the liquid was removed by vacuum filtration and the plate washed 3 times with 100µl wash buffer. Detection antibodies were diluted 1:25 in detection antibody diluent and 25µl added to each well. These were then incubated for 30 minutes following which the plate was vacuum filtered and washed a further 3 times with 100µl wash buffer. Streptavidin-PE was diluted 1:100 in wash buffer and 50µl were added to each well. This was incubated for 10 minutes and then filtered through the plate. The plate was then rinsed 3 times in 100µl of re-suspension buffer. The beads were then re-suspended in 125µl of re-suspension buffer and analysed using the Luminex 200IS system.

2.14 Confocal microscopy NF-κB

NF-κB nuclear translocation was measured using quantitative image analysis (Noursadeghi et al, 2008). HaCaT cells were plated out onto sterile glass cover slips in 24 well plates at $4x10^5$cells/ml (1ml/well). Following 1 day in culture (or when reached 80% confluency) the culture media was removed and the cells dosed with 1ml of the required concentration of DNCB, SDS, LPS or vehicle control in culture media. Cells were incubated for 1 hour or 2 hours. Following incubation, culture media was aspirated and the cells were fixed in 3.7% wt/v paraformaldehyde in TBS for 15 minutes. Following this, cells were washed 3 times with TBS. The cells were then permeabilised with permeabilisation buffer 0.2% Triton-X100 in TBS for 10 minutes at room temperature and washed again 3 times in TBS. Cells were then incubated with blocking buffer (10% normal goat serum in TBS) for 30 minutes at room temperature. The blocking buffer was then removed and primary antibody Rabbit anti-NF-κB p65 (Santa Cruz sc-372) used at 1/50 in blocking buffer added and left overnight at 4°C. The following day, antibody was removed and the cells washed 3 times with TBS. Secondary antibody Goat anti-Rabbit AF-633 (Invitrogen A21072) used at 1/500 in blocking buffer was added for 1h at room temperature. Following 1 hour incubation, secondary antibody was removed and the cells washed 3 times with TBS. Cells were

then incubated with DAPI (2 μg/ml in TBS) for 5 minutes followed by 3 washes with TBS. Cover slips were then mounted in mounting solution (Vectashield hard set) and stored at 4°C in the dark until analysis by confocal microscopy.

2.15 Detection of Intra-cellular Reactive Oxygen Species (ROS)

HaCaT cells were plated in 96-well collagen-I coated microplates (BD BioCoat® Collagen-I Cellware) at a density of $8x10^4$cells/ml in 100μl per well and incubated overnight at 37ºC with 5% CO_2. Cells were then dosed with between 2.5μM and 40μM DNCB (or positive control between 1.8μM and 29μM Menadione) for 24 hours. After 24 hours, 50μl of pre-warmed Staining Solution (2.8μl of 1mg/ml Hoechst dye and 86.5μl of 1000μM chloromethyl-dihydrodichlorofluorescein diacetate (cm-H_2DCFDA) probe (Life Technologies) in 5.5ml of pre-warmed culture media) was added to each well and incubated for 30 minutes in the dark at room temperature. Following incubation, 100μl of pre-warmed Fixation Solution (1.6ml 37% Formaldehyde solution to 4.4ml PBS) was added. The plate was then incubated for 30 minutes in the dark at room temperature. Following incubation, the fixation solution was removed and the cells washed with 100μl of PBS. The PBS was then removed and 200μl PBS added and the plate sealed. The plate was analysed using the Cellomics Array Scan V using Target Activation BioApplication software.

2.16 Peripheral blood mononuclear cell - dendritic cells (PBMC-DC)

This experiment was conducted under a study approved by the joint University College London/University College London Hospitals National Health Service Trust Research Ethics Committee and written informed consent obtained from the blood donor.

Human blood (100ml) was diluted in HBSS (60ml), layered onto Lymphoprep (Axis-Shield) and centrifuged at 800 x g (without brake) for 20 minutes at room temperature. Peripheral blood mononuclear cells (PBMCs) were obtained from the interphase by pipetting, and washed 3 times in HBSS (Gibco). Monocytes ($CD14^+$ cells) were isolated from PBMCs by magnetic positive selection with CD14 micro-beads using the MACS™ separator according to manufactures instructions (Miltenyi Biotec). The resultant monocytes were maintained at $1x10^6$ cells/ml in RPMI-1640 medium

containing 100ng/ml Granulocyte Macrophage-Colony Stimulating Factor (GM-CSF) and 50ng/ml Interleukin-4 (IL-4) (both gifts from Schering-Plough research institute, Kenilworth NJ) at 37^{o}C in 5% CO_2. Following 2 days in culture, the cells were re-fed by replacing half the media with fresh media containing GM-CSF and IL-4. After 4 days in culture, the PBMC-immature dendritic cells were exposed to either; 0.15% DMSO (vehicle control), 100ng/ml LPS (*E.coli* O111:B4, Invitrogen), or filtered conditioned media (from HaCaTs previously exposed to various concentrations of DNCB, SDS or DMSO). The conditioned media were diluted 1:2 in RPMI without cytokines and the cells cultured for 20hrs.

2.17 Flow Cytometry

Following incubation, the supernatants were removed by centrifugation and the PBMC-DCs were blocked for 1hr at 4^{o}C in blocking buffer (HBSS containing 10% goat serum and 0.05% sodium azide). Cells were then stained for 30 minutes at 4^{o}C in 50µl blocking buffer containing:

- CD83 (FITC) IgG1 (HB15e, BD Biosciences) diluted 1:20
- CD86 (PE) IgG1 (2331 FUN-1, BD Biosciences) diluted 1:50
- DC-SIGN (APC) IgG2b (DCN46, BD Biosciences) diluted 1:50
- or matched isotope controls (IgG1 and IgG2b) (BD Biosciences) diluted 1:50

Following incubation with antibodies, the cells were washed twice with HBSS and re-suspended in 100µl of HBSS containing 1% BSA and 0.05% sodium azide. Propidium iodide (2µl) was added and the cells analysed using a FACSCalibur (BD Biosciences). The flow cytometery data were analysed using FlowJo 8.0 (Tree Star).

2.18 Statistical analysis

One way analysis of variance (ANOVA) with Dunnett's multiple correction post hoc test was used to analyse cytokine release data. One way analysis of variance (ANOVA) with Tukey's multiple correction post hoc test was used for the analysis of real time PCR data. All statistical analysis (with the exception of the microarray data) was done using GraphPad Prism v 5.0 software.

3 KERATINOCYTE MODEL SELECTION AND PRODUCTION OF INFLAMMATORY/IMMUNOMODULATORY CYTOKINES

3.1 Introduction

Cytokines and chemokines are small protein mediators critical for the orchestration of immune responses through their influence on cellular communication and movement. Keratinocytes play a role in the initiation and elicitation of cutaneous immune responses by expressing many cytokines, such as IL-1α (Luger et al, 1981; Ansel et al, 1983; Phillips et al, 1995), IL-1β (Kupper et al, 1986; Zepter et al, 1997), IL-1RA (Haskill et al, 1991; Phillips et al, 1995; Bigler et al, 1992), IL-6 (Kupper et al, 1989; Khan et al, 1993; Ishimaru et al, 2013), IL-7 (Ariizumi et al, 1995), IL-8 (Larsen et al, 1989; Li et al, 1996; Barker et al, 1990; Andrew et al, 1999), TNF-α (Kock et al, 1990), IL-10 (Rivas and Ullrich, 1992), IL-12 (Aragane et al, 1994; Yawalkar et al, 1996), IL-15 (Blauvelt et al, 1996), IL-18 (Stoll et al, 1997; Naik et al, 1999), IL-23 (Larsen 2009) and IL-33 (Meephansan et al, 2012; Taniguchi et al, 2013), IFNα/β (Fujisawa et al, 1997), chemokines, such as MCP-1 (Barker et al, 1990, 1991) and RANTES (Li et al, 1996) and growth factors such as TGFα (Coffey et al, 1987), TGFβ (Bascom et al, 1989), VEGF (Trompezinski, 2004) and GM-CSF (Pastore et al, 1997; Kupper et al, 1988).

In response to pathogens, the cytokine signature produced by keratinocytes is complex, varying between different pathogens, species and strata of the epidermis. Following viral infection, keratinocytes have been shown to produce interferons α, β and γ as well as pro-inflammatory cytokines IL-1β, IL-18, TNFα and GM-CSF (Surasombatpattana *et al*, 2011; Reinholz et al, 2013; Shao et al, 2010). Keratinocyte cytokine profiles have been shown to differ between different species of fungus (Shiraki et al, 2006), and strains of Malassezia (Donnarumma et al, 2014), indicating that cytokine responses can vary significantly between different pathogens. The differentiation state of keratinocytes also appears to influence their capacity for cytokine production, as bacterial stimuli have been shown to induce antimicrobial peptides and pro-

inflammatory cytokines, the levels of which differed between the stratum basale and stratum granulosum in human skin (Percoco et al, 2013).

Cutaneous immune responses to chemical allergens have also stimulated detectable levels of cytokines and chemokines in the epidermis: IL-1α (Enk and Katz 1992a/c., Haas et al, 1992), IL-1β (Enk and Katz 1992a/c), IL-6 (Cumberbatch et al, 1996; Holliday et al, 1996; Flint et al, 1998), IL-10 (Enk and Katz 1992b; Nickoloff et al, 1994), IL-12 (Muller et al, 1994), IL-18 (Stoll et al 1997), IFNγ (Enk and Katz 1992a), TNFα (Piguet et al,1991., Haas et al, 1992; Flint 1998; Enk and Katz 1992a/c), IP-10 (Enk and Katz 1992a/c), MIP-2 (Enk and Katz 1992a/c) and GM-CSF (Enk and Katz 1992a/c). However, in many studies it was not possible to identify which skin cell type is responsible for the production of each cytokine. In response to chemical allergens, keratinocytes specifically have been shown to transcribe or release IL-1α (Corsini 1998, Curtis et al, 2007; Coquette et al, 2003; Newby et al, 2000), IL-1β (Zepter, 1997), IL-8 (Newby et al, 2000, Coquette et al, 2003; Mohamadzadeh, 1994), IL-18 (Stoll et al 1997; Naik et al, 1999), IL-23 (Larsen et al, 2009) and TNFα (Newby et al, 2000).

Numerous cytokines are involved in orchestrating cutaneous immune responses. IL-1β, IL-18 and TNFα have been shown to be critical for Langerhans cell (LC) migration in contact hypersensitivity (Cumberbatch et al, 1995, 1997, 2001; Shornick et al, 2001), while IL-10 inhibits this process (Wang et al, 1999). The combined effect of these signals causes down-regulation of E-cadherin and dissociation of LC from neighbouring keratinocytes (Jakob and Udey, 1998). Following detachment, migration out of the epidermis is driven by a CXCL12 chemokine gradient originating from dermal fibroblasts and signalling via CXCR4 on LC (Ouwehand et al, 2008). CCR7 is up-regulated upon LC/DC maturation (Saeki et al, 1999; Forster et al, 1999), allowing movement towards CCL19 and CCL21 (Ohl et al, 2004; Saeki et al, 1999; Gunn et al, 1999; Haessler et al, 2011), which originate from the lymphatics (Gunn et al, 1998). During migration, LCs mature to an activated phenotype characterised by a transient increase in antigen processing, and up-regulation of MHCII and co-stimulatory molecules, for efficient antigen presentation. Co-stimulatory/adhesion molecules, e.g. CD83, CD86 and CD54, have been shown to be up-regulated by cytokines, for example IL-1α (Matjeka et al, 2012).

In the lymph node, activated DCs release cytokines that influence T cell differentiation to determine the type of response, e.g. IL-12 released from DCs has been demonstrated to stimulate naïve $CD4^+$ T cells to differentiate into Th1 cells (Hsieh et al, 1993; Manetti et al, 1993), while TGFβ, IL-6, IL-21 skewed differentiation to Th17 (Veldhoen et al, 2006; Zhou et al, 2007; Korn et al, 2007). Recently, a skin-homing Th22 cell population has been identified (Trifari et al, 2009; Duhen et al, 2009), which were generated from interactions with DCs expressing IL-6 and TNFα (Duhen et al, 2009). The T cell polarisation cytokines released by a DC population may be determined by the cytokine environment in which the DCs encountered antigen, as well as by the nature of the antigen.

Elicitation of CHS to chemical allergens has been shown to be driven by $CD4^+$ Th1, $CD8^+$ type 1 cytotoxic T cells (Wang et al, 2000), $CD4^+$ Th17 (Larsen et al, 2009; Pennino et al, 2010), and NK cells (Carbone et al, 2010), as well as infiltration of macrophages and neutrophils (Goebeler 2001). T cells home to the skin in response to CCL27 (CCR10), CCL17 and CCL22 (CCR4) (Reiss et al, 2001; Hudak et al, 2002, Morales et al, 1999; Homey et al, 2002). Other immune cells migrate in response to chemokines produced by keratinocytes such as MCP-1, RANTES (Goebeler 2001), CXCL10 (IP-10), CXCL9 (MIG) and CXCL11 (ITAC) (Klunker et al, 2003). In human skin biopsies from patch test positive sites (during elicitation) to various allergens, IFNγ, IL4, IL-17 and IL-23 all showed increased expression (Zhao et al, 2009).

In vitro systems have some advantages over *ex vivo* skin tissue for investigating cytokine expression by keratinocytes. They are based on a single cell type, compared to the mixed cell population in skin. It is also technically more feasible to measure cytokines quantitatively *in vitro*, because in skin they are difficult to extract and short-lived due to receptor binding. 3D reconstructed human epidermis (RHE) cultures have been developed to provide stratified keratinocyte models that are similar to epidermis *in vivo* (Ponec et al, 2003; Poumay et al, 2004). These systems have been used to measure irritancy in standard toxicological testing by MTT and IL-1α (Spielmann et al, 2007), and in assay development for biomarkers to assess skin sensitisation potential, such as IL-1α (dos Santos et al, 2011), IL-1α and IL-8 (Coquette et al, 2003; Poumay et

al, 2004; Spiekstra et al, 2009), IL-8, CCL20 and CCL27 (Spiekstra et al, 2005), and a panel of genes (McKim et al, 2012).

In this chapter we will investigate cytokine responses to DNCB *in vitro* and their association with death, and characterise the use of 3D skin models for investigating the response.

The aims of this chapter are to: characterise keratinocyte-derived inflammatory mediator production in response to chemical allergen; understand the kinetics of DNCB induced inflammatory mediator release, its relationship with cytotoxicity and the kinetics of mediator gene expression; and determine the optimum *in vitro* model to study the response of keratinocytes to chemical allergen

3.2 Results

Morphology of the EpiDerm™ and EpiDermFT™ models

EpiDerm™ and EpiDermFT™ models were fixed and stained using haematoxylin and eosin (H&E). The EpiDerm models (Figure 3-1a and 3-1b) comprise stratified, differentiated keratinocytes forming clear stratum: basale; spinosum; granulosum and corneum. Keratohyalin granules are also evident in the stratum granulosum. The stratification of the keratinocytes in the EpiDerm model is well defined and represents an accurate model of keratinocyte differentiation in human skin.

The EpiDermFT models (Figure 3-2) were also characterised by H&E staining. These models had a very deep dermal fibroblast layer, which appeared viable except at the base of the dermis (Figure 3-2a). The epidermal keratinocytes in these full thickness models did not retain the viable, differentiated strata (Figure 3-2b) seen in the keratinocyte only model (Figure 3-1c). This model has a much denser stratum corneum than expected, potentially over-developed due to a lack of viable suprabasal keratinocytes. The dermal epidermal junction (DEJ) is also clearly split. The models exposed to 750μM DNCB for 24 hours also had split DEJ (Figure 3-2c) and a dense stratum corneum. In response to DNCB the basal keratinocytes appear pyknotic indicating these cells are undergoing apoptosis (Figure 3-2d).

A comparative study of cytokine, chemokine and growth factor production by HaCaT, EpiDerm and EpiDermFT models

HaCaT cells, EpiDerm and EpiDermFT models were exposed to DNCB or SDS. 1μg/ml LPS combined with 1μg/ml IFNγ, a strong pro-inflammatory stimulus, was also tested to provide a positive control for cytokine release. Cells were exposed for 1, 4 (data not shown) or 24 hours and the release of 31 different cytokines was measured by multiplex ELISA. Figure 3-3 summarises the cytokines and chemokines that could be detected in the supernatant from these models, both constitutively and in response to DNCB or SDS or in response to LPS and IFNγ.

a

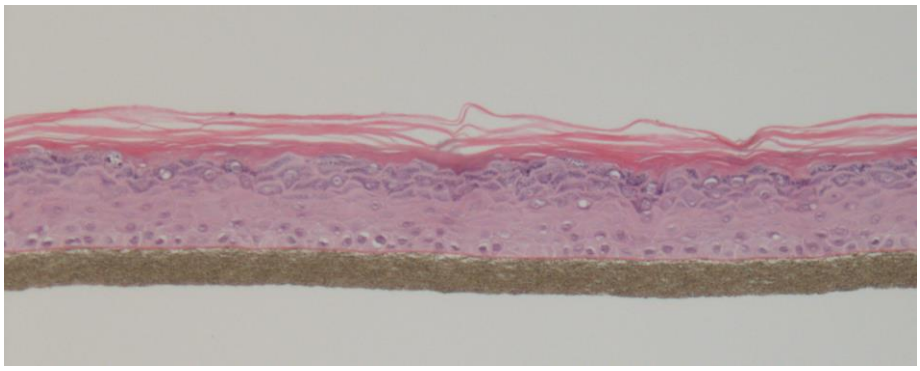

b

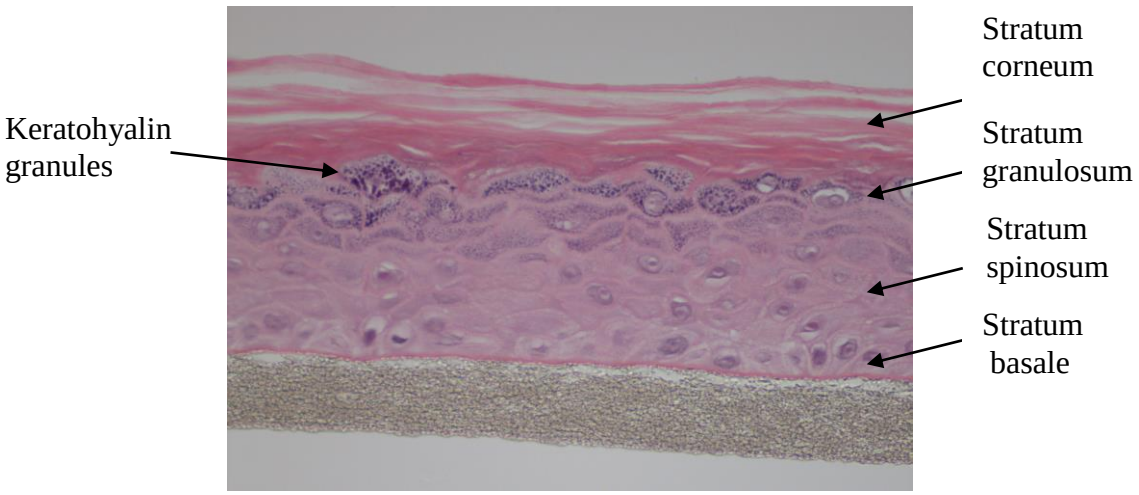

Figure 3-1 Morphology of the EpiDerm models

The EpiDerm models were stained with H&E and overall structure examined at x10 magnification (a) and x40 magnification (b). Stratum corneum, stratum granulosum (containing keratohyalin granules), stratum spinosum and stratum basale were all evident.

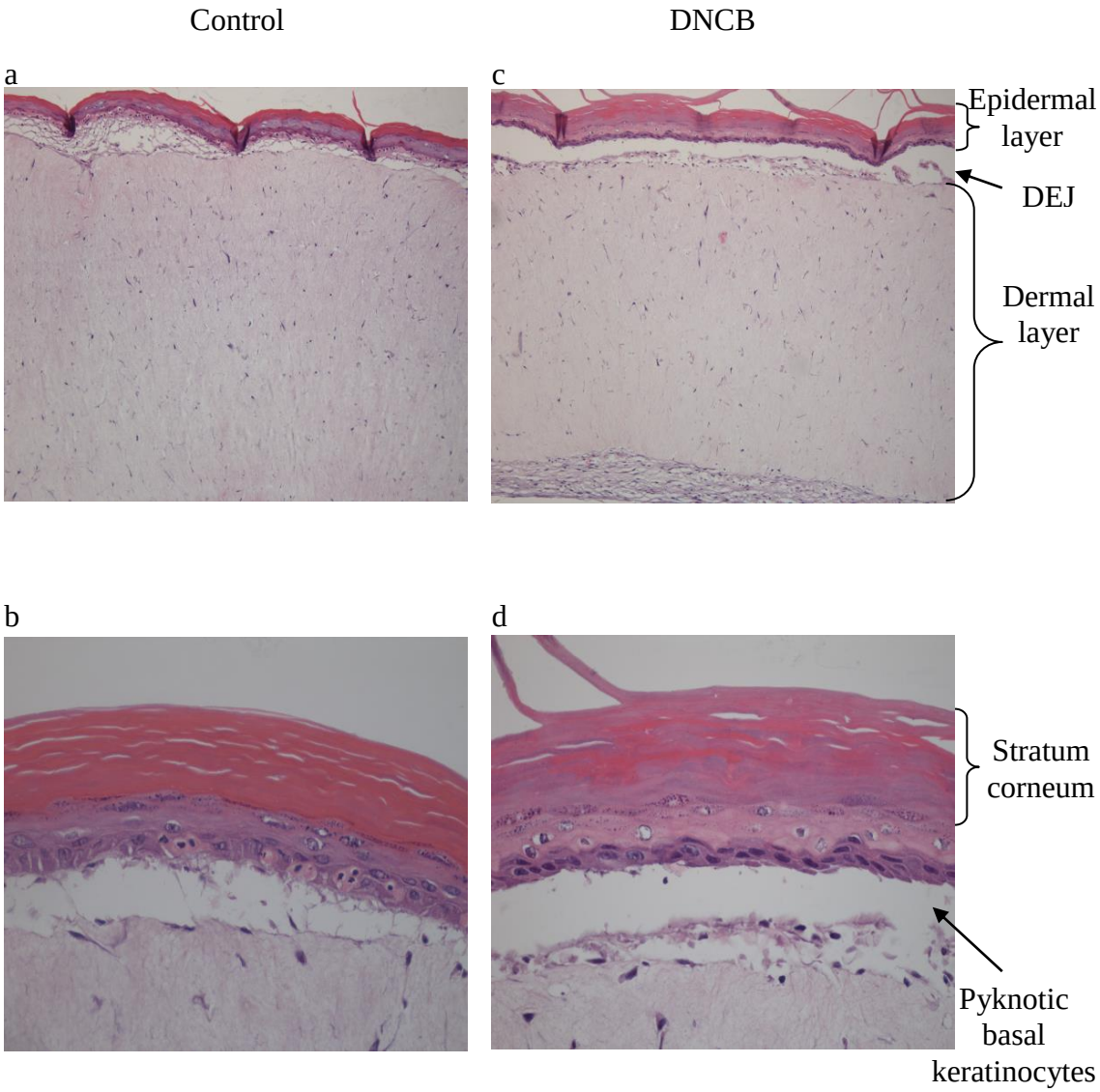

Figure 3-2 Morphology of EpiDermFT models

The morphology of the EpiDermFT model was assessed by H&E staining. Histological examination of untreated control models: x10 magnification (a) x40 magnification (b) and models exposed to 750μM DNCB for 24 hours: x10 magnification (c) x40 magnification (d) show them to be compromised. Both control and treated models have a deep dermal layer, a split dermal-epidermal junction (DEJ) and dense stratum corneum. The DNCB treated models have pyknotic basal keratinocytes.

It is possible that some of the cytokines that weren't identified were present but under the level of detection of this technology (e.g. TNFα). There is some overlap in the cytokines produced in the HaCaT cells and EpiDerm models; however a much larger number of cytokines, chemokines and growth factors were detected in the EpiDermFT models. Many of the cytokines detected were also present at much higher concentrations in the media from the EpiDermFT models compared with the EpiDerm or HaCaT models. IL-1α could only be detected in media from HaCaT cells following total cell death (e.g. when they were snap frozen – data not shown).

Each of the models was able to respond to LPS and IFNγ by inducing production and release of a number of cytokines. In the HaCaT cells (Figure 3-4a), FGF-basic, GCSF, HGF, IFNα, IL-10, IL-1ra, IL-2, IL-2R, IL-6, IL-7, IP-10, MCP-1, MIG, MIP-1α, RANTES and VEGF were all induced in response LPS and IFNγ compared with controls. The levels of IL-8 however decreased slightly in response to LPS and IFNγ.

In the EpiDerm (keratinocyte only) models, 13 cytokines were induced following exposure to LPS and IFNγ (Figure 3-4b). These were FGF-basic, GCSF, IL-17, IL-1ra, IL-2R, IL-7, IL-8, IP-10, MCP-1, MIG, RANTES, VEGF and IL-1α. In the EpiDermFT (keratinocyte and fibroblast) model, Eotaxin, FGF-basic, IFNα, IL-12, IL-17, IL-1ra IL-2R, IL-7, MIG, MIP-1α, RANTES, VEGF, IL-1α, IP-10, HGF, MCP-1, and GCSF were all induced following exposure to LPS and IFNγ (Figure 3-4c). GM-CSF, IL-6 and IL-8 were also detectable in the culture media, however the levels appeared unchanged in response to LPS and IFNγ (compared with vehicle controls).

Figures 3-5 and 3-6 show overviews of the cytokine responses of HaCaT cells, EpiDerm and EpiDermFT models in response to DNCB and SDS respectively. The cytokine data for HaCaTs and EpiDerm is explored in more detail below.

Figure 3-7 shows how 3 cytokines IL-1ra, IL-6 and IL-8 are expressed in response to DNCB, SDS, LPS and LPS and IFNγ. DNCB stimulates greater expression of all three cytokines compared to the other stimuli.

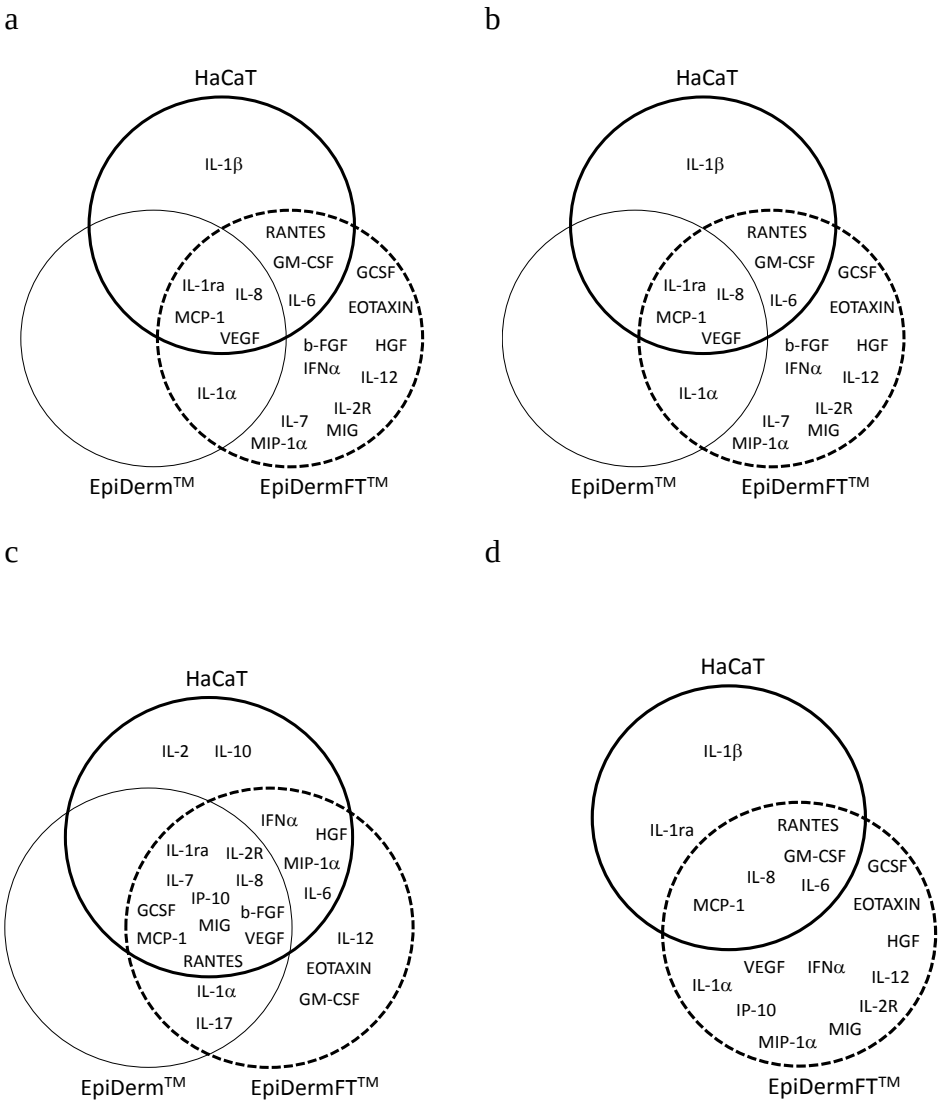

Figure 3-3 Cytokine production in response to stimulation with DNCB, SDS, LPS and IFNγ

Culture supernatant was collected from HaCaT, EpiDerm and EpiDermFT models following 24 hour culture with DMSO vehicle control (a), all concentrations of DNCB (b), 1μg/ml LPS and IFNγ (c) or all concentrations of SDS (d). The supernatants were assayed for release of 31 different mediators by ELISA. The Venn diagram indicates mediators that could be detected in each model (EpiDerm cultures were not tested with SDS).

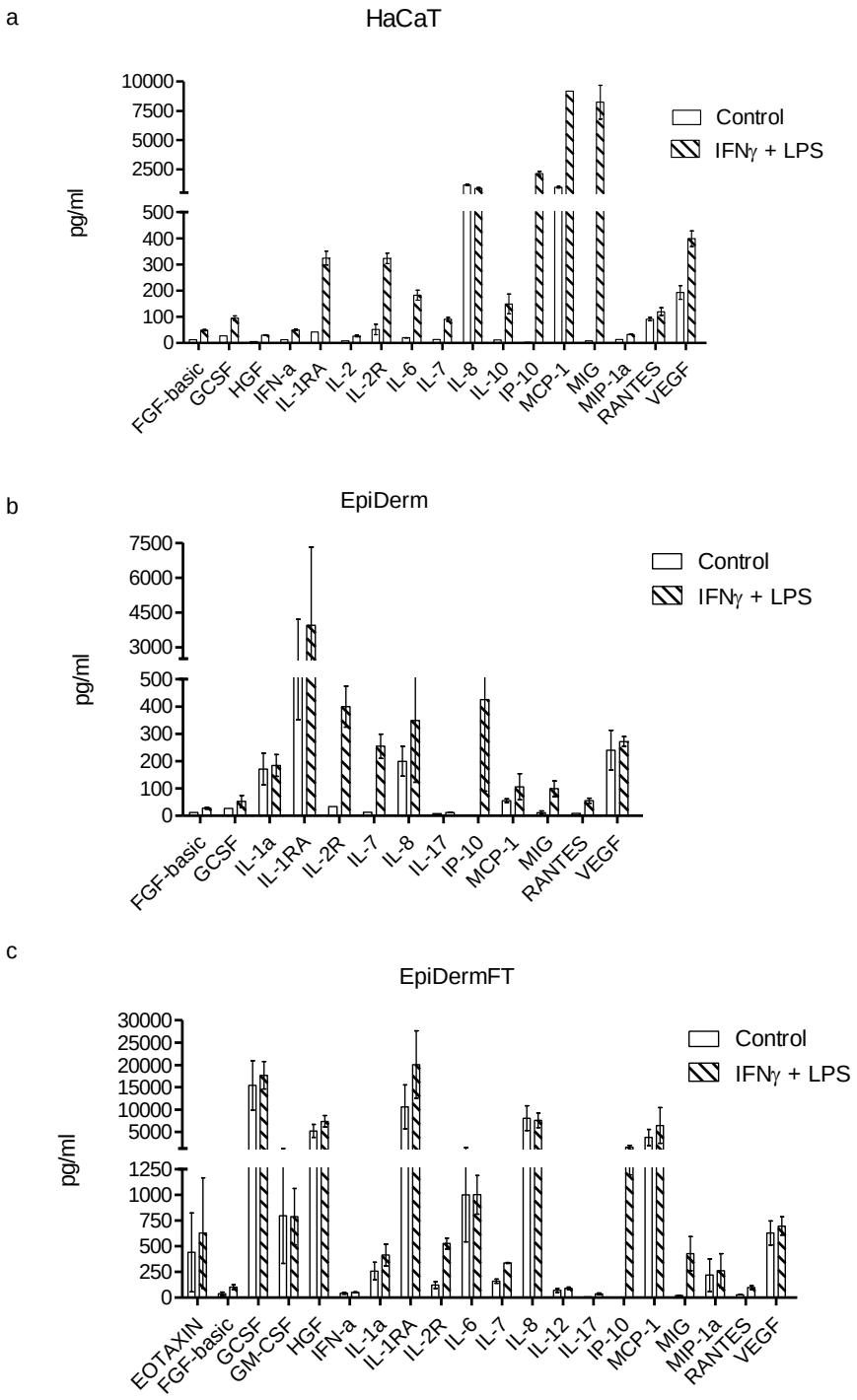

Figure 3-4 Cytokine production in response to stimulation with LPS and IFNγ

HaCaT cells (a), EpiDerm (b) and EpiDermFT models (c) were exposed to culture media control (empty bars) or 1μg/ml LPS and IFNγ (filled) for 24 hours. Supernatants were assayed for release of soluble mediators into the media by ELISA. The graph shows mean and SD for three experiments.

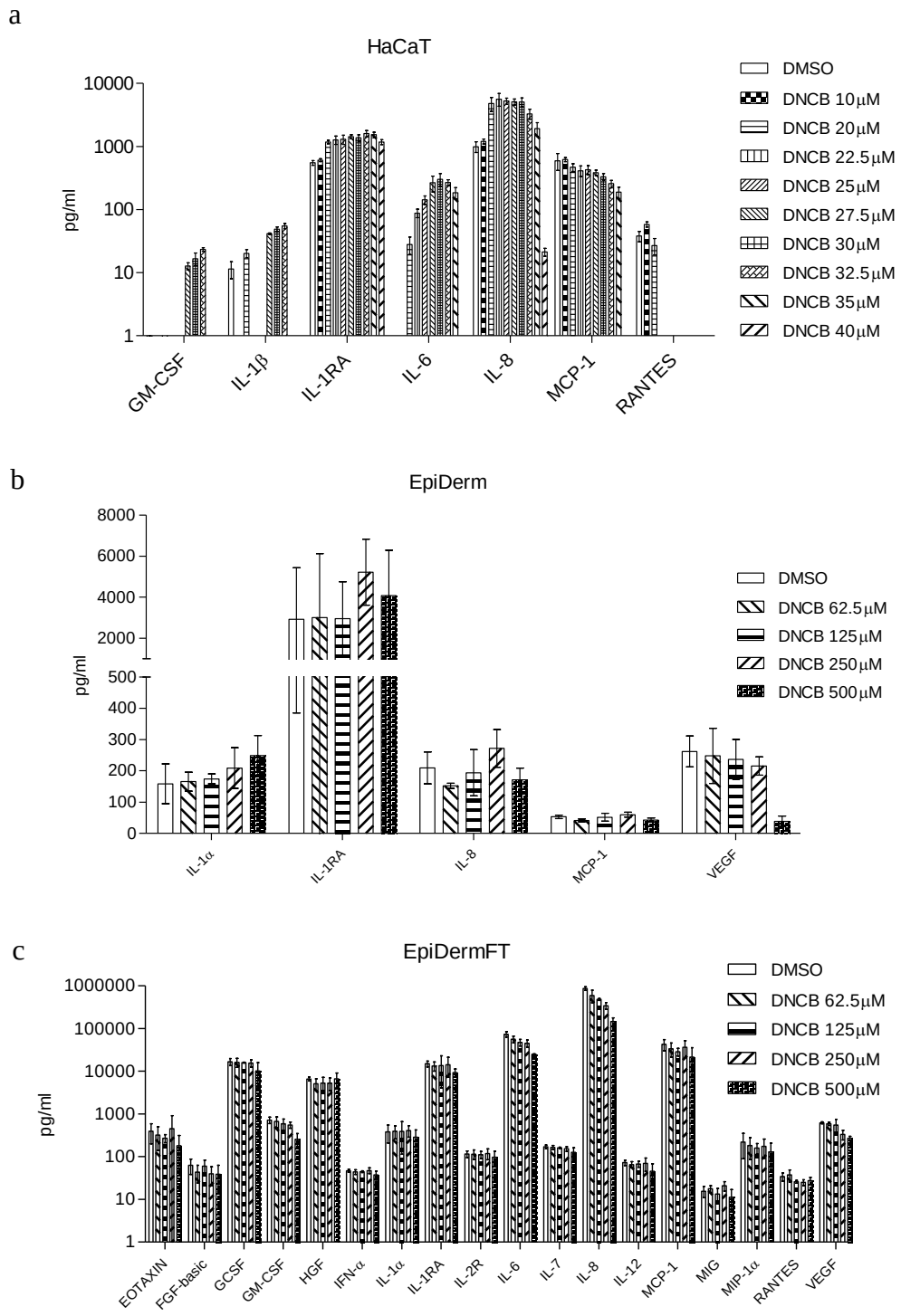

Figure 3-5 Cytokine production in response to stimulation with DNCB

HaCaT cells (a), EpiDerm (b) and EpiDermFT models (c) were exposed to 0.2% DMSO (empty bars) or DNCB for 24 hours. Supernatants were assayed for release of soluble mediators into the media by ELISA. The graph shows mean and SD for three experiments.

a

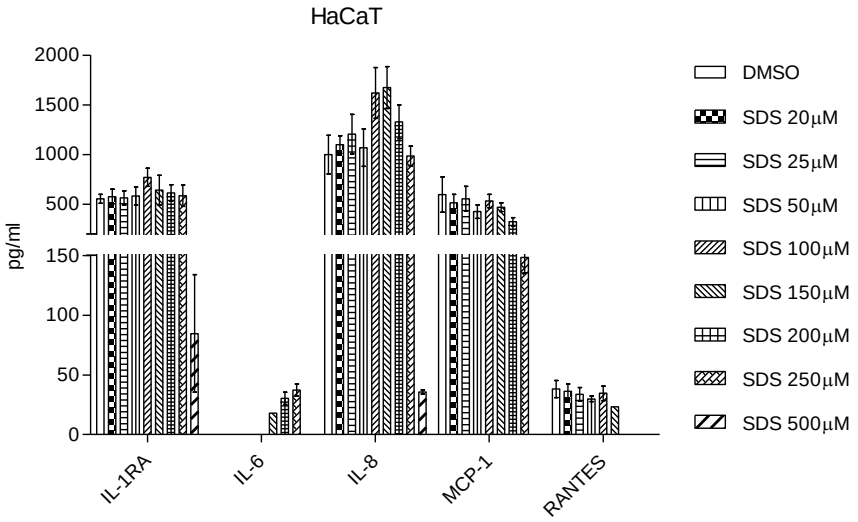

b

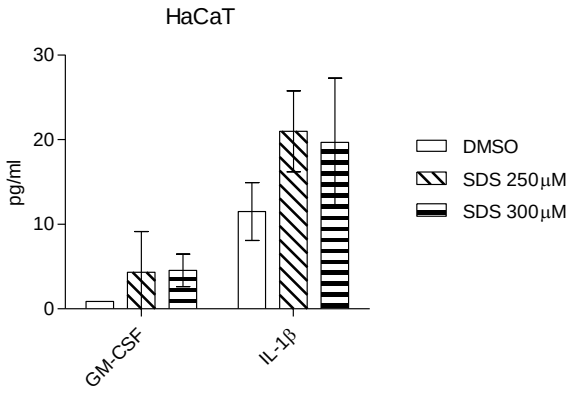

c

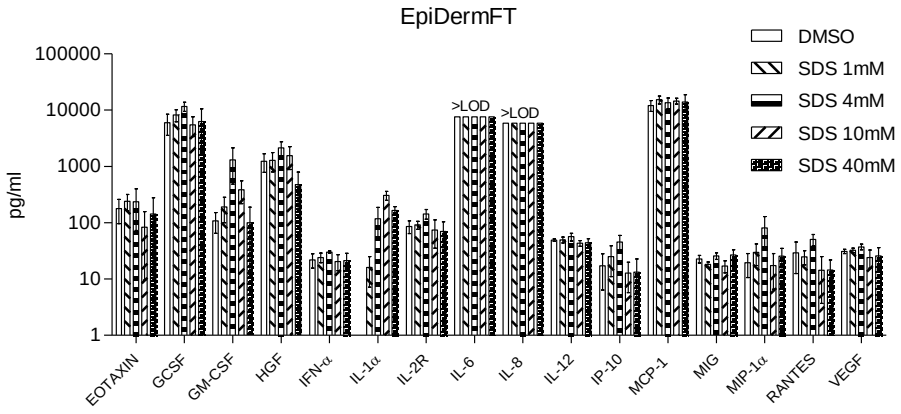

Figure 3-6 Cytokine production in response to stimulation with SDS

HaCaT cells (a and b) and EpiDermFT models (c) were exposed to 0.2% DMSO (empty bars) or SDS for 24 hours. Supernatants were assayed for release of soluble mediators into the media by ELISA. The graph shows mean and SD for three experiments. IL-6 and IL-8 levels from EpiDermFT (c) were greater than the limit of detection (LOD).

a

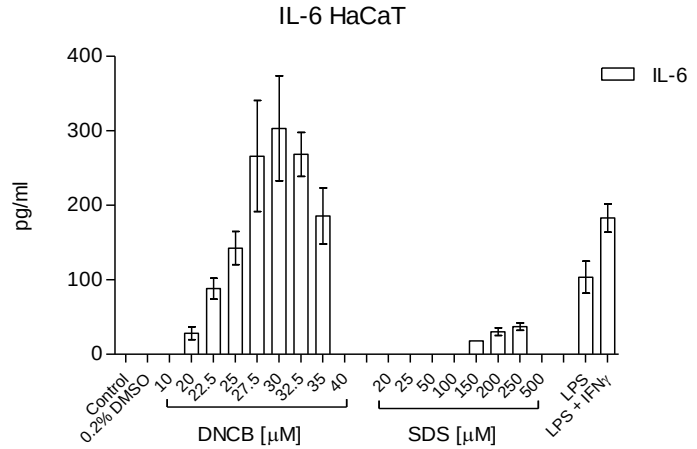

b

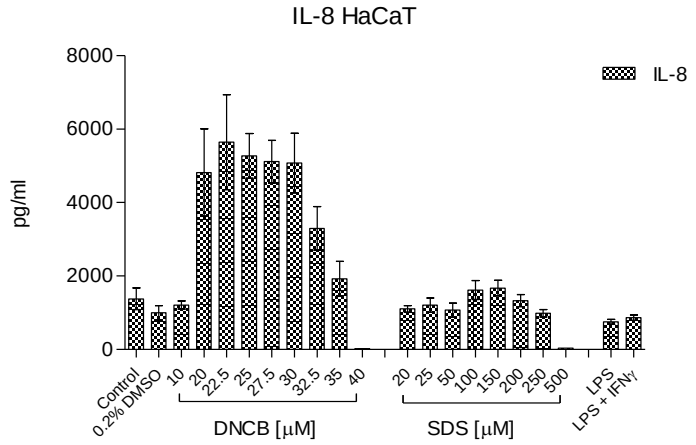

c

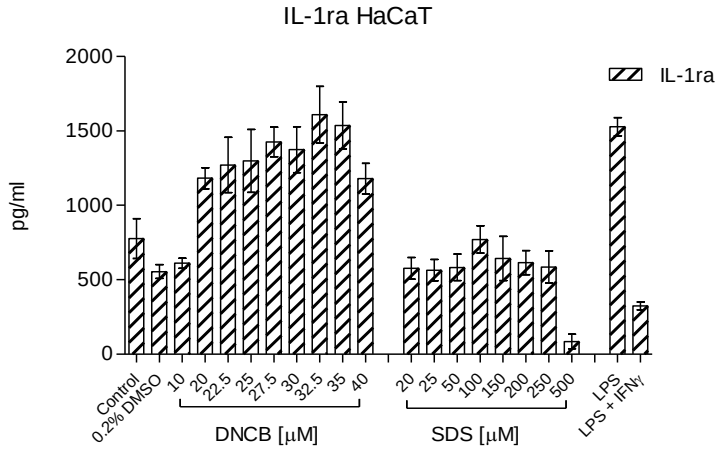

Figure 3-7 Comparison of cytokine production from different stimuli

HaCaT cells were exposed to meida (control), 0.2% DMSO, DNCB, SDS, 1μg/ml LPS or 1μg/ml LPS and IFNγ for 24 hours. Supernatants were assayed for release of IL-6, IL-8 or IL-1ra into the media by ELISA. The graph shows mean and SD for three experiments.

HaCaT viability in response to DNCB and SDS

The ability of HaCaT cells to reduce MTT was used as an assessment of viability in response to DNCB and SDS. HaCaTs were exposed to a range of concentrations of DNCB or SDS for 24 hours before addition of MTT (Figure 3-8a). The concentration at which 50% cell death occurred was approximately 30μM DNCB and between 250 and 500μM SDS.

EpiDerm viability in response to DNCB and SDS

EpiDerm models from 3 different keratinocyte donors were topically exposed to SDS, DNCB or 0.2% DMSO (vehicle control) for 1, 4 (data not shown due to no change in cell viability) or 24 hours. Model viability was measured by LDH leakage (for DNCB) in order for the tissue to be utilised in histological examination, or MTT (for SDS) (Figure 3-8b). Following 24 hour exposure to 500μM DNCB, the EpiDerm models were 60% viable compared with vehicle control treated models. The concentration at which 50% cell death occurred was approximately 3.5mM for SDS. The error represented on this graph was intra-donor, as the viability of each chemical exposed model was compared to its donor matched control. Variation was substantially larger between donors.

EpiDermFT viability in response to DNCB and SDS

After exposure of the EpiDermFT models to the same DNCB concentrations as those used for the EpiDerm model, no cell death could be detected (data not shown). Following extensive optimisation of the level of DMSO required for adequate model penetration, it was speculated that a lack of cell death seen in the EpiDermFT models was due to reduction of MTT by the fibroblasts in the dermal layer. This was confirmed by splitting the dermal and epidermal layers after exposure to chemicals but before MTT assay. In response to DNCB in 0.4% DMSO one donor (Figure 3-8c) showed a cytotoxic response to DNCB. The dose response for cytotoxicity begins at a lower concentration in the epidermal layer compared with the dermal layer, perhaps due to chemical penetration through the layers. At low concentrations of chemical there is an increase in MTT activity compared with vehicle controls. However, two subsequent donors did not show any signs of cytotoxicity in the epidermis or dermis (data not

shown). EpiDermFT models were also exposed, topically, to 0.04-40mM SDS or 0.2% DMSO (vehicle control) for 24 hours. The ability of the models to reduce MTT was measured as an assessment of viability (Figure 3-8c). For SDS one donor is shown which is representative of all three donors. The concentration at which 50% cell death occurs following exposure to SDS was at a concentration between 4 and 10mM.

EpiDerm models show minimal changes in cytokine release in response to DNCB

The release of cytokines into the culture supernatant by EpiDerm models topically exposed to DNCB or 0.2% DMSO (vehicle control) for 1, 4 or 24 hours was measured. Only 5 out of 31 soluble mediators could be detected from EpiDerm media; these were IL-1α, IL-1ra, IL-8, MCP-1 and VEGF. All five were detected even in the absence of chemical. Following exposure to DNCB for 1 or 4 hours the concentrations of these factors in the supernatant remained unchanged (data not shown). Following 24 hour exposure to DNCB (Figure 3-9), there was a tendency for IL-1α and IL-1RA concentrations to increase as concentration of chemical increased, and viability decreased. In contrast, the concentrations of MCP-1 and IL-8 increased slightly at 250μM, but decreased below background levels at 500μM. The concentrations of VEGF fell sharply and significantly ($p<0.01$) following exposure to 500μM DNCB. The inter-donor variability for these cultures was very high, and hence it was difficult to demonstrate statistical significance for these changes.

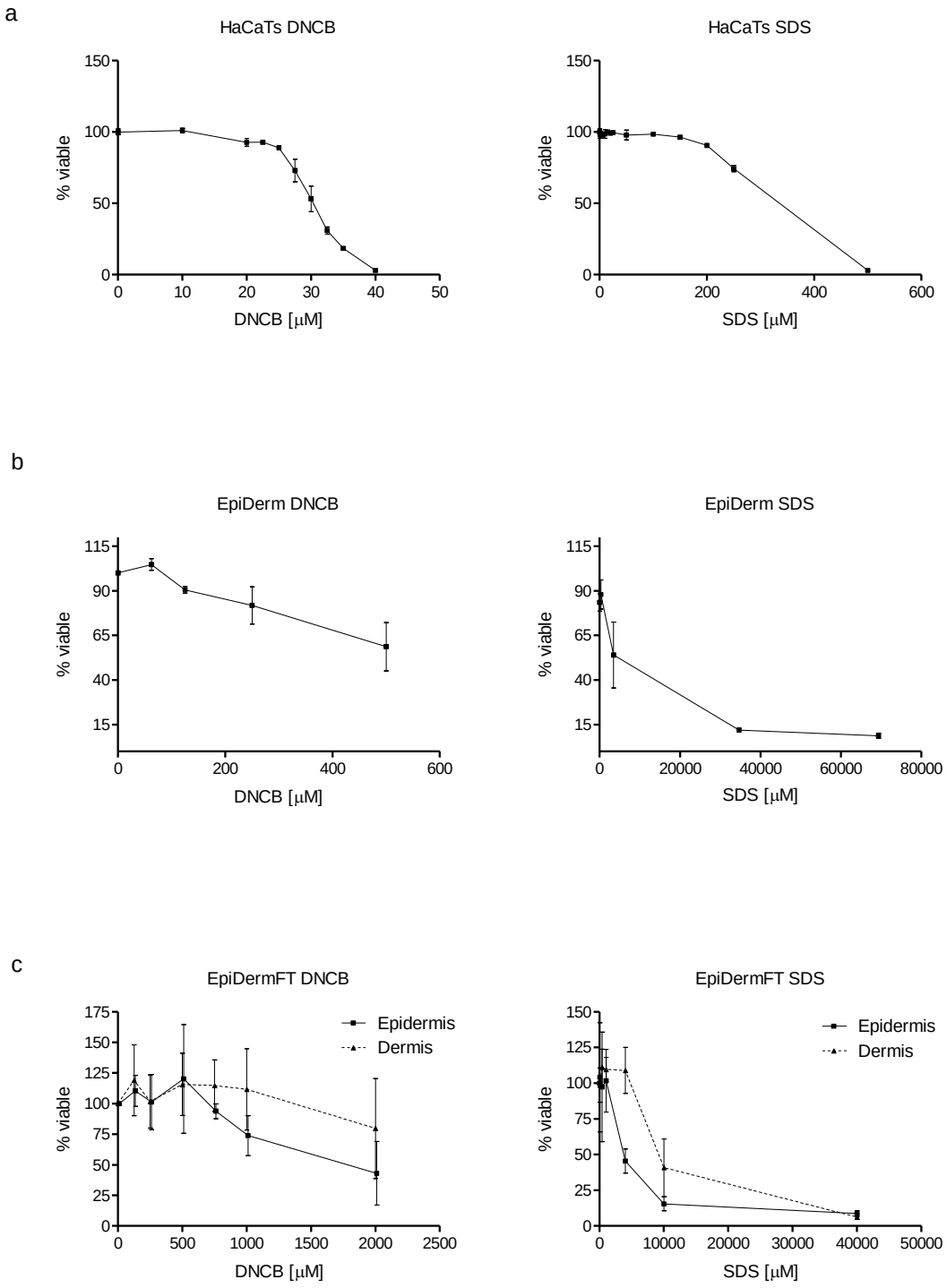

Figure 3-8 Cytotoxicity in response to stimulation with DNCB or SDS

HaCaT cells (a), EpiDerm (b) and EpiDermFT models (c) were cultured in the presence of a range of concentrations of DNCB or SDS for 24 hours (0μM = 0.2% DMSO vehicle control). The ability of the cells to reduce MTT or release LDH (EpiDerm with DNCB) was measured as an assessment of viability. The graph shows mean and SD for three experiments. The EpiDerm SDS graph (b) was generated from data provided by Samantha Fletcher.

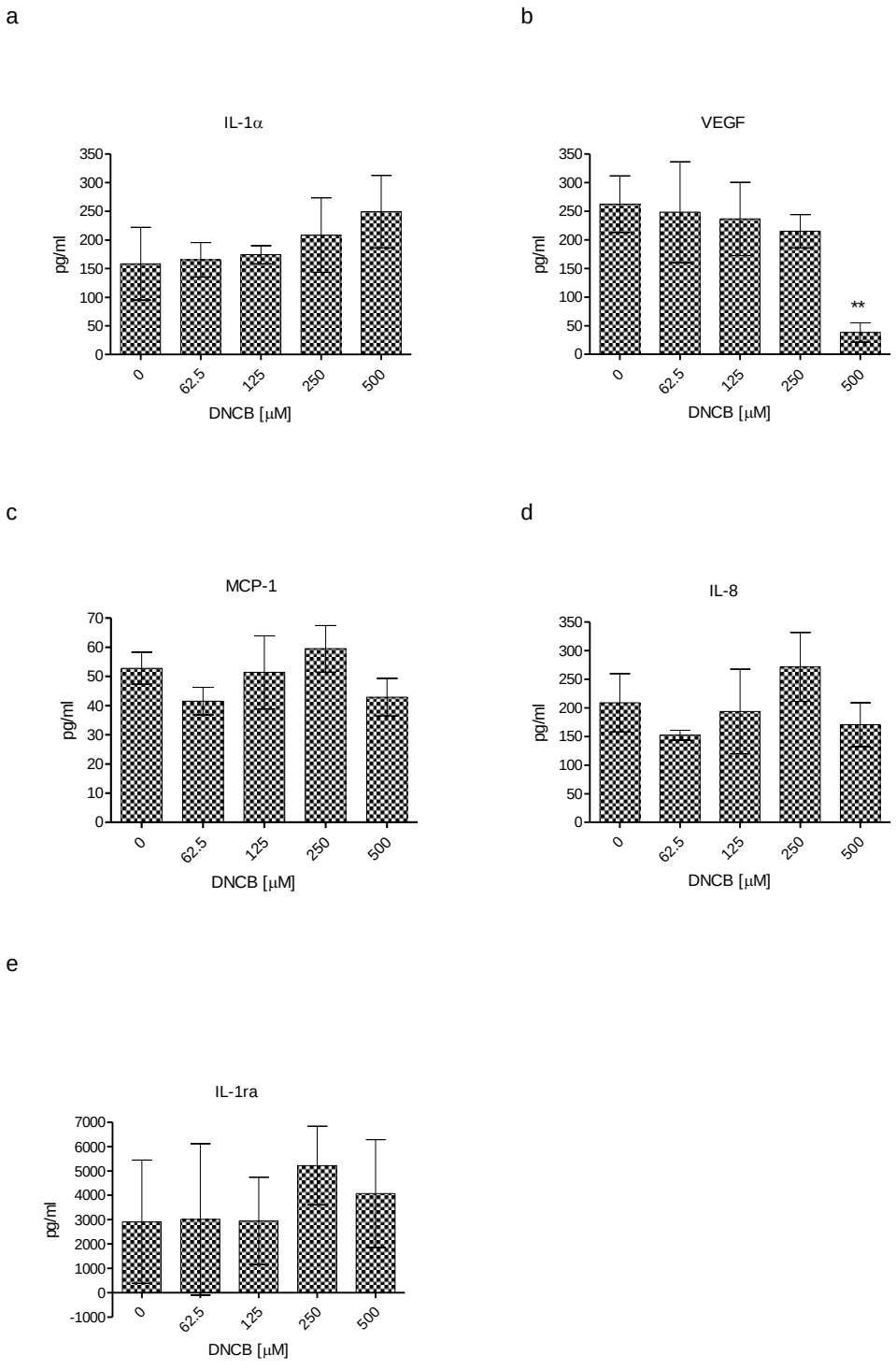

Figure 3-9 Cytokine release from EpiDerm following exposure to DNCB

EpiDerm models were cultured in the presence of a range of concentrations of DNCB (0μM= 0.2% DMSO vehicle control) for 24 hours. Supernatants were assayed for release of soluble mediators by ELISA. The graph shows mean and SD for three experiments (3 different donors). Statistical analysis: One way ANOVA with post-test Dunnett's multiple comparison test *$p<0.05$, **$p<0.01$, ***$p<0.001$.

Cytokine release is amplified in HaCaT cells following exposure to DNCB compared with SDS

Due to the high donor variability in cytokine production seen in the EpiDerm models (and the histological analysis of the EpiDermFT models), the release of cytokine into the culture supernatant by HaCaT cells, exposed to a range of DNCB and SDS concentrations for 24 hours, was measured.

Out of the 31 cytokines and chemokines measured, only 7 could be consistently detected in the HaCaT media in response to vehicle control, DNCB or SDS. These included three cytokines seen in the EpiDerm model (IL-1ra, IL-8 and MCP-1) and additionally IL-1β, IL-6, GM-CSF and RANTES. VEGF was detected inconsistently and varied with different batches of antibodies (Invitrogen). IL-1α could only be detected following total cell death in response to snap freezing (data not shown).

At high (cytotoxic) concentrations of either DNCB or SDS, there was a strong inhibition of release of all mediators except IL-1ra, which was increased in the presence of DNCB (Figures 3-10, 3-11 and 3-12). In contrast, intermediate doses of DNCB, but not SDS stimulated significant increase in the release of IL-1ra, IL-6, IL-8 and RANTES (Figures 3-11 and 3-12). Interestingly the dose response profiles for each mediator were slightly different.

In summary HaCaT cells responded to subtoxic concentrations of the sensitiser DNCB by the release of the inflammatory mediators IL-6, IL-8 and RANTES, and by the release of the anti-inflammatory mediator IL-1ra.

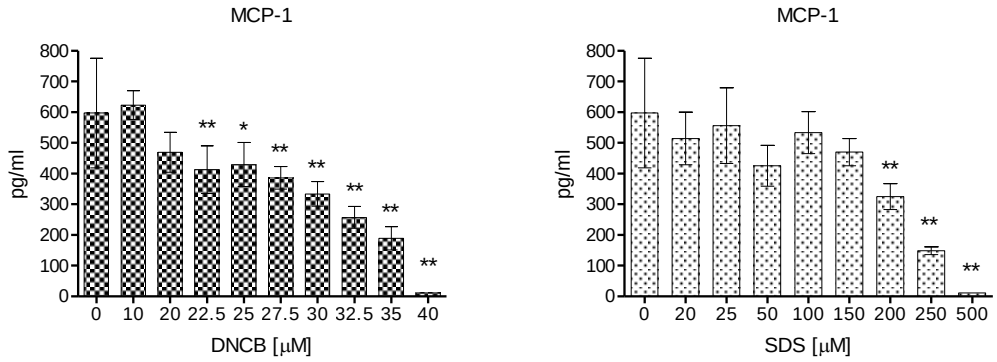

Figure 3-10 MCP-1 production in response to DNCB and SDS

HaCaT cells were cultured in the presence of a range of concentrations of DNCB (filled) or SDS (empty) for 24 hours (0μM = 0.2% DMSO vehicle control). Supernatants were assayed for release of MCP-1 by ELISA. The graph shows mean and SD for three experiments. Statistical analysis: One way ANOVA with post-test Dunnett's multiple comparison test *$p<0.05$, **$p<0.01$, ***$p<0.001$.

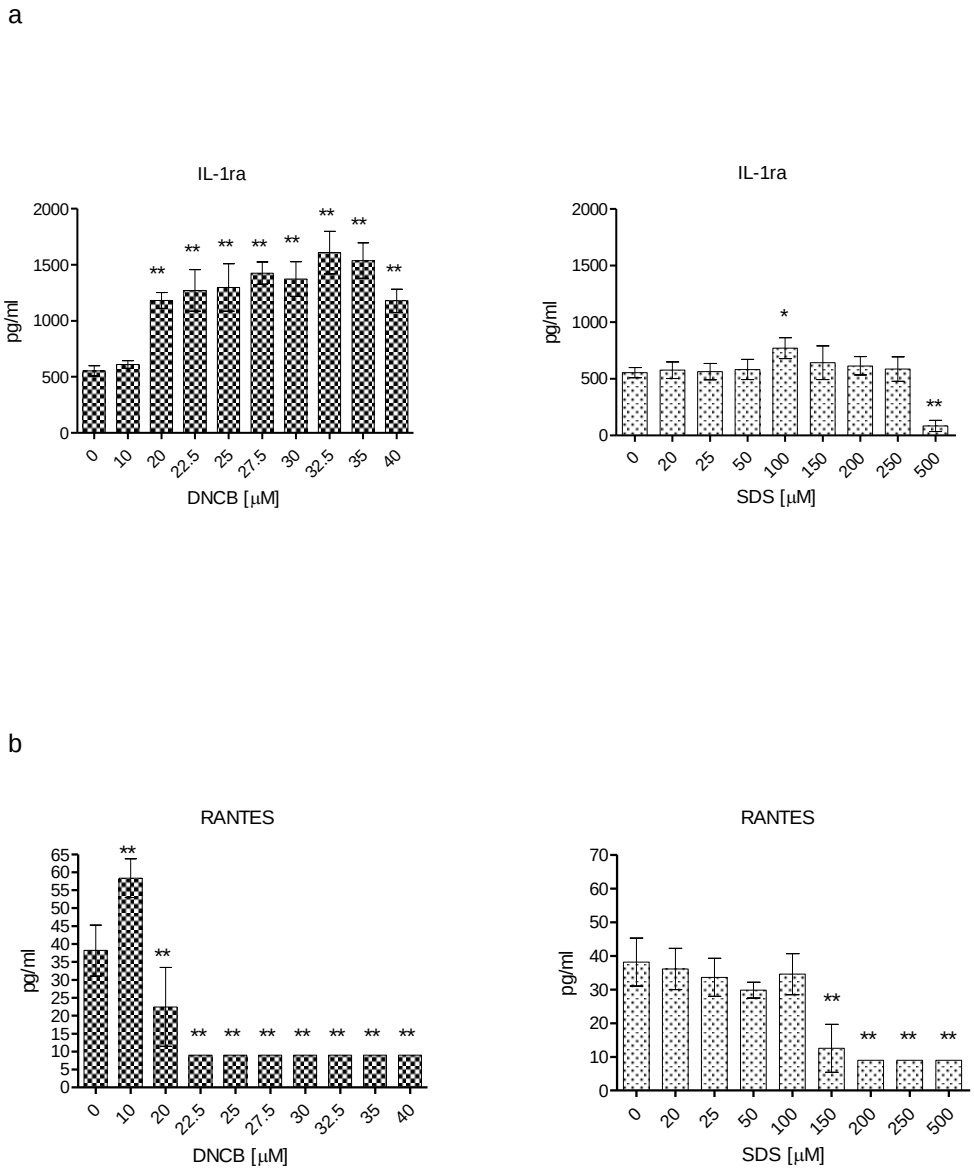

Figure 3-11 IL-1ra and RANTES production in response to DNCB and SDS

HaCaT cells were cultured in the presence of a range of concentrations of DNCB (filled) or SDS (empty) for 24 hours (0μM = 0.2% DMSO vehicle control). Supernatants were assayed for release of IL-1ra (a) and RANTES (b) by ELISA. The graph shows mean and SD for three experiments. Statistical analysis: One way ANOVA with post-test Dunnett's multiple comparison test *p<0.05, **p<0.01, ***p<0.001.

a

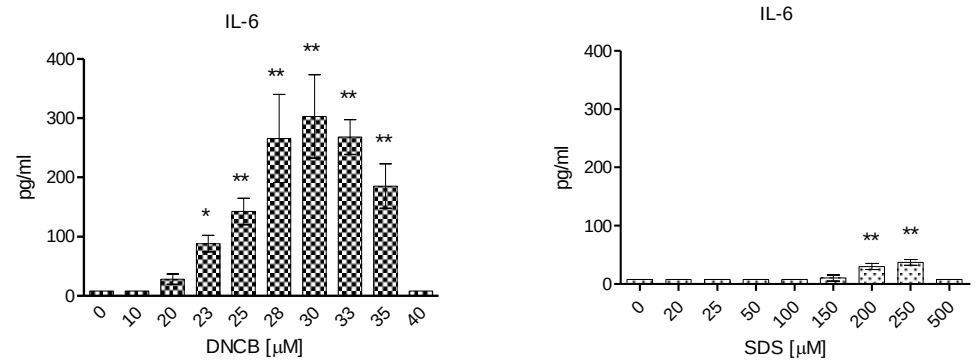

b

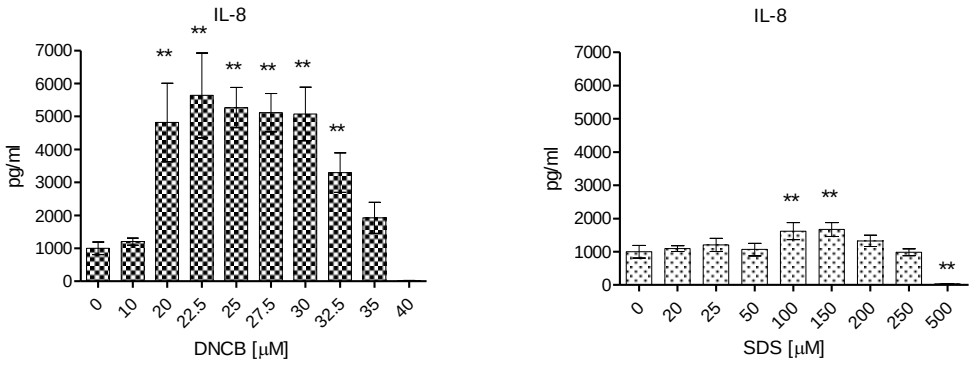

Figure 3-12 IL-6 and IL-8 production in response to DNCB and SDS

HaCaT cells were cultured in the presence of a range of concentrations of DNCB (filled) or SDS (empty) for 24 hours (0μM = 0.2% DMSO vehicle control). Supernatants were assayed for release of IL-6 (a) and IL-8 (b) by ELISA. The graph shows mean and SD for three experiments. Statistical analysis: One way ANOVA with post-test Dunnett's multiple comparison test *$p<0.05$, **$p<0.01$, ***$p<0.001$

IL-1β, IL-6, IL-8 and GM-CSF release from HaCaT cells in response to DNCB is dependent on time

The release of IL-1β, IL-6, IL-8 and GM-CSF by HaCaT cells in response to DNCB was investigated further by looking at earlier time points (1, 4 and 24 hours). IL-1β, although present at very low levels, was detected in response to both DNCB and SDS after 24 hour exposure. The amount of IL-1β in response to DNCB was double that seen in response to SDS (Figure 3-13a). IL-1β was not detected at earlier time points in response to DNCB. GM-CSF was also detected at very low levels in response to both DNCB and SDS after 24 hour exposure. The response to DNCB was greater and dose-dependent (Figure 3-13b).

IL-6 could not be detected at 1 hour post exposure to DNCB or SDS (Figure 3-14a). There was a small increase at 4 hours with both SDS and DNCB. Following 24 hour DNCB exposure, the level of IL-6 was increased further, whereas there was not a significant increase in IL-6 in response to SDS (24 hours).

IL-8 was also only detected at minimal levels at 1 hour post exposure to DNCB or SDS (Figure 3-14b). In response to SDS there was a small increase at both 4 hours and 24 hours. After 4 hour exposure to DNCB IL-8 levels were low, however, after 24 hour DNCB exposure, IL-8 was markedly increased in response to DNCB compared to vehicle control.

a

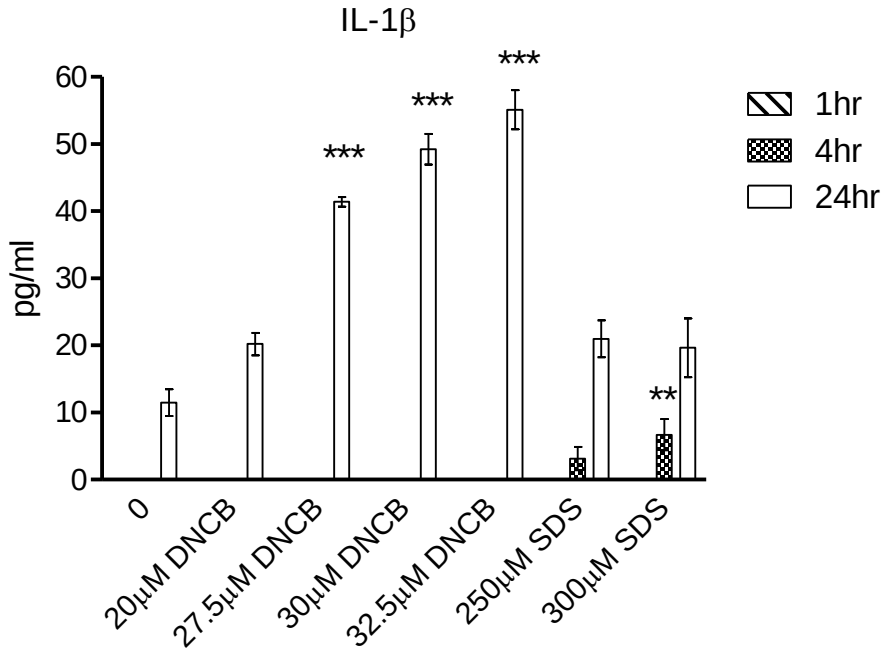

b

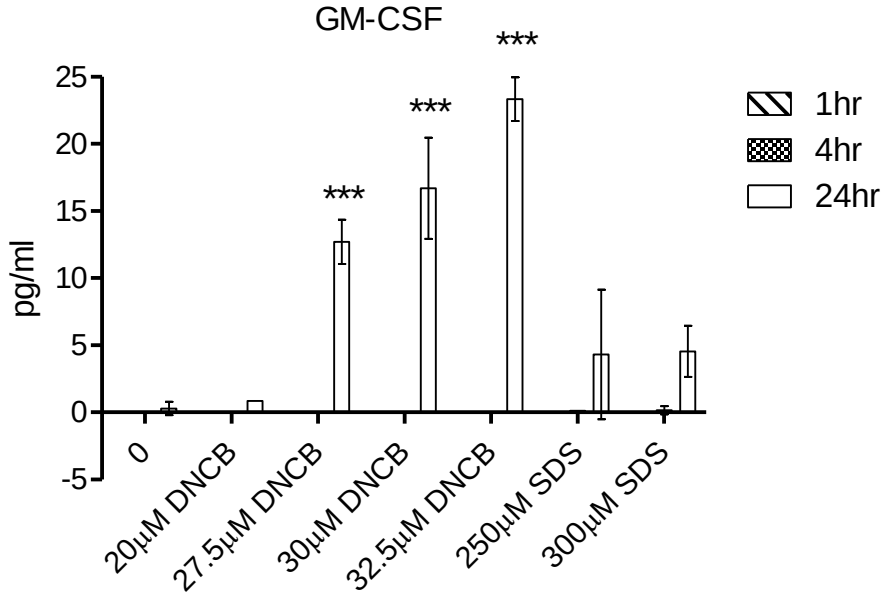

Figure 3-13 IL-1β and GM-CSF production in response to DNCB over time

HaCaT cells were cultured in the presence of a range of concentrations of DNCB or SDS for 1 hour, 4 hours or 24 hours (0μM = 0.2% DMSO vehicle control). Supernatants were assayed for release of IL-1β (a) and GM-CSF (b) by ELISA. The graph shows mean and SD for three experiments. Statistical analysis: ANOVA with post-hoc Dunnett's modification *$p<0.05$, **$p<0.01$, ***$p<0.001$.

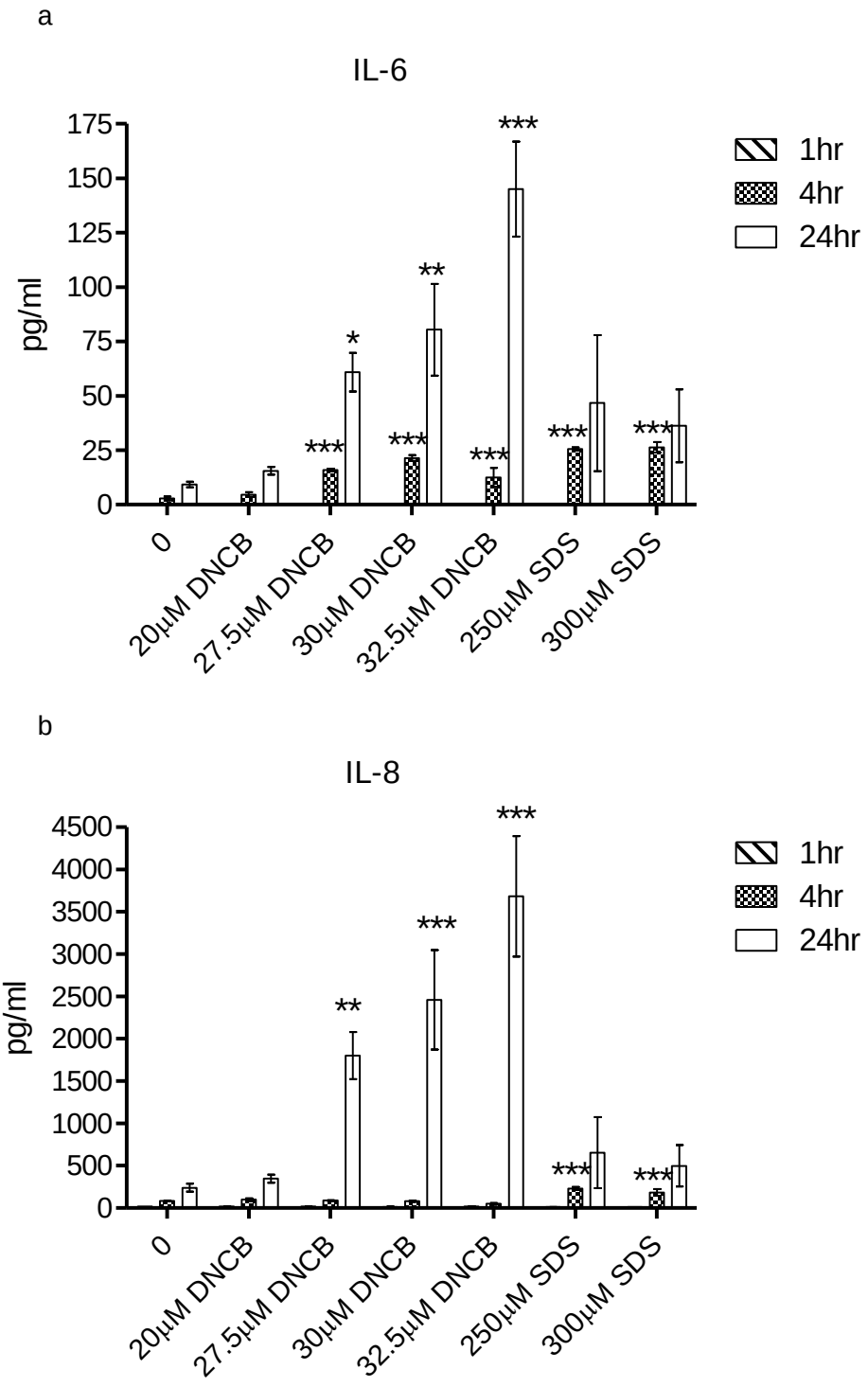

Figure 3-14 IL-6 and IL-8 production in response to DNCB over time

HaCaT cells were cultured in the presence of a range of concentrations of DNCB or SDS for 1 hour, 4 hours or 24 hours (0μM = 0.2% DMSO vehicle control). Supernatants were assayed for release of IL-6 (a) and IL-8 (b) by ELISA. The graph shows mean and SD for three experiments. Statistical analysis: ANOVA with post-hoc Dunnett's modification *p<0.05, **p<0.01, ***p<0.001.

IL-1β, IL-6 and IL-8 are actively transcribed following exposure to DNCB

In order to understand the kinetics of the IL-1β, IL-6 and IL-8 protein release, these cytokines were analysed at the transcript (mRNA) level. HaCaT cells were exposed to 20-32μM DNCB or 0.2% DMSO for 1 hour (Figure 3-15) or 4 hours (Figure 3-16) or 24 hours (Figure 3-17). Total mRNA was extracted and analysed by qRT-PCR for expression of IL-1β, IL-6 and IL-8 mRNA. Following 1 hour exposure to DNCB, IL-1β, IL-6 and IL-8 appear to be actively down-regulated (or of lower expression) compared with vehicle control. IL-1β expression was 1.4 fold lower, IL-6 was found to be 4 fold lower and IL-8 was 2.2 fold down-regulated compared to vehicle control (Figure 3-15). Following 4 hour exposure, there were dose-dependent increases in expression of IL-1β, IL-6 and IL-8 (Figure 3-16). The maximum fold changes compared with vehicle control expression were 1.9 for IL-1β, 22.4 for IL-6 and 7.8 for IL-8. Following 24 hour exposure to DNCB (Figure 3-17), the IL-1β and IL-8 transcripts remained upregulated in a dose-dependent manner compared to vehicle control, with maximum fold increases of 11.5 for IL-1β and 5.7 for IL-8. However, IL-6 was 1.9 fold down-regulated (or of lower expression) compared to vehicle control following 24 hour exposure to DNCB.

The relationship between gene expression and protein release for IL-1β, IL-6 and IL-8

For IL-1β, a 1.9 fold increase in transcription of the gene occured at 4 hours and increased to 11.5 at 24 hours, whereas the protein was only detected at 24 hours, and then at only modest amounts (maximum 55pg/ml). Transcription occurred more quickly for IL-8, with increases in transcription of 7.8 fold at 4 hours and 5.7 fold following 24 hours. This corresponded to a peak IL-8 protein level of 3500pg/ml at 24 hours. The IL-6 transcript was up-regulated 22.4 fold at 4 hours and appeared to be switched off at 24 hours. This correlated with a peak IL-6 protein level at 24 hours of 145pg/ml.

The EpiDerm models treated with DNCB for 24 hours were also assessed for the expression of IL-1β, IL-6 and IL-8 transcripts (Figure 3-18). IL-6 could not be detected, and due to large variation in the data, no statistically significant changes were observed.

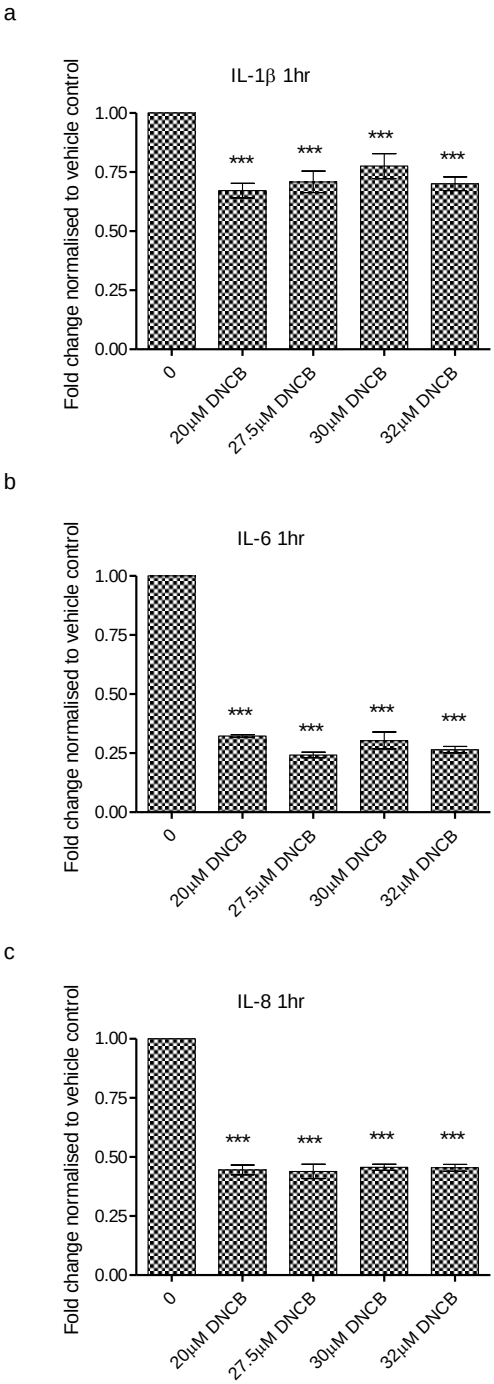

Figure 3-15 Transcription of IL-1β, IL-6 and IL-8 in response to DNCB

HaCaT cells were cultured in the presence of a range of concentrations of DNCB for 1 hour (0μM = 0.2% DMSO vehicle control). Total mRNA was extracted and analysed for expression of IL-1β (a), IL-6 (b) and IL-8 (c) transcripts by qRT-PCR. Data is shown as fold change (relative to vehicle control), normalised to HPRT expression. The graph shows mean and SD for three experiments. Statistical analysis: ANOVA with post-hoc Tukey's modification *$p<0.05$, **$p<0.01$, ***$p<0.001$.

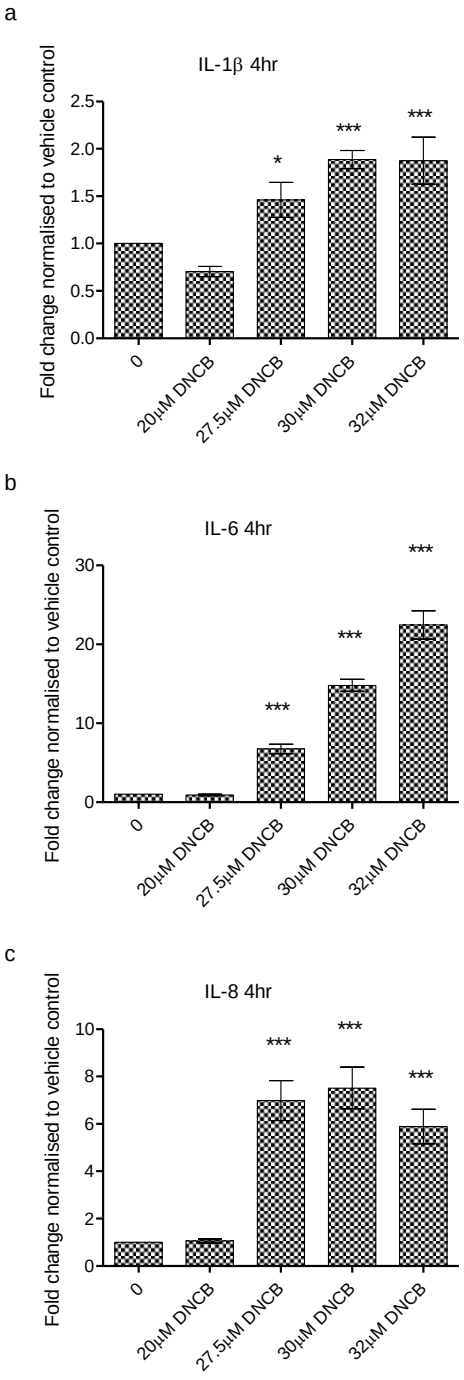

Figure 3-16 Transcription of IL-1β, IL-6 and IL-8 in response to DNCB

HaCaT cells were cultured in the presence of a range of concentrations of DNCB for 4 hours (0μM = 0.2% DMSO vehicle control). Total mRNA was extracted and analysed for expression of IL-1β (a), IL-6 (b) and IL-8 (c) transcripts by qRT-PCR. Data is shown as fold change (relative to vehicle control), normalised to HPRT expression. The graph shows mean and SD for three experiments. Statistical analysis: ANOVA with post-hoc Tukey's modification *$p<0.05$, **$p<0.01$, ***$p<0.001$.

a

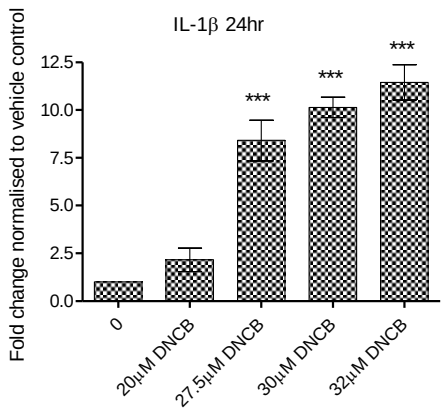

b

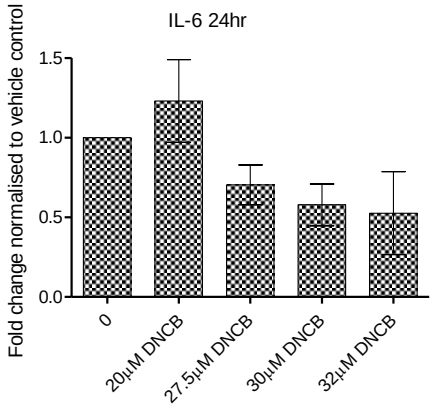

c

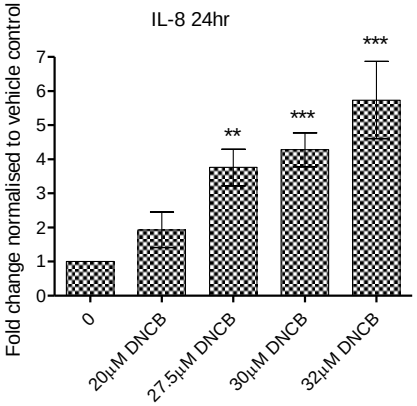

Figure 3-17 Transcription of IL-1β, IL-6 and IL-8 in response to DNCB

HaCaT cells were cultured in the presence of a range of concentrations of DNCB for 24 hours (0μM = 0.2% DMSO vehicle control). Total mRNA was extracted and analysed for expression of IL-1β (a), IL-6 (b) and IL-8 (c) transcripts by qRT-PCR. Data is shown as fold change (relative to vehicle control), normalised to HPRT expression. The graph shows mean and SD for three experiments. Statistical analysis: ANOVA with post-hoc Tukey's modification *$p<0.05$, **$p<0.01$, ***$p<0.001$.

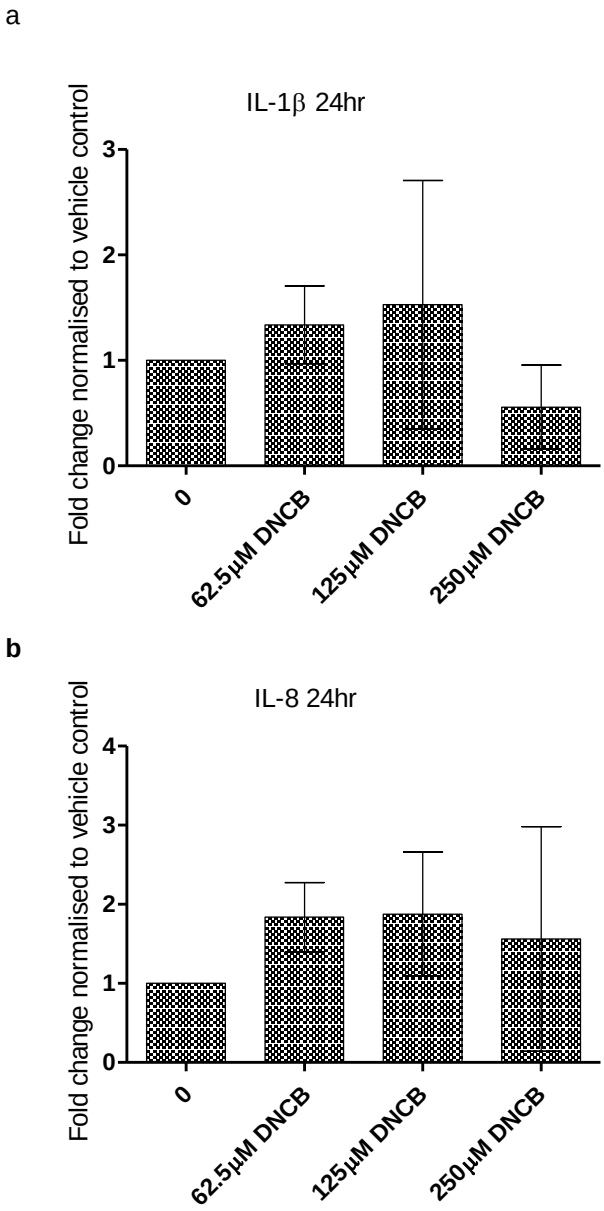

Figure 3-18 Transcription of IL-1β and IL-8 in response to DNCB

EpiDerm models were cultured in the presence of a range of concentrations of DNCB for 24 hours (0µM = 0.2% DMSO vehicle control). Total mRNA was extracted and analysed for expression of IL-1β (a) and IL-8 (b) transcripts by qRT-PCR. Data is shown as fold change (relative to vehicle control), normalised to HPRT expression. The graph shows mean and SD for three experiments. Statistical analysis: ANOVA with post-hoc Tukey's modification *$p<0.05$, **$p<0.01$, ***$p<0.001$

3.3 Discussion

In this chapter, we evaluated three *in vitro* models (HaCaT, EpiDerm, EpiDermFT) for their use in the investigation of keratinocyte-derived cytokines in response to chemical allergen. The 3D models (EpiDerm, EpiDermFT) have been shown to be more representative of skin physiology than monolayer culture, as the keratinocytes differentiate into distinct strata (Ponec et al, 2000, 2002; Poumay et al, 2004,). We have confirmed this by histological examination of the EpiDerm cultures, which we found to resemble normal human epidermis. In contrast, the full thickness models did not show viable, differentiated lower strata. This may be due to reduced delivery of media components to the suprabasal keratinocytes through the fibroblast layer or a consequence of lengthy transport from the supplier. Other groups have found full thickness type cultures to be a valid model (Spiekstra et al, 2005, Holland et al, 2008, 2009), but these are normally produced and studied in the same laboratory. The cytokine expression from the EpiDermFT models was higher and more diverse than from EpiDerm or HaCaT, however the expression profiles from these and the EpiDerm models were not reproducible between donors (groups often pool donors to negate this; Poumay et al, 2004). For this reason, we decided that the EpiDerm and EpiDermFT models were not suitable for mechanistic investigation into cytokine and signalling responses. The keratinocyte-only 3D models (e.g. EpiDerm) are, however, proving valuable for toxicity testing of topically applied cosmetics, where cytotoxicity/irritancy is the primary end-point (Spielmann et al, 2007). Other groups are trying to improve these models by including other cell types such as $CD34^+$ LC-like cells (Facy et al, 2005), MUTZ derived-LCs (Ouwehand 2011) and $CD4^+$ T cells (van den Bogaard et al, 2014).

The HaCaT cells differ from normal human keratinocytes in being immortalised and blocked at a single differentiation state (Boukamp et al, 1988). Nevertheless, the cells do share many characteristics with keratinocytes *in vivo*, and have been widely used as a model to study keratinocyte molecular cell biology. In our context, HaCaT cytokine release showed the major advantage of good reproducibility between biological replicates. HaCaT also demonstrated sensitivity to different stimuli, allowing

discrimination between LPS/IFNγ and DNCB cytokine responses. For these reasons we chose to investigate the HaCaT cells further.

We used LPS with IFNγ, a combination of an innate and adaptive stimulus, as a positive pro-inflammatory control. The inclusion of IFNγ also simulates the microenvironment during the elicitation phase of CHS where Th1 and Tc1 cells are active. Indeed, we found more chemokines, cytokines and growth factors produced by the HaCaTs and EpiDerm model (keratinocyte-only cultures) in response to IFNγ/LPS compared to DNCB or SDS. In response to IFNγ/LPS, both of these models released IL-1ra, IL-2R, IL-7, IL-8, IP-10, MIG, MCP-1, RANTES, GCSF, VEGF, b-FGF. In addition to these, the HaCaT cells also expressed IL-2, IL-6, IL-10, IFNα, MIP1α and HGF, which were not seen in the EpiDerm model, while EpiDerm produced IL-1α and IL-17. A further experiment was conducted using EpiDerm with LPS alone (data not shown) where only IL-1ra, IL-8, MCP-1, VEGF, IL-1α were seen, indicating that the others are IFNγ driven (or a result of combined exposure).

Of the cytokines observed in response to combined innate/adaptive stimulus, IL-1ra, IL-2, IL-2R, IL-6, IL-7, IL-10, IP-10, MCP-1, MIG, MIP-1α, FGF, GCSF, IFNα, RANTES and HGF were expressed with an average fold change of more than 2 compared to control in either HaCaT or EpiDerm.

A number of pro-inflammatory cytokines and chemokines were induced by LPS/IFNγ in the HaCaT or EpiDerm cultures. IL-6 up-regulation in response to IFNγ/LPS has been demonstrated by others (Ishimaru et al, 2013; Teunissen et al, 1998). This cytokine has pro-inflammatory functions through stimulation of the acute phase response and triggering fever (reviewed in Heinrich et al, 1990). IL-6 is also a major regulator of the Th17/Treg balance (Kimura and Kishimoto, 2010), promoting differentiation of Th17 cells. Up-regulation of IFNα was also observed in response to IFNγ/LPS. IFNα is a major mediator of antiviral immunity, but also plays an important role in mediating macrophage and DC activation. IFNα release has been demonstrated in keratinocytes in response to virus (Shao et al, 2010) and at low mRNA levels following LPS stimulation (Fujisawa et al, 1997).

We detected chemokines for: granulocytes (MIP-1α) (and their differentiation factor G-CSF); monocytes and dendritic cells (IP-10, MCP-1); NK and T cells (IP-10, MCP-1, MIG, RANTES); and eosinophils and basophils (RANTES). IP-10 (Luster and Ravetch,1987, Kaplan et al, 1987; Klunker et al, 2003), MIG (Tensen et al, 1999; Klunker et al, 2003), and MCP-1 (Barker et al, 1990, 1991), are known to be induced by IFNγ, and showed the largest expression levels and fold-increases in our data. The neutrophil/granulocyte chemoattractant, IL-8, was constitutively expressed at a high level, but was not affected by IFNγ/LPS in our data. This is in agreement with Li et al (1996) and Barker et al (1990), but IL-8 was found to be activated by others (Teunissen et al, 1998; Song 2002).

Growth factors HGF and b-FGF were also up-regulated. b-FGF is known to be produced by keratinocytes (Halaban et al, 1988), and is involved in tissue re-modelling following infection. HGF is usually produced by mesenchymal cells, not keratinocytes, and acts on epithelial cells. It was not seen in EpiDerm, so it is possible that immortalised HaCaTs are capable of producing HGF as an autocrine-proliferation signal.

Other mediators induced in response to LPS/IFNγ, IL-1ra, IL-10 and IL-2R are known to have immunosuppressive function. IL-1ra inhibits pro-inflammatory IL-1 signalling (reviewed in Arend, 1990), IL-10 down-regulates Th1 cytokine expression (reviewed in Moore et al, 2001) and dendritic /Langerhans cell function, and soluble IL-2R (reviewed in Caruso, 1993) sequesters IL-2, a cytokine that stimulates T cell survival, proliferation and differentiation (reviewed in Boyman and Sprent, 2012). Interestingly, we also saw IL-2 upregulated in response to IFNγ/LPS (but to a much lower extent than IL-2R), as well as IL-7, another T cell survival cytokine. To our knowledge neither IL-2 nor sIL-2R expression from keratinocytes has previously been observed. Yasumura et al (1994) were unable to detect sIL-2R in the supernatant of human keratinocytes but did observe membrane-bound receptor on a small proportion of the population. It is possible that keratinocytes produce IL-2R as a reaction to IFNγ to suppress T-cell activity. IL-7 has previously been shown to be transcribed in keratinocytes in response to IFNγ (Ariizumi et al, 1995). We saw an increase in extracellular IL-1ra, while Phillips et al (1995) saw no change in intracellular IL-1ra in response to IFNγ. IL-10 has previously been found

to be induced by IFNγ in human keratinocytes (Zeitvogel et al, 2008), which is consistent with our result. Altogether, the combination of IL-1ra, IL-10 and IL-2R may reflect an active negative feedback loop to regulate the strong pro-inflammatory stimulus induced by the LPS/IFNγ combination.

To characterise the keratinocyte-derived cytokine profile in response to a model chemical allergen, we exposed HaCaTs and EpiDerm to DNCB. In order to distinguish the allergen response from chemical-induced cell death, we also investigated responses to a model irritant, SDS. In both keratinocyte models (HaCaT and EpiDerm), IL-1ra, IL-8, MCP-1 and VEGF were detected. Expression of IL-1β, IL-6, RANTES and GM-CSF was measured in HaCaTs but not EpiDerm, while IL-1α was only seen in EpiDerm. Generally, the expression from EpiDerm was lower than that from HaCaTs, and much more variable. The variability observed could potentially be due to slight differences in the thickness of the stratum corneum between EpiDerm models.

IL-1α was not detected from HaCaTs in response to DNCB, but was seen following snap freezing (data not shown), which suggests release of pre-stored intracellular IL-1α (Corsini et al, 1998; Coquette et al, 2003). IL-1α expression from EpiDerm showed a tendency to increase, albeit at a low level in response to DNCB (although highly variable between donors). A low level of IL-1α in response to DNCB compared with irritant is consistent with the literature (Poumay et al, 2004; dos Santos et al, 2011; Coquette et al, 1999, 2003). This difference between IL-1α releases might be explained by a tendency for chemical allergens to induce apoptosis, compared with irritant necrotic death and cell rupture (Pastore et al, 1995).

Several other cytokines showed narrow dose responses to DNCB, where release of cytokine occurred at concentrations just under the threshold at which the chemical induced cytotoxicity. This suggests that the cells activate these cytokines when highly stressed.

In response to DNCB or SDS, the same cytokines were detected following treatment with either chemical, but some of the expression profiles were significantly different. Pro-inflammatory cytokines IL-1β and IL-6 were highly up-regulated in response to

DNCB but not SDS, which may be part of a sensitiser-specific signature. Low level IL-1β release following sensitiser exposure has been seen previously (Zepter et al, 1997), but to our knowledge sensitiser-induced IL-6 expression specifically from keratinocytes has not been observed before. IL-6 has been seen in epidermis exposed to chemical-allergen (Cumberbatch et al, 1996; Holliday et al, 1996; Flint et al, 1998), but cannot be assigned to a particular cell type with certainty.

Expression of IL-1ra from HaCaTs increases in response to DNCB at similar concentrations to those which induce IL-1β. IL-1ra has been shown to be predominantly intracellular, pre-stored in keratinocytes (Haskill et al, 1991), potentially as a form of immediate regulation of IL-1 signalling. The fold increase of IL-1ra was lower than that of IL-1β, and there was no change in the SDS-induced IL-1ra expression. Spiekstra et al (2009) quote an EC50 value for IL-1ra production from skin models in response to DNCB which implies that they have observed an increase, however the full data is not disclosed.

The chemokine IL-8 had a similar sensitiser-specific profile to IL-6 and IL-1β. IL-8 expression in response to sensitisers has been observed by others (Newby et al, 2000, Coquette et al, 2003; Mohamadzadeh, 1994). A down-regulation of RANTES was seen at high concentrations of both DNCB and SDS, however with DNCB there was a significant release at lower concentrations. Goebeler et al, 2001 showed RANTES to be present in skin during ACD elicitation reactions. MCP-1 decreased in line with the cytotoxicity profile for both chemicals, suggesting it is only produced by unstressed cells. MCP-1 has, however, been seen in skin during elicitation of contact allergy (Goebeler et al, 2001). It is possible this is due to the effect of IFNγ on keratinocytes (Barker et a, 1991), as we saw a large induction of MCP-1 in our data in response to LPS/IFNγ.

GM-CSF, a growth and differentiation factor for granulocytes and monocytes, only showed low levels of expression, but again displayed a much greater response with DNCB compared to SDS. Terunuma et al (2001) found GM-CSF mRNA to be up-regulated in response to SDS and Ni, but not with DNCB, although they tested at 3μM, approximately 10 fold lower than concentrations at which we saw a response. Enk and

Katz (1992a/c) also found up-regulation of GM-CSF in skin following exposure to sensitiser and irritant.

Having identified the pro-inflammatory mediators characteristic of a response to sensitiser (IL-1β, IL-6, IL-8), we investigated the kinetics of their transcription. The highest fold change of transcription following DNCB exposure was seen in IL-6 at 4 hours, but it was short-lived and down-regulated by 24 hours. It is known that IL-6 is regulated during CHS responses, as, following exposure to oxazalone, the levels in skin peak at 4 hours and decrease by 24 hours (Flint et al, 1998). These timeframes are consistent with our mRNA observations. Similar protein fold changes are seen with IL-6 and IL-8 from the high, short transcription activity of IL-6 compared with a lower sustained transcription for IL-8. IL-1β only increases in mRNA at 24hr, which is consistent with the slightly lower protein fold change observed.

Only a small number of mediators were produced in response to DNCB. This could be because this highly restricted signal would be sufficient to initiate a priming cascade to drive the adaptive response *in vivo*. Alternatively, it could be that the keratinocyte cytokine profile contributes to cross-talk between skin resident cells including macrophages, fibroblasts, dendritic or Langerhans cells that develops into a more diverse set of cytokine/chemokine signals to initiate the response. In either case, the keratinocyte-derived cytokines that we found to be sensitiser specific may play roles at key points in the development of ACD. Due to the vast number of keratinocytes in skin, it is likely that the IL-1β and GM-CSF they produce are important factors influencing LC migration (Cumberbatch et al, 1997; shornick et al. 2001) and maturation (Witmer-pack et al, 1987;Caux et al, 1992; Heufler et al, 1988; Enk et al, 1993), for presentation of hapten-antigen to T-cells in the lymph node. The expression of RANTES and IL-8 will drive chemotaxis of T cells and granulocytes into the skin. The production of IL-1ra demonstrates the capacity of keratinocytes to help regulate the inflammatory response. It has been shown that IL-6 is critical for CHS to DNP-HSA (Palm and Medzhitov, 2009), however its function in initiation of the response is less clear. It is possible that the keratinocyte-derived IL-6 might promote the Th17 and Th1 responses (Serada 2008) known to be important in CHS (Wang et al, 2000; Larsen et al, 2009; Pennino et al, 2010). Alternatively, IL-6 could modify the processing of skin-

protein by cutaneous dendritic cells, leading to presentation of atypical epitopes and triggering autoimmune-like responses (Drakesmith et al, 1998).

We would expect to see TNFα in these responses (Cumberbatch and Kimber, 1995), and indeed we did detect a signal in response to DNCB and not SDS, however the level was below the range of the standard curve for the ELISA and only equated to a maximum level of 5pg/ml. It is possible that we missed the peak TNFα expression, as other groups have found TNFα to be released early (Piguet et al, 1992; Haas et al, 1992). Low levels of TNFα were also seen in response to IFNγ in PAM212 cells (Ariizumi et al, 1995) or LPS in an epidermoid carcinoma cell line (Kock et al, 1990). In mouse skin, the expression of TNFα (mRNA and protein) following exposure to the sensitiser oxazolone are under tight temporal constraints. This transient and localised transcriptional expression peaks and drops within 20 minutes, and protein expression is maximal at 2 hours, returning to normal by 4 hours (Flint et al, 1998).

We could not detect active extracellular IL-18 by standard ELISA or western blot (data not shown). IL-18 has been found at very low levels in supernatant and immunoprecipitation was required to concentrate IL-18 enough to measure (Naik et al, 1999). Van Och et al (2005) measured a dose response of intracellular IL-18 (but not extracellular) in HEL-30 cells exposed to DNCB. It is possible that active IL-18 is not present (Mee et al, 2000) due to the processing required by active caspase-1 (Ghayur et al, 1997), which is not thought to be present in keratinocytes (Akeda et al, 2014). Recent literature suggests that IL-23 (Larsen 2009) may also play a role in allergic contact dermatitis by enhancing the Th17 response, however we haven't measured this cytokine.

In this chapter, we have compared 3D keratinocyte models to the HaCaT cell line, and found HaCaTs to be the most suitable for mechanistic studies. Combined innate and adaptive stimulus induced keratinocyte release of both pro-inflammatory and immunoregulatory cytokines. In response to chemicals, we found a characteristic cytokine signature that differentiates a model sensitiser from a model irritant, in particular IL-1β, IL-6 and IL-8. In the following chapters we investigate the signalling pathways associated with the cytokine changes we identified.

4 DIFFERENTIAL GENE EXPRESSION IN THE TRANSCRIPTOME OF KERATINOCYTES FOLLOWING EXPOSURE TO DNCB AND SDS

4.1 Introduction

In the previous chapter, we saw a characteristic cytokine signature related to DNCB exposure. In this chapter, to understand the specificity of this response, we investigated the mechanisms behind the cytokine release and associated chemical-induced pathways. To achieve this, we studied changes in the keratinocyte transcriptome in response to DNCB exposure.

A number of groups have investigated transcriptional changes in response to sensitising chemicals. The majority of these studies have been on dendritic or dendritic-like cells (Ryan et al, 2004; Johansson et al, 2011; Miyazawa and Takashima, 2012; Yoshikawa et al, 2010; Schoeters et al, 2007; Python et al, 2009; Szameit et al, 2009), with the objective of finding a small number of genes to predict sensitisation potential (Gildea et al, 2006; Hooyberghs et al, 2008; Lambrechts et al, 2010; Johansson et al, 2013). Early array studies into keratinocyte gene expression analysed the response of 3D skin models to irritant chemicals for the identification of irritancy biomarkers (Fletcher et al, 2001; Borlon et al, 2007). More recently, several groups have performed array studies focussing on sensitising chemicals and keratinocytes (Yoshikawa et al, 2010; Saito et al, 2013; Vandebriel et al, 2010; Van der Veen et al, 2013), which have led to development of keratinocyte-based assays to predict sensitisation potential (Emter et al, 2013; McKim et al, 2010). Due to the focus on biomarker discovery, the interpretation of transcriptomic changes in these studies has been limited. However, differentially expressed genes from keratinocyte transcriptomic studies (Saito et al, 2013; Yoshikawa et al, 2010; Vandebriel et al, 2010; Van der Veen et al, 2013) seem to be associated with four themes: transcription factors (ATF3, cFOS); heat shock proteins (HSPA1B, HSPA6, HSPH1, DNAJB1, DNAJB4); cytokines and related proteins (IL-1β, IL-8, TNFAIP3); and oxidative stress/Nrf2 (HMOX1, NQO1, TXNRD1, GCLC, GCLM).
Pathway analysis, which highlights the canonical biological processes that are over-represented in gene expression data, has emerged as a method to help interpret large data sets in terms of mechanisms of action. The pathways within sensitiser-induced

gene expression data sets are only now being explored. Van der Veen et al (2013) have recently shown Nrf2, MAPK, Toll like receptor signalling and cytokine pathways to be involved in keratinocyte responses to sensitiser.

The aim of this chapter is to determine the differential gene expression in the transcriptome of the keratinocyte cell line HaCaT following exposure to a chemical sensitiser, DNCB, and to confirm the specificity of the response through comparison with the chemical irritant SDS. We also aim to identify the ontologies and pathways that are significantly over-represented in the data to provide mechanistic interpretation.

4.2 Results

Array data analysis

The array data files from HaCaT cells exposed to DNCB, SDS or vehicle control were analysed using the single colour advanced analysis settings in GeneSpringGX v12.6 (Agilent). During loading, flags were assigned as not detected if the data spots were: not positive and significant; or not above background. Saturated, non uniform or population outliers were designated with compromised flags. Log_2 transformation was applied to the data (raw signals of 0 were set to 1 before transformation). The data were then normalised by applying the percentile shift algorithm to centre the data from each array at the 75th percentile. Following this, the data were baseline transformed by subtracting the median of the vehicle control arrays (0.2% DMSO), entity by entity.

A box whisker plot of the normalised intensities from each array (Figure 4-1a) shows that they have similar distributions. Figure 4-1b shows a profile of 9 feature extraction values, representing quality control metrics, for each array. The profiles are consistent, providing confidence in comparisons between arrays.

Principal component analysis (PCA) was performed to check that there is discrimination between treatments in the data, that there are no confounding effects (e.g. between batches), and to look for potential outliers. Figure 4-2 shows a clear separation between vehicle control, DNCB and SDS. It also demonstrates progressively increasing separation from control with increasing doses of DNCB.

a

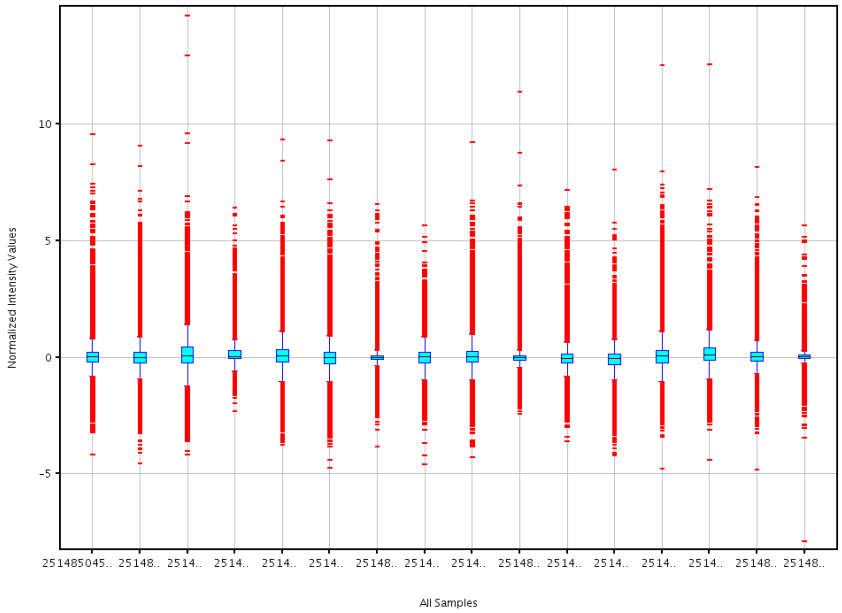

b

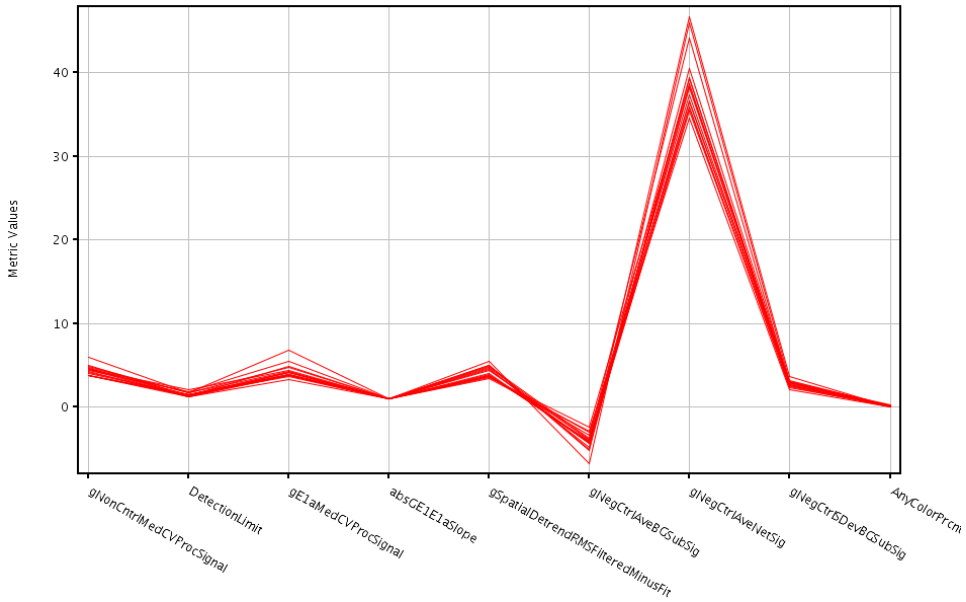

Figure 4-1 Summary of normalised intensities and quality control metrics

The quality and consistency of the array data were assessed by comparing the normalised intensity values of all probes from each array by box whisker plot (a) and comparing profiles of the quality control features for each array (b).

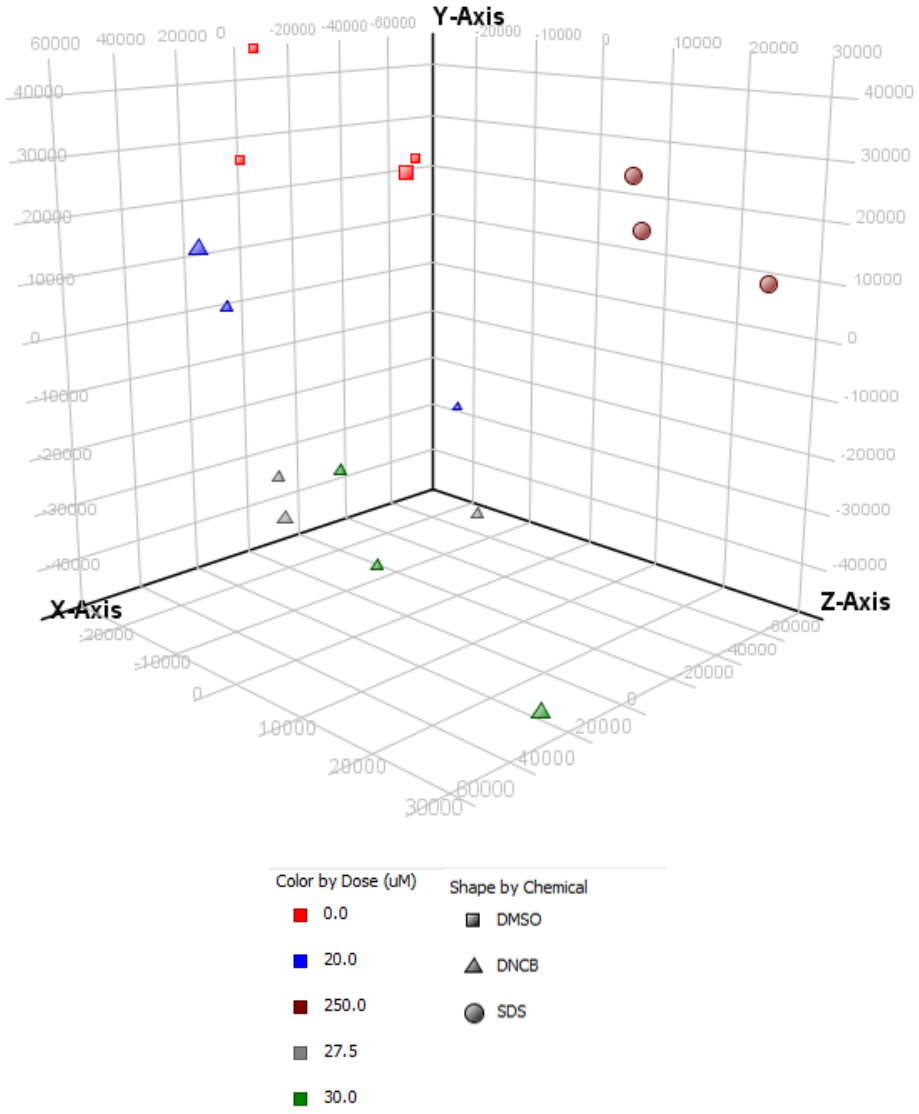

Figure 4-2 Principal component analysis plot

Principal component analysis (PCA) was used to establish the contribution of treatment vs. confounding effects to the variance of the data. The first 3 components are shown: x-axis component 1 (21.64%), y-axis component 2 (17.95%), z-axis component 3 (11.35%), % = percentage of total variance. Each point represents a single array (0µM = 0.2% DMSO vehicle control).

Data filtering

The data from the arrays were further filtered by flags. Only probes flagged as detected in at least 66 percent of samples (2/3 biological replicates) in any 1 out of 5 treatment conditions were accepted for inclusion in the analysis. This reduced the number of probes for analysis from 41093 to 29881. Statistical analysis was performed using this filtered list.

Differential gene expression following exposure to DNCB

The statistical significance of differentially expressed genes at each DNCB concentration compared with the DMSO control was calculated. A one-way ANOVA was selected for these data, as only one parameter (dose) was varied, with more than two conditions (0, 20, 27.5, 30μM DNCB). The Benjamini Hochberg false discovery rate (FDR) multiple testing correction was also applied to reduce chance events being highlighted as significant. 8396 genes out of 29881 had a corrected p-value < 0.05 for at least one dose of DNCB compared to the DMSO vehicle control. The data were further reduced by application of a fold change cut-off, to select only genes that were more than 2-fold differentially expressed (up or down), which resulted in 2147 genes. The majority of these were highly significant, with 1869 of these genes also found with a corrected p-value <0.01; 70 of which had a fold change of more than 10. The normalised intensity values of the 2147 differentially expressed genes with p(corr) < 0.05 and more than 2-fold change were visualised by line graph (Figure 4-3). This shows that most of the genes follow a dose response (up or down-regulated) following exposure to DNCB. Figure 4-4 shows representative examples of genes with dose responses to DNCB and highlights the similarity between the biological replicates.

Table 4-1 shows the top 60 genes (of 2147) ranked by absolute fold change at 30μM DNCB. The top 60 include cytokines and chemokines (such as IL-1α, IL-6, IL-8, CCL18), heat shock proteins, keratin-associated proteins and transcription factors.

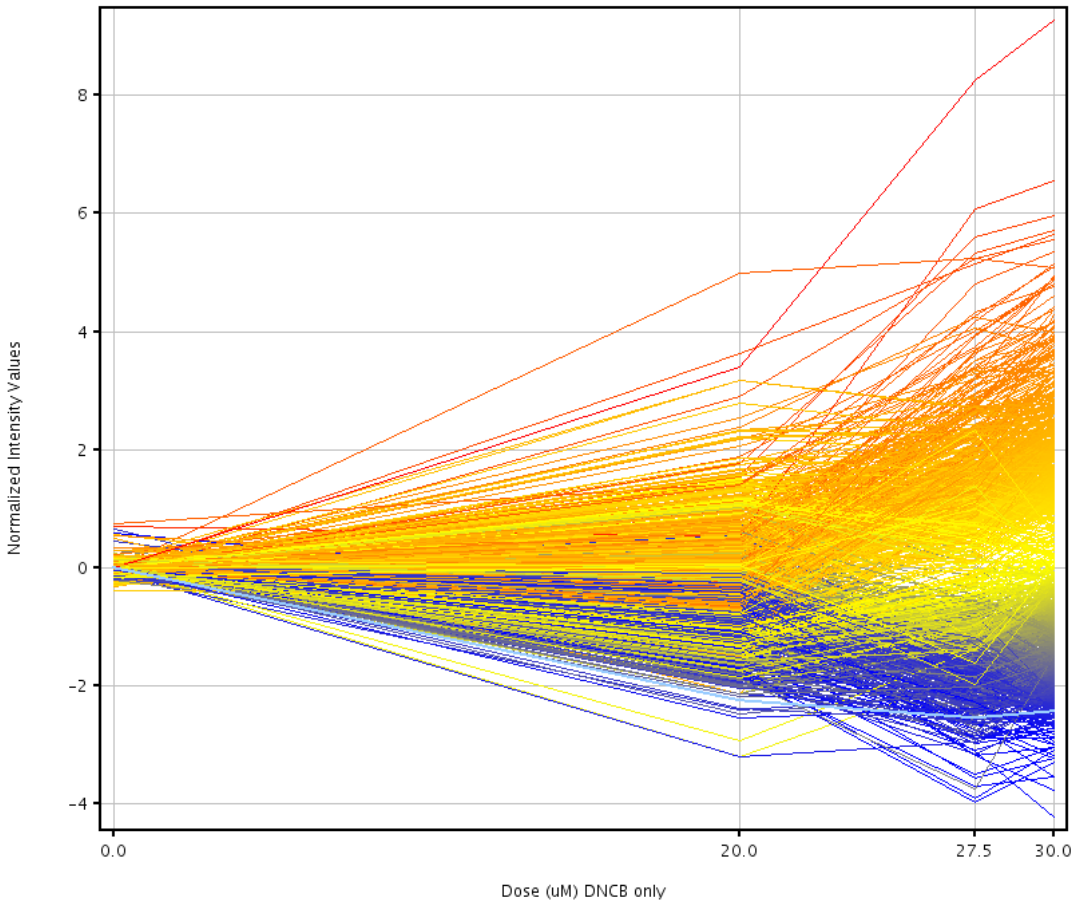

Figure 4-3 Dose response of differentially expressed genes (DNCB vs. control)

Normalised intensity values of 2147 significantly differentially expressed genes, with p(corr) < 0.05 and fold change greater than 2, plotted against dose of DNCB (0μM = 0.2% DMSO vehicle control). Lines are coloured by expression at 30μM (red = up-regulated, blue = down-regulated).

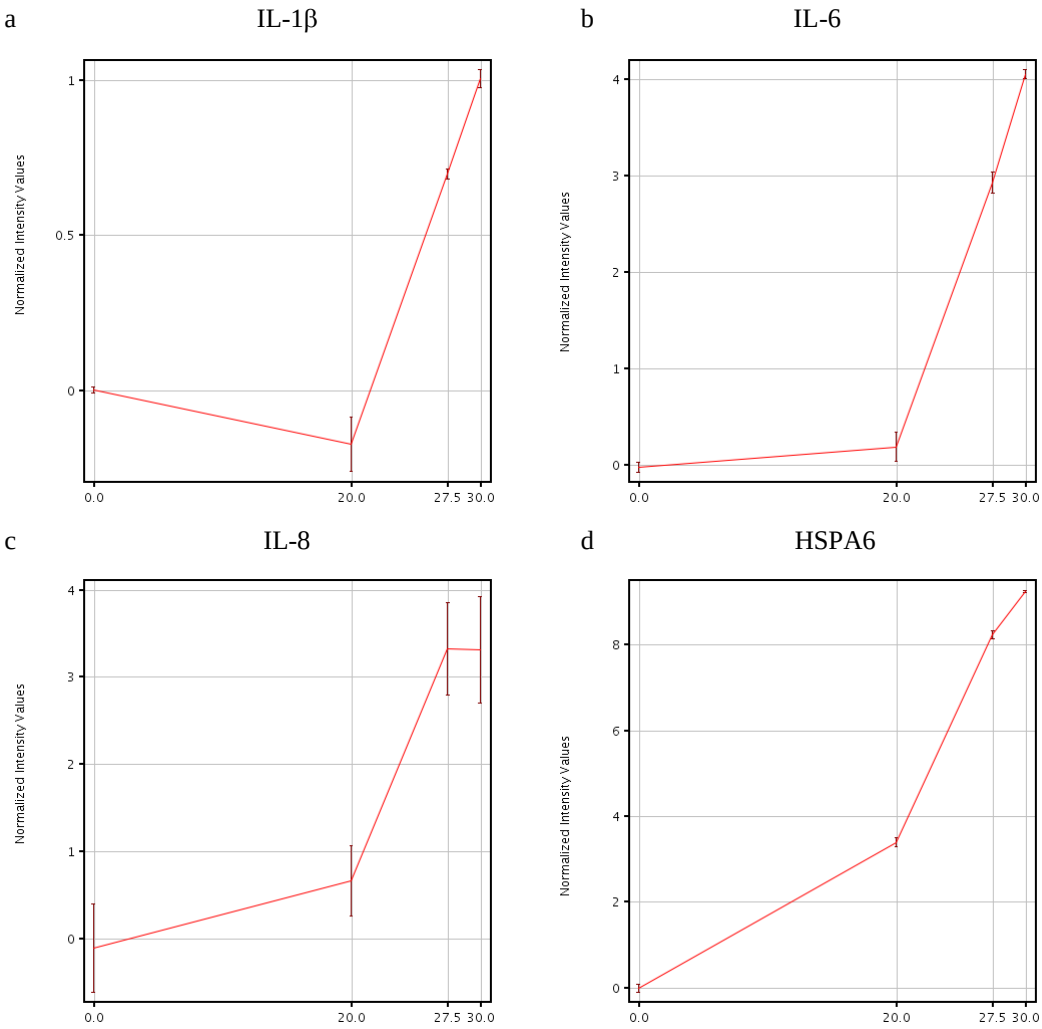

Figure 4-4 Expression of IL-1β, IL-6, IL-8 and HSPA6

Normalised intensity values (log_2 fold change – relative to 0.2% DMSO vehicle control) for IL-1β (a), IL-6 (b), IL-8 (c) and HSPA6 (d) in response to DNCB (concentration in μM on x-axis, 0μM = 0.2% DMSO vehicle control). Error bars show standard deviation of biological replicates (n=3 DNCB, n=4 DMSO).

Rank	Gene symbol	Gene name	Fold change DNCB 20μM	Regulation DNCB 20μM	Fold change DNCB 27.5μM	Regulation DNCB 27.5μM	Fold change DNCB 30μM	Regulation DNCB 30μM	ANOVA corrected p-value
1	HSPA6	heat shock 70kDa protein 6 (HSP70B')	10.53	up	301.74	up	611.87	up	4.12E-09
2	KRTAP1-5	keratin associated protein 1-5	2.90	up	47.97	up	61.85	up	1.18E-07
3	KRTAP3-2	keratin associated protein 3-2	1.14	down	41.14	up	57.66	up	7.00E-04
4	SPINK1	serine peptidase inhibitor, Kazal type 1	3.52	up	41.43	up	54.41	up	6.78E-07
5	MMP3	matrix metallopeptidase 3 (stromelysin 1, progelatinase)	8.11	up	40.95	up	51.00	up	9.17E-04
6	HTRA3	HtrA serine peptidase 3	12.58	up	35.64	up	50.81	up	9.97E-08
7	IL1RL1	interleukin 1 receptor-like 1	1.50	up	28.66	up	41.93	up	4.21E-07
8	KIAA1239	KIAA1239	1.30	up	17.63	up	34.55	up	9.97E-08
9	HMOX1	heme oxygenase (decycling) 1	31.57	up	37.68	up	33.82	up	2.41E-09
10	SPANXB2	SPANX family, member B2	2.58	up	18.82	up	33.81	up	3.07E-05
11	SPANXA1	sperm protein associated with the nucleus, X-linked, family member A1	4.03	up	17.48	up	30.28	up	1.48E-06
12	SNAI1	snail family zinc finger 1	1.69	down	8.75	up	29.56	up	8.21E-07
13	TRIM43	tripartite motif containing 43	1.26	up	11.63	up	29.14	up	2.93E-06
14	KRT34	keratin 34	1.25	down	14.38	up	28.50	up	2.15E-06
15	C11orf96	chromosome 11 open reading frame 96	1.05	up	15.19	up	28.09	up	3.53E-08
16	IL1A	interleukin 1, alpha	1.84	up	14.97	up	27.39	up	3.53E-06
17	NR4A1	nuclear receptor subfamily 4, group A, member 1	1.29	down	12.43	up	23.87	up	1.36E-08

Rank	Gene symbol	Gene name	Fold change DNCB 20μM	Regulation DNCB 20μM	Fold change DNCB 27.5μM	Regulation DNCB 27.5μM	Fold change DNCB 30μM	Regulation DNCB 30μM	ANOVA corrected p-value
18	ACTN2	actinin, alpha 2	1.01	down	6.35	up	20.36	up	6.63E-05
19	KRTAP1-3	keratin associated protein 1-3	1.02	up	3.65	up	18.98	up	3.29E-04
20	ARC	activity-regulated cytoskeleton-associated protein	1.55	down	8.66	up	18.71	up	8.64E-08
21	CCL18	chemokine (C-C motif) ligand 18 (pulmonary and activation-regulated)	1.39	down	13.23	up	18.54	up	4.98E-04
22	USP2	ubiquitin specific peptidase 2	2.28	up	11.15	up	17.84	up	1.67E-05
23	IL10RA	interleukin 10 receptor, alpha	1.33	down	9.37	up	17.81	up	4.12E-06
24	DEFB103B	defensin, beta 103B	1.60	up	7.93	up	17.51	up	1.81E-02
25	ATF3	activating transcription factor 3	1.30	up	10.38	up	17.48	up	1.28E-07
26	HBG1	hemoglobin, gamma A	1.38	down	6.74	up	17.43	up	6.76E-06
27	NR4A3	nuclear receptor subfamily 4, group A, member 3	1.72	down	11.14	up	17.30	up	4.21E-07
28	IL6	interleukin 6 (interferon, beta 2)	1.15	up	7.73	up	16.83	up	3.99E-07
29	CXCR4	chemokine (C-X-C motif) receptor 4	1.31	down	8.05	up	16.46	up	2.66E-06
30	LINC00520	long intergenic non-protein coding RNA 520	5.26	up	18.85	up	15.89	up	1.04E-05
31	CCK	Cholecystokinin	1.26	up	10.26	up	15.66	up	6.48E-06
32	PIWIL2	piwi-like RNA-mediated gene silencing 2	1.46	up	9.35	up	15.64	up	7.76E-06
33	HBG1	hemoglobin, gamma A	1.11	up	6.17	up	14.83	up	2.22E-06
34	VASN	Vasorin	2.50	down	6.80	up	14.66	up	4.27E-08

Rank	Gene symbol	Gene name	Fold change DNCB 20μM	Regulation DNCB 20μM	Fold change DNCB 27.5μM	Regulation DNCB 27.5μM	Fold change DNCB 30μM	Regulation DNCB 30μM	ANOVA corrected p-value
35	ZNF280A	zinc finger protein 280A	1.03	up	5.60	up	14.46	up	3.26E-06
36	MSX1	msh homeobox 1	1.45	down	6.67	up	14.21	up	2.10E-05
37	ATF3	activating transcription factor 3	1.47	up	9.90	up	13.93	up	3.99E-07
38	ANKRD1	ankyrin repeat domain 1 (cardiac muscle)	1.06	up	7.64	up	13.44	up	2.53E-05
39	TRIM53AP	tripartite motif containing 53A, pseudogene	1.02	up	4.69	up	13.17	up	1.28E-07
40	SPANXD	SPANX family, member D	1.80	up	7.72	up	13.10	up	8.09E-05
41	PIWIL2	piwi-like RNA-mediated gene silencing 2	1.40	up	8.31	up	12.77	up	1.98E-06
42	LOC440040	glutamate receptor, metabotropic 5 pseudogene	1.03	up	4.78	up	12.52	up	1.25E-06
43	IL13RA2	interleukin 13 receptor, alpha 2	5.66	up	16.09	up	12.50	up	5.56E-07
44	CD55	CD55 molecule, decay accelerating factor for complement (Cromer blood group)	1.46	up	7.86	up	12.31	up	4.27E-08
45	FOSB	FBJ murine osteosarcoma viral oncogene homolog B	1.11	up	6.70	up	12.24	up	2.16E-07
46	EGR4	early growth response 4	1.92	down	6.29	up	12.15	up	3.50E-05
47	GEM	GTP binding protein overexpressed in skeletal muscle	1.08	up	7.41	up	11.82	up	7.55E-07
48	LYRM9	LYR motif containing 9	3.46	down	13.09	down	11.81	down	2.17E-02
49	ZNF606	zinc finger protein 606	1.94	down	5.58	down	11.71	down	2.60E-02
50	DNAJB4	DnaJ (Hsp40) homolog, subfamily B, member 4	4.44	up	9.69	up	11.41	up	3.00E-06
51	KLF6	Kruppel-like factor 6	2.60	up	9.63	up	11.38	up	2.08E-05

Rank	Gene symbol	Gene name	Fold change DNCB 20μM	Regulation DNCB 20μM	Fold change DNCB 27.5μM	Regulation DNCB 27.5μM	Fold change DNCB 30μM	Regulation DNCB 30μM	ANOVA corrected p-value
52	KRTAP4-1	keratin associated protein 4-1	1.10	up	9.05	up	11.35	up	3.37E-04
53	FOS	FBJ murine osteosarcoma viral oncogene homolog	1.24	down	3.73	up	11.18	up	3.00E-06
54	DNAJB4	DnaJ (Hsp40) homolog, subfamily B, member 4	4.25	up	9.22	up	10.89	up	1.81E-06
55	WNK4	WNK lysine deficient protein kinase 4	3.23	down	5.86	down	10.88	down	1.85E-06
56	IL8	interleukin 8	1.70	up	10.70	up	10.64	up	1.50E-02
57	ZFAND2A	zinc finger, AN1-type domain 2A	1.70	up	6.89	up	10.32	up	3.53E-08
58	RGS16	regulator of G-protein signaling 16	1.60	down	3.17	up	10.19	up	2.06E-06
59	CNN1	calponin 1, basic, smooth muscle	1.14	down	5.48	up	10.15	up	1.12E-04
60	PPP1R15A	protein phosphatase 1, regulatory subunit 15A	2.20	up	7.50	up	10.10	up	5.65E-06

Table 4-1 Top 60 differentially expressed genes in response to DNCB ranked by fold change

List of the top 60 (from 2147) differentially expressed genes with p(corr) < 0.05 and fold change > 2 (relative to control), ranked by fold change (at 30μM DNCB).

Differential gene expression following exposure to SDS

The statistical significance of differentially expressed genes from SDS exposed HaCaT cells compared with the DMSO control was calculated. An unpaired t-test was selected for this data as there were only 2 conditions (0, 250μM SDS), and applied with the Benjamini Hochberg FDR multiple testing correction. In response to SDS, 4264 genes out of 29881 had a corrected p-value < 0.05. The data were further reduced by application of a fold change cut-off, to select only genes that were more than 2-fold differentially expressed (up or down), which resulted in 584 genes. The majority of these were highly significant, with 431 of these genes also found with a corrected p-value of 0.01; only 4 of which had a fold change of more than 10.

The normalised intensity values of the 584 differentially expressed genes with p(corr) < 0.05 and more than 2-fold change were visualised by line graph (Figure 4-5). Table 4-2 shows the top 30 genes (of 584) ranked by absolute fold change.

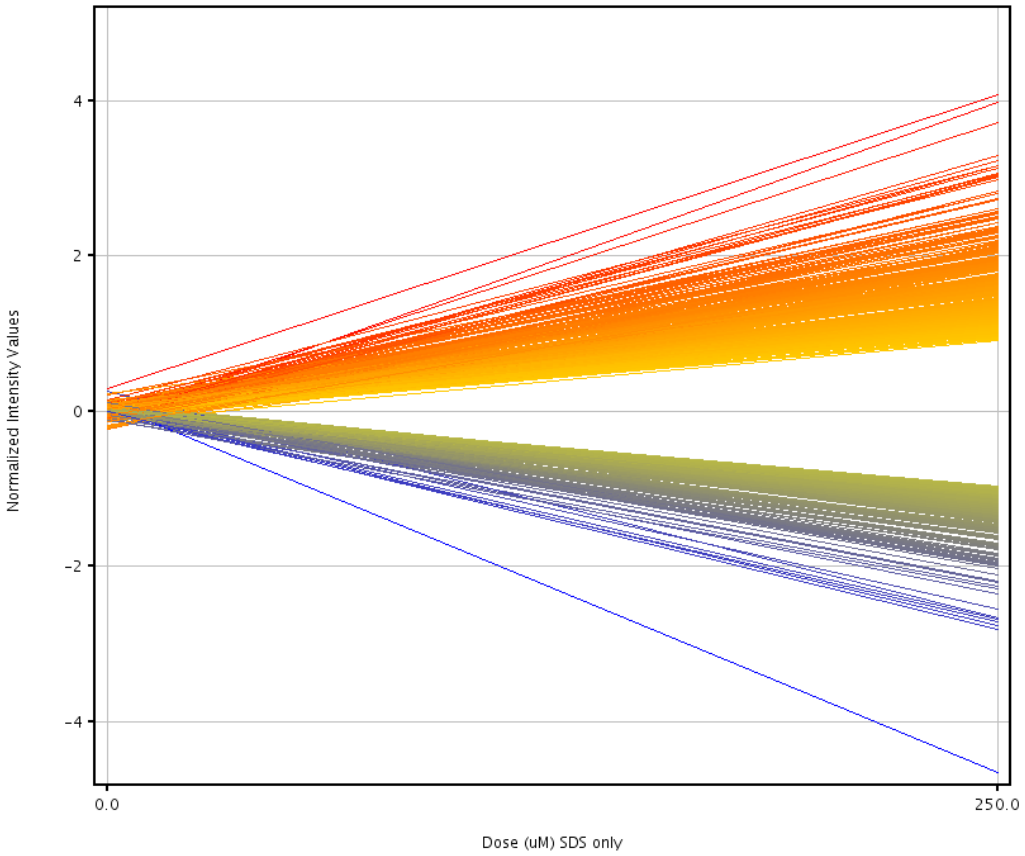

Figure 4-5 Dose response of differentially expressed genes (SDS vs. control)

Normalised intensity values of 584 significantly differentially expressed genes, with p(corr) < 0.05 and fold change greater than 2, plotted against dose of SDS (0μM = 0.2% DMSO vehicle control). Lines are coloured by expression at 250μM (red = up-regulated, blue = down-regulated).

Rank	Gene symbol	Gene name	Fold change SDS 250μM vs control	Regulation SDS 250μM vs control	T-test corrected p-value
1	MMP3	matrix metallopeptidase 3 (stromelysin 1, progelatinase)	17.14	up	2.23E-03
2	CGA	glycoprotein hormones, alpha polypeptide	13.84	up	6.68E-03
3	IL1RL1	interleukin 1 receptor-like 1	13.49	up	8.50E-04
4	KIAA1755	KIAA1755	10.20	up	1.57E-03
5	LINC00659	long intergenic non-protein coding RNA 659	8.57	up	3.19E-03
6	LPPR5	lipid phosphate phosphatase-related protein type 5	8.52	up	8.48E-03
7	THBS1	thrombospondin 1	8.33	up	4.74E-03
8	ENKUR	enkurin, TRPC channel interacting protein	8.04	up	4.47E-02
9	MIR100HG	mir-100-let-7a-2 cluster host gene (non-protein coding)	7.58	up	1.24E-03
10	CEP85L	centrosomal protein 85kDa-like	7.53	down	2.26E-02
11	CREB5	cAMP responsive element binding protein 5	7.12	up	6.39E-04
12	SEMA6D	sema domain, transmembrane domain (TM), and cytoplasmic domain, (semaphorin) 6D	6.85	down	6.54E-04
13	CHAC1	ChaC, cation transport regulator homolog 1 (E. coli)	6.85	up	1.24E-03
14	LINC01127	long intergenic non-protein coding RNA 1127	6.63	up	5.45E-04
15	PHLDA1	pleckstrin homology-like domain, family A, member 1	6.46	up	3.70E-04
16	IL1A	interleukin 1, alpha	5.96	up	6.54E-04
17	VAV3	vav 3 guanine nucleotide exchange factor	5.94	down	8.13E-04

Rank	Gene symbol	Gene name	Fold change SDS 250μM vs control	Regulation SDS 250μM vs control	T-test corrected p-value
18	CGA	glycoprotein hormones, alpha polypeptide	5.79	up	1.37E-02
19	LOC101059954	uncharacterized LOC101059954	5.67	up	8.44E-04
20	PRUNE2	prune homolog 2 (Drosophila)	5.64	up	5.07E-03
21	ANO2	anoctamin 2	5.62	up	1.21E-03
22	CD55	CD55 molecule, decay accelerating factor for complement (Cromer blood group)	5.56	up	4.77E-04
23	CCK	Cholecystokinin	5.45	up	5.86E-03
24	DNM3	dynamin 3	5.35	up	6.54E-04
25	CD55	CD55 molecule, decay accelerating factor for complement (Cromer blood group)	5.26	up	1.10E-03
26	LOC100507165	uncharacterized LOC100507165	5.19	up	3.19E-03
27	PHLDA1	pleckstrin homology-like domain, family A, member 1	5.13	up	7.12E-04
28	IFNE	interferon, epsilon	5.09	up	1.41E-03
29	INHBA	inhibin, beta A	5.05	up	4.48E-04
30	CCL2	chemokine (C-C motif) ligand 2	5.01	down	4.72E-04

Table 4-2 Top 30 differentially expressed genes in response to SDS ranked by fold change

List of the top 30 (from 584) differentially expressed genes with p(corr) < 0.05 and fold change > 2, ranked by fold change.

Overlap between the DNCB and SDS significantly differentially expressed genes

The overlap between the gene lists for DNCB and SDS with corrected p-values < 0.05 and fold changes more than 2 (compared with DMSO control) were visualised using a Venn diagram (Figure 4-6). Only 263 genes out of a combined set of 2468 differentially expressed genes were common between the two chemicals.

Gene ontology analysis

The database for annotation, visualisation and integrated discovery (DAVID) (http://david.abcc.ncifcrf.gov/tools.jsp) was used to understand the biological functions, classified by gene ontology (http://www.geneontology.org), involved in the response of HaCaT cells to DNCB and SDS. The DNCB and SDS final gene-lists resulting from normalisation, statistical analysis and 2-fold change cut off (as previously discussed) were loaded into DAVID software for enrichment analysis. Using this software the genes were mapped to associated biological functions and the most statistically over-represented gene ontologies were ranked by modified Fisher exact p-value (Hosack et al, 2003). 1553 out of 2147 genes on the DNCB list could be identified in DAVID. The most over-represented gene ontologies in response to DNCB generally involved regulation of transcription (Table 4-3). Using the gene-list from SDS exposed HaCaT cells, 458 out of 584 genes could be identified in DAVID. The enriched terms in response to SDS (Table 4-4) were mainly associated with the regulation of cell death.

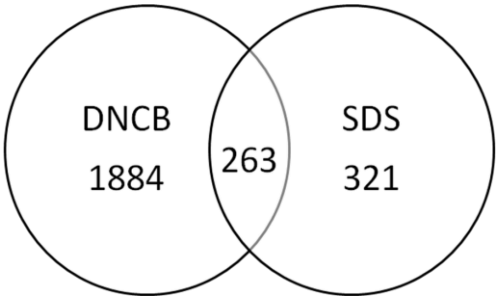

Figure 4-6 Overlap between the DNCB and SDS differentially expressed genes

The overlap between the significantly differentially expressed genes following 4 hour exposure to DNCB or SDS, represented by Venn diagram. Differentially expressed genes had corrected p-values < 0.05 and fold changes more than 2 at any dose.

Gene Ontology Term	Count	Percentage	p-value
GO:0045449~regulation of transcription	338	26.24224	4.49E-39
GO:0006350~transcription	287	22.28261	5.36E-36
GO:0006355~regulation of transcription, DNA-dependent	255	19.79814	4.02E-35
GO:0051252~regulation of RNA metabolic process	258	20.03106	8.48E-35
GO:0016481~negative regulation of transcription	65	5.046584	1.80E-08
GO:0010629~negative regulation of gene expression	69	5.357143	2.44E-08
GO:0045892~negative regulation of transcription, DNA-dependent	54	4.192547	3.57E-08
GO:0051253~negative regulation of RNA metabolic process	54	4.192547	6.26E-08
GO:0051172~negative regulation of nitrogen compound metabolic process	69	5.357143	7.76E-08
GO:0045934~negative regulation of nucleobase, nucleoside, nucleotide and nucleic acid metabolic process	68	5.279503	1.02E-07
GO:0006357~regulation of transcription from RNA polymerase II promoter	86	6.677019	3.07E-07
GO:0031327~negative regulation of cellular biosynthetic process	71	5.512422	3.34E-07
GO:0010558~negative regulation of macromolecule biosynthetic process	69	5.357143	5.71E-07
GO:0009890~negative regulation of biosynthetic process	71	5.512422	7.44E-07
GO:0000122~negative regulation of transcription from RNA polymerase II promoter	41	3.18323	1.32E-06
GO:0010033~response to organic substance	83	6.444099	1.59E-06
GO:0043067~regulation of programmed cell death	89	6.909938	4.81E-06
GO:0010941~regulation of cell death	89	6.909938	5.57E-06
GO:0042981~regulation of apoptosis	88	6.832298	5.72E-06
GO:0009611~response to wounding	64	4.968944	6.65E-06
GO:0051789~response to protein stimulus	22	1.708075	7.58E-06

Gene Ontology Term	Count	Percentage	p-value
GO:0007243~protein kinase cascade	49	3.804348	8.60E-06
GO:0045765~regulation of angiogenesis	16	1.242236	1.36E-05
GO:0032570~response to progesterone stimulus	9	0.698758	2.49E-05
GO:0045766~positive regulation of angiogenesis	10	0.776398	3.01E-05
GO:0010605~negative regulation of macromolecule metabolic process	79	6.13354	3.38E-05
GO:0006954~inflammatory response	43	3.338509	3.42E-05
GO:0002237~response to molecule of bacterial origin	18	1.397516	4.99E-05
GO:0031328~positive regulation of cellular biosynthetic process	74	5.745342	5.61E-05
GO:0010557~positive regulation of macromolecule biosynthetic process	71	5.512422	6.90E-05
GO:0040012~regulation of locomotion	29	2.251553	8.68E-05
GO:0009891~positive regulation of biosynthetic process	74	5.745342	8.81E-05
GO:0032675~regulation of interleukin-6 production	11	0.854037	9.26E-05

Table 4-3 Gene ontologies associated with DNCB exposure

List of over-represented gene ontologies from DAVID ranked by p-value. Count = number of differentially expressed genes from the data annotated in the ontology. Percentage = count divided by number of genes in the ontology (times 100%).

Gene Ontology Term	Count	Percentage	p-value
GO:0042981~regulation of apoptosis	42	10.74169	2.58E-08
GO:0043067~regulation of programmed cell death	42	10.74169	3.43E-08
GO:0010941~regulation of cell death	42	10.74169	3.78E-08
GO:0009891~positive regulation of biosynthetic process	36	9.207161	4.11E-07
GO:0031328~positive regulation of cellular biosynthetic process	35	8.951407	8.55E-07
GO:0043065~positive regulation of apoptosis	25	6.393862	5.60E-06
GO:0043068~positive regulation of programmed cell death	25	6.393862	6.29E-06
GO:0010942~positive regulation of cell death	25	6.393862	6.80E-06
GO:0042127~regulation of cell proliferation	36	9.207161	6.93E-06
GO:0010557~positive regulation of macromolecule biosynthetic process	31	7.928389	1.86E-05
GO:0008284~positive regulation of cell proliferation	23	5.882353	2.94E-05
GO:0010243~response to organic nitrogen	9	2.30179	3.40E-05
GO:0012501~programmed cell death	29	7.41688	3.63E-05
GO:0051094~positive regulation of developmental process	18	4.603581	4.37E-05
GO:0007398~ectoderm development	15	3.836317	4.63E-05
GO:0008544~epidermis development	14	3.580563	8.25E-05
GO:0032101~regulation of response to external stimulus	13	3.324808	8.26E-05
GO:0010604~positive regulation of macromolecule metabolic process	35	8.951407	9.65E-05
GO:0008219~cell death	31	7.928389	1.05E-04
GO:0014075~response to amine stimulus	7	1.790281	1.12E-04
GO:0016265~death	31	7.928389	1.18E-04

Gene Ontology Term	Count	Percentage	p-value
GO:0070482~response to oxygen levels	12	3.069054	1.21E-04
GO:0040012~regulation of locomotion	14	3.580563	1.27E-04
GO:0010648~negative regulation of cell communication	16	4.092072	1.39E-04
GO:0009968~negative regulation of signal transduction	15	3.836317	1.43E-04
GO:0009611~response to wounding	25	6.393862	1.58E-04
GO:0002687~positive regulation of leukocyte migration	5	1.278772	1.78E-04
GO:0006915~apoptosis	27	6.905371	1.82E-04
GO:0051173~positive regulation of nitrogen compound metabolic process	28	7.161125	2.21E-04

Table 4-4 Gene ontologies associated with SDS exposure

List of over-represented gene ontologies from DAVID ranked by p-value. Count = number of differentially expressed genes from the data annotated in the ontology. Percentage = count divided by number of genes in the ontology (times 100%).

Pathway analysis

To understand the canonical biological pathways affected in HaCaT cells in response to DNCB, the gene expression data were analysed using both Ingenuity pathway analysis (IPA) (Qiagen, http://www.ingenuity.com) and MetaCore (Thomson Reuters, http://thomsonreuters.com/metacore/). These software tools were selected due to the stringent curation of their biological interaction knowledge databases. Additionally, the MetaCore software contains a number of contact allergy specific pathways. These analyses are, however, limited by the amount of information and number of pathways in the databases.

Pathway enrichment analysis was performed to determine the most populated canonical pathways of the statistically significant ($p(corr) < 0.05$ and fold change > 2) differentially expressed genes in response to DNCB. The most represented canonical pathways ranked by p-value are shown in Table 4-5 (IPA) and Table 4-6 (MetaCore). The ratio (the number of genes differentially expressed, divided by the number of genes in the pathway) gives an indication of the proportion of the pathway changing in the data. P-values are calculated as the probability of the number of positive matches on a pathway, with a false discovery rate applied. There is some overlap between the IPA and MetaCore analyses, however, often the same core gene network is included under different pathway titles in the two tools.

Several of the differentially expressed genes cause over-representation of many pathways. These include cytokines (IL-1α, IL-1β, IL-6, IL-8, CCL2, CCL3 and CCL4), heat shock proteins (Hsp60, Hsp70) and transcription factors (c-Jun, c-Fos, AP-1, EGR1, CEBPβ, Fra-1, ATF and IκB), which appear on numerous canonical pathways. Three interesting pathways were selected from each analysis to give examples of visual representation of the pathway expression data. Genes involved in the IL-6 (Figure 4-7), IL-10 (Figure 4-8) and TLR (Figure 4-9) signalling pathways were differentially expressed (using IPA). In MetaCore, the same genes from the data were represented in: "Immune response IL-1 signalling" (Figure 4-10), "Immune response HSP60 and HSP70 TLR signalling" (Figure 4-11), and "KEAP1/NRF2 as a cellular sensor for skin sensitisers" (Figure 4-12) pathways.

Rank	Pathway	p-value	Ratio
1	IL-10 Signaling	5.50E-05	0.224
2	ILK Signaling	4.07E-04	0.144
3	Role of Hypercytokinemia/hyperchemokinemia in the Pathogenesis of Influenza	8.91E-04	0.243
4	Aldosterone Signaling in Epithelial Cells	8.91E-04	0.147
5	Agranulocyte Adhesion and Diapedesis	1.02E-03	0.14
6	IL-6 Signaling	1.32E-03	0.155
7	Cholecystokinin/Gastrin-mediated Signaling	1.74E-03	0.16
8	Role of IL-17F in Allergic Inflammatory Airway Diseases	1.95E-03	0.22
9	Granulocyte Adhesion and Diapedesis	2.29E-03	0.137
10	Hepatic Fibrosis / Hepatic Stellate Cell Activation	2.51E-03	0.13
11	IL-17A Signaling in Fibroblasts	2.63E-03	0.229
12	NRF2-mediated Oxidative Stress Response	3.31E-03	0.131
13	HMGB1 Signaling	3.98E-03	0.144
14	Glucocorticoid Receptor Signaling	4.17E-03	0.118
15	Differential Regulation of Cytokine Production in Intestinal Epithelial Cells by IL-17A and IL-17F	4.47E-03	0.261
16	IL-17 Signaling	4.47E-03	0.167
17	Acute Phase Response Signaling	6.92E-03	0.127
18	Differential Regulation of Cytokine Production in Macrophages and T Helper Cells by IL-17A and IL-17F	7.08E-03	0.278
19	PPAR Signaling	1.07E-02	0.144

Rank	Pathway	p-value	Ratio
20	Toll-like Receptor Signaling	1.10E-02	0.155
21	Role of Macrophages, Fibroblasts and Endothelial Cells in Rheumatoid Arthritis	1.10E-02	0.109
22	Role of IL-17A in Arthritis	1.29E-02	0.167
23	Glutathione Biosynthesis	1.45E-02	0.667
24	Retinoate Biosynthesis I	1.70E-02	0.2
25	Transcriptional Regulatory Network in Embryonic Stem Cells	2.09E-02	0.175
26	LXR/RXR Activation	2.24E-02	0.125
27	Embryonic Stem Cell Differentiation into Cardiac Lineages	2.95E-02	0.3
28	Methylglyoxal Degradation III	2.95E-02	0.3
29	JAK/Stat Signaling	3.02E-02	0.139
30	CD40 Signaling	3.63E-02	0.141

Table 4-5 IPA pathway analysis

List of the top 30 statistically over-represented canonical pathways from the DNCB gene-list using IPA ranked by corrected p-value. Ratio = number of genes differentially expressed, divided by the number of genes in the pathway

Rank	Pathway	p-value	FDR	Ratio
1	Immune response_IL-1 signaling pathway	7.21E-10	5.21E-07	0.3182
2	Immune response_IL-17 signaling pathways	7.37E-09	2.62E-06	0.2500
3	Immune response_HMGB1/RAGE signaling pathway	1.09E-08	2.62E-06	0.2642
4	Immune response_IL-18 signaling	6.10E-08	1.10E-05	0.2333
5	Role of Endothelin-1 in inflammation and vasoconstriction in Sickle cell disease	1.50E-07	2.17E-05	0.2895
6	The innate immune response to contact allergens	3.47E-07	3.86E-05	0.3030
7	Immune response_TREM1 signaling pathway	3.73E-07	3.86E-05	0.2203
8	Reproduction_GnRH signalling	6.81E-07	6.15E-05	0.1944
9	Immune response_HMGB1/TLR signaling pathway	8.57E-07	6.89E-05	0.2778
10	Transcription_Role of AP-1 in regulation of cellular metabolism	1.49E-06	1.07E-04	0.2632
11	Immune response_IL-3 activation and signaling pathway	2.04E-06	1.34E-04	0.2903
12	Putative pathways of hormone action in neurofibromatosis type 1	2.38E-06	1.38E-04	0.3333
13	Immune response_Gastrin in inflammatory response	2.49E-06	1.38E-04	0.1884
14	Transcription_Role of VDR in regulation of genes involved in osteoporosis	3.78E-06	1.95E-04	0.1967
15	Immune response_Substance P-stimulated expression of proinflammatory cytokines via MAPKs	5.04E-06	2.43E-04	0.2326
16	Immune response_HSP60 and HSP70/ TLR signaling	6.75E-06	2.87E-04	0.2037
17	Immune response_CCL2 signaling	6.75E-06	2.87E-04	0.2037
18	Signal transduction_PTMs in IL-17-induced CIKS-independent signaling pathways	9.64E-06	3.87E-04	0.2174

Rank	Pathway	p-value	FDR	Ratio
19	Immune response_TLR2 and TLR4 signaling pathways	1.17E-05	4.23E-04	0.1930
20	Immune response_Role of PKR in stress-induced antiviral cell response	1.17E-05	4.23E-04	0.1930
21	Expression targets of Tissue factor signaling in cancer	1.48E-05	4.83E-04	0.3182
22	Immune response_MIF-mediated glucocorticoid regulation	1.48E-05	4.83E-04	0.3182
23	Immune response_Signaling pathway mediated by IL-6 and IL-1	1.54E-05	4.83E-04	0.2667
24	Development_ERBB-family signalling	1.62E-05	4.87E-04	0.2308
25	PDE4 regulation of cyto/chemokine expression in arthritis	1.75E-05	5.05E-04	0.2041
26	IGF family signaling in colorectal cancer	1.95E-05	5.43E-04	0.1833
27	The role of KEAP1/NRF2 pathway in skin sensitization	2.58E-05	6.90E-04	0.2500
28	Immune response_Classical complement pathway	3.03E-05	7.81E-04	0.1923
29	Development_Regulation of epithelial-to-mesenchymal transition (EMT)	3.67E-05	9.07E-04	0.1719
30	Role of keratinocytes and Langerhans cells in skin sensitization	3.76E-05	9.07E-04	0.2800

Table 4-6 Metacore pathway analysis

List of the top 30 statistically over-represented canonical pathways from the DNCB gene-list using Metacore ranked by p-value. FDR = false discovery rate.

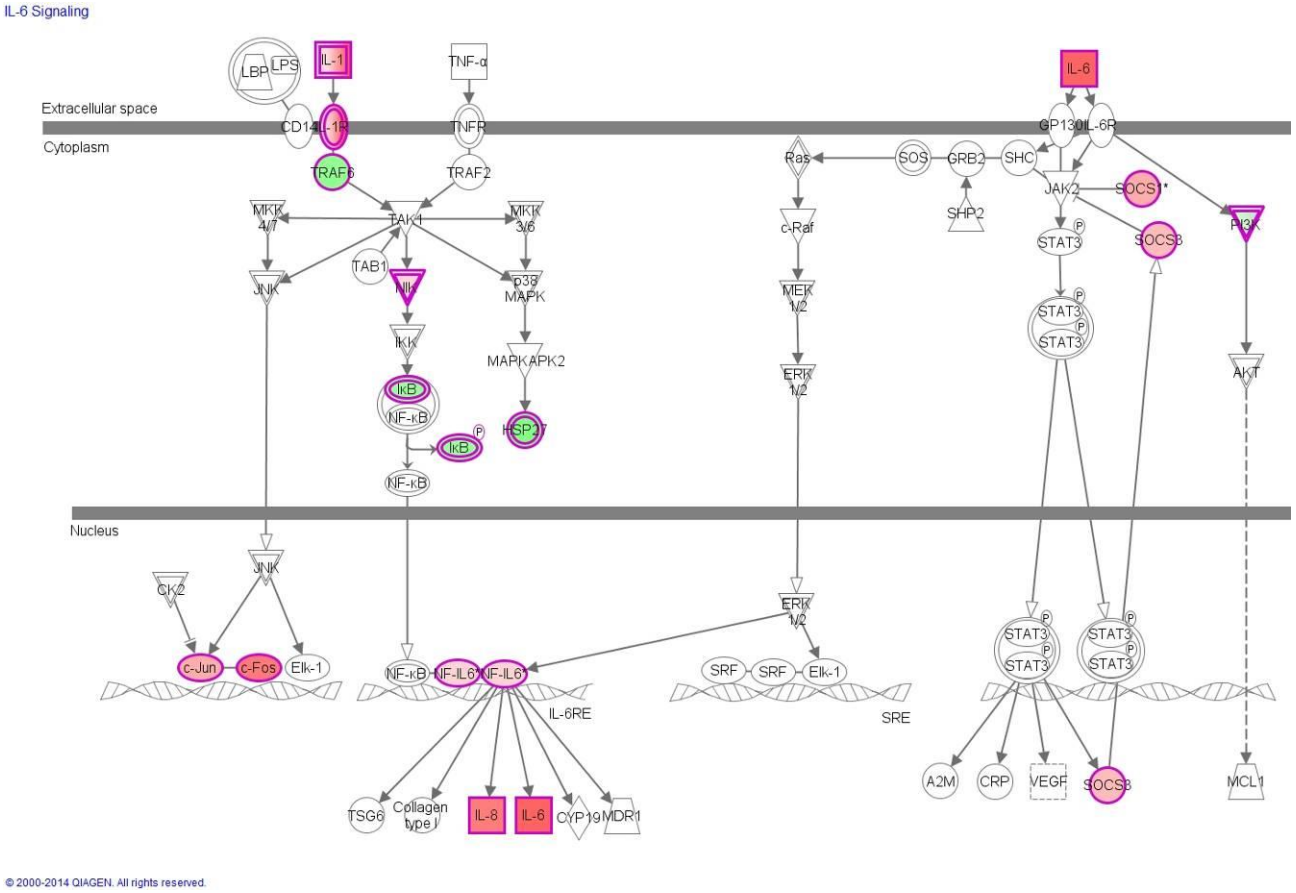

Figure 4-7 IL-6 signalling pathway

Differentially expressed genes involved in the IL-6 signalling pathway from IPA. Up-regulated genes (red) and down-regulated genes (green), intensity of colour indicates level of fold change.

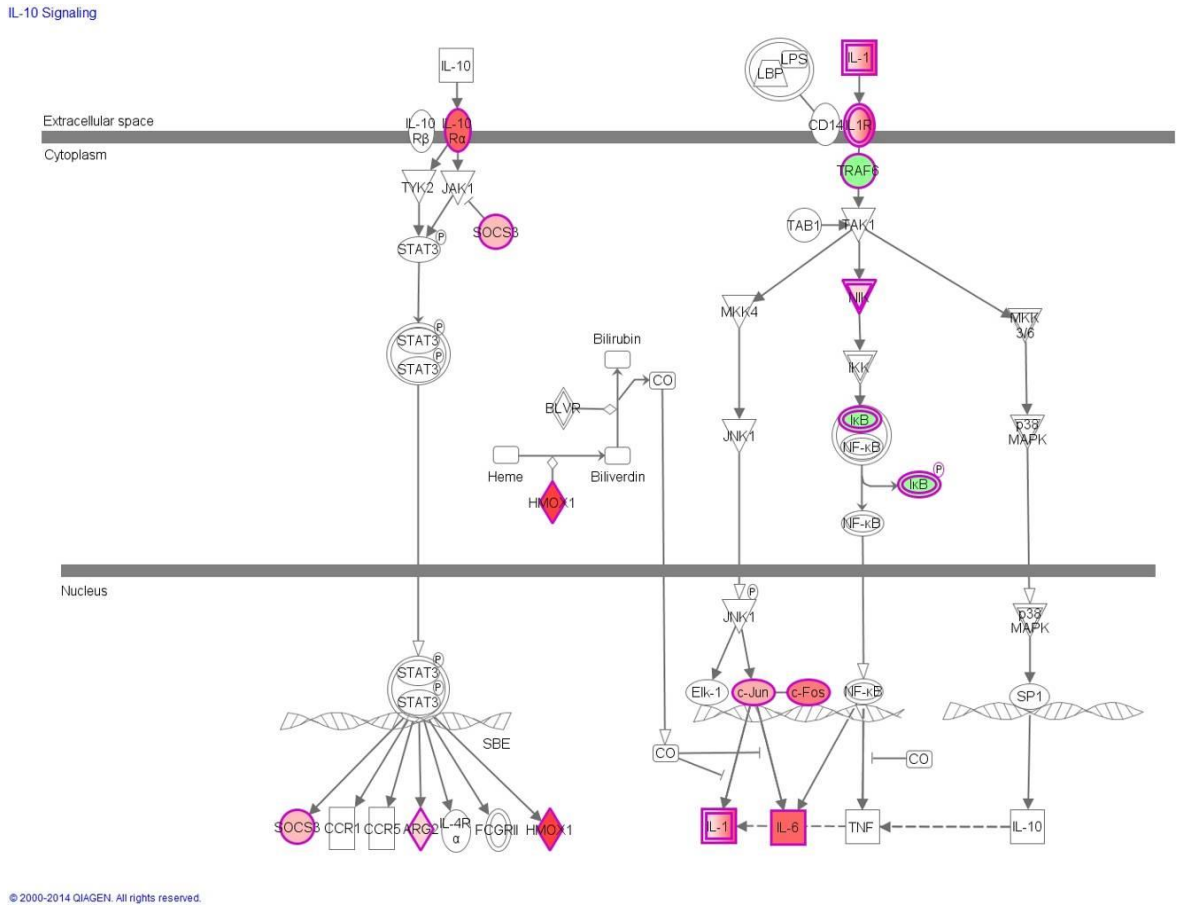

Figure 4-8 IL-10 signalling pathway

Differentially expressed genes involved in the IL-10 signalling pathway from IPA. Up-regulated genes (red) and down-regulated genes (green), intensity of colour indicates level of fold change.

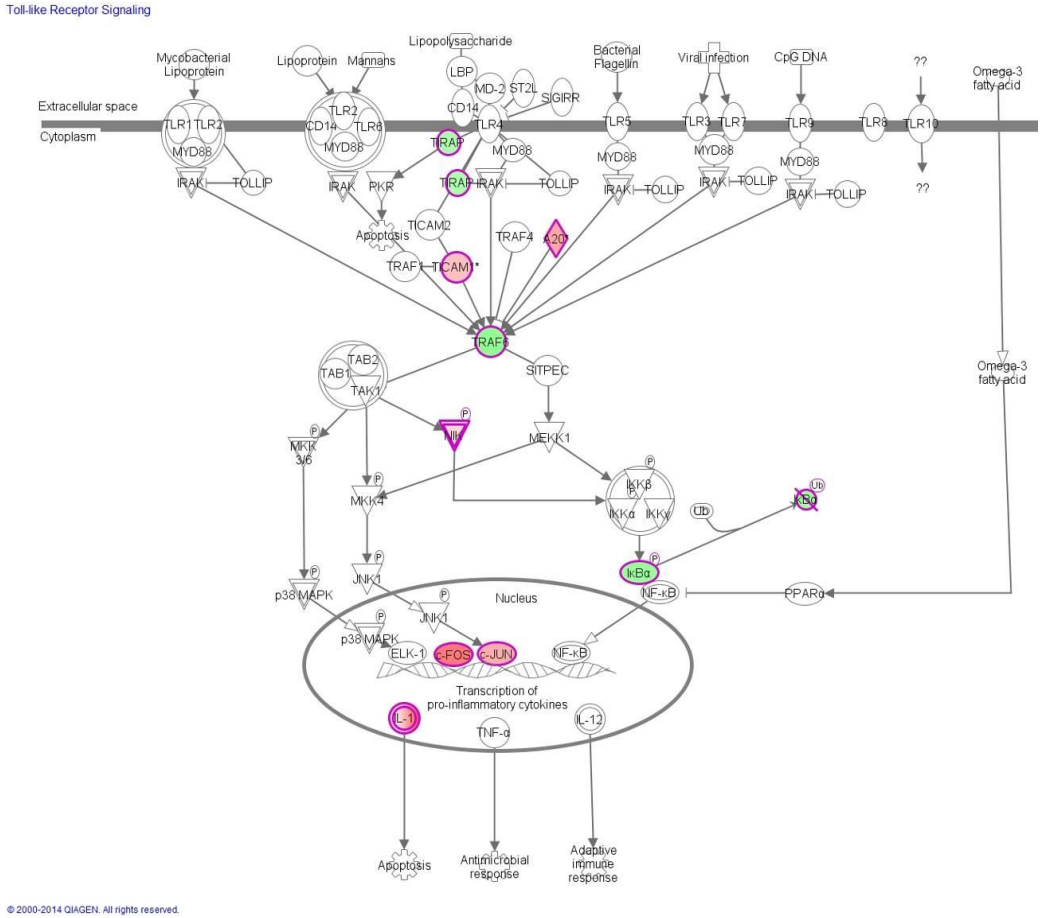

Figure 4-9 Toll-like receptor signalling pathway

Differentially expressed genes involved in the TLR signalling pathway from IPA. Up-regulated genes (red) and down-regulated genes (green), intensity of colour indicates level of fold change.

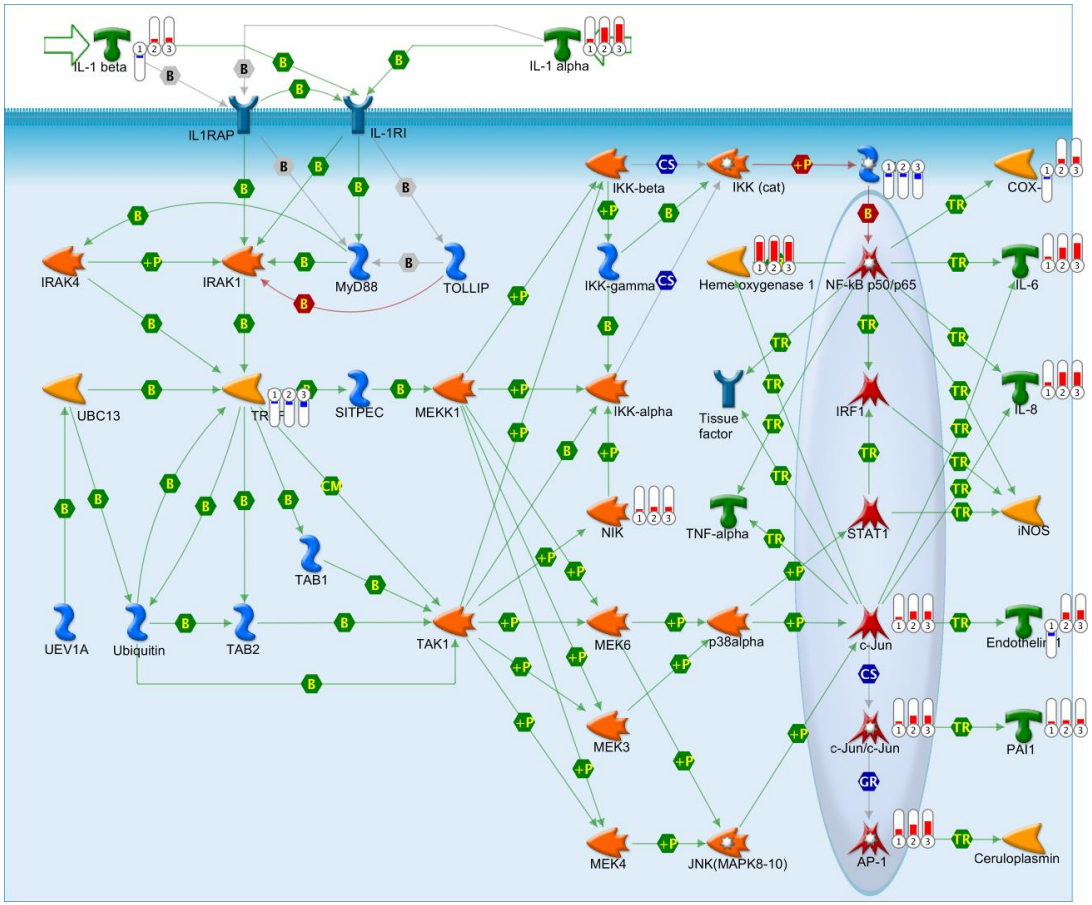

Figure 4-10 Immune response IL-1 signalling pathway

Differentially expressed genes involved in the IL-1 signalling pathway from MetaCore. The thermometers show up-regulated (red) and down-regulated (blue) gene changes at 20μM (1), 27.5μM (2) and 30μM (3).

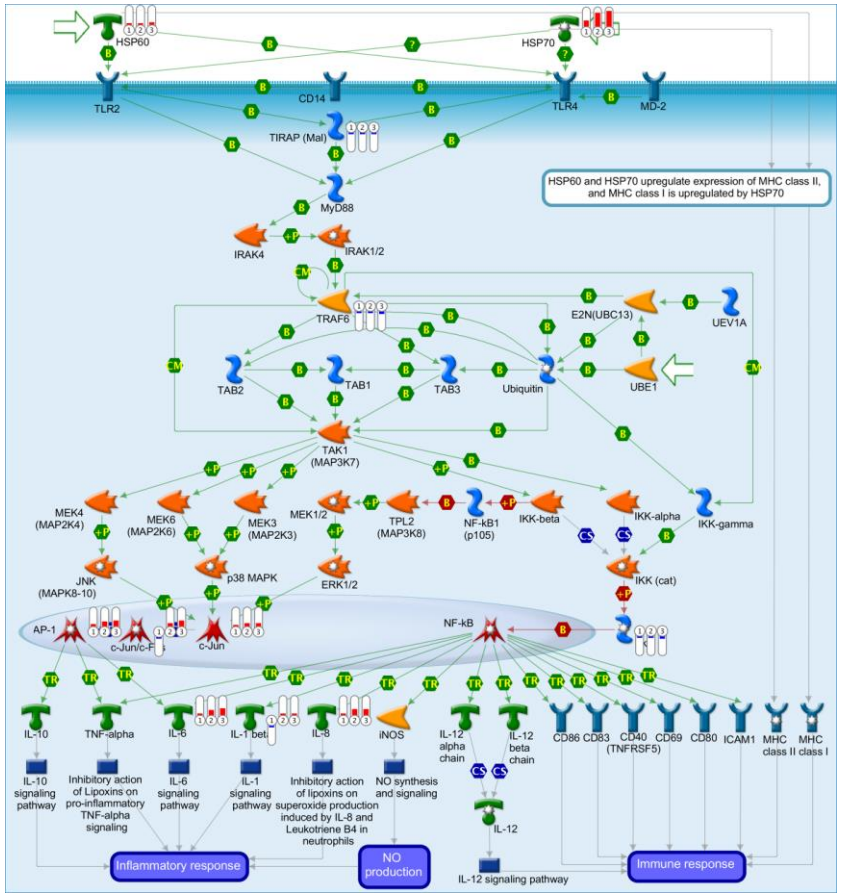

Figure 4-11 Immune response HSP60 and HSP70 TLR signalling pathway

Differentially expressed genes involved in the Hsp/TLR signalling pathway from MetaCore. The thermometers show up-regulated (red) and down-regulated (blue) gene changes at 20μM (1), 27.5μM (2) and 30μM (3).

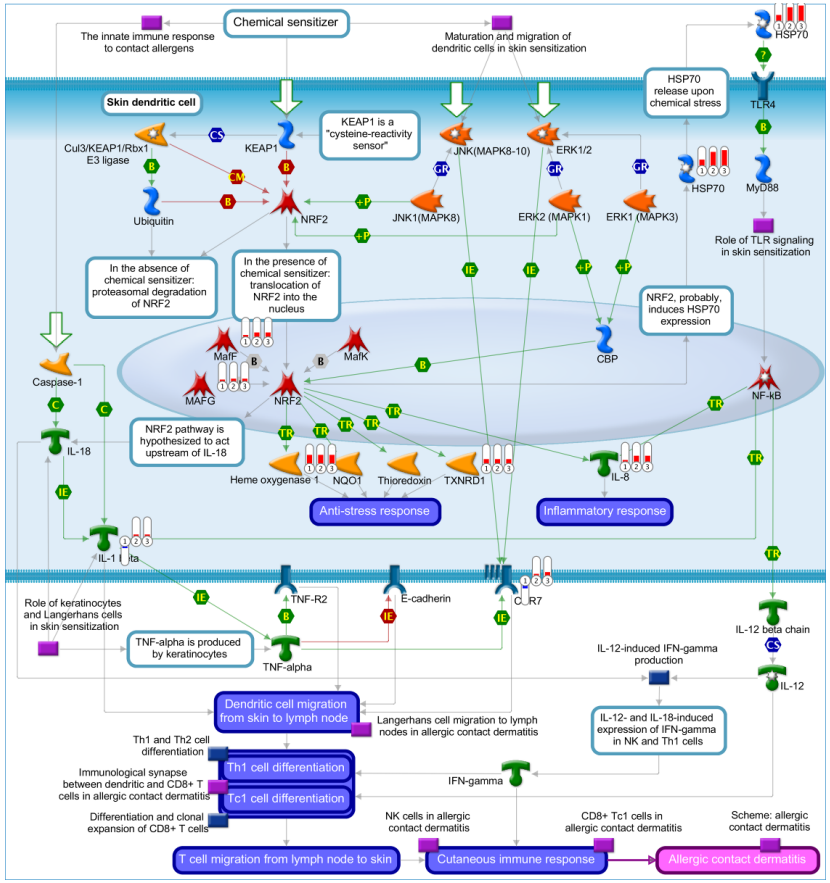

Figure 4-12 KEAP1/NRF2 pathway as a cellular sensor for skin sensitisers

Differentially expressed genes involved in the Nrf2 signalling pathway from MetaCore. The thermometers show up-regulated (red) and down-regulated (blue) gene changes at 20μM (1), 27.5μM (2) and 30μM (3).

Upstream regulator analysis

In order to identify potential triggers of the differential gene expression, the data were analysed in IPA to find upstream regulators that drive similar gene expression profiles. A closer match of up- and down-regulation leads to greater statistical significance. Upstream regulators include drugs, chemicals and endogenous molecules.

From this analysis, TNF, MEK/ERK, JNK, p38MAPK, NF-κB, TLR, and EGFR signalling (or their chemical inhibitors) were highlighted (Table 4-7). Three of these upstream regulators (p38MAPK, JNK and NF-κB) are shown as examples, alongside the corresponding gene profiles from our data (Figure 4-13 and 4-14).

Transcription factor target analysis

Another analysis method to investigate which factors control the differentially expressed genes in the data is to detect over-represented transcription factor:promoter binding sites. The open access, web-based oPOSSUM software (http://opossum.cisreg.ca/oPOSSUM3) was used for this purpose. The standard JASPAR CORE profile database was used with the following default settings: a minimum specificity of 8 bits, and a matrix match threshold of 85% with 5000/5000 upstream/downstream sequence were chosen. The top 30 transcription factors (sorted by z-score) are listed (Table 4-8).

Rank	Upstream regulator	Molecule type	Predicted activation state	Activation z-score	p-value of overlap
1	TNF	Cytokine	Activated	3.303	2.51E-16
2	PDGF BB	Complex	Activated	3.216	6.81E-15
3	SB203580	chemical - kinase inhibitor	Inhibited	-2.446	3.13E-13
4	IL1B	Cytokine	Activated	3.411	1.11E-12
5	25-hydroxycholesterol	chemical reagent	Activated	2.157	2.44E-12
6	P38 MAPK	Group	Activated	2.809	2.49E-12
7	CREB1	transcription regulator	Activated	3.066	5.28E-12
8	PD98059	chemical - kinase inhibitor	Inhibited	-3.773	1.29E-11
9	IRAK4	Kinase			1.87E-11
10	NFkB (complex)	Complex	Activated	2.909	2.02E-11
11	poly rI:rC-RNA	chemical reagent	Activated	3.449	2.68E-11
12	LDL	Complex		1.88	2.82E-11
13	IKBKB	Kinase		1.088	3.12E-11
14	lipopolysaccharide	chemical drug	Activated	3.999	3.36E-11
15	IL10	Cytokine		-0.671	4.70E-11
16	SP600125	chemical - kinase inhibitor	Inhibited	-3.097	2.45E-10
17	prostaglandin E2	chemical - endogenous mammalian	Activated	2.285	2.48E-10
18	TREM1	transmembrane receptor	Activated	2.25	2.58E-10
19	U0126	chemical - kinase inhibitor	Inhibited	-3.541	3.67E-10
20	thapsigargin	chemical toxicant	Activated	2.93	6.58E-10
21	cholesterol	chemical - endogenous mammalian		0.747	9.33E-10

Rank	Upstream regulator	Molecule type	Predicted activation state	Activation z-score	p-value of overlap
22	Jnk	Group	Activated	2.278	1.04E-09
23	TAC1	Other	Activated	2.376	1.66E-09
24	SFTPA1	transporter	Inhibited	-2.646	1.66E-09
25	Pka	complex		1.664	1.82E-09
26	BAPTA-AM	chemical reagent	Inhibited	-2.401	2.10E-09
27	cycloheximide	chemical reagent		1.142	2.88E-09
28	PPRC1	transcription regulator	Activated	2.401	3.82E-09
29	EGF	growth factor	Activated	3.197	3.84E-09
30	IL4	cytokine		1.876	4.25E-09

Table 4-7 Upstream regulator analysis

List of top 30 upstream regulators matching the gene expression profile induced by DNCB, ranked by p-value, from IPA.

a

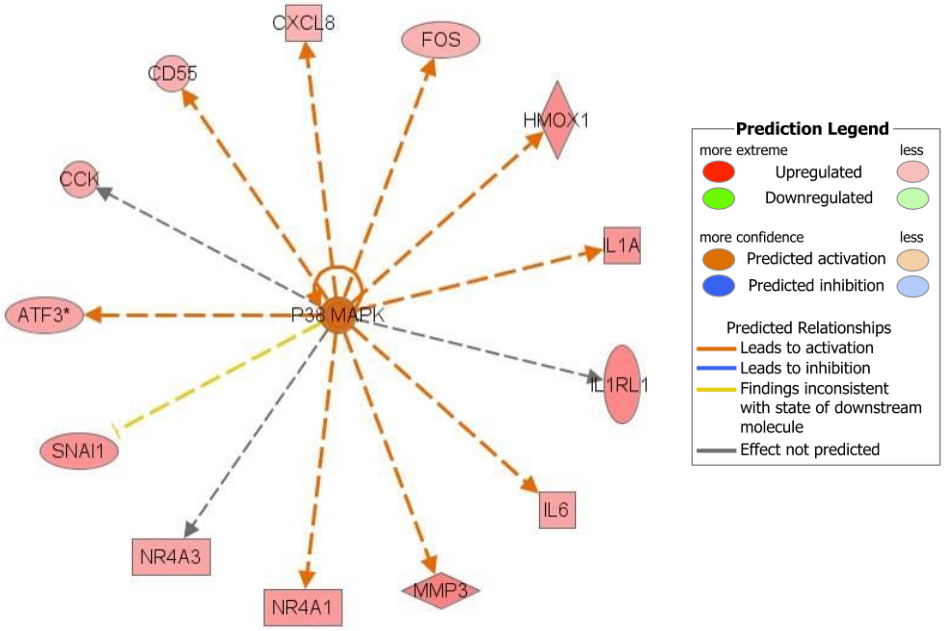

b

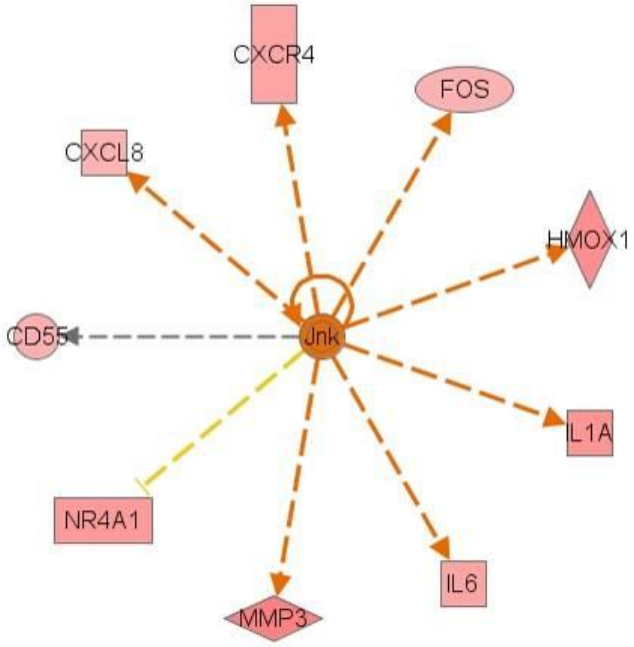

Figure 4-13 p38MAPK and JNK as upstream regulators

Upstream regulators consistent with modulation of many of the differentially expressed genes include p38MAPK (a) and JNK (b), from IPA. Orange arrows = predicted activation, yellow arrows = inconsistent effect compared to upstream regulator, grey arrow = association with unknown direction. Red nodes = up-regulated gene in our data.

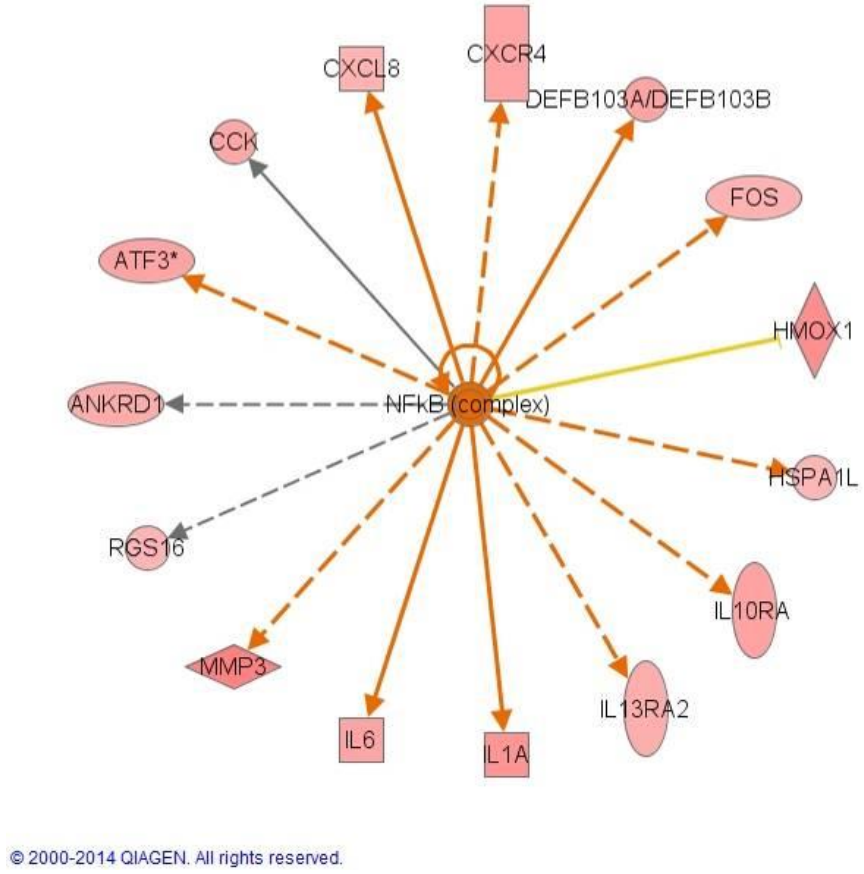

Figure 4-14 NF-κB as an upstream regulator

NF-κB was highlighted as a potential upstream regulator consistent with modulation of many of the differentially expressed genes, from IPA. Orange arrows = predicted activation, yellow arrows = inconsistent effect compared to upstream regulator, grey arrow = association with unknown direction; solid lines = direct interaction. Red nodes = up-regulated gene in our data.

Transcription factor	Family	z-score	Fisher score
SP1	BetaBetaAlpha-zinc finger	26.086	41.418
Klf4	BetaBetaAlpha-zinc finger	22.166	52.038
Egr1	BetaBetaAlpha-zinc finger	19.959	30.373
MZF1_1-4	BetaBetaAlpha-zinc finger	17.869	30.006
MZF1_5-13	BetaBetaAlpha-zinc finger	16.712	35.152
SRF	MADS	16.529	16.963
NF-kappaB	Rel	15.382	33.832
NFYA	NFY CCAAT-binding	15.038	18.468
HIF1A::ARNT	Helix-Loop-Helix	14.034	32.222
REL	Rel	14.024	26.299
Arnt	Helix-Loop-Helix	13.735	25.797
ELK1	Ets	13.571	26.699
Arnt::Ahr	Helix-Loop-Helix	11.314	25.139
SPI1	Ets	11.178	27.077
ELF5	Ets	10.609	30.924
Mycn	Helix-Loop-Helix	10.498	18.287
NFKB1	Rel	9.844	18.248
SPIB	Ets	9.844	37.179
IRF1	IRF	9.539	16.336
FOXO3	Forkhead	9.531	18.689
USF1	Helix-Loop-Helix	9.301	24.834
FEV	Ets	9.264	25.244
Stat3	Stat	9.16	28.072
RELA	Rel	8.843	24.486
ZNF354C	BetaBetaAlpha-zinc finger	8.819	40.238
TEAD1	Homeo	8.745	12.536
Myc	Helix-Loop-Helix	8.66	18.038
INSM1	BetaBetaAlpha-zinc finger	8.613	22.643
E2F1	E2F	8.452	18.353

Table 4-8 Transcription factor target analysis

List of the top 30 transcription factors controlling the differential gene expression induced by DNCB, ranked by z-score, from oPOSSUM. Fisher score = negative natural logarithm of the p-values.

Network analysis

In order to gain a less restricted view of the data, network analysis was performed. Pathway analysis is restricted to known canonical pathways, whereas network analysis allows overlaying of data onto all known protein:protein interactions.

A human interactome database (http://wiki.cytoscape.org/Data_Sets, Annotated human interactome 2007, courtesy of Andrew Garrow) was loaded into the Cytoscape 3.1 platform (http://www.cytoscape.org/). This database contains information about which proteins are known from literature to interact with each other. In Cytoscape, the proteins are designated nodes and the interactions edges, which allows the formation of a network diagram. A DNCB gene-list ($p(corr) < 0.05$ and fold change > 1.5) was overlaid onto this network and the non-changing proteins in the network filtered out, leaving only the differentially expressed genes (Figure 4-15). Detailed views focused on individual hubs are shown in Figures 4-16 and 4-17.

Gene expression of cytokines, chemokines, heat shock and keratin-related proteins

We searched for interleukins (Table 4-9) and chemokines (Table 4-10) in the gene expression data to obtain a general view of cytokine and chemokine transcription in response to DNCB. Also, many of the top fold change genes were heat-shock or keratin-related proteins, therefore we specifically searched for these families in the data (Table 4-11 and 4-12).

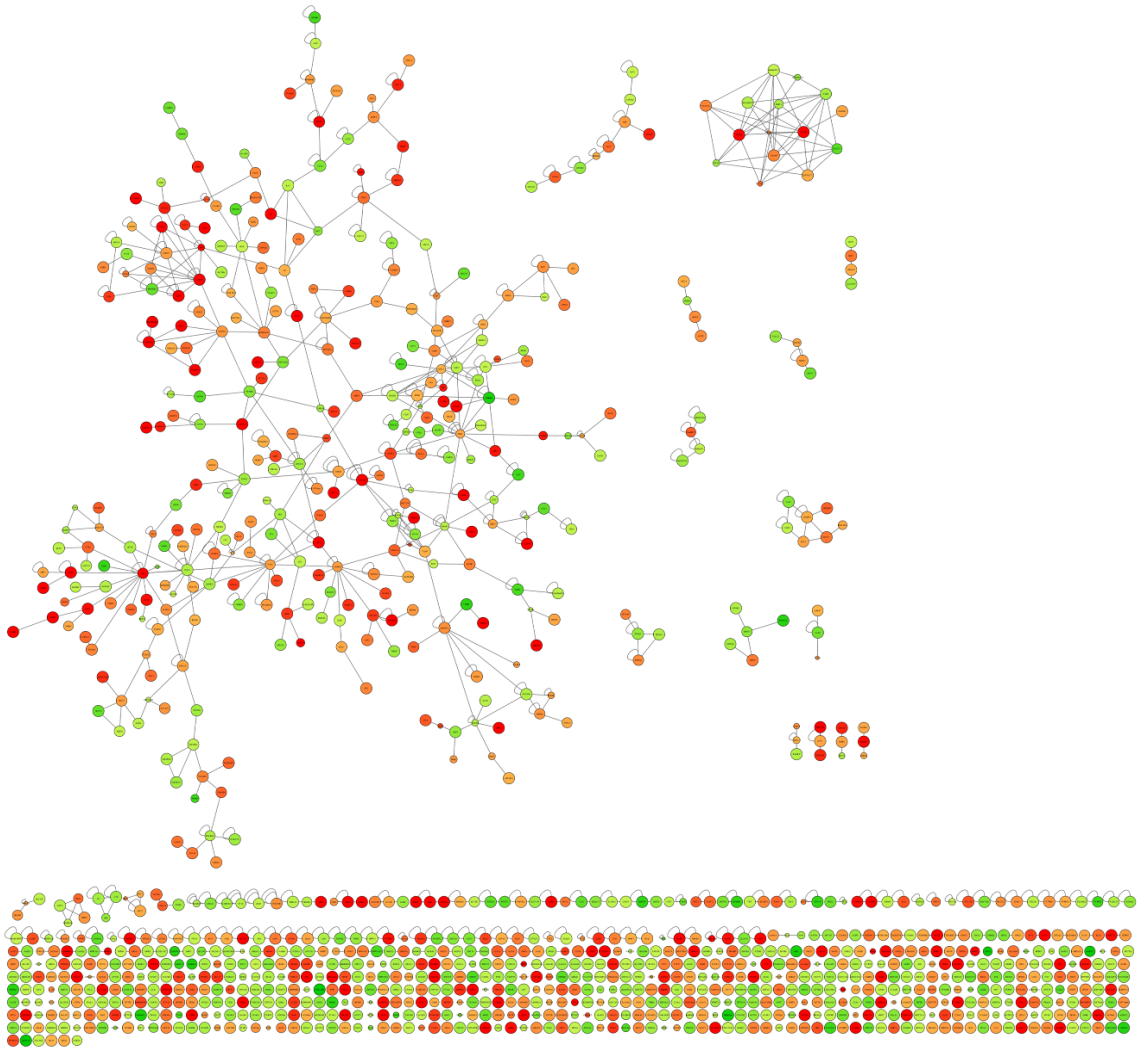

Figure 4-15 Network analysis: full network

The significantly differentially expressed genes in response to DNCB (p(corr) < 0.05 and fold change > 1.5) were overlaid onto a human interactome network. Nodes coloured by fold change (red = up-regulated, green = down-regulated). Nodes sized by p(corr), largest = most significant.

a

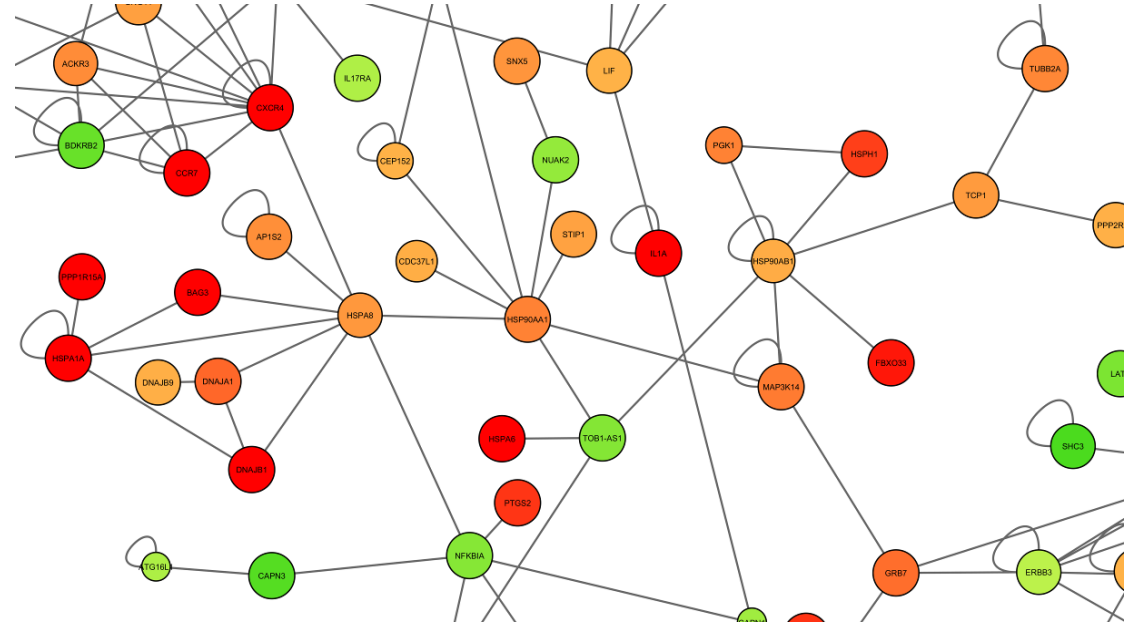

b

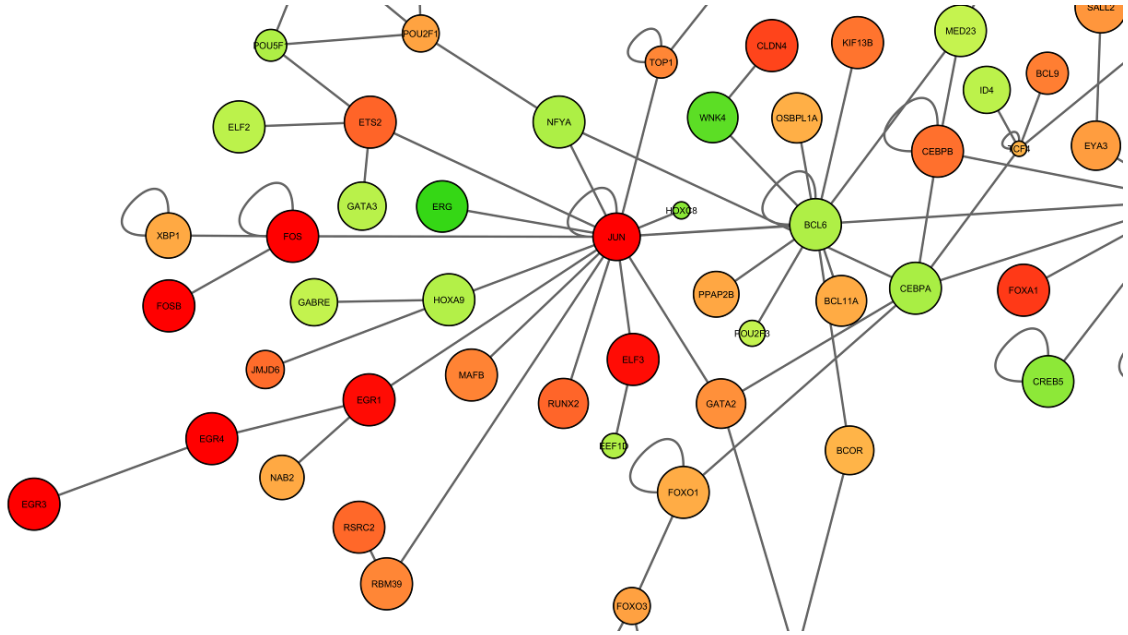

Figure 4-16 Network analysis: sub-networks - Heat shock proteins and JUN

Detailed view of the network focussing on heat shock proteins (a) and JUN (b) sub-networks. Nodes coloured by fold change (red = up-regulated, green = down-regulated). Nodes sized by p(corr), largest = most significant.

a

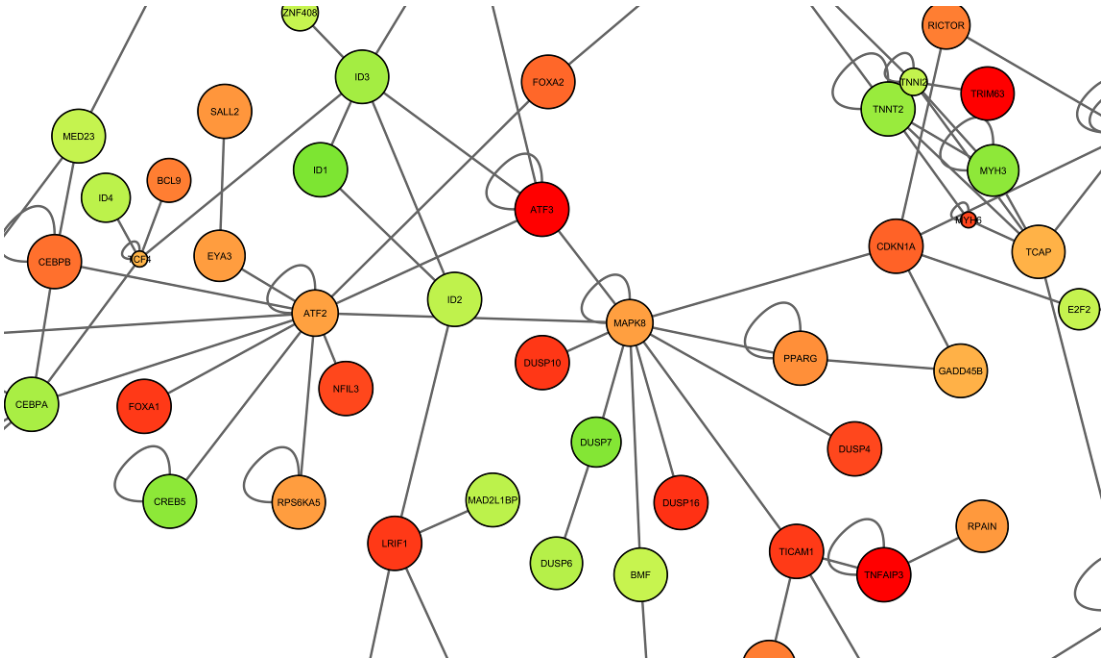

b

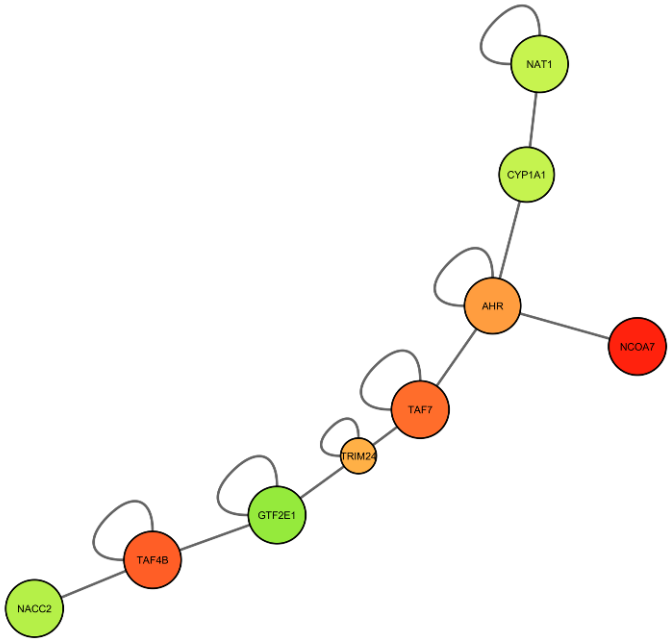

Figure 4-17 Network analysis: sub-networks – MAPK and AhR

Detailed view of the network focussing on MAPK (a) and AhR (b) sub-networks. Nodes coloured by fold change (red = up-regulated, green = down-regulated). Nodes sized by p(corr), largest = most significant.

Gene symbol	Gene name	FC (abs) DNCB 30μM	Regulation DNCB	p (Corr) DNCB	FC (abs) SDS 250μM	Regulation SDS	p (Corr) SDS
IL1RL1	interleukin 1 receptor-like 1	41.927	up	5.073E-05	13.491	Up	9.811E-05
IL1A	interleukin 1, alpha	27.385	up	7.639E-06	5.961	Up	7.224E-05
IL10RA	interleukin 10 receptor, alpha	17.810	up	6.836E-04	1.127	Up	8.716E-01
IL6	interleukin 6 (interferon, beta 2)	16.827	up	5.301E-06	1.315	Up	1.894E-02
IL13RA2	interleukin 13 receptor, alpha 2	12.498	up	5.766E-05	4.554	Up	7.224E-05
IL8	interleukin 8	10.644	up	4.512E-02	2.348	Up	2.768E-01
IL16	interleukin 16	3.263	down	3.512E-03	1.433	Up	8.478E-02
IL1R2	interleukin 1 receptor, type II	2.441	up	4.514E-04	3.855	Up	7.224E-05
IL1RN	interleukin 1 receptor antagonist	2.095	up	4.037E-03	1.000	down	9.970E-01
IL1B	interleukin 1, beta	2.002	up	1.676E-05	1.609	Up	2.708E-04
IL7R	interleukin 7 receptor	1.979	up	4.158E-02	2.303	Up	1.310E-02
IL7R	interleukin 7 receptor	1.945	up	6.966E-02	2.562	Up	2.294E-02
IL33	interleukin 33	1.937	up	3.899E-01	1.115	down	4.747E-01
IL17RA	interleukin 17 receptor A	1.812	down	5.073E-05	1.154	down	2.198E-02
IL1R2	interleukin 1 receptor, type II	1.785	up	4.967E-02	3.632	Up	1.018E-03
IL11	interleukin 11	1.633	down	2.123E-03	1.810	Up	7.832E-03

Table 4-9 Gene expression of interleukins

A list of interleukins that have a fold change greater than 1.5 in response to DNCB (at 30μM).

Gene symbol	Gene name	FC (abs) DNCB 30μM	Regulation DNCB	p (Corr) DNCB	FC (abs) SDS 250μM	Regulation SDS	p (Corr) SDS
CCL18	chemokine (C-C motif) ligand 18 (pulmonary and activation-regulated)	18.544	up	1.67E-03	1.079	down	8.96E-01
CXCR4	chemokine (C-X-C motif) receptor 4	16.464	up	1.57E-04	1.366	up	2.32E-01
CCL3	chemokine (C-C motif) ligand 3	6.770	up	2.59E-03	1.610	up	3.25E-01
CX3CL1	chemokine (C-X3-C motif) ligand 1	4.707	up	2.27E-03	1.229	down	3.30E-01
CCL3L3	chemokine (C-C motif) ligand 3-like 3	4.490	up	2.27E-03	1.077	up	8.67E-01
CCR7	chemokine (C-C motif) receptor 7	4.105	up	7.28E-04	1.459	up	1.33E-01
CCL4	chemokine (C-C motif) ligand 4	3.141	up	5.21E-03	1.684	up	2.32E-01
CCL26	chemokine (C-C motif) ligand 26	3.009	up	4.10E-04	1.022	down	8.66E-01
CCL26	chemokine (C-C motif) ligand 26	2.959	up	1.05E-04	1.078	down	3.16E-01
CCL3L3	chemokine (C-C motif) ligand 3-like 3	2.772	up	7.98E-03	1.183	up	5.03E-01
CCR2	chemokine (C-C motif) receptor 2	2.613	up	2.72E-02	1.978	up	6.64E-02
CCL2	chemokine (C-C motif) ligand 2	2.553	down	7.35E-05	5.008	down	6.63E-05
CX3CL1	chemokine (C-X3-C motif) ligand 1	2.191	up	1.71E-01	1.310	down	5.68E-01
CCL7	chemokine (C-C motif) ligand 7	2.069	down	7.05E-03	2.098	down	8.27E-03
CCL25	chemokine (C-C motif) ligand 25	2.039	up	5.52E-02	1.194	up	4.62E-01
CXCR5	chemokine (C-X-C motif) receptor 5	2.033	up	4.85E-01	1.072	down	8.60E-01

Gene symbol	Gene name	FC (abs) DNCB 30μM	Regulation DNCB	p (Corr) DNCB	FC (abs) SDS 250μM	Regulation SDS	p (Corr) SDS
ACKR3	atypical chemokine receptor 3	1.866	up	2.27E-03	1.537	down	2.09E-02
CXCR2P1	chemokine (C-X-C motif) receptor 2 pseudogene 1	1.730	down	7.98E-03	1.178	up	8.67E-01
CCR3	chemokine (C-C motif) receptor 3	1.681	up	4.28E-01	1.046	up	9.14E-01
CCR4	chemokine (C-C motif) receptor 4	1.574	up	4.29E-01	3.995	up	3.25E-01

Table 4-10 Gene expression of chemokines

A list of chemokines that have a fold change greater than 1.5 in response to DNCB (at 30μM).

Gene symbol	Gene name	FC (abs) DNCB 30μM	Regulation DNCB	p (Corr) DNCB	FC (abs) SDS 250μM	Regulation SDS	p (Corr) SDS
HSPA6	heat shock 70kDa protein 6 (HSP70B')	611.867	up	3.31E-07	1.840	down	7.17E-03
HSPA1L	heat shock 70kDa protein 1-like	9.920	up	4.83E-06	2.037	down	1.57E-03
HSPA1A	heat shock 70kDa protein 1A	8.479	up	4.83E-06	1.417	down	1.97E-02
HSPA1A	heat shock 70kDa protein 1A	7.477	up	1.72E-06	1.419	down	7.17E-03
HSPB8	heat shock 22kDa protein 8	3.754	up	6.91E-04	1.897	up	7.45E-02
HSPH1	heat shock 105kDa/110kDa protein 1	3.619	up	1.36E-06	1.159	up	7.38E-02
HSPA12A	heat shock 70kDa protein 12A	3.574	down	2.14E-02	1.414	down	4.72E-01
HSPA1A	heat shock 70kDa protein 1A	3.502	up	4.83E-06	1.335	down	7.17E-03
HSPB3	heat shock 27kDa protein 3	2.926	down	9.59E-05	1.167	down	2.12E-01
HSPH1	heat shock 105kDa/110kDa protein 1	2.842	up	6.77E-07	1.106	up	1.68E-01
HSPD1	heat shock 60kDa protein 1 (chaperonin)	2.655	up	1.04E-03	1.096	down	6.10E-01
HSP90AA1	heat shock protein 90kDa alpha (cytosolic), class A 1	1.978	up	8.72E-04	1.115	up	3.00E-01
HSP90AA1	heat shock protein 90kDa alpha (cytosolic), class A 1	1.962	up	1.48E-02	1.257	down	4.52E-01
HSPA4	heat shock 70kDa protein 4	1.866	up	1.08E-03	1.003	up	9.60E-01
HSPB9	heat shock protein, alpha-crystallin-related, B9	1.813	down	1.96E-03	1.240	up	1.54E-01
AHSA1	AHA1, activator of heat shock 90kDa protein ATPase homolog 1 (yeast)	1.811	up	1.08E-03	1.009	up	9.31E-01
HSPA8	heat shock 70kDa protein 8	1.753	up	1.96E-03	1.095	up	4.60E-01

Gene symbol	Gene name	FC (abs) DNCB 30μM	Regulation DNCB	p (Corr) DNCB	FC (abs) SDS 250μM	Regulation SDS	p (Corr) SDS
HSP90AB6P	heat shock protein 90kDa alpha (cytosolic), class B member 6, pseudogene	1.723	up	4.87E-01	1.133	down	8.76E-01
HSP90AA1	heat shock protein 90kDa alpha (cytosolic), class A 1	1.701	up	2.17E-02	1.039	down	8.48E-01
HSP90AB1	heat shock protein 90kDa alpha (cytosolic), class B 1	1.687	up	1.36E-04	1.012	up	8.48E-01
HSPA13	heat shock protein 70kDa family, member 13	1.647	up	1.51E-03	1.203	up	1.54E-01
HSPD1	heat shock 60kDa protein 1 (chaperonin)	1.616	up	1.56E-04	1.074	up	1.68E-01

Table 4-11 Gene expression of heat shock proteins

A list of heat shock proteins that have a fold change greater than 1.6 in response to DNCB (at 30μM).

Gene symbol	Gene name	FC (abs) DNCB 30μM	Regulation DNCB	p (Corr) DNCB	FC (abs) SDS 250μM	Regulation SDS	p (Corr) SDS
KRTAP1-5	keratin associated protein 1-5	61.849	up	9.15E-05	1.558	Up	1.39E-01
KRTAP3-2	keratin associated protein 3-2	57.664	up	2.16E-02	1.294	down	8.54E-01
KRT34	keratin 34	28.499	up	1.69E-04	2.179	Up	3.70E-02
KRTAP1-3	keratin associated protein 1-3	18.977	up	8.84E-03	1.939	Up	3.09E-01
KRTAP4-1	keratin associated protein 4-1	11.352	up	5.25E-03	1.000	Up	1.00E+00
KRTAP4-6	keratin associated protein 4-6	7.793	up	8.84E-03	1.074	Up	8.65E-01
KRTAP1-1	keratin associated protein 1-1	5.818	up	1.77E-04	1.240	Up	3.25E-01
KRTAP3-1	keratin associated protein 3-1	4.609	up	3.82E-03	1.018	down	9.47E-01
KRT27	keratin 27	4.027	up	7.19E-02	2.980	Up	1.55E-01
KRTAP2-3	keratin associated protein 2-3	3.897	up	2.50E-03	1.920	Up	4.09E-02
KRTAP9-2	keratin associated protein 9-2	2.737	up	4.77E-01	1.865	down	6.13E-01
KRT6B	keratin 6B	2.138	down	2.15E-03	2.382	Up	6.03E-04
KRTAP1-1	keratin associated protein 1-1	2.051	up	2.05E-02	1.477	down	3.10E-01
KRT23	keratin 23 (histone deacetylase inducible)	1.856	down	2.23E-03	1.645	Up	1.65E-02

Gene symbol	Gene name	FC (abs) DNCB 30μM	Regulation DNCB	p (Corr) DNCB	FC (abs) SDS 250μM	Regulation SDS	p (Corr) SDS
KRTAP19-1	keratin associated protein 19-1	1.825	up	3.32E-01	2.002	Up	2.88E-01
KRTAP4-12	keratin associated protein 4-12	1.710	up	2.17E-01	1.145	Down	6.22E-01
KGFLP2	keratinocyte growth factor-like protein 2	1.675	down	5.66E-01	1.440	Down	6.22E-01
KRT33B	keratin 33B	1.624	up	1.74E-01	1.017	up	9.58E-01
KRTAP2-3	keratin associated protein 2-3	1.567	up	4.19E-01	1.036	up	9.31E-01

Table 4-12 Gene expression of keratins and keratin associated proteins

A list of keratins and keratin associated proteins that have a fold change greater than 1.5 in response to DNCB (at 30μM).

4.3 Discussion

In this chapter, we investigated the transcriptional response of HaCaT cells to a model sensitiser (DNCB) and a model irritant (SDS). We observed large differences in gene expression between the two chemicals, as was initially evident from our principal component analysis of the raw signal intensities from the arrays. The overlap between significantly differentially expressed genes was small, and gene ontology analysis showed that different processes were being affected. In general, the most over-represented gene ontologies in response to DNCB were regulation of transcription, whereas in response to SDS they were mainly regulation of cell death. These differences might be caused by the different chemistries of DNCB and SDS. The electrophilic nature of DNCB makes it likely to covalently modify any exposed nucleophilic amino acids on proteins (Aleksic et al, 2007), and it is possible that this could change their functional state and lead to changes in transcription. Conversely, SDS is an amphiphilic anionic surfactant that can cause membrane disruption leading to necrotic cell death (Pastore et al, 1995).

From the transcriptomic analysis, we see differential expression of cytokines, chemokines and growth factors, which are consistent with the cytokine release seen from HaCaT cells in the previous chapter. For example, IL-1β, IL-6 and IL-8 were 2, 17 and 10.6-fold up-regulated (respectively) on the arrays, which correspond to 2, 15 and 8-fold seen in chapter 3 by qRT-PCR. Also, the increase in IL-1RA and decrease in MCP-1 seen at the protein level in chapter 3 were mirrored in the array data (IL-1RA 2.1-fold up, MCP-1 2.6-fold down). IL-1α, although not found to be released by the cells in the previous chapter, was 27-fold up-regulated at the transcriptional level, indicating that it is actively synthesised but remains pre-stored (Cohen et al, 2010; Corsini et al, 1998; Coquette et al, 2003). TNFα was only 1.37-fold increased at 4 hours, however, it was the most significant upstream regulator found in pathway analysis, and also, TNFα induced protein 3 (TNFAIP3) was up to 5-fold upregulated, indicating that TNFα may have been present at an earlier time.

In response to DNCB, transcription of IL-1 family cytokines and receptors included both stimulatory and inhibitory components, suggesting activation of IL-1 signalling in a tightly regulated manner. For instance, we saw up-regulation of agonists IL-1α and IL-1β as well as the antagonist IL-1RA and the inhibitory decoy receptor interleukin-1 receptor type 2 (IL-1R2). Keratinocytes have been shown by others to express IL-1R2 (Lukiw et al, 1999; Yamaki et al, 2010), which inhibits local inflammation induced by IL-1 (Rauschmayr et al, 1997), since it binds IL-1 but lacks a signal transmission domain, preventing a response to the ligand. IL-1R2 also binds to intracellular IL-1α and protects it from cleavage to its active form (Zheng et al, 2013). This may contribute to the lack of IL-1α release we observed in response to DNCB.

Another gene from the IL-1 family, interleukin-1 receptor-like 1 (IL-1RL1) was significantly up-regulated in response to DNCB, with the highest fold change of all interleukin-related genes (42-fold). Its ligand, IL-33, was also up-regulated although just under 2-fold, and has been shown to be expressed in the nucleus of keratinocytes (Moussion et al, 2008). IL-33 signalling is known to drive Th2 responses (Schmitz et al, 2005), and more recently $CD8^+$ responses (Bonilla et al, 2012). Recent evidence has shown that IL-33 plays an important role in responses to contact allergens. The abrogation of IL-33 has been shown to reduce ear swelling in mouse CHS (Taniguchi et al, 2013), and it has been found to be expressed in human skin during ACD (Mattii et al, 2013). Our data indicate that these *in vivo* responses may be driven by keratinocyte-derived IL-33.

In addition to pro-inflammatory cytokines, we saw transcription of genes that suggest anti-inflammatory components of the response. For example, the receptor for the anti-inflammatory cytokine IL-10 (IL-10RA) and the decoy receptor for IL-13 (IL-13RA2; Kawakami et al, 2001) were strongly up-regulated in HaCaT cells. Also, unexpectedly, the IL-17 receptor (IL-17RA) was slightly down-regulated (1.8-fold), which would act to reduce the effect of Th17 cells known to be involved in ACD (Larsen et al, 2009; Pennino et al, 2010).

We also saw down-regulation of IL-11 in response to DNCB. It is possible that down-regulation of IL-11 may increase the CHS response, since administration of recombinant human IL-11 decreases CHS reactions (Peterson et al, 2000).

Many chemokines that drive the infiltration of both innate and adaptive immune cells into the epidermis were found to be modulated in response to DNCB. In addition to IL-8 and MCP-1 (previously discussed), several of the other differentially expressed chemokines are known to be involved in ACD. CCL3, a chemotractant for granulocytes, and CCL4, a chemoattractant for T cells, NK cells and monocytes, were both up-regulated in our data and have been shown to be expressed in skin during elicitation to contact allergens (Goebeler et al, 2001). CCL18, which is known to attract naïve T cells (Adema et al, 1997) and cause maturation of macrophages (Schraufstatter et al, 2012), has been seen *in vivo* during elicitation to contact sensitisers (Goebeler et al, 2001; Pivarcsi et al, 2004). The $CD4^+$ T cell chemoattractant IL-16 (reviewed in Center et al, 1996) is also known to be involved in CHS (Yoshimoto et al, 2000). It is expressed in the epidermis during sensitisation and elicitation to TNCB and oxazolone (Masuda et al, 2005), and polymorphisms in its promoter have been associated with increased susceptibility to ACD (Reich et al, 2003). In contrast to this, we observed a decrease in IL-16 in response to DNCB, therefore it is possible that a different cell type is the source of IL-16 during CHS.

The other differentially expressed chemokines have not previously been associated with CHS. However, given their ability to attract granulocytes (CCL26), T cells (CCL25, CX3CL1), monocytes (CCL7), macrophages and dendritic cells (CCL25), their up-regulation is likely to assist cutaneous immune responses to chemical exposure. For example, CX_3CL1 is a T cell chemoattractant that also facilitates adhesion to T cells (Bazan et al, 1997), and is expressed in human skin and keratinocyte cell lines (Sugaya et al, 2003). Therefore, it is plausible that it may be involved in elicitation of CHS. Further study would be required to determine which of the differentially expressed chemokines have essential roles in CHS.

In addition to the chemokine expression, transcription of several chemokine receptors was seen. Some of these have been observed previously on keratinocytes: CCR3 has

been found to be expressed in keratinocytes in response to IL-4 (Kagami et al, 2005); CCR4 and CXCR4 have been shown to be expressed by keratinocytes (Kroeze et al, 2012); and CXCR4 is also involved in the regulation of keratinocyte proliferation (Takekoshi et al, 2013). Differentially expressed chemokine receptors CCR2 and CCR7, from our study, were not previously detected in skin (Kroeze et al, 2012), and CXCR5 has, to our knowledge, not been reported to be expressed on keratinocytes.

We saw a striking up-regulation of many heat shock proteins (Hsp) in response to DNCB, which was not seen in response to SDS. Many of these had gene expression fold-changes greater than 10 that were highly significant. The differentially expressed Hsp clustered together in network analysis, alongside DnaJ proteins, also known as Hsp40. Hsp are essential for protein folding and degradation, and the DnaJ family regulate the activity of Hsp70 by stimulating ATP hydrolysis, enabling Hsp70 to bind to unfolded polypeptides (Qiu et al, 2006). The Hsp response to DNCB was also highlighted in pathway analysis, where the Hsp60/70 pathway was one of the most significant found. In common with our observation, others have seen transcription of Hsp in keratinocytes in response to sensitisers: HSPA1B (Vandebriel et al, 2010); HSPA6, HSPH1, DNAJB4 (Saito et al, 2013); DNAJB1 and DNAJB4 (Yoshikawa et al, 2010). Keratinocytes have been shown to produce Hsp70 and Hsp27 in response to osmotic stress (Garmyn et al, 2001). Yusuf et al (2009) saw reduced CHS responses to DNFB with inhibition of Hsp27 or Hsp70. There is also some evidence that peptides chaperoned by Hsp70 are presented more efficiently (Binder et al, 2001; Ishii et al, 1999) and result in larger DTH elicitation responses (Roman and Moreno, 1997). Hsp are thought to act as endogenous danger signals, since they are released from necrotic cells and are able to stimulate DC maturation (Basu et al, 2000), potentially through TLR4 (Ohashi et al, 2000).

It is possible that we saw such a large up-regulation of Hsp to process mis-folded protein caused by covalent modification by DNCB. DnaJ/Hsp40 has been shown to be important for ubiqutination processing of keratin in keratinocytes (Yamazaki et al, 2012). In our data, as well as the Hsp, we also saw many other genes from the ubiquitination pathway, including USP2, SPINK1, HTRA3 (all more than 10-fold up-regulated) and NEDD4L, UBE2B, UBE2D3, UCHL1, USP36 more than 2-fold up-regulated in response to DNCB.

We saw a large number of keratins and keratin associated proteins (KRTAP) highly up-regulated. These are known to contain a high percentage of nucleophilic residues (Rogers et al, 2006). It is possible that sensitisers haptenate these keratin proteins (Aleksic et al, 2008; Simonsson et al, 2011) and lead to loss of function, meaning that transcription is necessary to restore the cellular architecture.

Several of the gene expression analysis methods suggest the involvement of NF-κB in the response to DNCB. In the pathway analysis, NF-κB itself was not seen to be differentially expressed, however, its negative regulator IκB was down-regulated, and NF-κB inducing kinase (NIK) was up-regulated. NF-κB was also highlighted as an important upstream regulator due to the up-regulation of IL-1, IL-6, IL-8 and β-defensin. Transcriptional activity of NF-κB and its sub-components REL and RELA was inferred to be highly significant, based on up-regulation of their transcriptional targets in transcription factor analysis.

There is substantial evidence for involvement of MAPK pathways in the response to DNCB. Many of the significant pathways included up-regulation of transcription factors that are downstream of MAP kinases, e.g. ATF3, c-Jun, c-Fos, C/EBP (NF-IL6). The most striking evidence was from the upstream regulator analysis, which, due to the expression of related genes, highlighted p38MAPK, JNK, CREB (downstream of ERK) and inverse relationships with chemical inhibitors of p38MAPK, JNK and MEK1,2 (upstream of ERK). Transcription factor analysis showed the relevance of MAPK activated transcription factors Myc, ELK1 and other ETS family transcription factors. JNK was also found as a central hub in network analysis, connected to modulated DUSP 4, 6, 7, 10 and 16 which are MAPK phosphatases (reviewed in Jeffrey et al, 2007). p38MAPK and JNK phosphorylation has previously been seen in skin explants and reconstituted human epidermis exposed to DNFB or oxazolone (Koeper et al, 2007), and inhibition of p38MAPK, but not JNK or ERK, reduced CHS reactions to DNFB in mice (Ayush et al, 2013). In contrast, inhibition of JNK, but not p38MAPK or ERK, decreased TNCB-induced IL-18 expression from PAM212 keratinocytes (Yun et al, 2010).

We saw some evidence for Nrf2/ARE activity from pathway analysis, where pathways related to Nrf2 and glutathione synthesis were found to be significantly modulated in our data. The Nrf2 pathway featured in the pathway analysis due to up-regulation of MafF and MafG (which bind Nrf2 to form a transcription factor complex), and HMOX-1, TXNRD1, IL-8, GCLC and GCLM. DNCB has been shown to inhibit thioredoxin reductase (TXNRD1) and increased transcription maybe acting to recover function (Arner et al, 1995). Others have seen transcription of Nrf2-dependent genes, including HMOX-1, TXNRD1, IL-8, GCLC, GCLM, NQO1 and AKR1C2, in keratinocytes in response to sensitisers (Vandebriel et al, 2010; Saito et al, 2013; Yoshikawa et al, 2010; Van der Veen et al, 2013; Emter et al, 2013). Several groups have observed Nrf2 activation following exposure to sensitisers in DC or DC-like cells (Ade et al, 2009; Lewis et al, 2006; Megherbi et al, 2009; Migdal et al, 2013), which could be due to direct binding to Keap-1 (Kobayashi et al, 2009) or generation of sufficient reactive oxygen species (ROS) to activate Keap-1, causing release and translocation of Nrf2. *In vitro* keratinocyte assays are being developed that aim to predict sensitisation potential based on this hypothesis. KeratinoSens is based on a luciferase reporter gene under the control of the ARE of AKR1C2 in HaCaT cells (Emter et al, 2010), and SenCeeTox measures Nrf2-related genes AKR1C2, NQO1, TXN, IL-8, HMOX-1, ALDH3A1, MAFF and GCLC among 11 genes used in the prediction (McKim et al, 2010, 2012). In addition to the ARE, involvement of the xenobiotic response element (XRE) is implied by our data, since the aryl hydrocarbon receptor (AhR) and its nuclear translocator (ARNT) were highly ranked in the transcription factor analysis, and AhR was also the hub of a small cluster in the network analysis. This receptor is activated by planar aromatic hydrocarbons, and binds the XRE triggering the expression of genes related to chemical metabolism.

The pathway and transcription factor analyses of the data have given us insight into the signalling cascades that might be triggered by DNCB (MAPK, NF-κB and Nrf2). We can also use the data to speculate about potential receptor-mediated initiation of these signalling cascades. For example, NF-κB and MAPK are downstream of the IL-1R and TLRs, and we see modulation of other genes on these cascades (such as IL-1RL1, IL-1R2, TRAF6, TIRAP, TICAM1 and agonists IL-1, IL-33), as well as the TLR ligands LPS and PolyIC appearing in the list of upstream regulators. These observations

suggest the possibility that DNCB could initiate IL-1 or TLR signalling, either directly or via production of danger signals. Another possibility is the EGFR/ErbB receptors, which are upstream of MAPK. We saw the ErbB pathway amongst the highest ranked pathways, and EGF in the list of significant upstream regulators. We also saw ErbB4 and the ErbB feedback inhibitor 5-fold modulated in the data. Both EGFR and ErbB have cysteine rich extracellular domains that DNCB could bind. Alternatively, HB-EGF, a ligand for both EGFR and ErbB4, was also upregulated (4-fold).

In this chapter, we have investigated the transcriptional changes in keratinocytes in response to DNCB (summarised in Figure 4-18), and have generated some potential mechanisms by which DNCB triggers cytokine release based on mRNA profiles. In the next chapter, we will investigate the functional protein responses of some of the candidate mechanisms, including the intracellular signalling cascades NF-κB and p38MAPK, their involvement with cytokine release and potential triggering mechanisms (ROS generation and EGFR signalling).

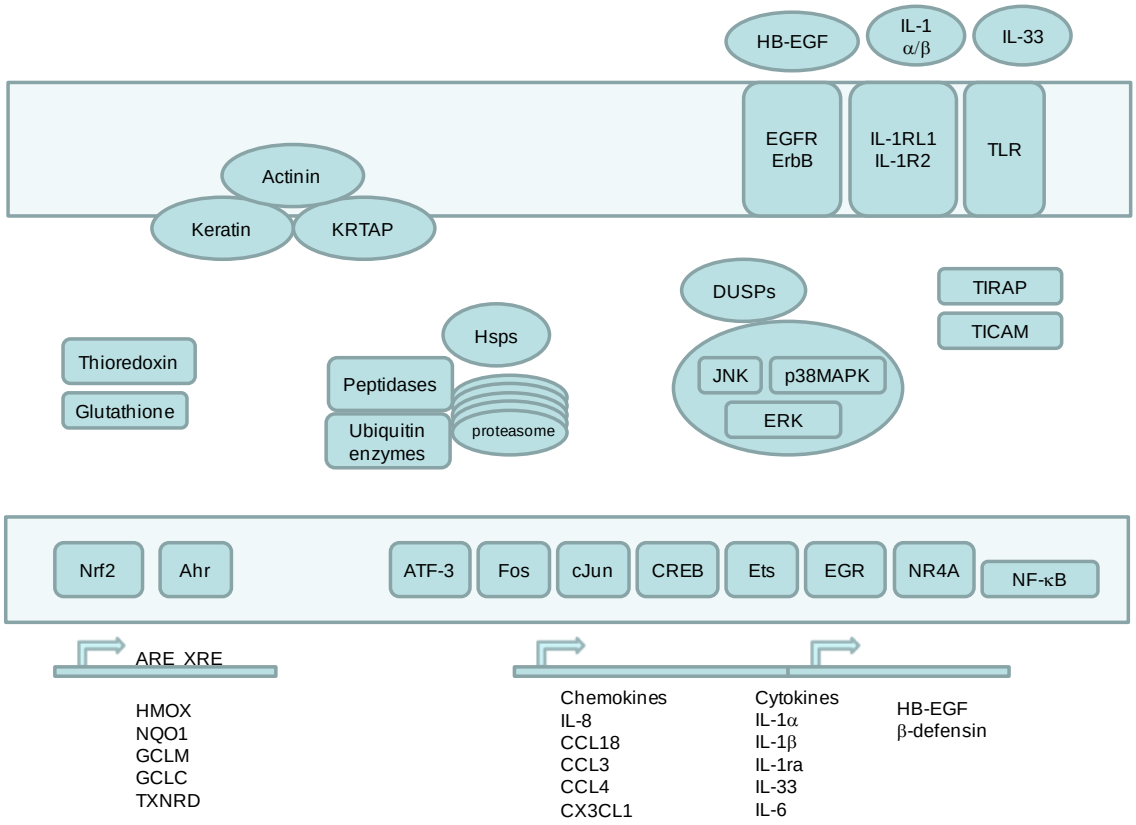

Figure 4-18 Summary of the interpretation of the transcriptomics data

The schematic includes directly modulated genes, and pathways, upstream regulators and transcription factors highlighted in analysis of the transcriptomics data.

5 ACTIVATION OF INTRACELLULAR SIGNALLING CASCADES IN HACAT CELLS FOLLOWING EXPOSURE TO DNCB

5.1 Introduction

In the previous chapter, we investigated the transcriptional response of keratinocytes to DNCB, and saw changes in the expression of genes driven by the p38MAPK, ERK, JNK, NF-κB and Nrf2 signalling cascades. In this chapter, we will investigate these mRNA findings at the functional protein level and determine if any are responsible for the sensitiser-specific cytokine profile (IL-1β, IL-6, IL-8) seen in chapter 3.

It is known that IL-1β, IL-6 and IL-8 have promoter binding sites for NF-κB (Kunsch and Rosen, 1993; Libermann and Baltimore, 1990; Hiscott et al, 1993) and for MAPK-activated transcription factors such as c-Jun and Fos (AP-1) (Faggioli et al, 2004; Cucinotta et al, 2008; Roman et al, 2000). Therefore, it is possible that one or more of these signalling pathways is driving the release of these cytokines in response to sensitiser.

Sensitiser-induced MAPK and NF-κB intracellular signalling have mostly been investigated in dendritic cells (DC) (Ade et al, 2007; Aiba et al, 2003; Antonios et al, 2009; Arrighi et al, 2001; Boisleve et al 2004; Boisleve et al 2005; Bruchhausen et al, 2003; Mizuashi et al, 2005; Trompezinski 2008) or DC-like cells (Cruz et al, 2002; Hirota et al, 2009; Suzuki et al, 2009; Matos et al, 2005a/b; Mitjans et al 2008; Miyazawa et al, 2008; Megherbi et al, 2009; Nukada et al, 2008; Iijima et al, 2003). In most cases, p38MAPK is activated in response to sensitisers, while the data are less consistent for ERK, JNK and NF-κB, and depend on the chemical or time-point investigated. The objective of several of these studies was to characterise the role of MAPK and NF-κB signalling cascades in DC maturation, measured by expression of CD83, CD86, CCR7 or HLA-DR (Ade et al, 2007; Antonios et al, 2009; Boisleve et al, 2004).

More recently, p38MAPK, ERK and JNK were also shown to be activated in keratinocytes in response to DNFB, PPD and oxazolone (Frankart et al, 2012; Galbiati

et al, 2011; Koeper et al, 2007), and NF-κB activation was observed in response to TNBS, DNBS and PPD (Galbiati et al, 2011; Miyazaki et al, 2000). MAPK signalling has been shown to be activated in skin (*in vivo*) during DNFB-induced CHS (Ayush et al, 2013), and inhibition of p38MAPK reduced the CHS ear swelling response (Ayush et al, 2013; Pastore et al, 2005).

In addition to evidence for MAPK and NF-κB activation, in the previous chapter we also found indications that sensitiser-induced cytokine gene expression changes may be triggered by EGFR/ErbB or ROS. Both of these triggers are known to stimulate the MAPK pathways (Teng et al, 2007; EGFR signalling reviewed in Lemmon and Schlessinger, 2010), and therefore represent possible mechanisms to initiate the response.

As one of the sensitiser-specific cytokines, IL-1β, has been shown to induce DCs to migrate and mature in CHS (Cumberbatch et al, 1997; Shornick et al, 2001), in addition to establishing which pathways drive the sensitiser-specific cytokine release from keratinocytes, it would be interesting to know if they have a functional effect on DCs.

The objectives of this chapter are therefore to: identify which signalling pathways are activated in response to DNCB (including the likely candidates from the previous chapter); determine which signalling cascades have a role in DNCB-driven IL-1β, IL-6 and IL-8 expression; investigate likely triggering mechanisms of these signalling pathways (receptor or ROS mediated); and test if the sensitiser-specific cytokine release has a functional effect on DC maturation.

5.2 Results

Activation of p38MAPK signalling pathway in response to DNCB

HaCaT cells were cultured in the presence of DNCB, LPS or IFNγ over a time course of 30 minutes to 24 hours. Cell lysate proteins were separated by SDS-PAGE, and di-phosphorylated (Thr^{180}/Tyr^{182}) p38MAPK (Figure 5-1a and c) and β-actin as a loading control (Figure 5-1b) were measured by western blot. One of two representative experiments is shown. In response to DNCB, p38MAPK was phosphorylated at 30 minutes, 1, 4 and 8 hours, but not at 24 hours. The phospho-p38MAPK response peaked at 1 hour and then decreased. LPS and IFNγ did not give a detectable phospho-p38MAPK signal by western blotting.

A similar experiment was performed with a reduced range of time points (30 minutes, 1 and 4 hours) and single concentrations of 30μM DNCB and 300μM SDS. Protein was extracted, and total and phosphorylated p38MAPK measured by Luminex ELISA (Figure 5-2). Data are shown as total and phosphorylated raw fluorescence measurements (a and b) and the ratio of phosphorylated:total (c and d). The graphs show mean and standard deviation (SD) from three experiments. The total protein levels of p38MAPK were relatively constant in the DNCB and SDS treated HaCaT cells. The phosphorylated:total p38MAPK ratios were significantly increased with DNCB and SDS, compared with control. The increase in the phosphorylated:total p38MAPK ratio seen in response to DNCB peaked at 1 hour, which is consistent with the western blot data.

Activation of Hsp27 in response to DNCB

Heat shock protein 27 (Hsp27) is downstream from p38MAPK in the signalling cascade. In an identical experiment to that previously described, total and phosphorylated (Ser^{82}) Hsp27 were measured by Luminex ELISA (Figure 5-3). The total protein levels of Hsp27 are constant across all treatments. The phosphorylated:total Hsp27 ratio increased in response to DNCB at all time-points, and at the early time-points (30 minutes, 1 hour) in response to SDS. All treatments, including vehicle control, show a time-dependent decrease in phospho-Hsp27.

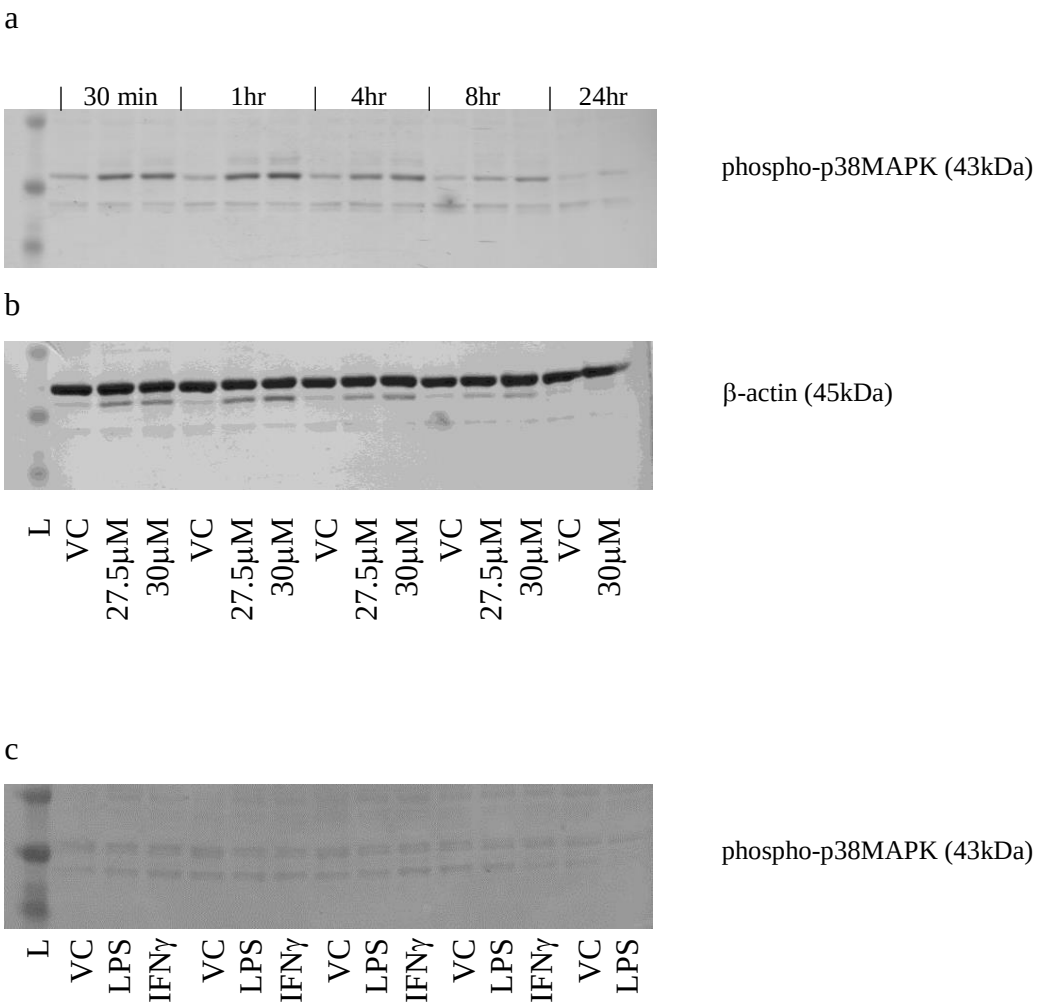

Figure 5-1 phospho-p38MAPK in response to DNCB, LPS or IFNγ

HaCaT cells were cultured in the presence of 0.2% DMSO (VC), 27.5 μM or 30μM DNCB (a and b), 1μg/ml LPS or IFNγ (c) over a time-course. Cell lysate proteins were separated by SDS-PAGE, and di-phosphorylated (Thr^{180}/Tyr^{182}) p38MAPK (a and c) and β-actin (b) were measured by western blot. One of two representative experiments is shown. L = molecular weight ladder.

a

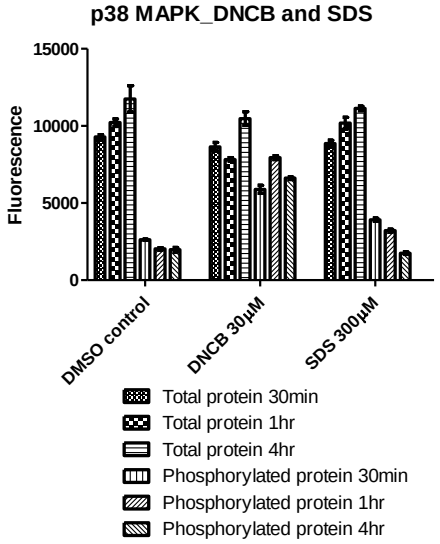

b

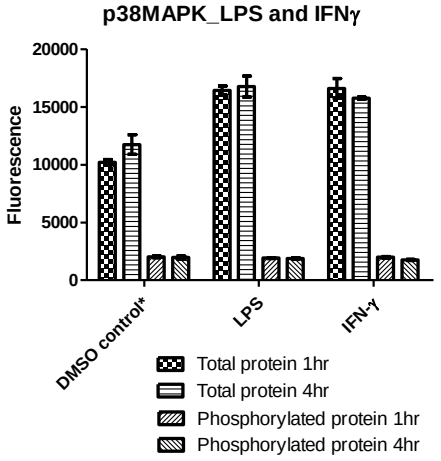

c

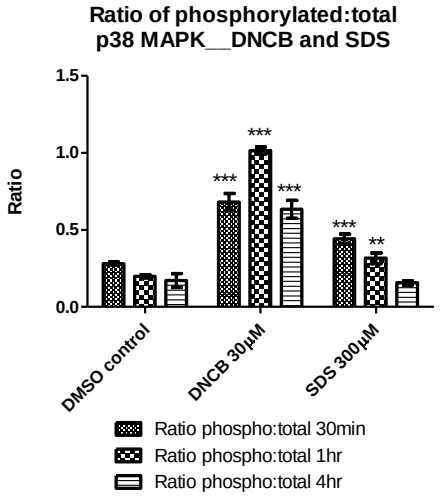

d

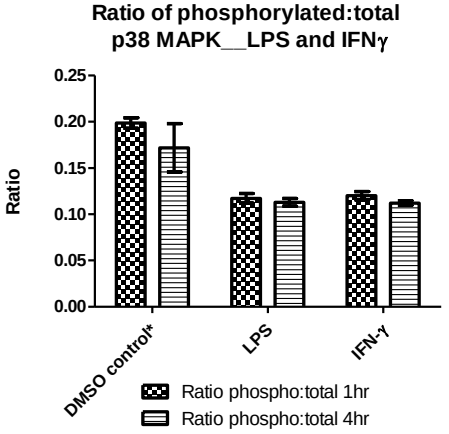

Figure 5-2 p38MAPK response to stimulation with DNCB, SDS, LPS and IFNγ

HaCaT cells were exposed to 0.2% DMSO (VC), 30µM DNCB or 300µM SDS (a and c), or 1µg/ml LPS or IFNγ (b and d) over a time-course. Protein was extracted, and total and phosphorylated p38MAPK were measured by Luminex ELISA. Data are shown as total and phosphorylated raw fluorescence measurements (a and b) and the ratio of phosphorylated:total (c and d). DMSO control data (in b and d) from DNCB/SDS experiments. The graphs show mean and SD from three experiments. Statistical analysis (c only): Two-way ANOVA with Bonferroni post-test (* $p < 0.05$, ** $p < 0.01$, *** $p < 0.001$).

a

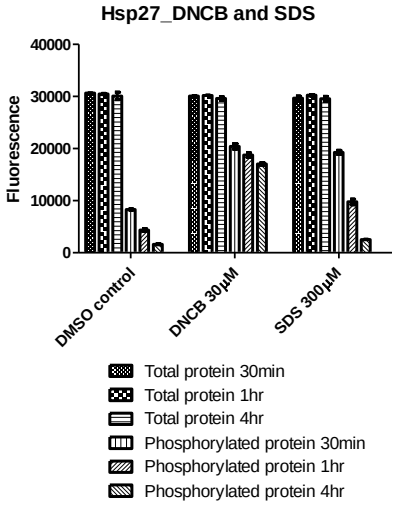

b

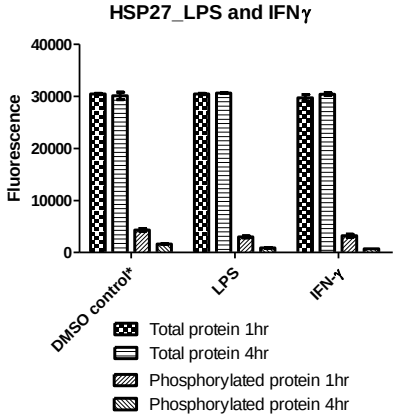

c

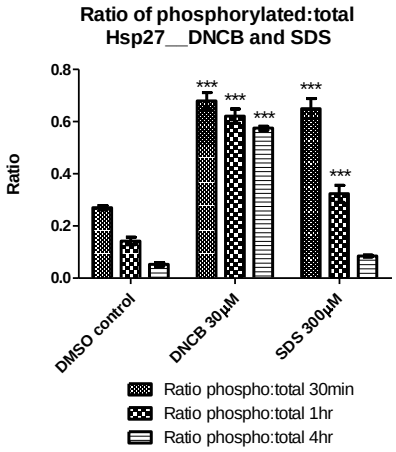

d

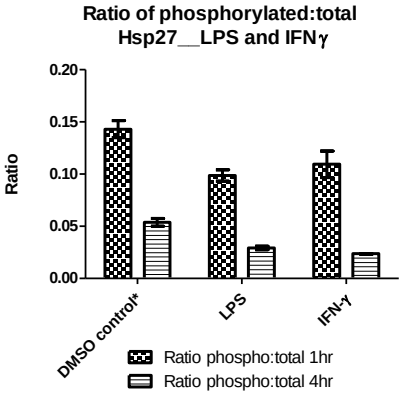

Figure 5-3 Hsp27 response to stimulation with DNCB, SDS, LPS and IFNγ

HaCaT cells were exposed to 0.2% DMSO (VC), 30µM DNCB or 300µM SDS (a and c), or 1µg/ml LPS or IFNγ (b and d) over a time-course. Protein was extracted, and total and phosphorylated Hsp27 were measured by Luminex ELISA. Data are shown as total and phosphorylated raw fluorescence measurements (a and b) and the ratio of phosphorylated:total (c and d). DMSO control data (in b and d) from DNCB/SDS experiments. The graphs show mean and SD from three experiments. Statistical analysis (c only): Two-way ANOVA with Bonferroni post-test (* $p < 0.05$, ** $p < 0.01$, *** $p < 0.001$).

Inhibition of p38MAPK signalling

HaCaT cells were exposed to increasing concentrations of the p38MAPK inhibitor SB203580 (Cuenda et al, 1995) in the presence or absence of 30μM DNCB. The MTT assay was used to assess cell viability (Figure 5-4). There was minimal effect on cell viability at all inhibitor concentrations up to 25μM. IL-1α was used as a positive control to check the efficacy of the p38MAPK inhibitor SB203580. Cells exposed to IL-1α without inhibitor showed increased phospho-p38MAPK, by western blotting (Figure 5-5). The level of phospho-p38MAPK decreased with increasing concentration of inhibitor, indicating that the inhibitor was working to suppress p38MAPK phosphorylation. A similar reduction in phosphorylation of p38MAPK has been seen previously in THP-1 cells (Frantz et al, 1998). We also measured phosphorylated Hsp27 by western blot (Figure 5-6). The level of IL-1α induced phopho-Hsp27 decreased with increasing concentration of the p38MAPK inhibitor.

IL-1β, IL-6 and IL-8 transcription in response to DNCB +/- p38MAPK inhibition

HaCaT cells were exposed to DNCB for 4 hours with increasing concentrations of the p38MAPK inhibitor SB203580. IL-1β, IL-6 and IL-8 mRNA expression were analysed by qRT-PCR (Figure 5-7). The data were plotted as fold change normalised to uninhibited vehicle control (0μM p38MAPK inhibitor, DMSO 0.15%). In the absence of DNCB, the vehicle control combined with low concentrations of inhibitor caused transcription of all three cytokines (peaking at 1-3μM SB203580). This increase was more apparent in IL-1β expression due to the lack of DNCB-induced response at 4 hours (Figure 5-7a). It is not clear what is driving the IL-1β difference with and without DNCB, it is possible that it could be due to an interaction between DNCB and the SB203580 inhibitor. The expression of IL-1β (Figure 5-7a) was unchanged in response to DNCB, and with inhibitor concentrations up to 5μM. Above this concentration of inhibitor, IL-1β message was down-regulated both in the presence and absence of DNCB. DNCB induced a strong up-regulation of IL-6 mRNA, which was significantly inhibited in response to p38MAPK inhibitor at concentrations above 5μM (Figure 5-7b). DNCB- mediated IL-8 mRNA expression was also significantly inhibited in response to p38MAPK inhibitor at concentrations of 1μM or above (Figure 5-7c).

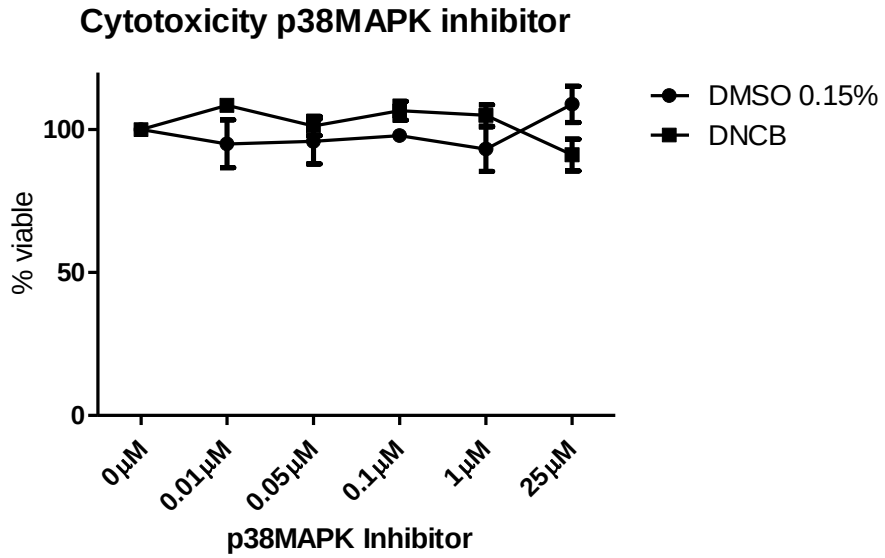

Figure 5-4 Cytotoxicity of the p38MAPK inhibitor SB203580

HaCaT cells were exposed to 0.15% DMSO (VC) or 30µM DNCB with increasing concentrations of the p38MAPK inhibitor SB203580. The MTT assay was used to assess cell viability. The graphs show mean and SD from three experiments.

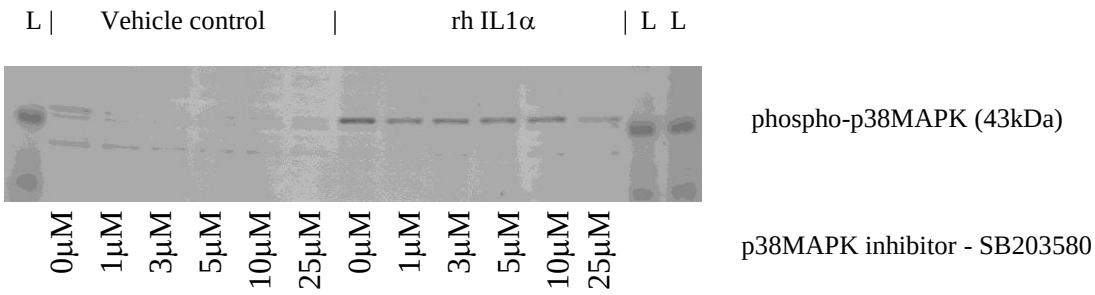

Figure 5-5 phospho-p38MAPK in response to IL-1α +/- p38MAPK inhibitor

HaCaT cells were cultured in the presence of 20ng/ml recombinant human IL-1α for 30 minutes +/- p38MAPK inhibitor SB203580 (0-25μM). Cell lysate proteins were separated by SDS-PAGE, and di-phosphorylated (Thr^{180}/Tyr^{182}) p38MAPK measured by western blot. L = molecular weight ladder.

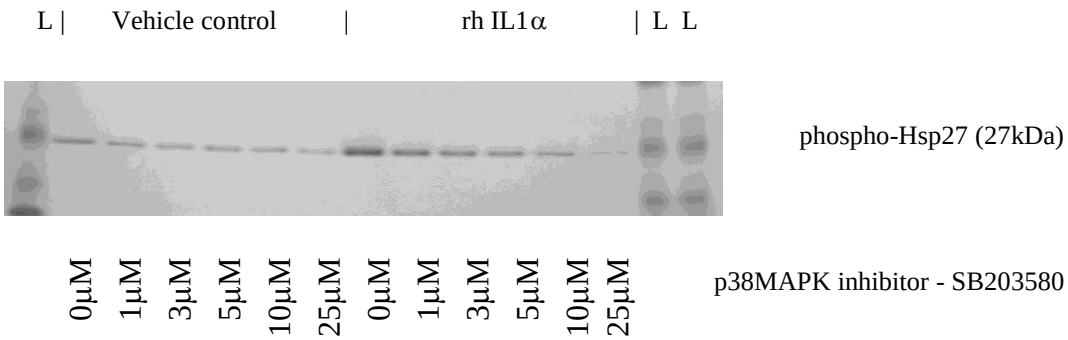

Figure 5-6 phospho-Hsp27 in response to IL-1α +/- p38MAPK inhibitor

HaCaT cells were cultured in the presence of 20ng/ml recombinant human IL-1α for 30 minutes +/- p38MAPK inhibitor SB203580 (0-25μM). Cell lysate proteins were separated by SDS-PAGE, and phosphorylated (Ser^{82}) Hsp27 measured by western blot. L = molecular weight ladder.

a

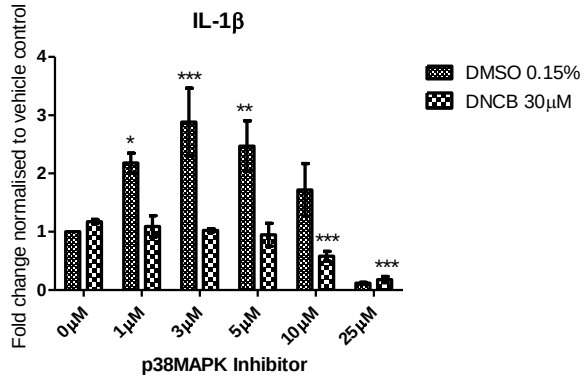

b

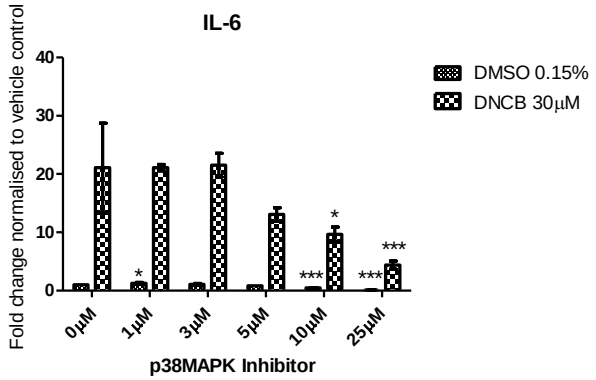

c

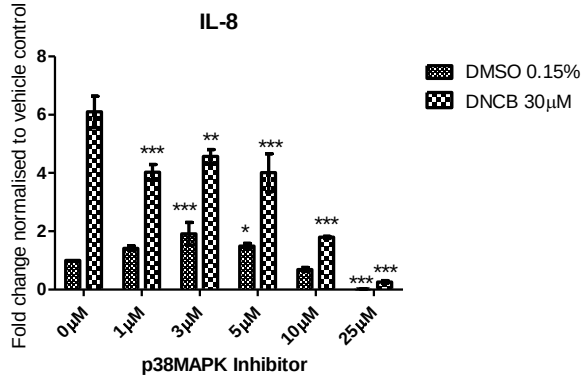

Figure 5-7 IL-1β, IL-6 and IL-8 transcription in response to DNCB +/- p38MAPK inhibition

HaCaT cells were exposed to 0.15% DMSO (VC) or 30μM DNCB, with increasing concentrations of the p38MAPK inhibitor SB203580. IL-1β, IL-6 and IL-8 mRNA expression was analysed by qRT-PCR. Data are fold change normalised to uninhibited vehicle control. The graphs show mean and SD from three experiments. Statistical analysis: One-way ANOVA with post-hoc Tukey's multiple comparison test * $p < 0.05$, ** $p < 0.01$, *** $p < 0.001$.

Activation of the ERK1/2 signalling pathway in response to DNCB

HaCaT cells were cultured in the presence of DNCB over a time-course of 30 minutes to 24 hours. Cell lysate proteins were separated by SDS-PAGE, and di-phosphorylated (Thr^{183}/Tyr^{185}) Erk1/2 (Figure 5-8a) and β-actin (Figure 5-8b) were measured by western blot. One of two representative experiments is shown. At 30 minutes, there was no change in the phosphorylation level of ERK1/2 with DNCB exposure compared to vehicle control. There was a decrease in phospho-ERK1/2 at 1 hour, followed by an increase at all later time-points in response to DNCB.

A similar experiment was performed with a reduced range of time points (30 minutes, 1 and 4 hours) and single concentrations of 30μM DNCB and 300μM SDS. Protein was extracted, and total and phosphorylated ERK1/2 measured by Luminex ELISA (Figure 5-9). Data are shown as total and phosphorylated raw fluorescence measurements (Figure 5-9a and b) and the ratio of phosphorylated:total (Figure 5-9c and d). The graphs show mean and SD from three experiments. The total protein levels of ERK1/2 were relatively constant with all treatments. The phosphorylated:total ERK1/2 ratio with vehicle control was much lower at 4 hours than at 30 minutes or 1 hour. DNCB induced a significant decrease in the ratio at 30 minutes and 1 hour, followed by a significant increase at 4 hours, consistent with the western blot. In contrast, following exposure to SDS, the phosphorylated:total ERK1/2 ratio was significantly increased at 30 minutes and 4 hours, but unchanged at 1 hour.

Activation of MEK and p90RSK in response to DNCB

MEK, the upstream signalling kinase to ERK1/2, and p90RSK, a downstream target of ERK1/2, were also investigated to further understand the modulation of the ERK signalling pathway. In an identical experiment to that previously described, total and phosphorylated MEK and p90RSK were measured by Luminex ELISA (Figures 5-10 and 5-11). The total protein levels of both were relatively constant in all treatments. The ratio of phosphorylated:total MEK decreased over time with vehicle control. Following exposure to DNCB, there were significant decreases in the phosphorylated:total ratios of MEK and p90RSK at 30 minutes and 1 hour. In contrast, SDS treatment led to significant increases in the phosphorylated:total ratios of MEK at all time points and p90RSK at 30 minutes and 4 hours.

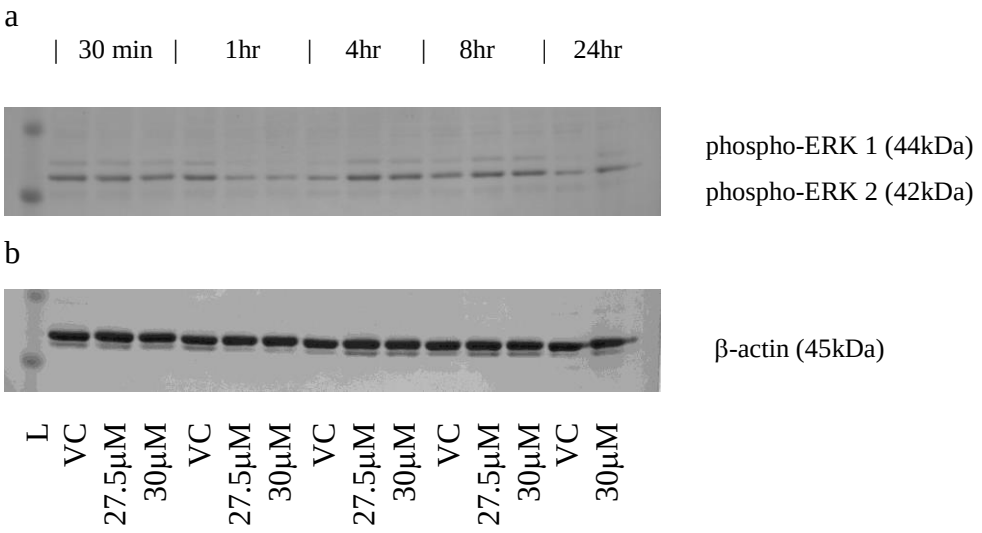

Figure 5-8 phospho-ERK1/2 in response to DNCB

HaCaT cells were cultured in the presence of 0.2% DMSO (VC), 27.5 μM or 30μM DNCB (a and b) over a time-course. Cell lysate proteins were separated by SDS-PAGE, and di-phosphorylated (Thr^{183}/Tyr^{185}) ERK1/2 (a) and β-actin (b) were measured by western blot. One of two representative experiments is shown. L = molecular weight ladder.

a

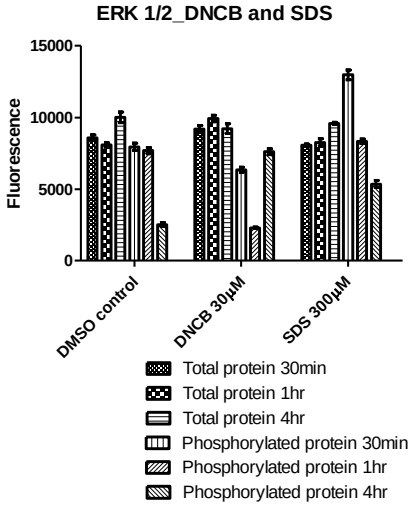

b

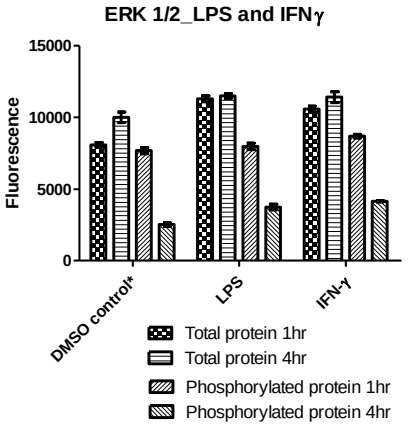

c

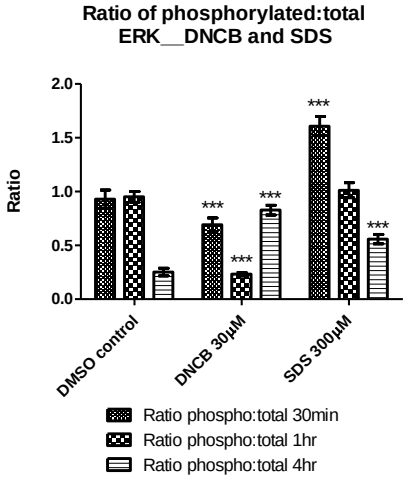

d

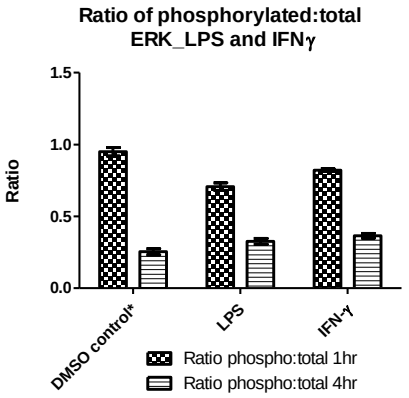

Figure 5-9 ERK1/2 response to stimulation with DNCB, SDS, LPS and IFNγ

HaCaT cells were exposed to 0.2% DMSO (VC), 30µM DNCB or 300µM SDS (a and c), or 1µg/ml LPS or IFNγ (b and d) over a time-course. Protein was extracted, and total and phosphorylated ERK1/2 were measured by Luminex ELISA. Data are shown as total and phosphorylated raw fluorescence measurements (a and b), and the ratio of phosphorylated:total (c and d). DMSO control data (in b and d) from DNCB/SDS experiments. The graphs show mean and SD from three experiments. Statistical analysis (c only): Two-way ANOVA with Bonferroni post-test (* $p < 0.05$, ** $p < 0.01$, *** $p < 0.001$).

a

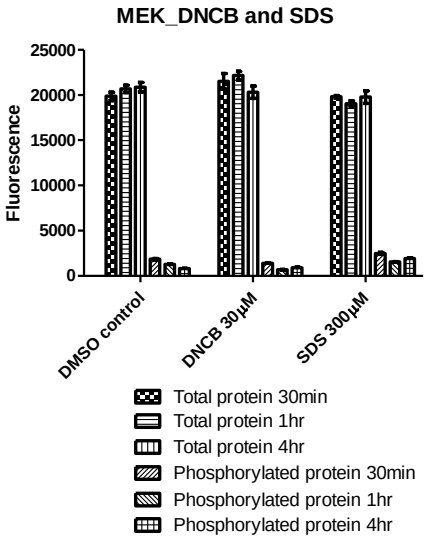

b

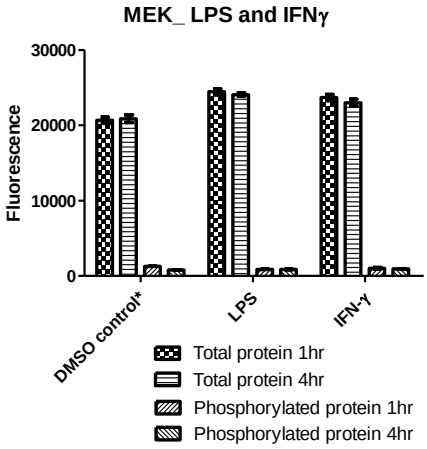

c

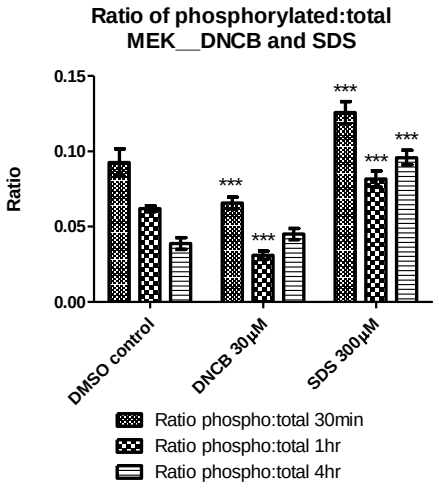

d

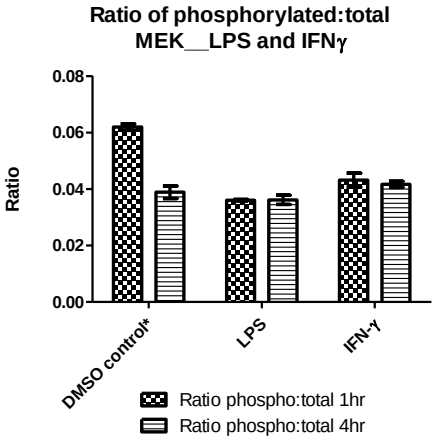

Figure 5-10 MEK response to stimulation with DNCB, SDS, LPS and IFNγ

HaCaT cells were exposed to 0.2% DMSO (VC), 30µM DNCB or 300µM SDS (a and c), or 1µg/ml LPS or IFNγ (b and d) over a time-course. Protein was extracted, and total and phosphorylated MEK were measured by Luminex ELISA. Data are shown as total and phosphorylated raw fluorescence measurements (a and b), and the ratio of phosphorylated:total (c and d). DMSO control data (in b and d) from DNCB/SDS experiments. The graphs show mean and SD from three experiments. Statistical analysis (c only): Two-way ANOVA with Bonferroni post-test (* $p < 0.05$, ** $p < 0.01$, *** $p < 0.001$).

a

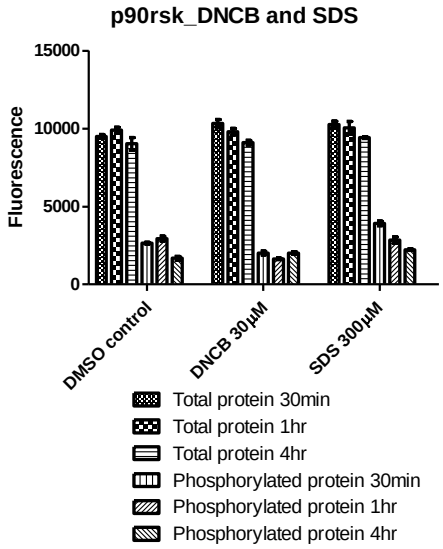

b

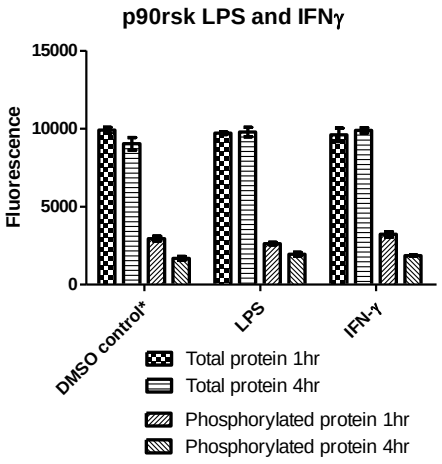

c

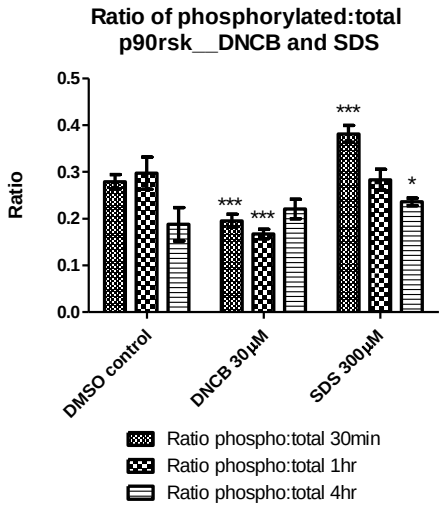

d

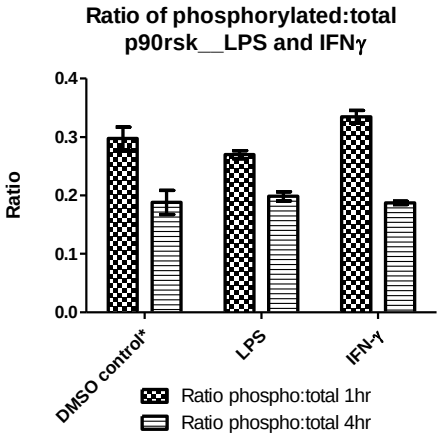

Figure 5-11 p90RSK response to stimulation with DNCB, SDS, LPS and IFNγ

HaCaT cells were exposed to 0.2% DMSO (VC), 30µM DNCB or 300µM SDS (a and c), or 1µg/ml LPS or IFNγ (b and d) over a time-course. Protein was extracted, and total and phosphorylated p90RSK were measured by Luminex ELISA. Data are shown as total and phosphorylated raw fluorescence measurements (a and b), and the ratio of phosphorylated:total (c and d). DMSO control data (in b and d) from DNCB/SDS experiments. The graphs show mean and SD from three experiments. Statistical analysis (c only): Two-way ANOVA with Bonferroni post-test (* $p < 0.05$, ** $p < 0.01$, *** $p < 0.001$).

Activation of the JNK signalling pathway in response to DNCB

HaCaT cells were cultured in the presence of DNCB over a time-course of 30 minutes to 24 hours. Cell lysate proteins were separated by SDS-PAGE, and di-phosphorylated (Thr^{183}/Tyr^{185}) p46 and p54 JNK (Figure 5-12) were measured by western blot. In response to DNCB, weak phospho-JNK signals were seen at 1 and 4 hours. Phospho-JNK could not be detected with vehicle control.

A similar experiment was performed with a reduced range of time points (30 minutes, 1 and 4 hours), and single concentrations of 30μM DNCB and 300μM SDS. Protein was extracted, and total and phosphorylated JNK measured by Luminex ELISA (Figure 5-13). Data are shown as total and phosphorylated raw fluorescence measurements (a and b) and the ratio of phosphorylated:total (c and d). The graphs show mean and standard deviation (SD) from three experiments. The total protein levels of JNK were relatively constant in the DNCB and SDS treated HaCaT cells. The phosphorylated:total JNK ratios were significantly increased with DNCB at 1 and 4 hours compared with control, consistent with the western blot data. The ratio was also increased from control at 30 minutes following exposure to SDS.

Activation of c-Jun and CREB in response to DNCB

c-Jun and CREB are transcription factors activated by MAP kinases. In an identical experiment to that previously described, total and phosphorylated c-Jun and CREB were measured by Luminex ELISA (Figures 5-14 and 5-15). The total protein levels of c-Jun increased over time with vehicle control, while total CREB was constant across all treatments. The phosphorylated:total c-Jun ratio increased at 1 and 4 hours in response to DNCB compared to control. SDS exposure produced much smaller changes in c-Jun phosphorylation. The ratio of phosphorylated:total CREB decreased over time with vehicle control. There were significant increases in the ratio at all time-points in response to DNCB, and at 30 minutes and 1 hour in response to SDS, compared to control.

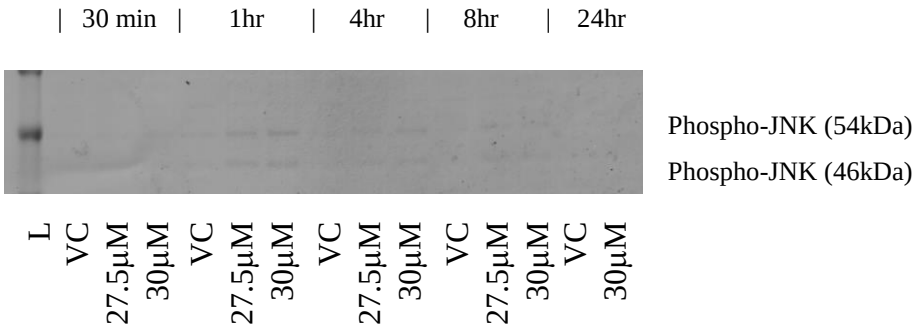

Figure 5-12 phospho-JNK in response to DNCB

HaCaT cells were cultured in the presence of 0.2% DMSO (VC), 27.5 μM or 30μM DNCB over a time-course. Cell lysate proteins were separated by SDS-PAGE, and di-phosphorylated (Thr^{183}/Tyr^{185}) p46 and p54 JNK were measured by western blot. L = molecular weight ladder.

a

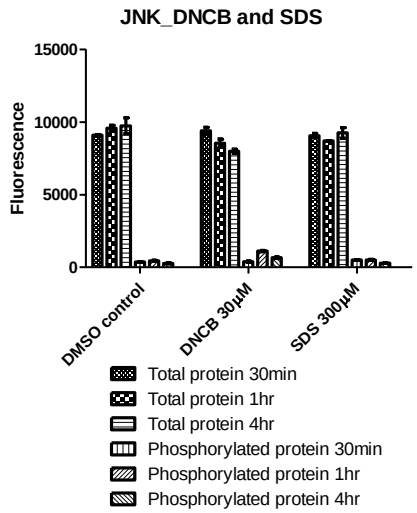

b

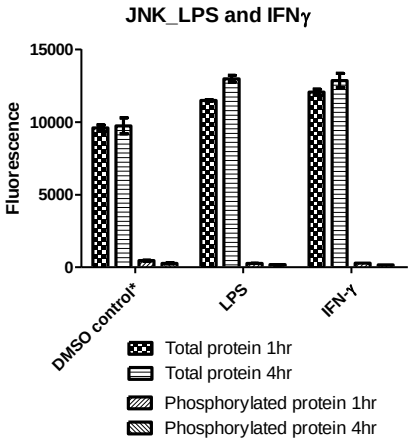

c

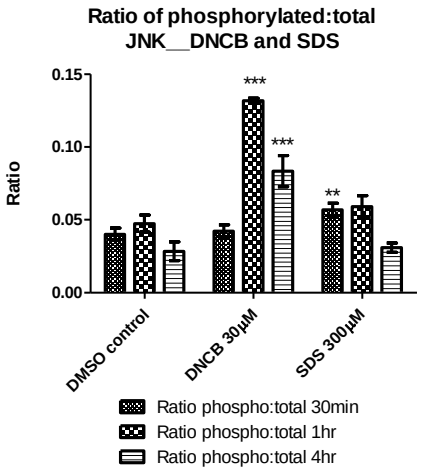

d

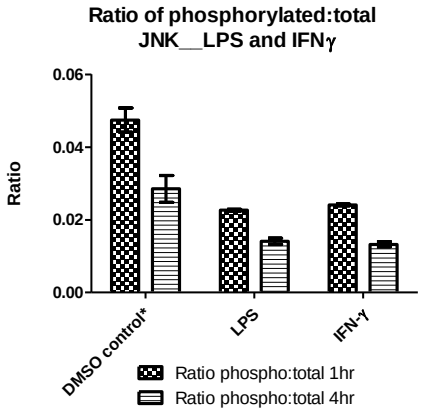

Figure 5-13 JNK response to stimulation with DNCB, SDS, LPS and IFNγ

HaCaT cells were exposed to 0.2% DMSO (VC), 30µM DNCB or 300µM SDS (a and c), or 1µg/ml LPS or IFNγ (b and d) over a time-course. Protein was extracted, and total and phosphorylated JNK were measured by Luminex ELISA. Data are shown as total and phosphorylated raw fluorescence measurements (a and b), and the ratio of phosphorylated:total (c and d). DMSO control data (in b and d) from DNCB/SDS experiments. The graphs show mean and SD from three experiments. Statistical analysis (c only): Two-way ANOVA with Bonferroni post-test (* $p < 0.05$, ** $p < 0.01$, *** $p < 0.001$).

a

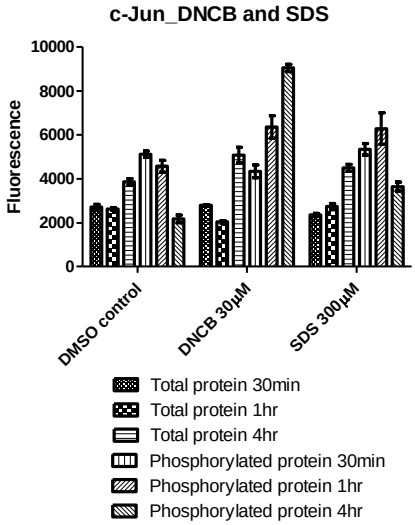

b

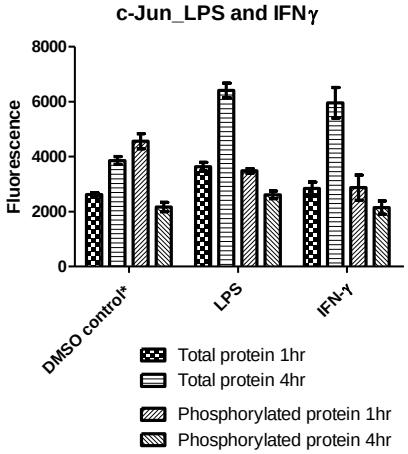

c

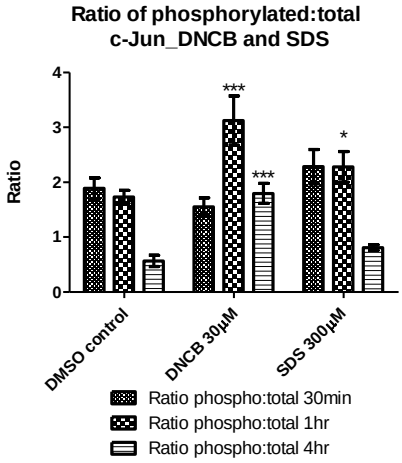

d

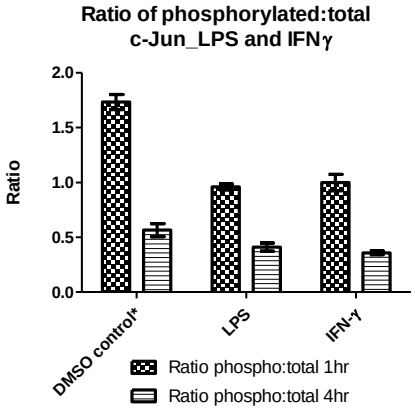

Figure 5-14 c-Jun response to stimulation with DNCB, SDS, LPS and IFNγ

HaCaT cells were exposed to 0.2% DMSO (VC), 30µM DNCB or 300µM SDS (a and c), or 1µg/ml LPS or IFNγ (b and d) over a time-course. Protein was extracted, and total and phosphorylated c-Jun were measured by Luminex ELISA. Data are shown as total and phosphorylated raw fluorescence measurements (a and b), and the ratio of phosphorylated:total (c and d). DMSO control data (in b and d) from DNCB/SDS experiments. The graphs show mean and SD from three experiments. Statistical analysis (c only): Two-way ANOVA with Bonferroni post-test (* $p < 0.05$, ** $p < 0.01$, *** $p < 0.001$).

a

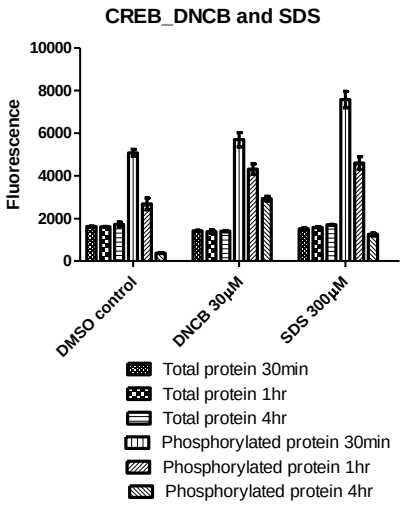

b

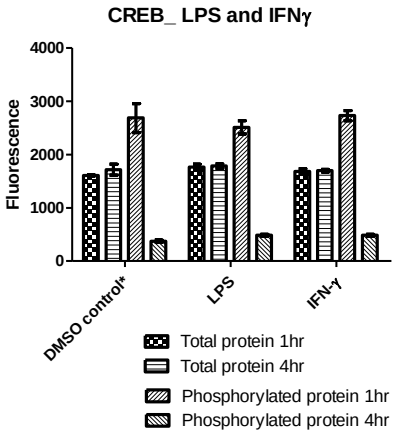

c

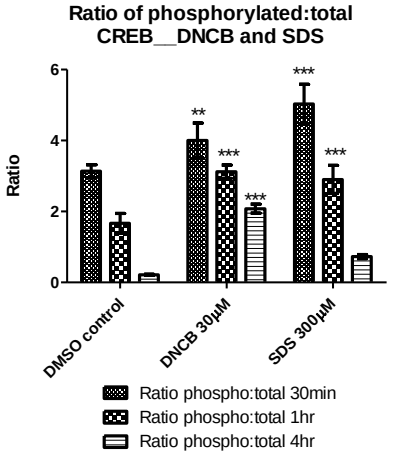

d

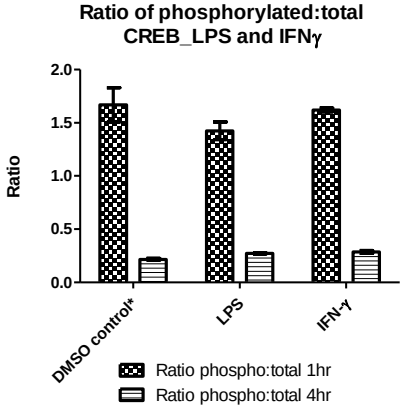

Figure 5-15 CREB response to stimulation with DNCB, SDS, LPS and IFNγ

HaCaT cells were exposed to 0.2% DMSO (VC), 30µM DNCB or 300µM SDS (a and c), or 1µg/ml LPS or IFNγ (b and d) over a time-course. Protein was extracted, and total and phosphorylated CREB were measured by Luminex ELISA. Data are shown as total and phosphorylated raw fluorescence measurements (a and b), and the ratio of phosphorylated:total (c and d). DMSO control data (in b and d) from DNCB/SDS experiments. The graphs show mean and SD from three experiments. Statistical analysis (c only): Two-way ANOVA with Bonferroni post-test (* $p < 0.05$, ** $p < 0.01$, *** $p < 0.001$).

Investigation of the NF-κB signalling pathway in response to DNCB

HaCaT cells were cultured in the presence of DNCB over a time-course of 30 minutes to 24 hours. Cell lysate proteins were separated by SDS-PAGE, and IκBα (Figure 5-16a) and β-actin as a loading control (Figure 5-16b) were measured by western blot. In response to DNCB, IκBα levels did not change at any dose or time-point.

A similar experiment was performed with a reduced range of time points (30 minutes, 1 and 4 hours) and single concentrations of 30μM DNCB and 300μM SDS. Protein was extracted, and total and phosphorylated IκBα measured by Luminex ELISA (Figure 5-17). Data are shown as total and phosphorylated raw fluorescence measurements (a and b) and the ratio of phosphorylated:total (c and d). The graphs show mean and standard deviation (SD) from three experiments. The total protein levels of IκBα were approximately constant in the DNCB and SDS treated HaCaT cells. The phosphorylated:total IκBα ratios were significantly decreased with DNCB and SDS at all time-points, compared with control.

HaCaT cells were exposed to 0.2% DMSO (VC), 20-32.5μM DNCB, 200-300μM SDS, or 1-2μg/ml LPS for 2 hours. NF-κB RelA was observed by confocal microscopy (Figure 5-18). Data shown are the confocal images (Figure 5-18a) for NF-κB RelA (red), DAPI (blue) for cells exposed to DMSO (VC) or 32μM DNCB for 2 hours. Figure 5-18b shows the ratio of NF-κB RelA inside the nucleus:outside the nucleus for each condition. Based on the assumption that measurements on individual cells are independent variables, there was a significant increase in nuclear NF-κB RelA translocation with all treatments compared to DMSO vehicle control.

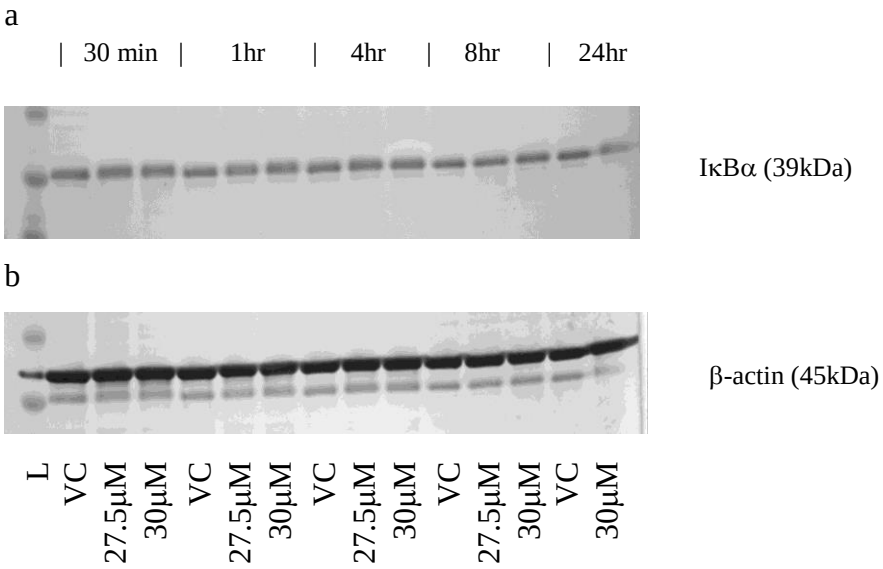

Figure 5-16 IκBα in response to DNCB

HaCaT cells were cultured in the presence of 0.2% DMSO (VC), 27.5 μM or 30μM DNCB over a time-course. Cell lysate proteins were separated by SDS-PAGE, and IκBα (a) and β-actin (b) were measured by western blot.

a

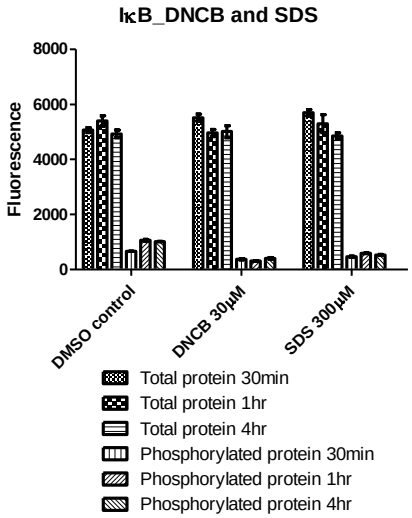

b

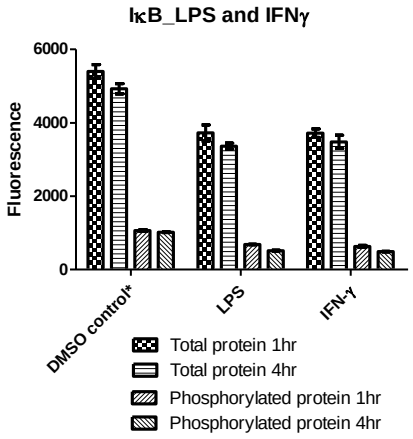

c

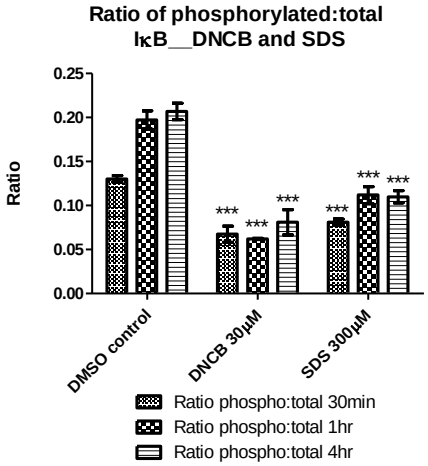

d

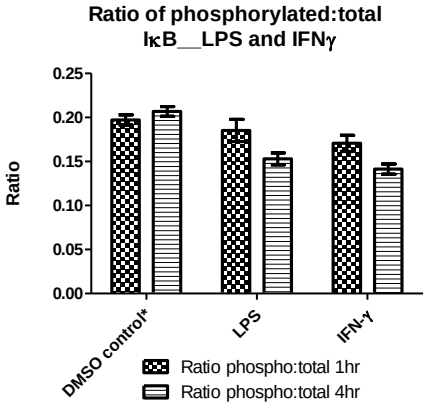

Figure 5-17 IκB response to stimulation with DNCB, SDS, LPS and IFNγ

HaCaT cells were exposed to 0.2% DMSO (VC), 30μM DNCB or 300μM SDS (a and c), or 1μg/ml LPS or IFNγ (b and d) over a time-course. Protein was extracted, and total and phosphorylated IκB were measured by Luminex ELISA. Data are shown as total and phosphorylated raw fluorescence measurements (a and b), and the ratio of phosphorylated:total (c and d). DMSO control data (in b and d) from DNCB/SDS experiments. The graphs show mean and SD from three experiments. Statistical analysis (c only): Two-way ANOVA with Bonferroni post-test (* $p < 0.05$, ** $p < 0.01$, *** $p < 0.001$).

a

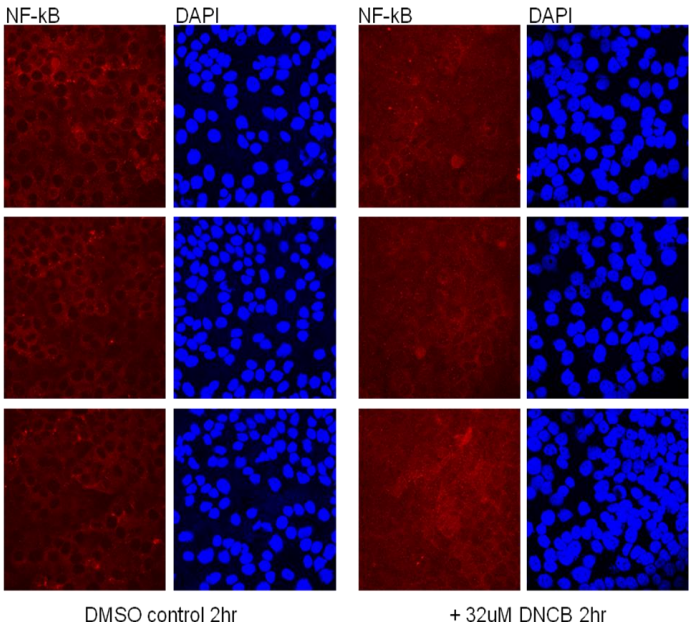

b

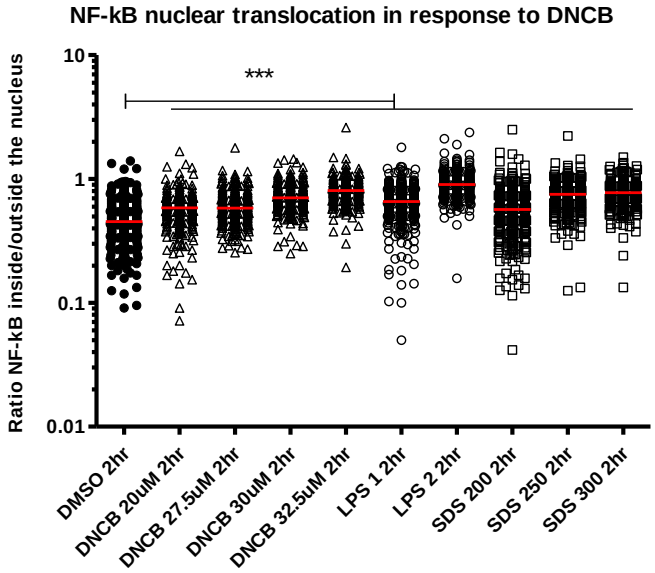

Figure 5-18 NF-κB translocation in response to DNCB, SDS and LPS

HaCaT cells were exposed to 0.2% DMSO (VC), 20-32.5μM DNCB, 200-300μM SDS, or 1-2μg/ml LPS for 2 hours. NF-κB RelA was observed by confocal microscopy. Data shown are the confocal images for NF-κB RelA (red), DAPI (blue) for cells exposed to DMSO (VC) or 32.5μM DNCB for 2 hours (3 replicates) (a). Ratio of NF-κB RelA inside the nucleus:outside the nucleus (each data point represents an individual cell) for each condition (b). Statistical analysis: One-way ANOVA with post-hoc Dunnett's multiple comparison test * $p < 0.05$, ** $p < 0.01$, *** $p < 0.001$. All treatments were significant compared to DMSO vehicle control with $p < 0.001$ (***).

Inhibition of NF-κB signalling

HaCaT cells were exposed to increasing concentrations of the NF-κB inhibitor BAY11-7082 (Pierce et al, 1997). TNFα was used as a positive control to check the efficacy of the NF-κB inhibitor BAY11-7082. Cells exposed to TNFα without inhibitor show large increases in IL-1β, IL-6 and IL-8 mRNA expression (Figure 5-19, n=1). The levels of each cytokine decrease with increasing concentration of inhibitor, indicating that the inhibitor was working to suppress NF-κB signalling.

HaCaT cells were exposed to 30μM DNCB with increasing concentrations of the NF-κB inhibitor. IL-1β, IL-6 and IL-8 mRNA expression were analysed by qRT-PCR (Figure 5-20). Data shown are fold change normalised to uninhibited vehicle control (0μM inhibitor, 0.15%DMSO). The NF-κB inhibitor caused a concentration dependent decrease in the vehicle induced expression of IL-1β, IL-6 and IL-8. DNCB-induced IL-1β and IL-8 showed a small increase in expression with increasing concentrations of inhibitor up to 3μM (although not significant), followed by a significant decrease at 25μM. DNCB-induced IL-6 expression was unchanged by inhibitor concentration up to 10μM, followed by a decrease at 25μM.

a

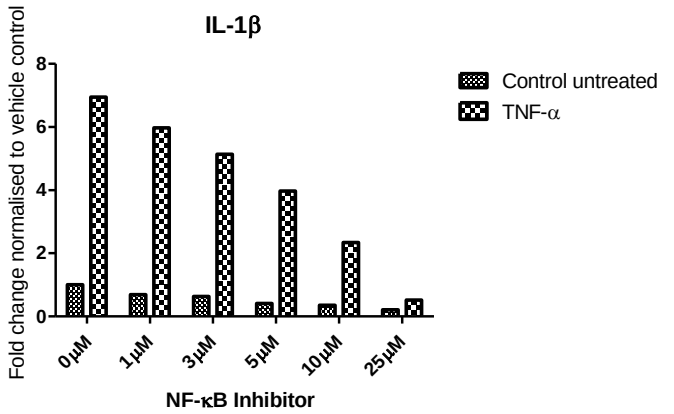

b

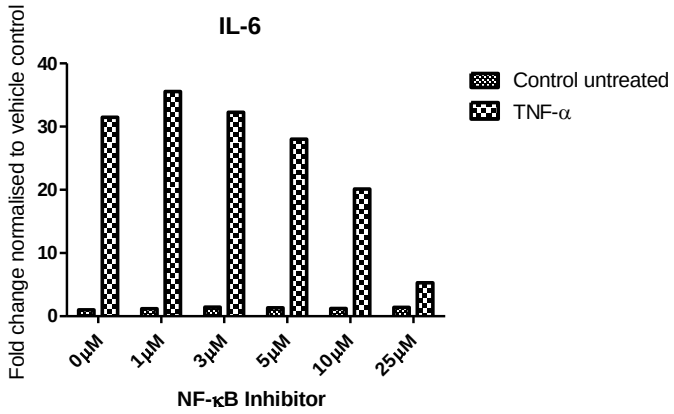

c

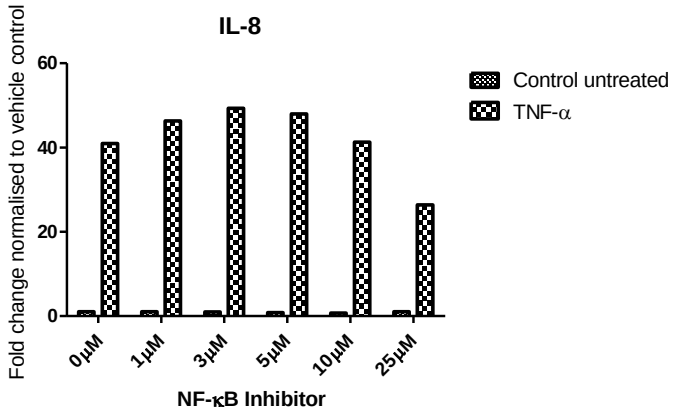

Figure 5-19 IL-1β, IL-6 and IL-8 transcription in response to TNFα +/- NF-κB inhibition

HaCaT cells were exposed to vehicle control (culture media) or 20ng/ml TNFα with increasing concentrations of the NF-κB inhibitor BAY11-7082. IL-1β (a), IL-6 (b) and IL-8 (c) mRNA expression were analysed by qRT-PCR. Data are fold change normalised to uninhibited vehicle control. No statistical analysis as n=1.

a

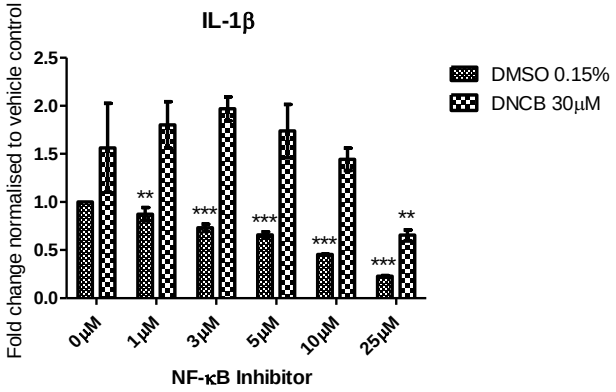

b

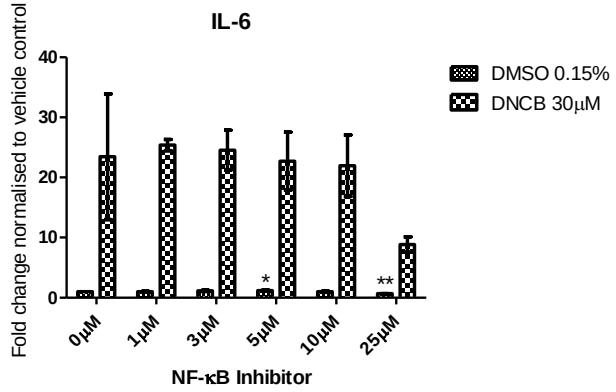

c

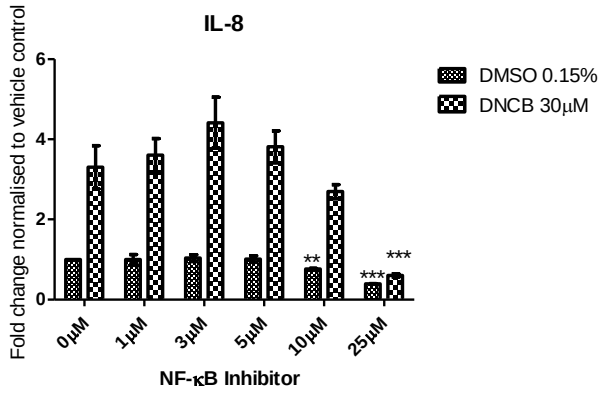

Figure 5-20 IL-1β, IL-6 and IL-8 transcription in response to DNCB +/- NF-κB inhibition

HaCaT cells were exposed to 0.15% DMSO (VC) or 30μM DNCB with increasing concentrations of the NF-κB inhibitor BAY11-7082. IL-1β (a), IL-6 (b) and IL-8 (c) mRNA expression were analysed by qRT-PCR. Data are fold change normalised to uninhibited vehicle control. The graphs show mean and SD from three experiments. Statistical analysis: one-way ANOVA with Tukey's multiple comparison test.

Activation of STAT3 and STAT6 in response to DNCB, SDS, LPS and IFNγ

HaCaT cells were exposed to 0.2% DMSO (VC), 30μM DNCB or 300μM SDS (Figure 5-21a and c), or 1μg/ml LPS or IFNγ (Figure 5-21b and d) over a time-course. Protein was extracted, and phosphorylated STAT3 (Figure 5-21a and b) and phosphorylated STAT6 (Figure 5-21c and d) (not total) was measured by Luminex ELISA. The phosphorylated STAT3 responses to DNCB, SDS and vehicle control showed the same decrease with time. No significant changes in phosphorylated STAT3 or STAT6 were seen with any of the treatments.

Activation of Tyk2 in response to DNCB, SDS, LPS and IFNγ

HaCaT cells were exposed to 0.2% DMSO (VC), 30μM DNCB or 300μM SDS (Figure 5-22a), or 1μg/ml LPS or IFNγ (Figure 5-22b) over a time-course. Protein was extracted, and phosphorylated Tyk2 (not total) was measured by Luminex ELISA. Phosphorylated Tyk2 significantly increased at 1 and 4 hours in response to DNCB compared to control. No changes were seen following exposure to SDS.

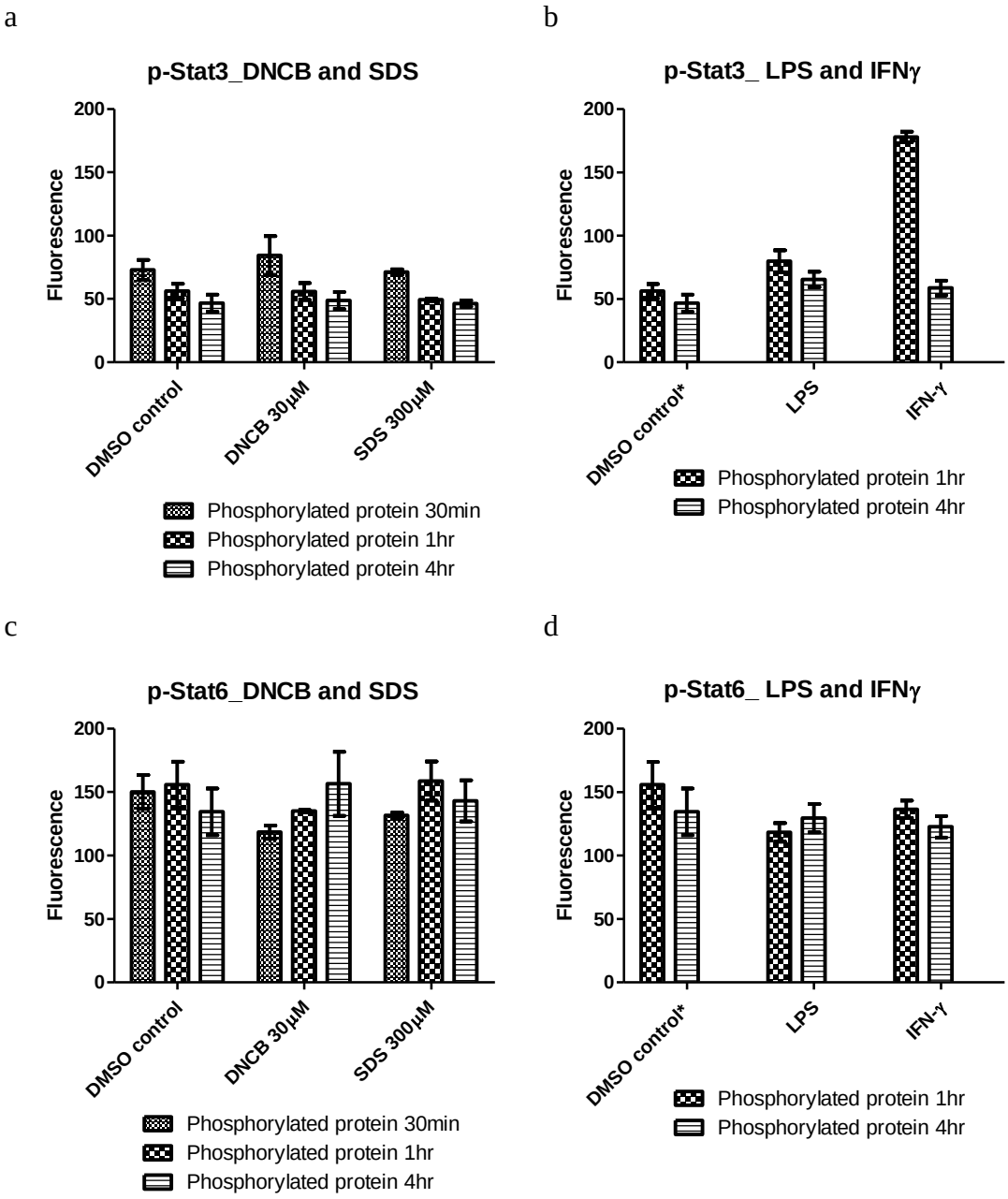

Figure 5-21 phospho-STAT3 and phospho-STAT6 response to DNCB, SDS, LPS and IFNγ

HaCaT cells were exposed to 0.2% DMSO (VC), 30µM DNCB or 300µM SDS (a and c), or 1µg/ml LPS or IFNγ (b and d) over a time-course. Protein was extracted, and phosphorylated STAT3 (a and b) and phosphorylated STAT6 (c and d) (not total) were measured by Luminex ELISA. Data are shown as phosphorylated raw fluorescence measurements. DMSO control data (in b and d) from DNCB/SDS experiments. The graphs show mean and SD from three experiments. Statistical analysis (a and c only): Two-way ANOVA with Bonferroni post-test (* $p < 0.05$, ** $p < 0.01$, *** $p < 0.001$).

a

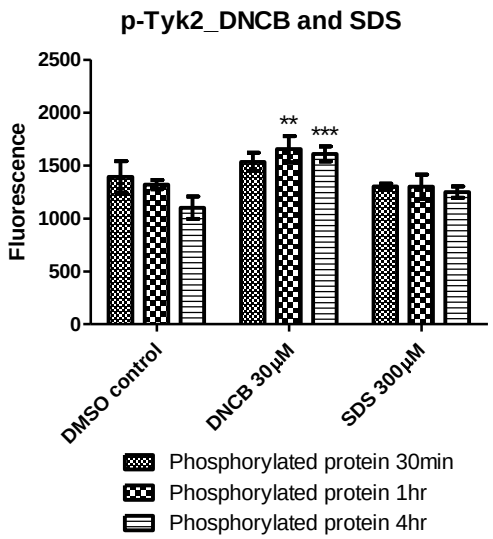

b

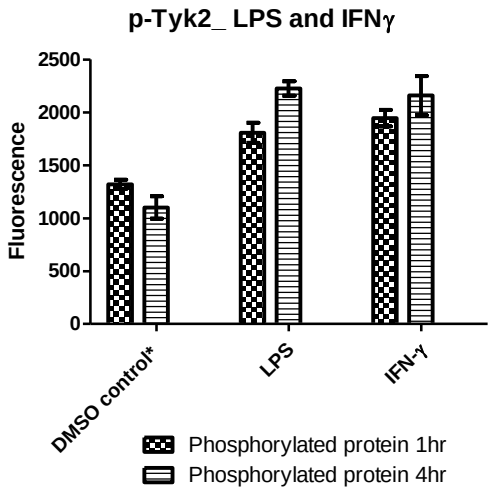

Figure 5-22 phospho-Tyk2 and phospho-Histone H3 response to DNCB, SDS, LPS and IFNγ

HaCaT cells were exposed to 0.2% DMSO (VC), 30µM DNCB or 300µM SDS (a), or 1µg/ml LPS or IFNγ (b) over a time-course. Protein was extracted, and phosphorylated Tyk2 (not total) was measured by Luminex ELISA. Data are shown as phosphorylated raw fluorescence measurements. DMSO control data (in b) from DNCB/SDS experiments. The graphs show mean and SD from three experiments. Statistical analysis (a only): Two-way ANOVA with Bonferroni post-test (* $p < 0.05$, ** $p < 0.01$, *** $p < 0.001$).

Activation of phospho-tyrosine in response to DNCB

HaCaT cells were cultured in the presence of 0.2% DMSO (VC) or 30μM DNCB for 8 hours. Cell lysate proteins were separated by SDS-PAGE, and total phospho-tyrosine measured by western blot (Figure 5-23). The lysate from the DNCB treated cells showed a large molecular weight band just above 171kDa (referenced by the ladder), that was not present in the vehicle control. There was also a band at approximately 117kDa (referenced by the ladder) that was present in the control but not the DNCB exposed cells.

Investigation of EGFR activation in response to DNCB

To determine if the tyrosine-phosphorylated large molecular weight protein seen in response to DNCB (Figure 5-23) was phosphorylated EGFR (MW approximately 185kDa), HaCaT cells were cultured in the presence of 0.2% DMSO (VC) or 20-30μM DNCB for 8 hours. Cell lysates were separated by SDS-PAGE, and phospho-EGFR/ErbB1 (Tyr^{1173}) measured by western blot (Figure 5-24). Phospho-EGFR/ErbB1 (Tyr^{1173}) was detected at a similar intensity in all samples (control and DNCB treated).

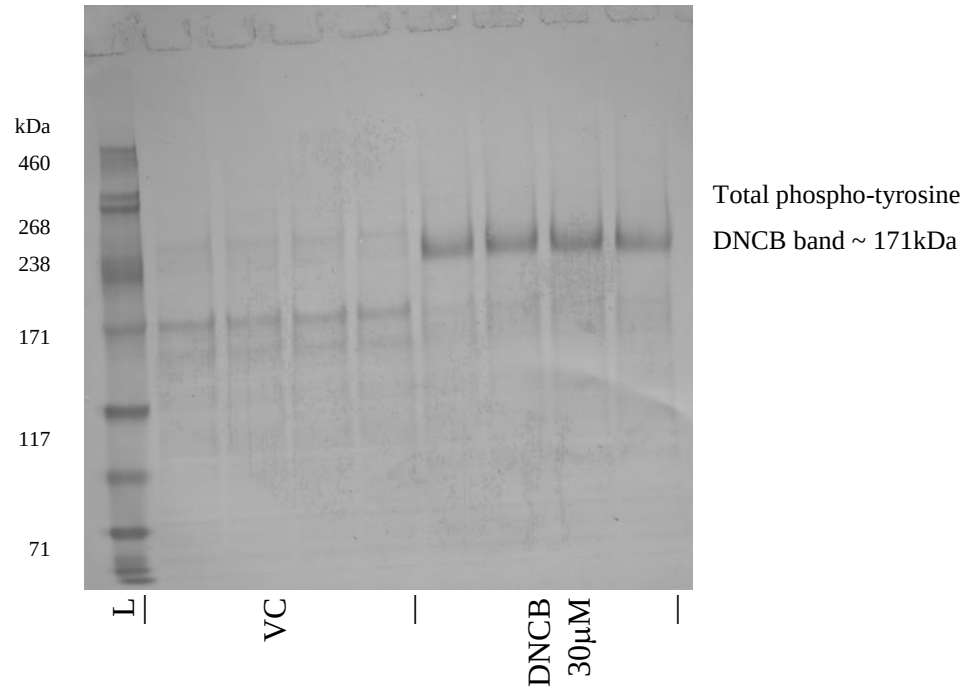

Figure 5-23 phospho-tyrosine in response to DNCB

HaCaT cells were cultured in the presence of 0.2% DMSO (VC) or 30μM DNCB for 8 hours. Cell lysate proteins were separated by SDS-PAGE, and total phospho-tyrosine measured by western blot (4 replicates loaded). One of two representative experiments is shown.

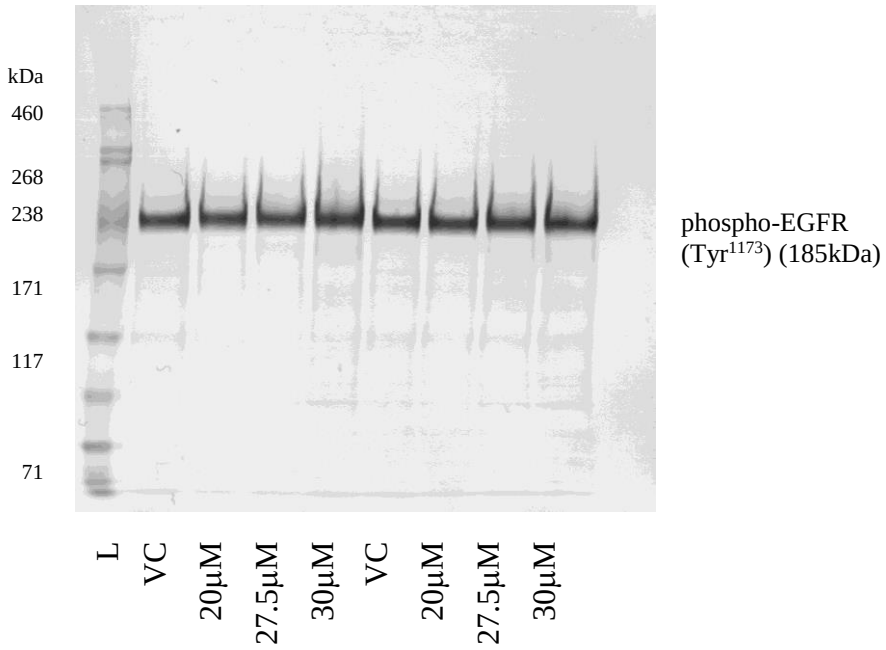

Figure 5-24 phospho-EGFR in response to DNCB

HaCaT cells were cultured in the presence of 0.2% DMSO (VC) or 20-30µM DNCB for 8 hours. Cell lysate proteins were separated by SDS-PAGE, and phospho-EGFR/ErbB1 (Tyr^{1173}) measured by western blot.

Generation of reactive oxygen species (ROS) in response to DNCB

HaCaT cells were cultured in the presence of 0.2% DMSO (VC), 2.5-40μM DNCB or menadione as a positive control (Loor et al, 2010) for 24 hours. Cells were incubated with ROS detection probe (CM-H_2DCFDA), which can detect hydrogen peroxide (H_2O_2), hydroxyl radical (HO•), peroxyl radical (ROO•) and peroxynitrite anion ($ONOO^-$). Intracellular probe fluorescence was measured by high throughput imaging using the Cellomics Array scan (by Samantha Windebank). The percentage of responding cells represents the percentage of cells with an average fluorescence over a threshold defined so that 15% of control treated cells are included (Figure 5-25a and b). There was a significant dose-dependent increase in the percentage of responding cells following exposure to DNCB, which was similar to the positive control menadione. Mean cellular total intensity represents the mean of the total intensities measured from each cell. The mean cellular average intensity represents the mean of the average intensities measured from each cell. The mean intensity SD represents the mean of the standard deviations of the intensities measured from each cell. All three of these data metrics showed a significant dose-dependent increase in response to DNCB, up to a fold change of approximately 3 times control. Altogether, these results demonstrate substantial generation of reactive oxygen species triggered by exposure to DNCB.

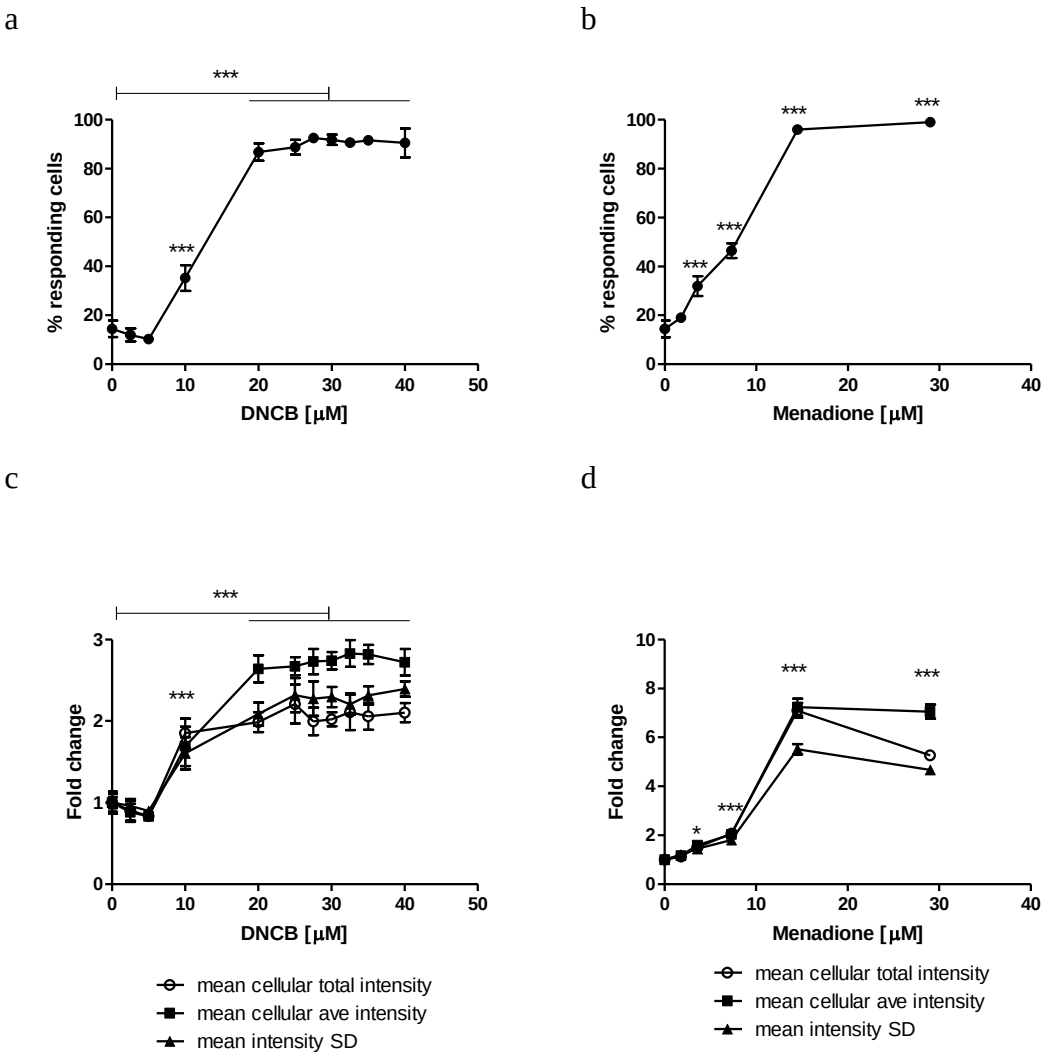

Figure 5-25 ROS generation in response to DNCB and menadione

HaCaT cells were cultured in the presence of 2.5-40µM DNCB or 1.8-29µM menadione for 24 hours (0µM = 0.2% DMSO vehicle control). Cells were incubated with ROS detection probe (CM-H_2DCFDA), and intracellular probe fluorescence measured by high throughput imaging using the Cellomics Array scan. Statistical analysis: one-way ANOVA with Tukey's multiple comparison test: (* $p < 0.05$, ** $p < 0.01$, *** $p < 0.001$). a and c, 10µM DNCB or above $p < 0.001$ (***). Measurement of ROS by Samantha Windebank.

Response of PBMC-DC to HaCaT conditioned media

Peripheral blood mononuclear cells (PBMCs) were obtained from human blood. Monocytes ($CD14^+$ cells) were isolated from PBMCs and cultured with GM-CSF and IL-4 to stimulate differentiation into immature dendritic cells. These PBMC derived DC were exposed for 20 hours to either: 0.15% DMSO (control); 100ng/ml LPS; or filtered conditioned media from HaCaT cells previously exposed to various concentrations of DNCB, SDS or DMSO. Expression of DC-SIGN, CD83 and CD86 were analysed by flow cytometry. To ensure analysis of the live DC population, cells were gated by FSC and SSC, then for DC-SIGN positive cells and for live cells by propidium iodine stain (Figure 5-26).

In response to DMSO (directly not as conditioned media), PBMC-DC had a slightly greater expression of CD83 and CD86, while LPS exposed cells showed a marked increase in expression of both compared to untreated cells (Figure 5-27).

Following exposure to supernatant from HaCaT cells exposed to 27.5- 40μM DNCB, PBMC-DC showed a small dose-dependent increase in CD83 and CD86 expression (Figure 5-28), although the magnitude was much less than that produced by LPS.

A similar experiment was performed with a range of concentrations of DNCB and SDS, with biological replicates for each treatment (Figure 5-29). In all cases only a small increase in CD83 or CD86 was seen, which was much lower than the increase observed with LPS-stimulated PBMC-DC.

a

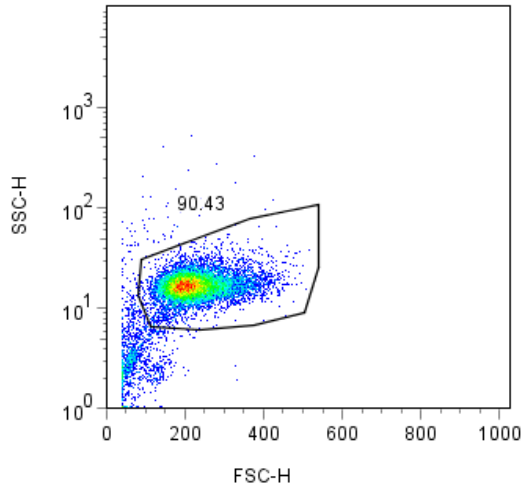

b

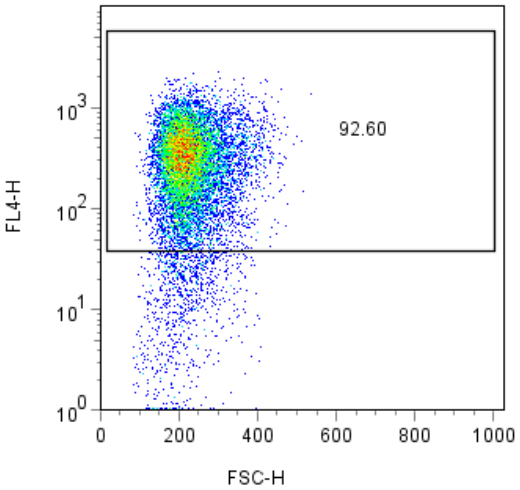

c

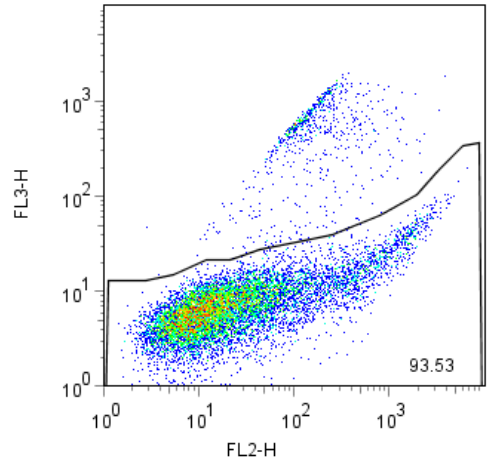

Figure 5-26 Gating of PBMC-DC

The PBMC-derived DC population were first gated by FSC and SSC (a), then for DC-SIGN positive cells (FL4-H) (b), followed by live/dead propidium iodine stain (FL3-H) (c). This gating was applied to all DC analyses.

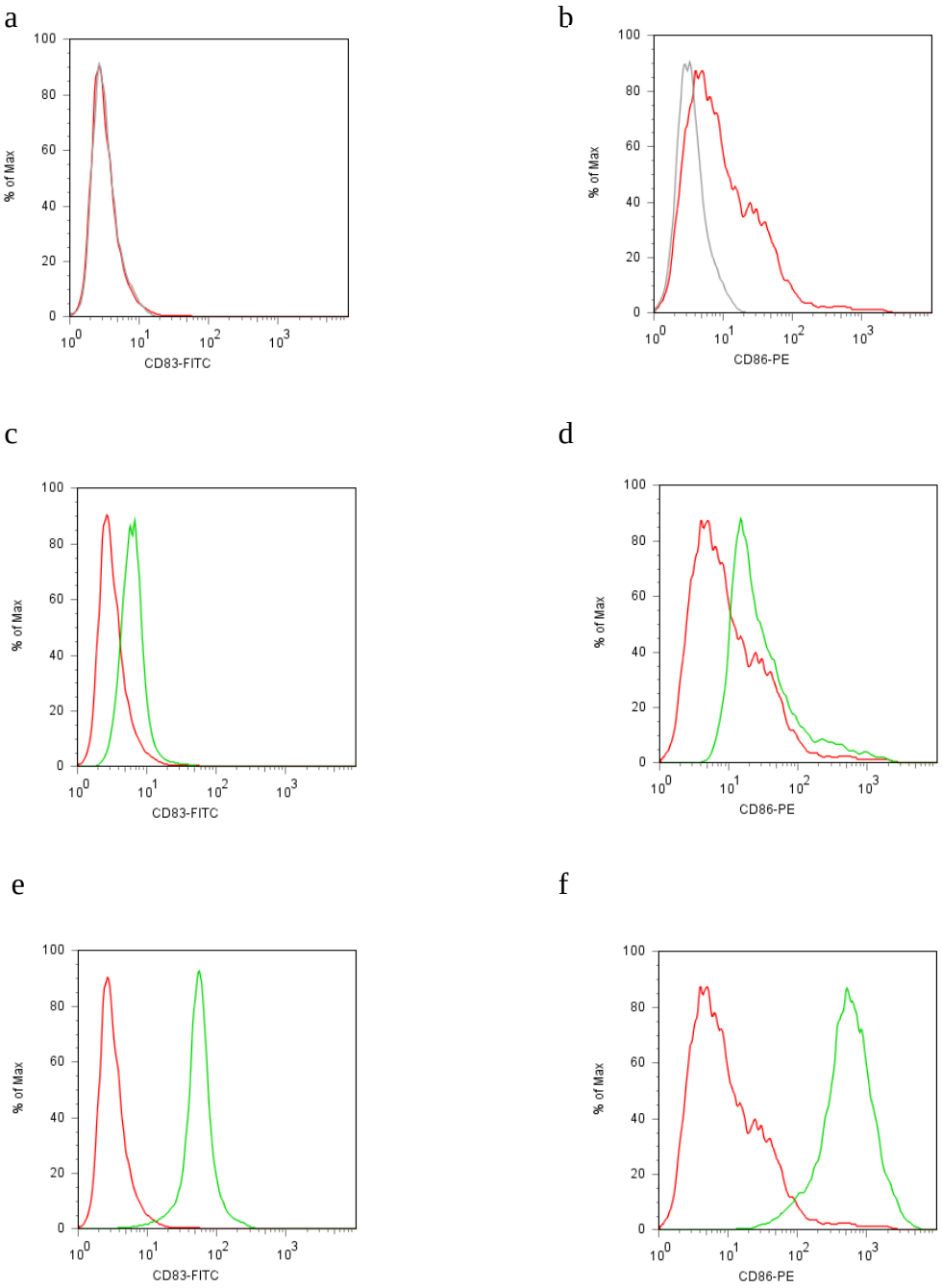

Figure 5-27 PBMC-DC CD83 and CD86 expression in response to LPS

PBMC-derived DC were untreated (a and b), or exposed directly to DMSO (c and d) or 100ng/ml LPS (e and f) for 20 hours. CD83 (a, c and e) and CD86 (b, d and f) expression were measured by flow cytometry. Graphs show isotype control (grey), unstimulated DC (red), DMSO or LPS exposed (green).

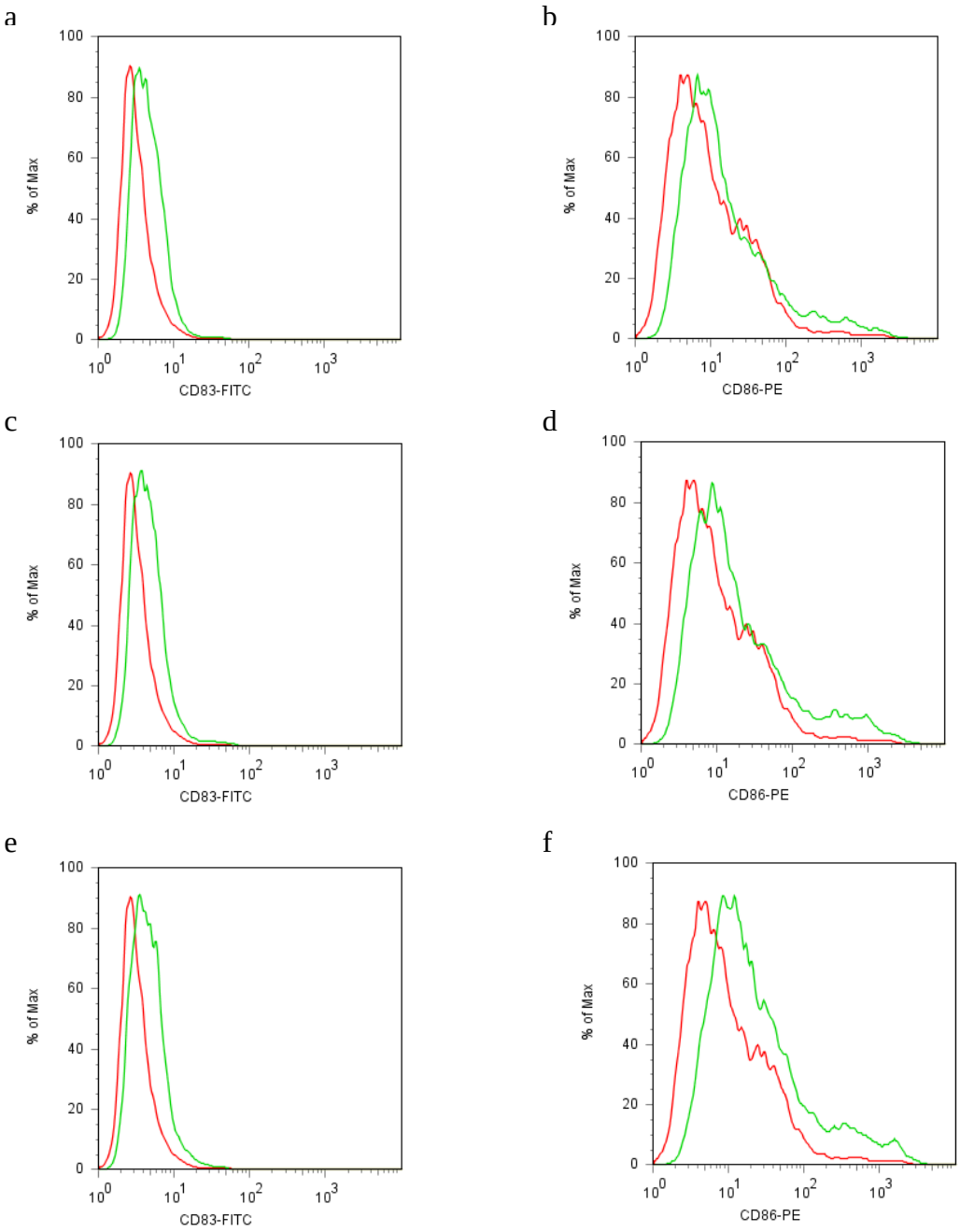

Figure 5-28 PBMC-DC CD83 and CD86 expression in response to supernatant from DNCB-treated HaCaT cells

PBMC-derived DC were exposed to supernatant from HaCaT cells exposed to 27.5µM DNCB (a and b), 32.5µM DNCB (c and d) or 40µM DNCB (e and f). CD83 (a, c and e) and CD86 (b, d and f) expression were measured by flow cytometry. Graphs show unstimulated DC (red), supernatant-exposed (green).

a

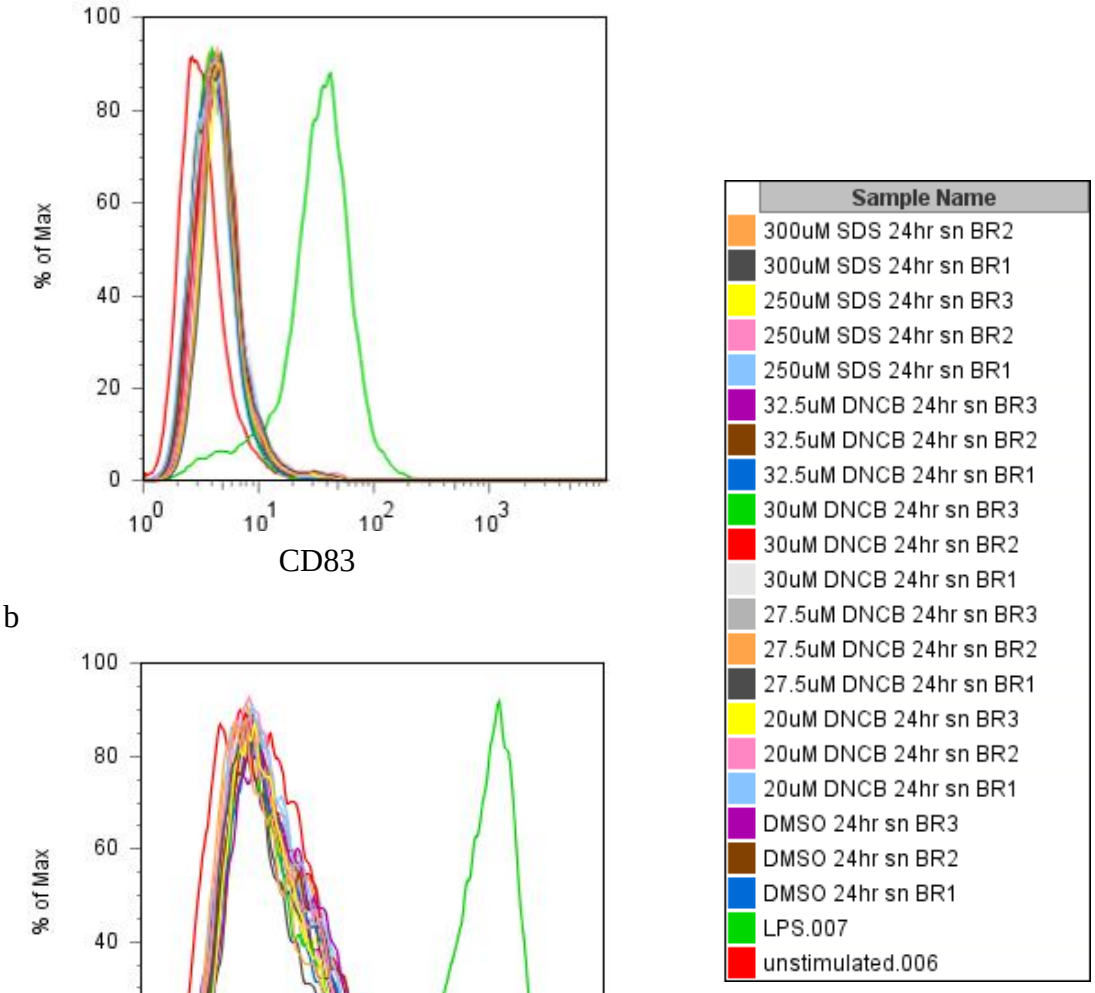

Figure 5-29 PBMC-DC CD83 and CD86 expression in response to supernatant from DNCB and SDS-treated HaCaT cells

PBMC-derived DC were exposed for 20 hours to supernatant from HaCaT cells exposed to 0.15% DMSO, or a range of concentrations of SDS or DNCB, or directly to LPS. CD83 (a) and CD86 (b) expression were measured by flow cytometry. BR = biological replicate.

5.3 Discussion

In this chapter, we have investigated the signalling cascades and triggers highlighted at the mRNA level in chapter 4, and their functional link to the sensitiser-specific cytokine profile seen in chapter 3. We first investigated the MAPK pathways, p38MAPK, ERK and JNK, as well as some of their downstream targets: c-Jun, CREB, Hsp27 and p90RSK.

We found that p38MAPK was phosphorylated in response to DNCB, with a peak of about 5 times the control level at 1 hour, and sustained phosphorylation until at least 8 hours. In response to SDS, p38MAPK phosphorylation also increased, but to a much lesser extent, and was not sustained. Several authors have reported phosphorylation of p38MAPK in response to sensitiser, at time points from 15 minutes to 8 hours, specifically: DNFB in reconstructed human epidermis (RHE) models (Frankart et al, 2012); p-phenylenediamine (PPD) in the NCTC2544 human keratinocyte cell line (Galbiati 2011); DNFB and oxazolone in (mouse and human) skin extracts and human RHE models (Koeper et al, 2007); and DNFB in mouse ear skin (Ayush et al, 2013). In contrast to these and our results, Yun et al (2010) did not see phosphorylation of p38MAPK in response to TNCB at 30 minutes in a mouse keratinocyte cell line, Pam212. The *in vivo* relevance of p38MAPK in CHS was demonstrated by a reduction of the ear swelling response to DNFB during p38MAPK inhibition (Ayush et al, 2013).

Following inhibition of p38MAPK, we saw decreases in DNCB-induced transcription of IL-1β, IL-6 and IL-8. These observations demonstrate a role for p38MAPK in driving the sensitiser-specific cytokine response in keratinocytes. Following p38MAPK inhibition in keratinocytes and other cell types, other groups have also seen reduced cytokine expression: IL-1β levels were decreased *in vivo* in mouse skin (Ayush et al, 2013); DNFB-driven IL-8 was inhibited in RHE (Frankart et al, 2012); DNCB-induced IL-1β and IL-8 expression were suppressed in PBMC-DC (Aiba et al, 2003); DNCB-induced IL-8 release was inhibited in THP-1 cells (Mitjans et al 2008; Nukada et al, 2008); LPS-induced IL-6 decreased in rat lung alveolar epithelial cells (Haddad, 2002); and IL-1β-induced IL-6 was reduced in mouse skeletal muscle cells (Luo et al, 2003).

Similarly, inhibition of Mnk1 (which is downstream of ERK and p38MAPK) inhibited anicomycin-induced IL-1β and IL-6 expression in keratinocytes (Kjellerup et al, 2007).

A reduced DNFB-stimulated CHS response (Yusuf et al, 2009) was also seen following inhibition of Hsp27, which is directly downstream of p38MAPK (Garmyn et al, 2001). In our data, Hsp27 was phosphorylated over at least 4 hours and to a similar extent to p38MAPK, adding to the evidence that the p38MAPK pathway is being activated in response to DNCB. The phospho-Hsp27 response to SDS was short-lived in comparison and similar to the SDS-induced p38MAPK profile.

We also investigated phosphorylation of ERK in response to DNCB. The ratio of phosphorylated:total ERK was a maximum of 4-fold down-regulated in DNCB-treated cells compared to control at 30 minutes and 1 hour, however, at 4 hours the phospho-ERK response to DNCB switched to about 4-fold up-regulated, acting slightly later than the p38MAPK response. The upstream kinase for ERK, MEK, was also reduced at 30 minutes and 1 hour, and was unchanged compared to control at 4 hours. The same profile was also seen with the downstream ERK target p90RSK. The reduction in activation of the ERK signalling cascade could be explained by previous observations of p38MAPK mediated inhibition of ERK (Zhang et al, 2001; Numazawa et al, 2003; Boisleve et al, 2005). Our data are consistent with this proposed mechanism, in that the maximum suppression of ERK, MEK and p90RSK occurred at the same time as peak p38MAPK phosphorylation.

In contrast to DNCB, phosphorylation of ERK, MEK and p90RSK were highly upregulated at 30 minutes and 4 hours in response to SDS. Overall, this indicates that activation of the ERK signalling cascade is responsive to SDS.

Other published data on ERK phosphorylation in response to sensitiser exposure show conflicting results, which may be partly due to the interaction with p38MAPK. ERK phosphorylation was found to be increased between 1 and 8 hours in response to: DNFB in RHE (Frankart et al, 2012); DNFB and oxazolone in (mouse and human) skin extracts (Koeper et al, 2007); and DNFB in mouse ear skin (Ayush et al, 2013). However, no changes in ERK phosphorylation were seen in human RHE models in

response to DNFB and oxazolone (Koeper et al, 2007); or in response to TNCB in Pam212 (Yun et al, 2010).

Several authors have investigated the effect of ERK signalling on cytokine release through inhibition of MEK, leading to reductions in: DNFB-induced IL-8 release in RHE (Frankart et al, 2012); DNCB-induced IL-1β expression in PBMC-DC (Aiba et al, 2003); DNCB-induced IL-8 release in THP-1 cells (Nukada et al, 2008); and IL-1β-induced IL-6 in mouse skeletal muscle cells (Luo et al, 2003).

We found that JNK was also phosphorylated in response to DNCB, at 1 and 4 hours, whereas very little change was detected with SDS. Several authors have reported phosphorylation of JNK at time points from 30 minutes to 3 hours, in response to: DNFB and oxazolone in (mouse and human) skin extracts and human RHE models (Koeper et al, 2007); TNCB in Pam212 cells (Yun et al, 2010); and DNFB in mouse ear skin (Ayush et al, 2013).

In addition to p38MAPK, ERK and JNK, we investigated activation of c-Jun and CREB, which are downstream targets of multiple MAPK pathways. In response to DNCB, we detected significant phosphorylation of both transcription factors; the ratios of phosphorylated:total c-Jun and CREB were 4-fold and 10-fold greater than control at 4 hours, respectively. In contrast, c-Jun was only slightly activated at 1 hour following exposure to SDS, and CREB was phosphorylated at early timepoints but not sustained at 4 hours.

In summary, our data demonstrate an important contribution of the MAPK signalling cascades in sensitiser induced cytokine release from keratinocytes. In general, DNCB appears to activate the oxidative stress-induced kinases p38MAPK and JNK, whereas SDS has a greater effect on the ERK pathway, more associated with cell proliferation.

In the gene expression changes in the previous chapter, we found evidence of NF-κB activation, as well as MAPK signalling, in response to DNCB. Therefore, we investigated the NF-κB response at the protein level. We measured total IκB, which

inhibits NF-κB translocation, therefore a decrease in IκB would correspond to NF-κB activation. However, we saw no change in total IκB levels following exposure to DNCB or SDS. In contrast, phosphorylated IκB was found to be down-regulated between 30 minutes and 4 hours, which was more pronounced with DNCB than SDS. IκB is ubiquitinated and degraded following phosphorylation (reviewed in Pasparakis, 2009), and therefore the decrease in phosphorylated IκB we observed might be explained by an increase in the rate of proteasomal degradation, leading to a decrease in phospho-IκB levels. This would be consistent with the observed increase in expression of proteins associated with the ubiquitination pathways in response to DNCB (see chapter 4). We also studied the translocation of NF-κB from the cytosol into the nucleus and found a small, but dose-dependent increase in nuclear NF-κB in response to DNCB, and when we inhibited NF-κB, we found reduced expression of DNCB-induced IL-1β, IL-6 and IL-8. The inhibitor dose-dependence was, however, not as pronounced as the inhibition of TNFα-induced IL-1β, IL-6 and IL-8. This difference could be due to the additional influence of MAPK driving DNCB-induced cytokine expression as well as NF-κB. HaCaT cells have been reported to have unusual NF-κB signalling compared to primary keratinocytes (Chaturvedi et al, 2001; Lewis et al, 2006) which may contribute to our conflicting results. However, in agreement with our results, Aiba et al (2003) saw a decrease in phospho-IκB and no change in total IκB in PBMC-DC in response to DNCB. In a different human keratinocyte cell line (NCTC-2544), total IκB was found to be reduced in response to p-phenylenediamine (PPD) (Galbiati et al, 2011), and NF-κB was activated in response to TNBS and DNBS in murine Pam212 keratinocytes (Miyazaki et al 2000). Also, NF-κB inhibition reduced poly(I:C)-induced IL-8 expression in HaCaT cells (Voss et al, 2012). Although our results are not all consistent with an activated NF-κB phenotype, on balance there is evidence of a role for NF-κB signalling in DNCB-induced cytokine release.

We found no changes in phosphorylation levels of STAT3 and STAT6 in response to DNCB or SDS, while phosphorylated Tyk2 (a member of the JAK family) increased by just 1.4-fold at 30 minutes and 1 hour following exposure to DNCB. In agreement with this, Valk et al (2002) saw no activation of STAT3 or STAT6 in PBMC-DC following

exposure to TNCB. These results suggest little involvement of JAK/STAT signalling, which is also consistent with the transcriptomics data from chapter 4.

In order to understand the possible upstream triggers for the activated signalling cascades, we have investigated the potential for ROS generation, or phosphorylation of receptor tyrosine kinases (RTK). We probed for total phosphotyrosine, and observed a strong band at just over 171kDa in response to DNCB, which was absent for control. This represented a large molecular weight protein with phosphorylated tyrosine residues, which we hypothesised to be a RTK. Exposure of PBMC-DC to sensitisers for just 15 minutes has been found by others to trigger increased phosphorylated tyrosine residues (proteins up to 135kDa measured) (Kuhn et al, 1998; Becker et al, 2003). We investigated whether the RTK could be EGFR, as EGFR/ErbB signalling is upstream of the MAPK cascades (reviewed in Lemmon and Schlessinger, 2010), and was highlighted in the analysis of the transcriptomics data in chapter 4. This receptor has a molecular weight of 185kDa, in the right range for the phosphotyrosine band, and a cysteine rich extracellular domain (reviewed in Lemmon and Schlessinger, 2010) that could undergo covalent modification by DNCB. To test this hypothesis, we probed for phosphorylated (Tyr^{1173}) EGFR. We found constitutive activation of this receptor with control, and no change following exposure to DNCB. Following our investigation, Frankart et al (2012) saw phospho-EGFR in RHE in response to DNFB between 1 and 4 hours, but not at 8 hours. It is possible that the time point we chose (8 hours) was too late to detect increased phosphorylated EGFR. Alternatively, the difference in results may be due to differences between RHE and HaCaT cells, since Frankart et al (2012) did not observe phospho-EGFR in their control samples. Other studies also provide evidence for involvement of EGFR activation in CHS. EGFRs were found to be internalised in normal human keratinocytes *in vitro* following DNFB exposure (Lambert et al, 2010), and *in vivo*, an EGFR inhibitor caused increased ear swelling during a CHS response to DNFB (Pastore et al, 2005). In common with Frankart et al (2012), we also detected increased transcription of HB-EGF (chapter 4), which is a ligand for both the EGFR and ErbB4. Given the constitutive activation of EGFR we observed in HaCaT cells, it is possible that the ErbB4 receptor has a more dynamic role in responding to chemical stress. ErbB4 has a molecular weight of 180kDa, and is therefore also a

plausible candidate for the phospho-tyrosine band; however, further investigation would be required to test this new hypothesis.

In addition to the possibility of DNCB binding directly to RTKs, DNCB could have an indirect effect through generation of ROS, which could modulate intra-cellular signalling. For example, it has been shown that ROS can trigger MAPK signalling cascades (Teng et al, 2007). To investigate the ROS hypothesis, we measured production of ROS in HaCaT cells following DNCB exposure, and found a significant dose-dependent response. In agreement with our data, other groups have shown that ROS are produced by sensitisers in DC-like cell lines (Miyazawa et al, 2012; Saito et al, 2013), and more recently in keratinocytes (Kim et al, 2012; Esser et al, 2012; Galbiati et al, 2014; Onami et al, 2014). Sensitisers have also been shown to decrease detectable free thiols on the surface of DC or DC-like cells (Hirota et al, 2009; Suzuki et al, 2009; Kagatani et al, 2010). This could be due to binding by the sensitiser or sensitiser-induced ROS. In either case, application of glutathione (GSH) or N-acetylcysteine have been found to reduce effects of sensitiser exposure including: tyrosine phosphorylation (Bruchhausen et al, 2003); MAPK activation (Bruchhausen et al, 2003; Matos et al, 2005 (2)); GSH depletion (Mizuashi et al, 2005); and DC maturation (CD80, CD86) (Iijima et al, 2003). Given the extent of ROS production, the hypothesis that DNCB-generated ROS initiate the intracellular signalling cascades remains plausible. Further investigation would be required to determine the relative contributions of ROS vs. direct DNCB binding in triggering the sensitiser-specific cytokine profile.

We hypothesise that the MAPK and NF-κB signalling cascades could be initiated by DNCB via two main routes: production of oxidative stress, or triggering of RTKs. Both of these mechanisms are likely to depend on the electrophilic nature of DNCB, either by direct binding to free cysteine residues or via increasing intracellular ROS, directly or by sequestering of antioxidant defences (e.g. glutathione, thioredoxin). In the oxidative stress case, Nrf2 signalling could be triggered following binding of ROS or DNCB to Keap1, allowing nuclear translocation of Nrf2 (Itoh et al, 1998). The contributions of direct DNCB binding or ROS to Nrf2 activation could be determined by measuring DNP-haptenated Keap1, or by observing the effect of reducing ROS levels on signalling, for example by over-expressing SOD and catalase. Oxidative stress is also

known to trigger MAPK pathways (p38MAPK, JNK), via effects on the upstream kinase ASK1 and PTP phosphatases. ASK1 kinase activity is inhibited by constitutive interaction with reduced thioredoxin (Saitoh et al, 1998). Following exposure to DNCB, depletion of reduced thioredoxin, combined with irreversible inhibition of thioredoxin reductase, may remove ASK1 inhibition and cause activation of p38MAPK and JNK (Ichijo et al, 1997). ROS have also been shown to cause reversible oxidation of cysteine residues at the catalytic site of MAPK phosphatases (MKP; cysteine-based PTP / DUSP), rendering them unable to de-phosphorylate activated MAPK and therefore potentiating signal transduction (Kamata et al, 2005; Robinson et al, 1999). It is possible that DNCB could also inhibit phosphatases, by irreversibly modifying the same free cysteine residue (or via increasing intracellular ROS). In order to assess these mechanisms, we could measure the effect of DNCB on ASK1 or MKP activity; or test whether DNCB can bind directly to MKP.

Independently of oxidative stress, DNCB could bind to extracellular cysteine residues on RTKs (e.g. ErbB, InsR, Ret), causing phosphorylation and activating the downstream cascades, MAPK and NF-κB. We could test this hypothesis by looking for DNCB bound to cysteine-rich RTKs and/or receptor phosphorylation in response to DNCB. Blocking / mutating these receptors would give us an idea of the contribution of receptor-mediated vs. ROS-mediated activation of MAPK signalling. A second stage in the response, caused by DNCB-induced transcription of ligands (e.g IL-1, DAMPs, growth factors) could be activation of IL-1R, TLR or RTK signalling. To test the impact of this on cytokine release, we could block IL-1R / TLRs, e.g. by knocking out MyD88. As these hypothesised mechanisms only depend on electrophilic reactivity, it is likely that other sensitising chemicals would follow the same mechanism, which could be easily tested with more chemicals.

To investigate if the functional effect of the sensitiser-specific cytokines was to induce DC maturation, we exposed PBMC-DC to conditioned media from HaCaT cells previously exposed to DNCB. We saw a small dose-dependent increase in CD83 and CD86, however, the magnitude was much lower than that produced by exposure to LPS, and not significant. Matjeka et al (2012) carried out a similar experiment, but used much higher, cytotoxic concentrations of sensitiser to generate keratinocyte-conditioned

media, and saw DC maturation, partly driven by IL-1α and other danger signals released after cell death. Therefore, it is unlikely that cytokines derived from keratinocytes exposed to sub-cytotoxic concentrations of sensitiser are influencing DC to mature during the induction of ACD.

Given that keratinocyte conditioned media did not activate DC maturation, we speculate that epidermal keratinocytes may be performing an alternative role in CHS. For example, they may contribute more to DC migration than maturation (e.g. via IL-1β). Keratinocyte cytokine release may affect other cells to increase production of cytokines that trigger DC maturation or migration. The keratinocytes could be more involved in chemotaxis (e.g. via IL-8, and other chemokines), recruiting immune cells to site of chemical exposure. It may be that the main role of the keratinocyte is to sequester harmful chemicals, especially in the thiol-rich outer skin layers, and produce chemokines and DAMPs on death (IL-1α, IL-33, HMGB1) which activate DC. The keratinocytes are also likely to be the main source of modified protein to act as antigen external to DCs for presentation on MHC.

6 GENERAL DISCUSSION

Contact hypersensitivity (CHS) is a well known adaptive immune response. However, although keratinocytes are the first cell type to encounter chemical allergen, their role in the induction of CHS has not been fully characterised. We have investigated the molecular mechanisms activated in keratinocytes in response to chemical allergen. In particular, we have studied sensitiser-induced transcriptional changes and activation of intracellular signalling cascades, and the resultant cytokine release, which may be important in the orchestration of skin cells to initiate an adaptive immune response.

To find a suitable *in vitro* model to characterise the role of keratinocytes in contact hypersensitivity, we evaluated the HaCaT cell line and 3-dimensional human skin models (EpiDerm, EpiDermFT). The 3D models offer significant advantages over monolayer culture, in that they are more representative of the physiology of human skin (Ponec et al, 2000, 2002; Poumay et al, 2004). In our experiments, histological examination of the EpiDerm model confirmed a fully differentiated and stratified tissue structure, representative of keratinocyte differentiation in human epidermis; however, we did not find that the full thickness models (EpiDermFT) had normal tissue physiology. Cytokine gene expression and protein release from the 3D models were found to be highly variable between donors. This was potentially due to variation in the thickness of the stratum corneum between models leading to differences in chemical exposure of the viable keratinocyte layers (Regnier et al, 1993). The variability in cytokine measurements excluded further use of these models to investigate the mechanisms behind sensitiser-induced mediator release.

In order to reduce variability and uncover mechanistic detail, we investigated the HaCaT cell line as a potential *in vitro* model. These cells are derived from spontaneously immortalised (but non-tumorigenic) human keratinocytes, first isolated from the distant periphery of an adult skin melanoma. They retain the ability to differentiate normally (unlike other keratinocyte cell lines) and can produce stratified epidermal tissue (Boukamp et al, 1988). Despite this, HaCaT cells do differ from normal human keratinocytes in being immortalised and cytogenetically abnormal (Boukamp et al, 1988). They contain mutations in both alleles of the p53 gene, which

results in a mutant p53 protein with an extended half life (Lehman et al, 1993). HaCaT cells have also been reported to have high constitutive NF-κB activity compared to primary keratinocytes (Chaturvedi et al, 1999; Qin et al, 1999; Lewis et al, 2006), however, we observed increased activation compared to this baseline, following exposure to DNCB. Although there are some differences between the HaCaT cell line and primary keratinocytes, they have many features in common, and HaCaT cells are frequently used as a model for human keratinocytes. Critically, for investigating molecular mechanisms in our studies, the measurements in HaCaT cells were extremely consistent, and sensitive to different stimuli. We have used HaCaT cells throughout our research; however, it would be interesting to verify our key results in primary keratinocytes.

Using HaCaT cells, we investigated the release of keratinocyte-derived mediators that may play a role in intercellular communication during the initiation of CHS. Following exposure to the chemical allergen DNCB, we saw increased release of cytokines (IL-1β, IL-1ra, IL-6), chemokines (IL-8, RANTES) and the growth factor GM-CSF. We compared this response to HaCaT cells exposed to the irritant SDS, to distinguish the allergen response from cell death, and found a sensitiser-specific signature of amplified release of IL-1β, IL-6 and IL-8. The transcription kinetics of these three cytokines were different. IL-6 expression, as well as being dose-dependent, was high but short lived, whereas IL-1β and IL-8 were sustained for longer, and increased after peak IL-6 expression, indicating that there might be feedback mechanisms operating between the cytokines. Expression of IL-1β and IL-8 has been seen previously from keratinocytes in response to sensitisers (Zepter et al, 1997; Newby et al, 2000, Coquette et al, 2003; Mohamadzadeh, 1994), whereas sensitiser-induced IL-6 expression has been observed in skin *in vivo* (Cumberbatch et al, 1996; Holliday et al, 1996; Flint et al, 1998), but not specifically from keratinocytes. Our results demonstrate that keratinocytes are a potential source of IL-6 in skin during CHS responses. In our study, the sensitiser-specific cytokine responses were closely linked to the level of chemical-induced stress on the cells, and were maximally activated at concentrations just below the cytotoxicity threshold. This led us to study a very narrow range of concentrations of DNCB, with careful consideration of the amount of cell death caused in each experiment.

After observing the sensitiser-specific cytokine release, we investigated changes in the HaCaT transcriptome in response to DNCB and SDS, to understand the pathways driving this response. We saw many DNCB-specific changes in gene expression that were not seen in response to SDS. In general, genes involved in the regulation of transcription were modulated with DNCB, suggesting an active cellular response, whereas for SDS the changes were mainly linked to cell death.

In the transcriptome response to DNCB, we observed up-regulation of IL-1β, IL-6 and IL-8, and also IL-1 family cytokines and receptors (IL-1α, antagonist IL-1ra, inhibitory decoy receptor IL-1R2, IL-1RL1 and its ligand IL-33), suggesting activation of IL-1 signalling in a tightly regulated manner. The transcription of IL-1α was 27-fold up-regulated, but we found that the IL-1α protein was only released by HaCaT cells following total cell death (snap freezing or extremely high concentrations of DNCB). This indicates that IL-1α is pre-stored in keratinocytes in response to sensitiser.

In addition to inflammatory cytokines, we found strong transcriptional up-regulation of many chemokines, suggesting that keratinocytes may have a role in attracting immune cells in response to sensitiser. The chemokines specifically up-regulated in response to DNCB and not SDS included: CCL18, CCL3, CX3CL1, CCL3L3, CCL4, CCL26 and CCL25. Collectively, these chemokines attract a range of cell types previously described at sites of CHS, including granulocytes, monocytes, dendritic cells, NK cells and T cells. Many of these chemokines have not previously been described as being expressed by keratinocytes in response to sensitisers.

As well as cytokine and chemokine mediators, we saw large increases in the expression of keratins, keratin associated proteins, and heat shock proteins that have a role in protein folding and degradation. We also observed modulation of proteases and ubiquitin-related genes. Together, these changes are indicative of increased turnover of proteins in the cell, which could be attributed to protein mis-folding caused by DNCB haptenation, or keratinocyte hyperplasia leading to tissue re-modelling.

To assist biological interpretation of the large number of gene expression changes, we performed pathway, transcription factor and upstream regulator analyses. In these

investigations, we found consistent evidence for the involvement of MAPK and NF-κB signalling in response to DNCB. In addition to the NF-κB and MAPK pathways, Nrf2 and AhR signalling, which trigger the ARE and XRE respectively, were also highlighted in transcription factor and pathway analysis.

Having identified potential signalling cascades from bioinformatics analysis of the transcriptomics experiments, we confirmed the functional involvement of these pathways in response to DNCB. We found that DNCB activated the oxidative stress-induced kinases JNK and p38MAPK, and transcription factors downstream of MAPK, c-Jun and CREB. In contrast, the SDS response was more associated with activation of the ERK pathway. We also saw involvement of NF-κB signalling in the keratinocyte response to DNCB, by direct measurement of NF-κB translocation. Using inhibitors, we demonstrated that the DNCB-specific IL-1β, IL-6 and IL-8 release required both p38MAPK and NF-κB signalling (independently).

In order to initiate a T cell-mediated response to chemical allergen, DCs migrate from skin to the local draining lymph nodes and express co-stimulatory molecules. The mechanism by which skin cells influence DCs to up-regulate these molecules has not been fully characterised. In an immune response to chemical allergen, in the absence of pathogen, endogenous danger signals (DAMPs) including cytokines are likely to be the trigger for DC migration and maturation, but the identity and cellular origin of the DAMPs involved is not clear. A successful CHS response also relies on presentation of chemical-derived antigen, and the source and route of processing and presentation of this antigen is uncertain. Hypotheses for antigen include: haptenation of protein followed by presentation of peptides containing the hapten; or presentation of atypical self-peptides due to mis-processing of haptenated protein or modification of the MHC groove by the chemical. Understanding more about these critical mechanisms for the initiation of CHS would help to establish why some chemicals are more effective at triggering CHS than others. These key challenges surrounding DC maturation and chemical-derived antigen are both dependent on events that occur in the skin, and understanding the mechanisms of the keratinocyte response to chemical allergen is an important step towards addressing these questions.

An important question is whether the restricted set of mediators, which were observed to be up-regulated in reponse to DNCB in this study, is sufficient to initiate priming of an adaptive immune response, or if cross-talk with other cell types is required. We hypothesised that the function of the sensitiser-induced keratinocyte-derived mediators could be to induce DC maturation. We exposed PBMC-DC to conditioned media from DNCB-stimulated keratinocytes (at sub-cytotoxic concentrations), and saw a small dose-dependent increase in DC maturation markers CD83 and CD86, although this increase was much smaller than that produced by LPS. It is likely that the limited amount of DC maturation we observed was due to the dose-dependent increase in keratinocyte-derived IL-1β, which has been shown to enhance antigen presentation by DCs (Enk et al, 1993). However, our data suggests it is unlikely that keratinocytes alone are able to incite DCs to fully mature following exposure to sub-cytotoxic concentrations of sensitiser; and DC maturation may require a degree of keratinocyte cell death in exposed tissue. IL-1α and IL-33, which we found to be up-regulated in response to DNCB, are released from intracellular stores following cell death, and are known to act as danger-associated molecular patterns (DAMPs, Cohen et al, 2010; Cayrol and Girard, 2009). IL-1α has been shown to be capable of activating dendritic cells to express co-stimulatory molecules (Matjeka et al, 2012), and IL-33 promotes Treg function (Schiering et al, 2014; Matta et al, 2014). As well as cytokine signalling mediators, we saw a large increase in transcription of heat shock proteins and β-defensin 103b, which may provide additional danger signalling to neighbouring cells in the epidermis, causing DC maturation (Basu et al, 2000; Funderberg et al, 2007) following keratinocyte cell death.

An alternative hypothesis, if a substantial level of cell death is not required, is that the keratinocyte-derived mediators we detected are part of communication with other skin cells to produce amplified or more diverse stimuli that can initiate an immune response. *In vivo* cutaneous immune responses to chemical allergens involve cytokines and chemokines (discussed previously) generated in the epidermis: IL-1α, IL-1β, IL-6, IL-10, IL-12, IL-18, IFNγ, TNFα, IP-10, MIP-2 and GM-CSF. It is not possible to accurately identify which skin cell type is responsible for the production of each cytokine, but the keratinocyte-derived cytokines we have observed could be directly contributing to this milieu or stimulating other cell types to create the correct

environment. For example, high levels of IL-6 and IL-8 can be induced in fibroblasts with keratinocyte-derived IL-1 (Boxman et al, 1996). The keratinocyte mediators may also trigger LCs to produce additional IL-1β and IL-6, or TNFα production from macrophages.

It is also possible that the main effect caused by intercellular mediators released from keratinocytes at sub-cytotoxic concentrations is to attract immune cellular infiltrate to the site of chemical exposure. This suggestion is supported by the large increase in expression of many chemokines in response to DNCB, and high levels of IL-8 release, known to be a chemoattractant for granulocytes and T cells (Harada et al, 1994). If the main role of keratinocytes in CHS is the production of chemokines, then keratinocytes may have a larger role in the elicitation, rather than the initiation of CHS responses. In support of an elicitation role, we saw release of a large number of mediators in response to a combined innate/adaptive immune stimulus, LPS/IFNγ, which is representative of the skin microenvironment during an active elicitation response. LPS/IFNγ-induced mediator release included pro-inflammatory cytokines (IL-2, IL-6, IL-7, IFNα), chemokines (MIP-1α, IP-10, MCP-1, MIG, RANTES), growth factors (HGF, FGF, GCSF), and immuno-suppressive mediators (IL-1ra, IL-10, IL-2R). These data suggest that keratinocytes could help to regulate elicitation responses through both stimulatory and inhibitory mechanisms. The role of keratinocytes in elicitation of CHS has not been well studied and warrants further investigation.

One intriguing aspect of the sensitiser-specific cytokine signature from keratinocytes, the high and short-lived expression of IL-6, may be connected to the question of the mechanism of antigen generation in CHS. IL-6 has previously been linked with autoimmune responses, by causing mis-processing in the endosome, resulting in the presentation of atypical epitopes (Drakesmith et al, 1998). Blocking the IL-6 receptor was also shown to inhibit experimental autoimmune encephalomyelitis, and suppress antigen-specific T cells (Serada et al, 2008). These data contribute to the hypothesis that keratinocyte-derived IL-6 might stimulate a sensitiser-induced 'autoimmune-like' reaction. This idea is supported by the increase in proteinase and proteasome expression indicated in our transcriptomics data. In addition to IL-6 driven mis-processing, it is possible that DNCB haptenates and causes mis-folding of many

proteins, which are processed to present peptides that appear non-self. This is consistent with the strong up-regulation of Hsps observed following exposure to DNCB, which may be transcribed as a response to mis-folded protein in order to accelerate their delivery to the proteasome.

Based on our observations, we can propose the molecular mechanisms that lead to the keratinocyte-derived cytokine release (Figure 6-1). DNCB is a highly reactive electrophilic chemical, and is therefore likely to covalently modify any exposed nucleophilic amino acids on protein (Aleksic et al, 2007, 2008). We found evidence to support non-specific protein modification, in that many of the changes seen in the transcriptome relate to proteins containing a high proportion of cysteine, or cysteine residues in critical functional domains e.g. KRTAPs, chemokines, phosphatases, and proteins involved in glutathione/thioredoxin and redox sensitive Keap1/Nrf2 pathways.

Direct binding of DNCB to cysteine residues on Keap1 may trigger activation of Nrf2 signalling (Kobayashi et al, 2009). DNCB is also known to sequester glutathione (Chia et al, 2010) and thioredoxin by direct binding, and irreversibly inhibit thioredoxin reductase (Nordberg et al, 1998). These reactions alter the redox balance of the cell, and allow endogenous ROS levels to rise. We found that DNCB produced a significant increase in intracellular ROS; it is possible that once the amount of ROS overwhelms antioxidant defences, the ROS will also contribute to the activation of redox-sensitive signalling cascades such as Nrf2 and stress-activated MAPK (p38MAPK, JNK). ASK1, a kinase upstream of p38MAPK and JNK, is inactivated by interaction with reduced thioredoxin, therefore a decrease in the level of thioredoxin can trigger p38MAPK and JNK signalling. Also, oxidation of functionally-critical cysteine residues on MKP (Salmeen and Barford, 2005), by ROS or DNCB binding, will inhibit the phosphatase activity, removing inhibition and allowing signal transduction to continue.

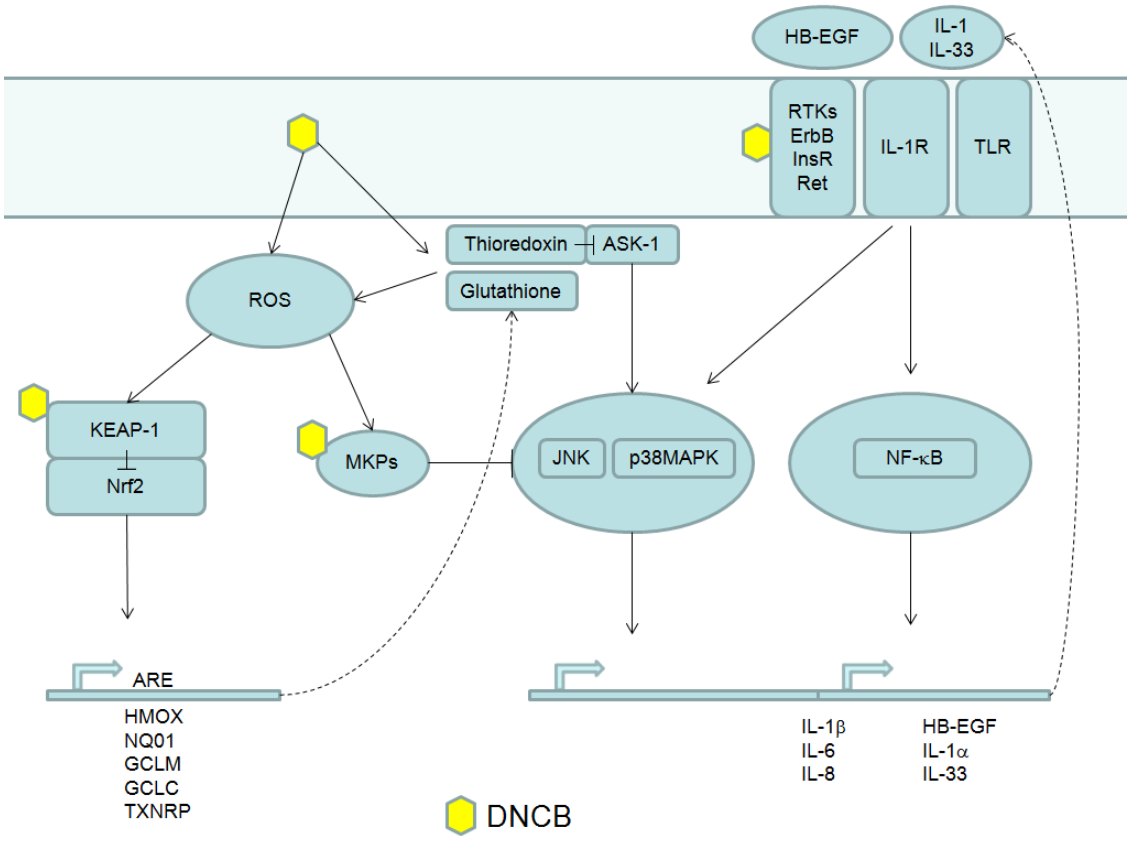

Figure 6-1 Potential molecular mechanisms driving keratinocyte responses to DNCB

In addition to cysteine-rich proteins, some receptor tyrosine kinases, such as EGFR/ErbB, InsR and Ret, have extracellular domains with a high proportion of cysteine residues (reviewed in Lemmon and Schlessinger, 2010), which, if bound by DNCB, could lead to activation of the receptor and downstream MAPK and NF-κB cascades. We saw phosphorylation of a large molecular weight protein, potentially activated following direct binding of DNCB to extracellular cysteine residues (e.g. ErbB receptors), or via binding to a ligand induced by DNCB. From the analysis of the transcriptomics data, we hypothesise that this protein is the ErbB4 receptor, driven by direct binding of DNCB or interaction with the ligand HB-EGF. Other receptors such as the IL-1R or TLRs are also implicated in the gene expression data, based on changes in IL-1R/TLR downstream signalling and up-regulation of IL-1α, IL-1β, IL-1ra and IL-33. Some of these receptor-mediated signals may be part of a secondary stage of the response, triggered following up-regulation of their respective ligands during the initial reaction to DNCB.

Our research has highlighted a number of other areas that would be interesting for further study. We have seen a specific cytokine response (IL-1β, IL-6 and IL-8) to DNCB induced via MAPK and NF-κB signalling pathways in HaCaT cells, and it would be interesting to see if the same response was found from primary keratinocytes. Given that many of the changes we observed may have been caused by nucleophilic substitution, it would also be interesting to determine whether other electrophilic chemical allergens induce a similar response, and if there are any differences between the pathways triggered. We found a strong band in response to DNCB on the phospho-tyrosine blot, which is likely to be an activated RTK, and we are keen to uncover the identity of this protein; we have hypothesised that it may be the ErbB4 receptor, and this could be easily tested. DNCB-dependent signalling via the TLR/NLR or IL-1 receptors is also likely from our data, and could be further characterised.

We have seen the potential of keratinocytes to produce DAMPs (including cytokines) in response to sensitiser, and it would be interesting to see how this depends on the nature and kinetics of cell death, and what their functional effect would be on DCs. It would also be interesting to determine how the cytokines released from keratinocytes at non-

cytotoxic concentrations act in conjunction with mediators from other cell types in skin to affect DC behaviour. Co-culture of sensitiser-exposed keratinocytes or conditioned media with other skin cells, such as fibroblasts, macrophages, mast cells or T cells, would enable characterisation of the full variety of cytokines that could be induced from keratinocyte-derived signals. Exposing PBMC-DC to secondary, co-culture media, combined with inhibition of individual cytokines, could then determine which of these mediators are capable of maturing DCs.

It would be particularly appealing to investigate which proteins are haptenated in skin, and what antigenic peptides are presented. To establish this, we could compare the repertoires of presented peptides following elution of peptide:MHC from DCs co-cultured with keratinocytes pre-treated with sensitiser or vehicle control. In addition to this, we would like to understand whether the processing and presentation pathways involved in generating antigenic peptide are directly perturbed by sensitisers or sensitiser-derived cytokines such as IL-6. Or whether sensitiser can bind directly to, and distort the MHC groove altering the range of peptides with affinity to bind MHC. It is possible that there is an autoimmune-like aspect to the development of CHS responses, due to atypical antigen presentation. We would like to determine whether sensitiser-induced IL-6 from keratinocytes has a functional role in driving atypical antigen presentation and autoimmune-like responses.

Further study surrounding the role of the keratinocyte in elicitation, specifically, which cell types respond to the keratinocytes-derived chemokines produced, how they interact and potentially regulate T cell function, could be of great importance for modulation of skin immune responses or vaccine development. A final but significant gap in our knowledge is the extent, phenotype and location of the memory T cells generated in CHS, particularly the density of hapten-antigen derived memory T cells residing in the skin as tissue- resident memory cells (Trm) and how long they prevail. A large clinical study involving skin biopsies from allergic vs non allergic subjects could be designed to investigate this.

REFERENCES

Achilleos,C., Tailhardat,M., Courtellemont,P., Varlet,B.L., & Dupont,D. Investigation of surface plasmon resonance biosensor for skin sensitizers studies. *Toxicol. In Vitro* **23**, 308-318 (2009).

Adam,J., Pichler,W.J., & Yerly,D. Delayed drug hypersensitivity: models of T-cell stimulation. *Br. J. Clin. Pharmacol.* **71**, 701-707 (2011).

Ade,N., Martinozzi-Teissier,S., Pallardy,M., & Rousset,F. Activation of U937 cells by contact sensitizers: CD86 expression is independent of apoptosis. *J. Immunotoxicol.* **3**, 189-197 (2006).

Ade,N. *et al.* NF-kappaB plays a major role in the maturation of human dendritic cells induced by NiSO(4) but not by DNCB. *Toxicol. Sci.* **99**, 488-501 (2007).

Ade,N. *et al.* HMOX1 and NQO1 genes are upregulated in response to contact sensitizers in dendritic cells and THP-1 cell line: role of the Keap1/Nrf2 pathway. *Toxicol. Sci.* **107**, 451-460 (2009).

Adema,G.J. *et al.* A dendritic-cell-derived C-C chemokine that preferentially attracts naive T cells. *Nature* **387**, 713-717 (1997).

Aiba,S. & Katz,S.I. Phenotypic and functional characteristics of in vivo-activated Langerhans cells. *The Journal of Immunology* **145**, 2791-2796 (1990).

Aiba,S., Terunuma,A., Manome,H., & Tagami,H. Dendritic cells differently respond to haptens and irritants by their production of cytokines and expression of co-stimulatory molecules. *Eur. J. Immunol.* **27**, 3031-3038 (1997).

Aiba,S. *et al.* p38 Mitogen-activated protein kinase and extracellular signal-regulated kinases play distinct roles in the activation of dendritic cells by two representative haptens, NiCl2 and 2,4-dinitrochlorobenzene. *J. Invest Dermatol.* **120**, 390-399 (2003).

Akeda,T. *et al.* CD8+ T cell granzyme B activates keratinocyte endogenous IL-18. *Arch. Dermatol. Res.* **306**, 125-130 (2014).

Albanesi,C. *et al.* Th1-and Th1-derived lymphokines differentially induce chemokine production by keratinocytes: implications for Th1 and Th2 cells recruitment into the skin. *Journal of Investigative Dermatology* **115**, 547 (2000).

Aleksic,M. *et al.* Investigating protein haptenation mechanisms of skin sensitisers using human serum albumin as a model protein. *Toxicol. In Vitro* **21**, 723-733 (2007).

Aleksic,M. *et al.* Mass spectrometric identification of covalent adducts of the skin allergen 2,4-dinitro-1-chlorobenzene and model skin proteins. *Toxicol. In Vitro* **22**, 1169-1176 (2008).

Aleksic,M. *et al.* Reactivity profiling: covalent modification of single nucleophile peptides for skin sensitization risk assessment. *Toxicol. Sci.* **108**, 401-411 (2009).

Ali,R.S. *et al.* Expression of the peptide antibiotics human beta defensin-1 and human beta defensin-2 in normal human skin. *J. Invest Dermatol.* **117**, 106-111 (2001).

Andrew,P.J., Harant,H., & Lindley,I.J. Up-regulation of interleukin-1beta-stimulated interleukin-8 in human keratinocytes by nitric oxide. *Biochem. Pharmacol.* **57**, 1423-1429 (1999).

Ansel,J.C., Luger,T.A., & Green,I. The effect of in vitro and in vivo UV irradiation on the production of ETAF activity by human and murine keratinocytes. *J. Invest Dermatol.* **81**, 519-523 (1983).

Antonios,D. *et al.* Metallic haptens induce differential phenotype of human dendritic cells through activation of mitogen-activated protein kinase and NF-kappaB pathways. *Toxicol. In Vitro* **23**, 227-234 (2009).

Aragane,Y. *et al.* IL-12 is expressed and released by human keratinocytes and epidermoid carcinoma cell lines. *J. Immunol.* **153**, 5366-5372 (1994).

Arend,W.P., Welgus,H.G., Thompson,R.C., & Eisenberg,S.P. Biological properties of recombinant human monocyte-derived interleukin 1 receptor antagonist. *J. Clin. Invest* **85**, 1694-1697 (1990).

Ariizumi,K., Meng,Y., Bergstresser,P.R., & Takashima,A. IFN-gamma-dependent IL-7 gene regulation in keratinocytes. *J. Immunol.* **154**, 6031-6039 (1995).

Arner,E.S., Bjornstedt,M., & Holmgren,A. 1-Chloro-2,4-dinitrobenzene is an irreversible inhibitor of human thioredoxin reductase. Loss of thioredoxin disulfide reductase activity is accompanied by a large increase in NADPH oxidase activity. *J. Biol. Chem.* **270**, 3479-3482 (1995).

Arrighi,J.F., Rebsamen,M., Rousset,F., Kindler,V., & Hauser,C. A critical role for p38 mitogen-activated protein kinase in the maturation of human blood-derived dendritic cells induced by lipopolysaccharide, TNF-alpha, and contact sensitizers. *J. Immunol.* **166**, 3837-3845 (2001).

Asea,A. *et al.* Novel signal transduction pathway utilized by extracellular HSP70: role of toll-like receptor (TLR) 2 and TLR4. *J. Biol. Chem.* **277**, 15028-15034 (2002).

Ashikaga,T. *et al.* Development of an in vitro skin sensitization test using human cell lines: the human Cell Line Activation Test (h-CLAT). I. Optimization of the h-CLAT protocol. *Toxicol. In Vitro* **20**, 767-773 (2006).

Asselineau,D., Bernhard,B., Bailly,C., & Darmon,M. Epidermal morphogenesis and induction of the 67 kD keratin polypeptide by culture of human keratinocytes at the liquid-air interface. *Exp. Cell Res.* **159**, 536-539 (1985).

Ayush,O. *et al.* Glutamine suppresses DNFB-induced contact dermatitis by deactivating p38 mitogen-activated protein kinase via induction of MAPK phosphatase-1. *J. Invest Dermatol.* **133**, 723-731 (2013).

Azam,P. *et al.* The cytokine-dependent MUTZ-3 cell line as an in vitro model for the screening of contact sensitizers. *Toxicol. Appl. Pharmacol.* **212**, 14-23 (2006).

Babior,B.M. The Respiratory Burst of Phagocytes. *Journal of Clinical Investigation* **73**, 599-601 (1984).

Bacci,S., Alard,P., Dai,R., Nakamura,T., & Streilein,J.W. High and low doses of haptens dictate whether dermal or epidermal antigen-presenting cells promote contact hypersensitivity. *Eur. J. Immunol.* **27**, 442-448 (1997).

Bachmann,M.F. *et al.* Peptide-induced T cell receptor down-regulation on naive T cells predicts agonist/partial agonist properties and strictly correlates with T cell activation. *Eur. J. Immunol.* **27**, 2195-2203 (1997).

Baggiolini,M., Walz,A., & Kunkel,S.L. Neutrophil-Activating Peptide-1 Interleukin-8, A Novel Cytokine That Activates Neutrophils. *Journal of Clinical Investigation* **84**, 1045-1049 (1989).

Barker,J.N., Allen,M.H., & MacDonald,D.M. The effect of in vivo interferon-gamma on the distribution of LFA-1 and ICAM-1 in normal human skin. *J. Invest Dermatol.* **93**, 439-442 (1989).

Barker,J.N., Sarma,V., Mitra,R.S., Dixit,V.M., & Nickoloff,B.J. Marked synergism between tumor necrosis factor-alpha and interferon-gamma in regulation of keratinocyte-derived adhesion molecules and chemotactic factors. *J. Clin. Invest* **85**, 605-608 (1990).

Barker,J.N. *et al.* Modulation of keratinocyte-derived interleukin-8 which is chemotactic for neutrophils and T lymphocytes. *Am. J. Pathol.* **139**, 869-876 (1991).

Barker,J.N. *et al.* Monocyte chemotaxis and activating factor production by keratinocytes in response to IFN-gamma. *J. Immunol.* **146**, 1192-1197 (1991).

Barker,J.N., Mitra,R.S., Griffiths,C.E., Dixit,V.M., & Nickoloff,B.J. Keratinocytes as initiators of inflammation. *Lancet* **337**, 211-214 (1991).

Barker,J.N.W.N., Allen,M.H., & MacDonald,D.M. Alterations Induced in Normal Human Skin by Invivo Interferon-Gamma. *British Journal of Dermatology* **122**, 451-458 (1990).

Baroja-Mazo,A. *et al.* The NLRP3 inflammasome is released as a particulate danger signal that amplifies the inflammatory response. *Nat. Immunol.* **15**, 738-748 (2014).

Barrat,F.J. *et al.* Nucleic acids of mammalian origin can act as endogenous ligands for Toll-like receptors and may promote systemic lupus erythematosus. *The Journal of Experimental Medicine* **202**, 1131-1139 (2005).

Bascom,C.C. *et al.* Complex regulation of transforming growth factor beta 1, beta 2, and beta 3 mRNA expression in mouse fibroblasts and keratinocytes by transforming growth factors beta 1 and beta 2. *Mol. Cell Biol.* **9**, 5508-5515 (1989).

Basham,T.Y., Nickoloff,B.J., Merigan,T.C., & Morhenn,V.B. Recombinant Gamma-Interferon Induces Hla-Dr Expression on Cultured Human Keratinocytes. *Journal of Investigative Dermatology* **83**, 88-90 (1984).

Basilico,C. & Moscatelli,D. The FGF family of growth factors and oncogenes. *Adv Cancer Res.* **59**, 115-165 (1992).

Basketter,D.A., York,M., McFadden,J.P., & Robinson,M.K. Determination of skin irritation potential in the human 4-h patch test. *Contact Dermatitis* **51**, 1-4 (2004).

Basu,S., Binder,R.J., Suto,R., Anderson,K.M., & Srivastava,P.K. Necrotic but not apoptotic cell death releases heat shock proteins, which deliver a partial maturation signal to dendritic cells and activate the NF-kappa B pathway. *Int. Immunol.* **12**, 1539-1546 (2000).

Bausinger,H., Lipsker,D., & Hanau,D. Heat-shock proteins as activators of the innate immune system. *Trends Immunol.* **23**, 342-343 (2002).

Bazan,J.F. *et al.* A new class of membrane-bound chemokine with a CX3C motif. *Nature* **385**, 640-644 (1997).

Becker,D., Valk,E., Zahn,S., Brand,P., & Knop,J. Coupling of contact sensitizers to thiol groups is a key event for the activation of monocytes and monocyte-derived dendritic cells. *J. Invest Dermatol.* **120**, 233-238 (2003).

Bigler,C.F., Norris,D.A., Weston,W.L., & Arend,W.P. Interleukin-1 receptor antagonist production by human keratinocytes. *J. Invest Dermatol.* **98**, 38-44 (1992).

Binder,R.J., Blachere,N.E., & Srivastava,P.K. Heat shock protein-chaperoned peptides but not free peptides introduced into the cytosol are presented efficiently by major histocompatibility complex I molecules. *J. Biol. Chem.* **276**, 17163-17171 (2001).

Biragyn,A. *et al.* Toll-like receptor 4-dependent activation of dendritic cells by beta-defensin 2. *Science* **298**, 1025-1029 (2002).

Bjerke,J.R., Tigalonova,M., & Matre,R. IgG-Fc receptors in stratum granulosum: an immunological defence in human skin? *Acta Derm. Venereol.* **74**, 429-432 (1994).

Black,A.P. *et al.* Human keratinocyte induction of rapid effector function in antigen-specific memory CD4+ and CD8+ T cells. *Eur. J. Immunol.* **37**, 1485-1493 (2007).

Blauvelt,A. *et al.* Interleukin-15 mRNA is expressed by human keratinocytes Langerhans cells, and blood-derived dendritic cells and is downregulated by ultraviolet B radiation. *J. Invest Dermatol.* **106**, 1047-1052 (1996).

Boelsma,E., Verhoeven,M.C., & Ponec,M. Reconstruction of a human skin equivalent using a spontaneously transformed keratinocyte cell line (HaCaT). *J. Invest Dermatol.* **112**, 489-498 (1999).

Boisleve,F., Kerdine-Romer,S., Rougier-Larzat,N., & Pallardy,M. Nickel and DNCB induce CCR7 expression on human dendritic cells through different signalling pathways: role of TNF-alpha and MAPK. *J. Invest Dermatol.* **123**, 494-502 (2004).

Boisleve,F., Kerdine-Romer,S., & Pallardy,M. Implication of the MAPK pathways in the maturation of human dendritic cells induced by nickel and TNF-alpha. *Toxicology* **206**, 233-244 (2005).

Bonilla,W.V. *et al.* The alarmin interleukin-33 drives protective antiviral CD8(+) T cell responses. *Science* **335**, 984-989 (2012).

Borlon,C. *et al.* The usefulness of toxicogenomics for predicting acute skin irritation on in vitro reconstructed human epidermis. *Toxicology* **241**, 157-166 (2007).

Boukamp,P. *et al.* Normal keratinization in a spontaneously immortalized aneuploid human keratinocyte cell line. *J. Cell Biol.* **106**, 761-771 (1988).

Boukamp,P. *et al.* Sustained nontumorigenic phenotype correlates with a largely stable chromosome content during long-term culture of the human keratinocyte line HaCaT. *Genes Chromosomes. Cancer* **19**, 201-214 (1997).

Boxman,I.L., Ruwhof,C., Boerman,O.C., Lowik,C.W., & Ponec,M. Role of fibroblasts in the regulation of proinflammatory interleukin IL-1, IL-6 and IL-8 levels induced by keratinocyte-derived IL-1. *Arch. Dermatol. Res.* **288**, 391-398 (1996).

Boyman,O. & Sprent,J. The role of interleukin-2 during homeostasis and activation of the immune system. *Nat. Rev. Immunol.* **12**, 180-190 (2012).

Brand,C.U., Hunziker,T., Limat,A., & Braathen,L.R. Large Increase of Langerhans Cells in Human Skin Lymph Derived from Irritant Contact-Dermatitis. *British Journal of Dermatology* **128**, 184-188 (1993).

Brasch,J., Burgard,J., & Sterry,W. Common Pathogenetic Pathways in Allergic and Irritant Contact-Dermatitis. *Journal of Investigative Dermatology* **98**, 166-170 (1992).

Bruchhausen,S., Zahn,S., Valk,E., Knop,J., & Becker,D. Thiol antioxidants block the activation of antigen-presenting cells by contact sensitizers. *J. Invest Dermatol.* **121**, 1039-1044 (2003).

Burns,D., Breathnach,S.M., Cox,N., & Griffiths,C. *Rooks textbook of dermatology*(Blackwell Science,2004).

Bursch,L.S. *et al.* Identification of a novel population of Langerin+ dendritic cells. *J. Exp. Med.* **204**, 3147-3156 (2007).

Butte,M.J., Keir,M.E., Phamduy,T.B., Sharpe,A.H., & Freeman,G.J. Programmed death-1 ligand 1 interacts specifically with the B7-1 costimulatory molecule to inhibit T cell responses. *Immunity.* **27**, 111-122 (2007).

Candi,E., Schmidt,R., & Melino,G. The cornified envelope: A model of cell death in the skin. *Nature Reviews Molecular Cell Biology* **6**, 328-340 (2005).

Carbone,T. *et al.* CD56highCD16-C. *J. Immunol.* **184**, 1102-1110 (2010).

Carr,M.M. *et al.* Early Cellular Reactions Induced by Dinitrochlorobenzene in Sensitized Human-Skin. *British Journal of Dermatology* **110**, 637-641 (1984).

Carriere,V. *et al.* IL-33, the IL-1-like cytokine ligand for ST2 receptor, is a chromatin-associated nuclear factor in vivo. *Proc. Natl. Acad. Sci. U. S. A* **104**, 282-287 (2007).

Caruso,C., Candore,G., Cigna,D., Colucci,A.T., & Modica,M.A. Biological significance of soluble IL-2 receptor. *Mediators. Inflamm.* **2**, 3-21 (1993).

Caux,C., zutter-Dambuyant,C., Schmitt,D., & Banchereau,J. GM-CSF and TNF-alpha cooperate in the generation of dendritic Langerhans cells. *Nature* **360**, 258-261 (1992).

Cavelier,C., Foussereau,J., & Massin,M. Nickel Allergy - Analysis of Metal Clothing Objects and Patch Testing to Metal Samples. *Contact Dermatitis* **12**, 65-75 (1985).

Cayrol,C. & Girard,J.P. The IL-1-like cytokine IL-33 is inactivated after maturation by caspase-1. *Proc. Natl. Acad. Sci. U. S. A* **106**, 9021-9026 (2009).

Cella,M., Sallusto,F., & Lanzavecchia,A. Origin, maturation and antigen presenting function of dendritic cells. *Current Opinion in Immunology* **9**, 10-16 (1997).

Celli,S., Lemaitre,F., & Bousso,P. Real-time manipulation of T cell-dendritic cell interactions in vivo reveals the importance of prolonged contacts for CD4+ T cell activation. *Immunity.* **27**, 625-634 (2007).

Center,D.M., Kornfeld,H., & Cruikshank,W.W. Interleukin 16 and its function as a CD4 ligand. *Immunol. Today* **17**, 476-481 (1996).

Cerdan,D., Grillon,C., Monsigny,M., Redziniak,G., & Kieda,C. Human keratinocyte membrane lectins: characterization and modulation of their expression by cytokines. *Biol. Cell* **73**, 35-42 (1991).

Chaturvedi,V. *et al.* Apoptosis in proliferating, senescent, and immortalized keratinocytes. *J. Biol. Chem.* **274**, 23358-23367 (1999).

Chaturvedi,V. *et al.* Abnormal NF-kappaB signaling pathway with enhanced susceptibility to apoptosis in immortalized keratinocytes. *J. Dermatol. Sci.* **26**, 67-78 (2001).

Cherry,N. *et al.* Surveillance of occupational skin disease: EPIDERM and OPRA. *Br. J. Dermatol.* **142**, 1128-1134 (2000).

Chia,A.J. *et al.* Differential effect of covalent protein modification and glutathione depletion on the transcriptional response of Nrf2 and NF-kappaB. *Biochem. Pharmacol.* **80**, 410-421 (2010).

Clark,R.A. *et al.* A novel method for the isolation of skin resident T cells from normal and diseased human skin. *J. Invest Dermatol.* **126**, 1059-1070 (2006).

Clark,R.A. *et al.* The vast majority of CLA+ T cells are resident in normal skin. *J. Immunol.* **176**, 4431-4439 (2006).

Coderch,L., De,P.M., Fonollosa,J., de la,M.A., & Parra,J. Efficacy of stratum corneum lipid supplementation on human skin. *Contact Dermatitis* **47**, 139-146 (2002).

Coderch,L., Lopez,O., de la,M.A., & Parra,J.L. Ceramides and skin function. *Am. J. Clin. Dermatol.* **4**, 107-129 (2003).

Coffey,R.J., Jr. *et al.* Production and auto-induction of transforming growth factor-alpha in human keratinocytes. *Nature* **328**, 817-820 (1987).

Cohen,I. *et al.* Differential release of chromatin-bound IL-1alpha discriminates between necrotic and apoptotic cell death by the ability to induce sterile inflammation. *Proc. Natl. Acad. Sci. U. S. A* **107**, 2574-2579 (2010).

Companjen,A.R., Prens,E., Mee,J.B., & Groves,R.W. Expression of IL-18 in human keratinocytes. *J. Invest Dermatol.* **114**, 598-599 (2000).

Coquette,A., Berna,N., Vandenbosch,A., Rosdy,M., & Poumay,Y. Differential expression and release of cytokines by an in vitro reconstructed human epidermis following exposure to skin irritant and sensitizing chemicals. *Toxicology in Vitro* **13**, 867-877 (1999).

Coquette,A. *et al.* Analysis of interleukin-1alpha (IL-1alpha) and interleukin-8 (IL-8) expression and release in in vitro reconstructed human epidermis for the prediction of in vivo skin irritation and/or sensitization. *Toxicol. In Vitro* **17**, 311-321 (2003).

Corsini,E., Primavera,A., Marinovich,M., & Galli,C.L. Selective induction of cell-associated interleukin-1alpha in murine keratinocytes by chemical allergens. *Toxicology* **129**, 193-200 (1998).

Corsini,E., Sheasgreen,J., Marinovich,M., & Galli,C.L. Use of differential display-polymerase chain reaction to identify genes selectively modulated by chemical allergens in reconstituted human epidermis. *Toxicol. In Vitro* **16**, 427-431 (2002).

Corsini,E. *et al.* Use of IL-18 production in a human keratinocyte cell line to discriminate contact sensitizers from irritants and low molecular weight respiratory allergens. *Toxicol. In Vitro* **23**, 789-796 (2009).

Cruz,M.T. *et al.* Differential activation of nuclear factor kappa B subunits in a skin dendritic cell line in response to the strong sensitizer 2,4-dinitrofluorobenzene. *Arch. Dermatol. Res.* **294**, 419-425 (2002).

Cucinotta,M. *et al.* Regulation of interleukin-8 gene at a distinct site of its promoter by CCAAT enhancer-binding protein homologous protein in prostaglandin E2-treated human T cells. *J. Biol. Chem.* **283**, 29760-29769 (2008).

Cuenda,A. *et al.* SB 203580 is a specific inhibitor of a MAP kinase homologue which is stimulated by cellular stresses and interleukin-1. *FEBS Lett.* **364**, 229-233 (1995).

Cumberbatch,M. & Kimber,I. Dermal tumour necrosis factor-alpha induces dendritic cell migration to draining lymph nodes, and possibly provides one stimulus for Langerhans' cell migration. *Immunology* **75**, 257-263 (1992).

Cumberbatch,M. & Kimber,I. Tumour necrosis factor-alpha is required for accumulation of dendritic cells in draining lymph nodes and for optimal contact sensitization. *Immunology* **84**, 31-35 (1995).

Cumberbatch,M., Dearman,R.J., & Kimber,I. Constitutive and inducible expression of interleukin-6 by Langerhans cells and lymph node dendritic cells. *Immunology* **87**, 513-518 (1996).

Cumberbatch,M., Dearman,R.J., & Kimber,I. Langerhans cells require signals from both tumour necrosis factor-alpha and interleukin-1 beta for migration. *Immunology* **92**, 388-395 (1997).

Cumberbatch,M., Griffiths,C.E., Tucker,S.C., Dearman,R.J., & Kimber,I. Tumour necrosis factor-alpha induces Langerhans cell migration in humans. *Br. J. Dermatol.* **141**, 192-200 (1999).

Cumberbatch,M., Dearman,R.J., Antonopoulos,C., Groves,R.W., & Kimber,I. Interleukin (IL)-18 induces Langerhans cell migration by a tumour necrosis factor-alpha- and IL-1beta-dependent mechanism. *Immunology* **102**, 323-330 (2001).

Curtis,A. *et al.* The effects of nickel and chromium on human keratinocytes: differences in viability, cell associated metal and IL-1alpha release. *Toxicol. In Vitro* **21**, 809-819 (2007).

Dahlen,S.E. *et al.* Leukotrienes Promote Plasma Leakage and Leukocyte Adhesion in Post-Capillary Venules - Invivo Effects with Relevance to the Acute Inflammatory Response. *Proceedings of the National Academy of Sciences of the United States of America-Biological Sciences* **78**, 3887-3891 (1981).

De Smedt,A.C., Van Den Heuvel,R.L., Van,T., V, Berneman,Z.N., & Schoeters,G.E. Capacity of CD34+ progenitor-derived dendritic cells to distinguish between sensitizers and irritants. *Toxicol. Lett.* **156**, 377-389 (2005).

Deyrieux,A.F. & Wilson,V.G. In vitro culture conditions to study keratinocyte differentiation using the HaCaT cell line. *Cytotechnology* **54**, 77-83 (2007).

Dinarello,C.A. The biology of interleukin-1. *Challenges in Medicine - 100Th Birthday of Ernst Jung - Prizes and Medals Awarded in 1996* **8**, 9-17 (1996).

Donnarumma,G. *et al.* Analysis of the response of human keratinocytes to Malassezia globosa and restricta strains. *Arch. Dermatol. Res.*(2014).

dos Santos,G.G. *et al.* A potential in vitro epidermal equivalent assay to determine sensitizer potency. *Toxicol. In Vitro* **25**, 347-357 (2011).

Dovezenski,N., Billetta,R., & Gigli,I. Expression and localization of proteins of the complement system in human skin. *J. Clin. Invest* **90**, 2000-2012 (1992).

Draize J.H., Woodward G, & Calvery H.O. Methods for study of irritation and toxicity of substances applied topically to the skin and mucous membranes. *Journal of Pharmacology and Experimental Therapeutics* **82**, 377-390 (1944).

Drakesmith,H. *et al.* In vivo priming of T cells against cryptic determinants by dendritic cells exposed to interleukin 6 and native antigen. *Proc. Natl. Acad. Sci. U. S. A* **95**, 14903-14908 (1998).

Duhen,T., Geiger,R., Jarrossay,D., Lanzavecchia,A., & Sallusto,F. Production of interleukin 22 but not interleukin 17 by a subset of human skin-homing memory T cells. *Nat. Immunol.* **10**, 857-863 (2009).

Dumitriu,I.E., Bianchi,M.E., Bacci,M., Manfredi,A.A., & Rovere-Querini,P. The secretion of HMGB1 is required for the migration of maturing dendritic cells. *J Leukoc Biol* **81**, 84-91 (2007).

Dyring-Andersen,B. *et al.* Increased number and frequency of group 3 innate lymphoid cells in nonlesional psoriatic skin. *Br. J. Dermatol.* **170**, 609-616 (2014).

Efimova,T., LaCelle,P., Welter,J.F., & Eckert,R.L. Regulation of human involucrin promoter activity by a protein kinase C, Ras, MEKK1, MEK3, p38/RK, AP1 signal transduction pathway. *J. Biol. Chem.* **273**, 24387-24395 (1998).

Eisen,H.N. Elicitation of delayed allergic skin reactions with haptens; the dependence of elicitation on hapten combination with protein. *J Exp. Med.* **95**, 473-487 (1952).

Eisenbarth,S.C., Colegio,O.R., O'Connor,W., Sutterwala,F.S., & Flavell,R.A. Crucial role for the Nalp3 inflammasome in the immunostimulatory properties of aluminium adjuvants. *Nature* **453**, 1122-1U13 (2008).

Emter,R., Ellis,G., & Natsch,A. Performance of a novel keratinocyte-based reporter cell line to screen skin sensitizers in vitro. *Toxicol. Appl. Pharmacol.* **245**, 281-290 (2010).

Emter,R. *et al.* Gene expression changes induced by skin sensitizers in the KeratinoSens cell line: Discriminating Nrf2-dependent and Nrf2-independent events. *Toxicol. In Vitro* **27**, 2225-2232 (2013).

Enk,A.H. & Katz,S.I. Early events in the induction phase of contact sensitivity. *J. Invest Dermatol.* **99**, 39S-41S (1992).

Enk,A.H. & Katz,S.I. Identification and induction of keratinocyte-derived IL-10. *J. Immunol.* **149**, 92-95 (1992).

Enk,A.H. & Katz,S.I. Early Molecular Events in the Induction-Phase of Contact Sensitivity. *Proceedings of the National Academy of Sciences of the United States of America* **89**, 1398-1402 (1992).

Enk,A.H., Angeloni,V.L., Udey,M.C., & Katz,S.I. An essential role for Langerhans cell-derived IL-1 beta in the initiation of primary immune responses in skin. *J. Immunol.* **150**, 3698-3704 (1993).

Esche,C., Stellato,C., & Beck,L.A. Chemokines: Key players in innate and adaptive immunity. *Journal of Investigative Dermatology* **125**, 615-628 (2005).

Esser,P.R. *et al.* Contact sensitizers induce skin inflammation via ROS production and hyaluronic acid degradation. *PLoS. One.* **7**, e41340 (2012).

Facy,V., Flouret,V., Regnier,M., & Schmidt,R. Reactivity of Langerhans cells in human reconstructed epidermis to known allergens and UV radiation. *Toxicol. In Vitro* **19**, 787-795 (2005).

Faggioli,L., Costanzo,C., Donadelli,M., & Palmieri,M. Activation of the Interleukin-6 promoter by a dominant negative mutant of c-Jun. *Biochim. Biophys. Acta* **1692**, 17-24 (2004).

Feigen,L.P. Actions of Prostaglandins in Peripheral Vascular Beds. *Federation Proceedings* **40**, 1987-1990 (1981).

Feliciani,C., Gupta,A.K., & Sauder,D.N. Keratinocytes and cytokine/growth factors. *Critical Reviews in Oral Biology & Medicine* **7**, 300-318 (1996).

Ferreira,S.H. & Nakamura,M. Prostaglandin Hyperalgesia .2. Peripheral Analgesic Activity of Morphine, Enkephalins and Opioid Antagonists. *Prostaglandins* **18**, 191-200 (1979).

Fletcher,S.T., Baker,V.A., Fentem,J.H., Basketter,D.A., & Kelsell,D.P. Gene expression analysis of EpiDerm following exposure to SLS using cDNA microarrays. *Toxicol. In Vitro* **15**, 393-398 (2001).

Flint,M.S., Dearman,R.J., Kimber,I., & Hotchkiss,S.A.M. Production and in situ localization of cutaneous tumour necrosis factor alpha (TNF-alpha) and interleukin 6 (IL-6) following skin sensitization. *Cytokine* **10**, 213-219 (1998).

Forster,R. *et al.* CCR7 coordinates the primary immune response by establishing functional microenvironments in secondary lymphoid organs. *Cell* **99**, 23-33 (1999).

Franchi,L. & Nunez,G. The Nlrp3 inflammasome is critical for aluminium hydroxide-mediated IL-1 beta secretion but dispensable for adjuvant activity. *European Journal of Immunology* **38**, 2085-2089 (2008).

Frankart,A., Coquette,A., Schroeder,K.R., & Poumay,Y. Studies of cell signaling in a reconstructed human epidermis exposed to sensitizers: IL-8 synthesis and release depend on EGFR activation. *Arch. Dermatol. Res.* **304**, 289-303 (2012).

Franklin,B.S. *et al.* The adaptor ASC has extracellular and 'prionoid' activities that propagate inflammation. *Nat. Immunol.* **15**, 727-737 (2014).

Frantz,B. *et al.* The activation state of p38 mitogen-activated protein kinase determines the efficiency of ATP competition for pyridinylimidazole inhibitor binding. *Biochemistry* **37**, 13846-13853 (1998).

Frey,J.R. & Wenk,P. [Experimental studies on the pathogenesis of contact eczema.]. *Dermatologica* **112**, 265-305 (1956).

Friedmann,P.S., Moss,C., Shuster,S., & Simpson,J.M. Quantitative Relationships Between Sensitizing Dose of Dncb and Reactivity in Normal Subjects. *Clinical and Experimental Immunology* **53**, 709-715 (1983).

Frohm,M. *et al.* The expression of the gene coding for the antibacterial peptide LL-37 is induced in human keratinocytes during inflammatory disorders. *J. Biol. Chem.* **272**, 15258-15263 (1997).

Fuchs,E. & Green,H. Changes in keratin gene expression during terminal differentiation of the keratinocyte. *Cell* **19**, 1033-1042 (1980).

Fujisawa,H., Kondo,S., Wang,B., Shivji,G.M., & Sauder,D.N. The expression and modulation of IFN-alpha and IFN-beta in human keratinocytes. *J. Interferon Cytokine Res.* **17**, 721-725 (1997).

Fukunaga,A., Khaskhely,N.M., Sreevidya,C.S., Byrne,S.N., & Ullrich,S.E. Dermal Dendritic Cells, and Not Langerhans Cells, Play an Essential Role in Inducing an Immune Response. *The Journal of Immunology* **180**, 3057-3064 (2008).

Funderburg,N. *et al.* Human -defensin-3 activates professional antigen-presenting cells via Toll-like receptors 1 and 2. *Proc. Natl. Acad. Sci. U. S. A* **104**, 18631-18635 (2007).

Galbiati,V. *et al.* Further development of the NCTC 2544 IL-18 assay to identify in vitro contact allergens. *Toxicol. In Vitro* **25**, 724-732 (2011).

Galbiati,V., Papale,A., Galli,C.L., Marinovich,M., & Corsini,E. Role of ROS and HMGB1 in Contact Allergen-Induced IL-18 Production in Human Keratinocytes. *J. Invest Dermatol.*(2014).

Gallucci,S., Lolkema,M., & Matzinger,P. Natural adjuvants: Endogenous activators of dendritic cells. *Nature Medicine* **5**, 1249-1255 (1999).

Gallucci,S. & Matzinger,P. Danger signals: SOS to the immune system. *Current Opinion in Immunology* **13**, 114-119 (2001).

Garmyn,M. *et al.* Human keratinocytes respond to osmotic stress by p38 map kinase regulated induction of HSP70 and HSP27. *J. Invest Dermatol.* **117**, 1290-1295 (2001).

Gauldie,J., Northemann,W., & Fey,G.H. IL-6 functions as an exocrine hormone in inflammation. Hepatocytes undergoing acute phase responses require exogenous IL-6. *J. Immunol.* **144**, 3804-3808 (1990).

Gebhardt,T. *et al.* Different patterns of peripheral migration by memory CD4+ and CD8+ T cells. *Nature* **477** , 216-219 (2011).

Gerberick,G.F. *et al.* A chemical dataset for evaluation of alternative approaches to skin-sensitization testing. *Contact Dermatitis* **50**, 274-288 (2004).

Gerberick,G.F. *et al.* Development of a peptide reactivity assay for screening contact allergens. *Toxicol. Sci.* **81**, 332-343 (2004).

Ghayur,T. *et al.* Caspase-1 processes IFN-gamma-inducing factor and regulates LPS-induced IFN-gamma production. *Nature* **386**, 619-623 (1997).

Giamarellos-Bourboulis,E.J. *et al.* Crystals of monosodium urate monohydrate enhance lipopolysaccharide-induced release of interleukin 1 beta by mononuclear cells through a caspase 1-mediated process. *Annals of the Rheumatic Diseases* **68**, 273-278 (2009).

Gildea,L.A. *et al.* Identification of gene expression changes induced by chemical allergens in dendritic cells: opportunities for skin sensitization testing. *J. Invest Dermatol.* **126**, 1813-1822 (2006).

Ginhoux,F. & Merad,M. Ontogeny and homeostasis of Langerhans cells. *Immunol. Cell Biol.* **88**, 387-392 (2010).

Gober,M.D., Fishelevich,R., Zhao,Y.M., Unutmaz,D., & Gaspari,A.A. Human natural killer T cells infiltrate into the skin at elicitation sites of allergic contact dermatitis. *Journal of Investigative Dermatology* **128** , 1460-1469 (2008).

Gocinski,B.L. & Tigelaar,R.E. Roles of CD4+ and CD8+ T cells in murine contact sensitivity revealed by in vivo monoclonal antibody depletion. *J. Immunol.* **144**, 4121-4128 (1990).

Goebeler,M. *et al.* Differential and sequential expression of multiple chemokines during elicitation of allergic contact hypersensitivity. *Am. J. Pathol.* **158**, 431-440 (2001).

Goldyne,M.E. Prostaglandins and Cutaneous Inflammation. *Journal of Investigative Dermatology* **64**, 377-385 (1975).

Goodman,W.A. *et al.* IL-6 signaling in psoriasis prevents immune suppression by regulatory T cells. *J. Immunol.* **183**, 3170-3176 (2009).

Griffiths,C.E., Voorhees,J.J., & Nickoloff,B.J. Characterization of intercellular adhesion molecule-1 and HLA-DR expression in normal and inflamed skin: modulation by recombinant gamma interferon and tumor necrosis factor. *J. Am. Acad. Dermatol.* **20**, 617-629 (1989).

Griffiths,C.E. *et al.* Exogenous topical lactoferrin inhibits allergen-induced Langerhans cell migration and cutaneous inflammation in humans. *Br. J. Dermatol.* **144**, 715-725 (2001).

Griffiths,C.E., Dearman,R.J., Cumberbatch,M., & Kimber,I. Cytokines and Langerhans cell mobilisation in mouse and man. *Cytokine* **32**, 67-70 (2005).

Groves,R.W. *et al.* Effect of in vivo interleukin-1 on adhesion molecule expression in normal human skin. *J. Invest Dermatol.* **98**, 384-387 (1992).

Groves,R.W., Allen,M.H., Ross,E.L., Barker,J.N., & MacDonald,D.M. Tumour necrosis factor alpha is pro-inflammatory in normal human skin and modulates cutaneous adhesion molecule expression. *Br. J. Dermatol.* **132**, 345-352 (1995).

Gruaz-Chatellard,D., Baumberger,C., Saurat,J.H., & Dayer,J.M. Interleukin 1 receptor antagonist in human epidermis and cultured keratinocytes. *FEBS Lett.* **294**, 137-140 (1991).

Gu,Y. *et al.* Activation of interferon-gamma inducing factor mediated by interleukin-1beta converting enzyme. *Science* **275**, 206-209 (1997).

Guillot,L. *et al.* Cutting edge: the immunostimulatory activity of the lung surfactant protein-A involves Toll-like receptor 4. *J. Immunol.* **168**, 5989-5992 (2002).

Gunn,M.D. *et al.* A chemokine expressed in lymphoid high endothelial venules promotes the adhesion and chemotaxis of naive T lymphocytes. *Proc. Natl. Acad. Sci. U. S. A* **95**, 258-263 (1998).

Gunn,M.D. *et al.* Mice lacking expression of secondary lymphoid organ chemokine have defects in lymphocyte homing and dendritic cell localization. *J. Exp. Med.* **189**, 451-460 (1999).

Haas,J., Lipkow,T., Mohamadzadeh,M., Kolde,G., & Knop,J. Induction of inflammatory cytokines in murine keratinocytes upon in vivo stimulation with contact sensitizers and tolerizing analogues. *Exp Dermatol* **1**, (1992).

Haddad,J.J. The involvement of L-gamma-glutamyl-L-cysteinyl-glycine (glutathione/GSH) in the mechanism of redox signaling mediating MAPK(p38)-dependent regulation of pro-inflammatory cytokine production. *Biochem. Pharmacol.* **63**, 305-320 (2002).

Haegel-Kronenberger,H. *et al.* Adhesive and/or signaling functions of CD44 isoforms in human dendritic cells. *J. Immunol.* **161**, 3902-3911 (1998).

Haessler,U., Pisano,M., Wu,M., & Swartz,M.A. Dendritic cell chemotaxis in 3D under defined chemokine gradients reveals differential response to ligands CCL21 and CCL19. *Proc. Natl. Acad. Sci. U. S. A* **108**, 5614-5619 (2011).

Halaban,R. *et al.* Paracrine stimulation of melanocytes by keratinocytes through basic fibroblast growth factor. *Ann. N. Y. Acad. Sci.* **548**, 180-190 (1988).

Harada,A. *et al.* Essential Involvement of Interleukin-8 (Il-8) in Acute-Inflammation. *J Leukoc Biol* **56**, 559-564 (1994).

Harder,J., Bartels,J., Christophers,E., & Schroder,J.M. A peptide antibiotic from human skin. *Nature* **387**, 861 (1997).

Harder,J. & Nunez,G. Functional expression of the intracellular pattern recognition receptor NOD1 in human keratinocytes. *J. Invest Dermatol.* **129**, 1299-1302 (2009).

Haskill,S. *et al.* Cdna Cloning of An Intracellular Form of the Human Interleukin-1 Receptor Antagonist Associated with Epithelium. *Proceedings of the National Academy of Sciences of the United States of America* **88**, 3681-3685 (1991).

Hauser,C., Saurat,J.H., Schmitt,A., Jaunin,F., & Dayer,J.M. Interleukin-1 Is Present in Normal Human-Epidermis. *Journal of Immunology* **136**, 3317-3323 (1986).

Heinrich,P.C., Castell,J.V., & Andus,T. Interleukin-6 and the Acute Phase Response. *Biochemical Journal* **265**, 621-636 (1990).

Heinrich,P.C. *et al.* Principles of interleukin (IL)-6-type cytokine signalling and its regulation. *Biochem. J.* **374**, 1-20 (2003).

Helle,M., Boeije,L., & Aarden,L.A. Functional discrimination between interleukin 6 and interleukin 1. *Eur. J. Immunol.* **18**, 1535-1540 (1988).

Helle,M., Brakenhoff,J.P., De Groot,E.R., & Aarden,L.A. Interleukin 6 is involved in interleukin 1-induced activities. *Eur. J. Immunol.* **18**, 957-959 (1988).

Hennen,J. *et al.* Cross talk between keratinocytes and dendritic cells: impact on the prediction of sensitization. *Toxicol. Sci.* **123**, 501-510 (2011).

Heufler,C., Koch,F., & Schuler,G. Granulocyte/macrophage colony-stimulating factor and interleukin 1 mediate the maturation of murine epidermal Langerhans cells into potent immunostimulatory dendritic cells. *J. Exp. Med.* **167**, 700-705 (1988).

Heufler,C. *et al.* Interleukin 7 is produced by murine and human keratinocytes. *J. Exp. Med.* **178**, 1109-1114 (1993).

Hirota,M. *et al.* Modification of cell-surface thiols elicits activation of human monocytic cell line THP-1: possible involvement in effect of haptens 2,4-dinitrochlorobenzene and nickel sulfate. *J. Toxicol. Sci.* **34**, 139-150 (2009).

Hiscott,J. *et al.* Characterization of a functional NF-kappa B site in the human interleukin 1 beta promoter: evidence for a positive autoregulatory loop. *Mol. Cell Biol.* **13**, 6231-6240 (1993).

Holland,D.B., Bojar,R.A., Jeremy,A.H., Ingham,E., & Holland,K.T. Microbial colonization of an in vitro model of a tissue engineered human skin equivalent--a novel approach. *FEMS Microbiol. Lett.* **279**, 110-115 (2008).

Holland,D.B., Bojar,R.A., Farrar,M.D., & Holland,K.T. Differential innate immune responses of a living skin equivalent model colonized by Staphylococcus epidermidis or Staphylococcus aureus. *FEMS Microbiol. Lett.* **290**, 149-155 (2009).

Holliday,M.R., Dearman,R.J., Basketter,D.A., & Kimber,I. Stimulation by oxazolone of increased IL-6, but not IL-10, in the skin of mice. *Toxicology* **106**, 237-242 (1996).

Homey,B. *et al.* CCL27/CCR10 interactions regulate T cell-mediated skin inflammation. *Journal of Investigative Dermatology* **119**, 301 (2002).

Hooyberghs,J. *et al.* A cell-based in vitro alternative to identify skin sensitizers by gene expression. *Toxicol. Appl. Pharmacol.* **231**, 103-111 (2008).

Hosack,D.A., Dennis,G., Jr., Sherman,B.T., Lane,H.C., & Lempicki,R.A. Identifying biological themes within lists of genes with EASE. *Genome Biol.* **4**, R70 (2003).

Howie,S.E. *et al.* Epidermal keratinocyte production of interferon-gamma immunoreactive protein and mRNA is an early event in allergic contact dermatitis. *J. Invest Dermatol.* **106**, 1218-1223 (1996).

Hsieh,C.S. *et al.* Development of TH1 CD4+ T cells through IL-12 produced by Listeria-induced macrophages. *Science* **260**, 547-549 (1993).

Hudak,S. *et al.* Immune surveillance and effector functions of CCR10(+) skin homing T cells. *J. Immunol.* **169**, 1189-1196 (2002).

Ibrahim,M.A.A., Chain,B.M., & Katz,D.R. The injured cell: the role of the dendritic cell system as a sentinel receptor pathway. *Immunology Today* **16**, 181-186 (1995).

Ichijo,H. *et al.* Induction of apoptosis by ASK1, a mammalian MAPKKK that activates SAPK/JNK and p38 signaling pathways. *Science* **275**, 90-94 (1997).

Iijima,N., Yanagawa,Y., & Onoe,K. Role of early- or late-phase activation of p38 mitogen-activated protein kinase induced by tumour necrosis factor-alpha or 2,4-dinitrochlorobenzene during maturation of murine dendritic cells. *Immunology* **110**, 322-328 (2003).

Illing,P.T. *et al.* Immune self-reactivity triggered by drug-modified HLA-peptide repertoire. *Nature* **486**, 554-558 (2012).

Inaba,K., Inaba,M., Naito,M., & Steinman,R.M. Dendritic Cell Progenitors Phagocytose Particulates, Including Bacillus-Calmette-Guerin Organisms, and Sensitize Mice to Mycobacterial Antigens In-Vivo. *Journal of Experimental Medicine* **178**, 479-488 (1993).

Inoue,K. *et al.* Mechanism underlying ATP release in human epidermal keratinocytes. *J. Invest Dermatol.* **134**, 1465-1468 (2014).

Ip,W.K. & Lau,Y.L. Distinct maturation of, but not migration between, human monocyte-derived dendritic cells upon ingestion of apoptotic cells of early or late phases. *J. Immunol.* **173**, 189-196 (2004).

Ishii,T. *et al.* Isolation of MHC class I-restricted tumor antigen peptide and its precursors associated with heat shock proteins hsp70, hsp90, and gp96. *J. Immunol.* **162**, 1303-1309 (1999).

Ishimaru,M., Tsukimoto,M., Harada,H., & Kojima,S. Involvement of P2Y(1)(1) receptor in IFN-gamma-induced IL-6 production in human keratinocytes. *Eur. J. Pharmacol.* **703**, 67-73 (2013).

Itoh,K. *et al.* Keap1 represses nuclear activation of antioxidant responsive elements by Nrf2 through binding to the amino-terminal Neh2 domain. *Genes Dev.* **13**, 76-86 (1999).

Iwasaki,A. & Medzhitov,R. Toll-like receptor control of the adaptive immune responses. *Nature Immunology* **5**, 987-995 (2004).

Iyer,S.S. *et al.* Necrotic cells trigger a sterile inflammatory response through the Nlrp3 inflammasome. *Proc. Natl. Acad. Sci. U. S. A* **106**, 20388-20393 (2009).

Jacobs,J.J.L., Lehe,C.L., Hasegawa,H., Elliott,G.R., & Das,P.K. Skin irritants and contact sensitizers induce Langerhans cell migration and maturation at irritant concentration. *Experimental Dermatology* **15**, 432-440 (2006).

Jakob,T. & Udey,M.C. Regulation of E-cadherin-mediated adhesion in Langerhans cell-like dendritic cells by inflammatory mediators that mobilize Langerhans cells in vivo. *J. Immunol.* **160**, 4067-4073 (1998).

Janeway,C., Travers,P., Walport,M., & Shlomchik,M. Immunobiology: The Immune System in Health and Disease. [6th Edition]. 2004. Garland Science.
Ref Type: Generic

Jeffrey,K.L., Camps,M., Rommel,C., & Mackay,C.R. Targeting dual-specificity phosphatases: manipulating MAP kinase signalling and immune responses. *Nat. Rev. Drug Discov.* **6**, 391-403 (2007).

Jiang,X. *et al.* Skin infection generates non-migratory memory CD8+ T(RM) cells providing global skin immunity. *Nature* **483**, 227-231 (2012).

Johansson,H., Lindstedt,M., Albrekt,A.S., & Borrebaeck,C.A. A genomic biomarker signature can predict skin sensitizers using a cell-based in vitro alternative to animal tests. *BMC. Genomics* **12**, 399 (2011).

Johansson,H., Albrekt,A.S., Borrebaeck,C.A., & Lindstedt,M. The GARD assay for assessment of chemical skin sensitizers. *Toxicol. In Vitro* **27**, 1163-1169 (2013).

Johnson,G.B., Brunn,G.J., Kodaira,Y., & Platt,J.L. Receptor-mediated monitoring of tissue well-being via detection of soluble heparan sulfate by Toll-like receptor 4. *J. Immunol.* **168**, 5233-5239 (2002).

Johnson,L.A. & Jackson,D.G. Inflammation-induced secretion of CCL21 in lymphatic endothelium is a key regulator of integrin-mediated dendritic cell transmigration. *Int. Immunol.* **22**, 839-849 (2010).

Kagami,S. *et al.* Interleukin-4 and interleukin-13 enhance CCL26 production in a human keratinocyte cell line, HaCaT cells. *Clin. Exp. Immunol.* **141**, 459-466 (2005).

Kagatani,S. *et al.* Oxidation of cell surface thiol groups by contact sensitizers triggers the maturation of dendritic cells. *J. Invest Dermatol.* **130**, 175-183 (2010).

Kalish,R.S., Wood,J.A., & LaPorte,A. Processing of urushiol (poison ivy) hapten by both endogenous and exogenous pathways for presentation to T cells in vitro. *J. Clin. Invest* **93**, 2039-2047 (1994).

Kamata,H. *et al.* Reactive oxygen species promote TNFalpha-induced death and sustained JNK activation by inhibiting MAP kinase phosphatases. *Cell* **120**, 649-661 (2005).

Kaplan,D.H., Jenison,M.C., Saeland,S., Shlomchik,W.D., & Shlomchik,M.J. Epidermal Langerhans Cell-Deficient Mice Develop Enhanced Contact Hypersensitivity. *Immunity* **23**, 611-620 (2005).

Kaplan,G., Luster,A.D., Hancock,G., & Cohn,Z.A. The Expression of A Gamma-Interferon Induced Protein (Ip-10) in Delayed Immune-Responses in Human-Skin. *Journal of Experimental Medicine* **166**, 1098-1108 (1987).

Kautz-Neu,K. *et al.* Langerhans cells are negative regulators of the anti-Leishmania response. *J. Exp. Med.* **208**, 885-891 (2011).

Kawai,T. & Akira,S. TLR signaling. *Seminars in Immunology* **19**, 24-32 (2007).

Kawakami,K., Taguchi,J., Murata,T., & Puri,R.K. The interleukin-13 receptor alpha2 chain: an essential component for binding and internalization but not for interleukin-13-induced signal transduction through the STAT6 pathway. *Blood* **97**, 2673-2679 (2001).

Kermani,F., Flint,M.S., & Hotchkiss,S.A. Induction and localization of cutaneous interleukin-1 beta mRNA during contact sensitization. *Toxicol. Appl. Pharmacol.* **169**, 231-237 (2000).

Khan,I.U., Mukhtar,H., & Haqqi,T.M. Chemical carcinogens increase IL-1 alpha and IL-6 gene transcripts in human keratinocytes. *Exp. Dermatol.* **2**, 84-88 (1993).

Kim,B.S. Innate Lymphoid Cells in the Skin. *J. Invest Dermatol.* **135**, 673-678 (2015).

Kim,D.H., Byamba,D., Wu,W.H., Kim,T.G., & Lee,M.G. Different characteristics of reactive oxygen species production by human keratinocyte cell line cells in response to allergens and irritants. *Exp. Dermatol.* **21**, 99-103 (2012).

Kimber,I., Dearman,R.J., Scholes,E.W., & Basketter,D.A. The local lymph node assay: developments and applications. *Toxicology* **93**, 13-31 (1994).

Kimber,I. *et al.* Skin sensitization testing in potency and risk assessment. *Toxicol. Sci.* **59**, 198-208 (2001).

Kimura,A. & Kishimoto,T. IL-6: regulator of Treg/Th17 balance. *Eur. J. Immunol.* **40**, 1830-1835 (2010).

Kissenpfennig,A. *et al.* Dynamics and function of Langerhans cells in vivo: dermal dendritic cells colonize lymph node areas distinct from slower migrating Langerhans cells. *Immunity.* **22**, 643-654 (2005).

Kjellerup,R.B., Kragballe,K., Iversen,L., & Johansen,C. Pro-inflammatory cytokine release in keratinocytes is mediated through the MAPK signal-integrating kinases. *Exp. Dermatol.* **17**, 498-504 (2008).

Klekotka,P.A., Yang,L., & Yokoyama,W.M. Contrasting roles of the IL-1 and IL-18 receptors in MyD88-dependent contact hypersensitivity. *J. Invest Dermatol.* **130**, 184-191 (2010).

Klunker,S. *et al.* A second step of chemotaxis after transendothelial migration: keratinocytes undergoing apoptosis release IFN-gamma-inducible protein 10, monokine induced by IFN-gamma, and IFN-gamma-inducible alpha-chemoattractant for T cell chemotaxis toward epidermis in atopic dermatitis. *J. Immunol.* **171**, 1078-1084 (2003).

Kobayashi,M. *et al.* Expression of toll-like receptor 2, NOD2 and dectin-1 and stimulatory effects of their ligands and histamine in normal human keratinocytes. *Br. J. Dermatol.* **160**, 297-304 (2009).

Kobayashi,M. *et al.* The antioxidant defense system Keap1-Nrf2 comprises a multiple sensing mechanism for responding to a wide range of chemical compounds. *Mol. Cell Biol.* **29**, 493-502 (2009).

Kobayashi,Y. *et al.* Identification of calcium-activated neutral protease as a processing enzyme of human interleukin 1 alpha. *Proc. Natl. Acad. Sci. U. S. A* **87**, 5548-5552 (1990).

Kock,A. *et al.* Human Keratinocytes Are A Source for Tumor-Necrosis-Factor-Alpha - Evidence for Synthesis and Release Upon Stimulation with Endotoxin Or Ultraviolet-Light. *Journal of Experimental Medicine* **172**, 1609-1614 (1990).

Koeper,L.M., Schulz,A., Ahr,H.J., & Vohr,H.W. In vitro differentiation of skin sensitizers by cell signaling pathways. *Toxicology* **242** , 144-152 (2007).

Kollisch,G. *et al.* Various members of the Toll-like receptor family contribute to the innate immune response of human epidermal keratinocytes. *Immunology* **114**, 531-541 (2005).

Kong,J., Grando,S.A., & Li,Y.C. Regulation of IL-1 family cytokines IL-1 alpha, IL-1 receptor antagonist, and IL-18 by 1,25-dihydroxyvitamin D-3 in primary keratinocytes. *Journal of Immunology* **176**, 3780-3787 (2006).

Kono,H. & Rock,K.L. How dying cells alert the immune system to danger. *Nature Reviews Immunology* **8**, 279-289 (2008).

Korn,T. *et al.* IL-21 initiates an alternative pathway to induce proinflammatory T(H)17 cells. *Nature* **448**, 484-487 (2007).

Krejci,N.C., Cuono,C.B., Langdon,R.C., & McGuire,J. In vitro reconstitution of skin: fibroblasts facilitate keratinocyte growth and differentiation on acellular reticular dermis. *J. Invest Dermatol.* **97**, 843-848 (1991).

Kroeze,K.L. *et al.* Autocrine regulation of re-epithelialization after wounding by chemokine receptors CCR1, CCR10, CXCR1, CXCR2, and CXCR3. *J. Invest Dermatol.* **132**, 216-225 (2012).

Kuhn,U. *et al.* Induction of tyrosine phosphorylation in human MHC class II-positive antigen-presenting cells by stimulation with contact sensitizers. *J. Immunol.* **160**, 667-673 (1998).

Kunsch,C. & Rosen,C.A. NF-kappa B subunit-specific regulation of the interleukin-8 promoter. *Mol. Cell Biol.* **13**, 6137-6146 (1993).

Kupper,T.S. *et al.* Human keratinocytes contain mRNA indistinguishable from monocyte interleukin 1 alpha and beta mRNA. Keratinocyte epidermal cell-derived thymocyte-activating factor is identical to interleukin 1. *J. Exp. Med.* **164**, 2095-2100 (1986).

Kupper,T.S., Lee,F., Birchall,N., Clark,S., & Dower,S. Interleukin 1 binds to specific receptors on human keratinocytes and induces granulocyte macrophage colony-stimulating factor mRNA and protein. A potential autocrine role for interleukin 1 in epidermis. *J. Clin. Invest* **82**, 1787-1792 (1988).

Kupper,T.S. *et al.* Production of IL-6 by keratinocytes. Implications for epidermal inflammation and immunity. *Ann. N. Y. Acad. Sci.* **557**, 454-464 (1989).

Kupper,T.S. & Fuhlbrigge,R.C. Immune surveillance in the skin: mechanisms and clinical consequences. *Nat. Rev. Immunol.* **4**, 211-222 (2004).

Kurdykowski,S. *et al.* Ultraviolet-B irradiation induces differential regulations of hyaluronidase expression and activity in normal human keratinocytes. *Photochem. Photobiol.* **87**, 1105-1112 (2011).

Lambert,S., Frankart,A., & Poumay,Y. p38 MAPK-regulated EGFR internalization takes place in keratinocyte monolayer during stress conditions. *Arch. Dermatol. Res.* **302**, 229-233 (2010).

Lambrechts,N. *et al.* Gene markers in dendritic cells unravel pieces of the skin sensitization puzzle. *Toxicol. Lett.* **196**, 95-103 (2010).

Landsteiner,K. & Jacobs,J. STUDIES ON THE SENSITIZATION OF ANIMALS WITH SIMPLE CHEMICAL COMPOUNDS. II. *J Exp. Med.* **64**, 625-639 (1936).

Larsen,C.G., Oppenheim,J.J., & Matsushima,K. Interleukin-1 Or Tumor Necrosis Factor Stimulate the Production of Neutrophil Activating Protein by Normal Human-Fibroblasts and Keratinocytes. *Journal of Investigative Dermatology* **92**, 467 (1989).

Larsen,C.G., Anderson,A.O., Oppenheim,J.J., & Matsushima,K. Production of Interleukin-8 by Human Dermal Fibroblasts and Keratinocytes in Response to Interleukin-1 Or Tumor Necrosis Factor. *Immunology* **68**, 31-36 (1989).

Larsen,C.P. *et al.* Migration and maturation of Langerhans cells in skin transplants and explants. *The Journal of Experimental Medicine* **172**, 1483-1493 (1990).

Larsen,J.M., Bonefeld,C.M., Poulsen,S.S., Geisler,C., & Skov,L. IL-23 and T(H)17-mediated inflammation in human allergic contact dermatitis. *J. Allergy Clin. Immunol.* **123**, 486-492 (2009).

Lavker,R.M. & Matoltsy,A.G. Substructure of keratohyalin granules of the epidermis as revealed by high resolution electron microscopy. *Journal of Ultrastruct Res.* **35**, 575-581 (1971).

Lebre,M.C. *et al.* Human keratinocytes express functional Toll-like receptor 3, 4, 5, and 9. *J. Invest Dermatol.* **127**, 331-341 (2007).

Lee,D.Y. & Cho,K.H. The effects of epidermal keratinocytes and dermal fibroblasts on the formation of cutaneous basement membrane in three-dimensional culture systems. *Arch. Dermatol. Res.* **296**, 296-302 (2005).

Lee,H.M. *et al.* Innate immune responses to Mycobacterium ulcerans via toll-like receptors and dectin-1 in human keratinocytes. *Cell Microbiol.* **11**, 678-692 (2009).

Lehman,T.A. *et al.* p53 mutations in human immortalized epithelial cell lines. *Carcinogenesis* **14**, 833-839 (1993).

Lemmon,M.A. & Schlessinger,J. Cell signaling by receptor tyrosine kinases. *Cell* **141**, 1117-1134 (2010).

Lenz,A., Heine,M., Schuler,G., & Romani,N. Human and murine dermis contain dendritic cells. Isolation by means of a novel method and phenotypical and functional characterization. *J. Clin. Invest* **92**, 2587-2596 (1993).

Leslie,C., Wall,M., Zelarney,P., & Voelker,D. Partial-Purification from Macrophages of A Phospholipase-A2 That Hydrolyzes Arachidonic-Acid from Phosphatidylcholine. *Federation Proceedings* **46**, 2285 (1987).

Levine,T.P. & Chain,B.M. Endocytosis by Antigen Presenting Cells - Dendritic Cells Are As Endocytically Active As Other Antigen Presenting Cells. *Proceedings of the National Academy of Sciences of the United States of America* **89**, 8342-8346 (1992).

Lewis,D.A., Hengeltraub,S.F., Gao,F.C., Leivant,M.A., & Spandau,D.F. Aberrant NF-kappaB activity in HaCaT cells alters their response to UVB signaling. *J. Invest Dermatol.* **126**, 1885-1892 (2006).

Lewis,J.B. *et al.* Ni(II) activates the Nrf2 signaling pathway in human monocytic cells. *Biomaterials* **27**, 5348-5356 (2006).

Li,H.F., Willingham,S.B., Ting,J.P.Y., & Re,F. Cutting edge: Inflammasome activation by alum and alum's adjuvant effect are mediated by NLRP3. *Journal of Immunology* **181**, 17-21 (2008).

Li,J., Ireland,G.W., Farthing,P.M., & Thornhill,M.H. Epidermal and oral keratinocytes are induced to produce RANTES and IL-8 by cytokine stimulation. *Journal of Investigative Dermatology* **106**, 661-666 (1996).

Li,J. *et al.* Induction of dendritic cell maturation by IL-18. *Cell Immunol.* **227**, 103-108 (2004).

Libermann,T.A. & Baltimore,D. Activation of interleukin-6 gene expression through the NF-kappa B transcription factor. *Mol. Cell Biol.* **10**, 2327-2334 (1990).

Lipkow,T., Saloga,J., Enk,A., Kolde,G., & Knop,J. Cellular Reactions in the Induction-Phase of the Allergic Contact-Dermatitis. *Allergologie* **14**, 176-179 (1991).

Liu-Bryan,R., Scott,P., Sydlaske,A., Rose,D.M., & Terkeltaub,R. Innate immunity conferred by Toll-like receptors 2 and 4 and myeloid differentiation factor 88 expression is pivotal to monosodium urate monohydrate crystal-induced inflammation. *Arthritis Rheum.* **52**, 2936-2946 (2005).

Livden,J.K. Fc gamma receptors on keratinocytes in psoriasis. *Arch. Dermatol. Res.* **280**, 12-17 (1988).

Loor,G. *et al.* Menadione triggers cell death through ROS-dependent mechanisms involving PARP activation without requiring apoptosis. *Free Radic. Biol. Med.* **49**, 1925-1936 (2010).

Loveless,S.E. *et al.* Further evaluation of the local lymph node assay in the final phase of an international collaborative trial. *Toxicology* **108**, 141-152 (1996).

Luger,T.A., Stadler,B.M., Katz,S.I., & Oppenheim,J.J. Epidermal-Cell (Keratinocyte)-Derived Thymocyte-Activating Factor (Etaf). *Journal of Immunology* **127**, 1493-1498 (1981).

Luger,T.A. & Schwarz,T. Evidence for An Epidermal Cytokine Network. *Journal of Investigative Dermatology* **95**, S100-S104 (1990).

Lukiw,W.J., Martinez,J., Pelaez,R.P., & Bazan,N.G. The interleukin-1 type 2 receptor gene displays immediate early gene responsiveness in glucocorticoid-stimulated human epidermal keratinocytes. *J. Biol. Chem.* **274** , 8630-8638 (1999).

Luo,G., Hershko,D.D., Robb,B.W., Wray,C.J., & Hasselgren,P.O. IL-1beta stimulates IL-6 production in cultured skeletal muscle cells through activation of MAP kinase signaling pathway and NF-kappa B. *Am. J. Physiol Regul. Integr. Comp Physiol* **284**, R1249-R1254 (2003).

Luster,A.D. & Ravetch,J.V. Biochemical characterization of a gamma interferon-inducible cytokine (IP-10). *J. Exp. Med.* **166**, 1084-1097 (1987).

Luthi,A.U. *et al.* Suppression of interleukin-33 bioactivity through proteolysis by apoptotic caspases. *Immunity.* **31**, 84-98 (2009).

Lutz,M.B. & Schuler,G. Immature, semi-mature and fully mature dendritic cells: which signals induce tolerance or immunity? *Trends Immunol.* **23**, 445-449 (2002).

Macagno,A., Napolitani,G., Lanzavecchia,A., & Sallusto,F. Duration, combination and timing: the signal integration model of dendritic cell activation. *Trends Immunol.* **28**, 227-233 (2007).

Macatonia,S.E., Knight,S.C., Edwards,A.J., Griffiths,S., & Fryer,P. Localization of Antigen on Lymph-Node Dendritic Cells After Exposure to the Contact Sensitizer Fluorescein Isothiocyanate - Functional and Morphological-Studies. *Journal of Experimental Medicine* **166**, 1654-1667 (1987).

Magnusson,B. & Kligman,A.M. The identification of contact allergens by animal assay. The guinea pig maximization test. *J. Invest Dermatol.* **52**, 268-276 (1969).

Mak,V.H.W. *et al.* Barrier Function of Human Keratinocyte Cultures Grown at the Air-Liquid Interface. *Journal of Investigative Dermatology* **96**, 323-327 (1991).

Malaisse,J. *et al.* Hyaluronan metabolism in human keratinocytes and atopic dermatitis skin is driven by a balance of hyaluronan synthases 1 and 3. *J. Invest Dermatol.* **134**, 2174-2182 (2014).

Manetti,R. *et al.* Natural killer cell stimulatory factor (interleukin 12 [IL-12]) induces T helper type 1 (Th1)-specific immune responses and inhibits the development of IL-4-producing Th cells. *J. Exp. Med.* **177**, 1199-1204 (1993).

Marchini,G. *et al.* Increased expression of HMGB-1 in the skin lesions of erythema toxicum. *Pediatr. Dermatol.* **24**, 474-482 (2007).

Mariathasan,S. *et al.* Cryopyrin activates the inflammasome in response to toxins and ATP. *Nature* **440**, 228-232 (2006).

MartIn-Fontecha,A. *et al.* Regulation of dendritic cell migration to the draining lymph node: impact on T lymphocyte traffic and priming. *J. Exp. Med.* **198**, 615-621 (2003).

Martin,S. *et al.* Peptide immunization indicates that CD8+ T cells are the dominant effector cells in trinitrophenyl-specific contact hypersensitivity. *J. Invest Dermatol.* **115**, 260-266 (2000).

Martin,S., Delattre,V., Leicht,C., Weltzien,H.U., & Simon,J.C. A high frequency of allergen-specific CD8+ Tc1 cells is associated with the murine immune response to the contact sensitizer trinitrophenyl. *Exp. Dermatol.* **12**, 78-85 (2003).

Martin,S.F. *et al.* Toll-like receptor and IL-12 signaling control susceptibility to contact hypersensitivity. *J. Exp. Med.* **205**, 2151-2162 (2008).

Martin,S.F. *et al.* T-cell recognition of chemicals, protein allergens and drugs: towards the development of in vitro assays. *Cell Mol. Life Sci.* **67**, 4171-4184 (2010).

Martinon,F., Burns,K., & Tschopp,J. The inflammasome: A molecular platform triggering activation of inflammatory caspases and processing of proIL-beta. *Molecular Cell* **10**, 417-426 (2002).

Martinon,F., Petrilli,V., Mayor,A., Tardivel,A., & Tschopp,J. Gout-associated uric acid crystals activate the NALP3 inflammasome. *Nature* **440**, 237-241 (2006).

Martinon,F., Mayor,A., & Tschopp,J. The Inflammasomes: Guardians of the Body. *Annual Review of Immunology* **27**, 229-265 (2009).

Marzulli,F.N. & Maibach,H.I. Dermatotoxicology. 1996. Taylor and Francis.
Ref Type: Generic

Mastorakos,G., Chrousos,G.P., & Weber,J.S. Recombinant Interleukin-6 Activates the Hypothalamic-Pituitary-Adrenal Axis in Humans. *Journal of Clinical Endocrinology & Metabolism* **77**, 1690-1694 (1993).

Masuda,K., Katoh,N., Soga,F., & Kishimoto,S. The role of interleukin-16 in murine contact hypersensitivity. *Clin. Exp. Immunol.* **140**, 213-219 (2005).

Matjeka,T., Summerfield,V., Noursadeghi,M., & Chain,B.M. Chemical toxicity to keratinocytes triggers dendritic cell activation via an IL-1alpha path. *J. Allergy Clin. Immunol.* **129**, 247-250 (2012).

Matos,T.J., Duarte,C.B., Goncalo,M., & Lopes,M.C. DNFB activates MAPKs and upregulates CD40 in skin-derived dendritic cells. *J. Dermatol. Sci.* **39**, 113-123 (2005).

Matos,T.J., Duarte,C.B., Goncalo,M., & Lopes,M.C. Role of oxidative stress in ERK and p38 MAPK activation induced by the chemical sensitizer DNFB in a fetal skin dendritic cell line. *Immunol. Cell Biol.* **83**, 607-614 (2005).

Matta,B.M. *et al.* IL-33 Is an Unconventional Alarmin That Stimulates IL-2 Secretion by Dendritic Cells To Selectively Expand IL-33R/ST2+ Regulatory T Cells. *J. Immunol.*(2014).

Mattii,M. *et al.* The balance between pro- and anti-inflammatory cytokines is crucial in human allergic contact dermatitis pathogenesis: the role of IL-1 family members. *Exp. Dermatol.* **22**, 813-819 (2013).

Matzinger,P. Tolerance, Danger, and the Extended Family. *Annual Review of Immunology* **12**, 991-1045 (1994).

McFadden,J.P., Wakelin,S.H., Holloway,D.B., & Basketter,D.A. The effect of patch duration on the elicitation of para-phenylenediamine contact allergy. *Contact Dermatitis* **39**, 79-81 (1998).

McKim,J.M., Jr., Keller,D.J., III, & Gorski,J.R. A new in vitro method for identifying chemical sensitizers combining peptide binding with ARE/EpRE-mediated gene expression in human skin cells. *Cutan. Ocul. Toxicol.* **29**, 171-192 (2010).

McKim,J.M., Jr., Keller,D.J., III, & Gorski,J.R. An in vitro method for detecting chemical sensitization using human reconstructed skin models and its applicability to cosmetic, pharmaceutical, and medical device safety testing. *Cutan. Ocul. Toxicol.* **31**, 292-305 (2012).

Medzhitov,R. *et al.* MyD88 is an adaptor protein in the hToll/IL-1 receptor family signaling pathways. *Molecular Cell* **2**, 253-258 (1998).

Mee,J.B., Alam,Y., & Groves,R.W. Human keratinocytes constitutively produce but do not process interleukin-18. *Br. J. Dermatol.* **143**, 330-336 (2000).

Meephansan,J., Komine,M., Tsuda,H., Tominaga,S., & Ohtsuki,M. Ultraviolet B irradiation induces the expression of IL-33 mRNA and protein in normal human epidermal keratinocytes. *J. Dermatol. Sci.* **65**, 72-74 (2012).

Megherbi,R. *et al.* Role of protein haptenation in triggering maturation events in the dendritic cell surrogate cell line THP-1. *Toxicol. Appl. Pharmacol.* **238**, 120-132 (2009).

Mempel,M. *et al.* Toll-like receptor expression in human keratinocytes: nuclear factor kappaB controlled gene activation by Staphylococcus aureus is toll-like receptor 2 but not toll-like receptor 4 or platelet activating factor receptor dependent. *J. Invest Dermatol.* **121**, 1389-1396 (2003).

Merad,M. *et al.* Langerhans cells renew in the skin throughout life under steady-state conditions. *Nat. Immunol.* **3**, 1135-1141 (2002).

Merad,M., Ginhoux,F., & Collin,M. Origin, homeostasis and function of Langerhans cells and other langerin-expressing dendritic cells. *Nature Reviews Immunology* **8**, 935-947 (2008).

Messmer,D. *et al.* High mobility group box protein 1: an endogenous signal for dendritic cell maturation and Th1 polarization. *J. Immunol.* **173**, 307-313 (2004).

Migdal,C. *et al.* Reactivity of chemical sensitizers toward amino acids in cellulo plays a role in the activation of the Nrf2-ARE pathway in human monocyte dendritic cells and the THP-1 cell line. *Toxicol. Sci.* **133**, 259-274 (2013).

Miller,L.S. *et al.* TGF-alpha regulates TLR expression and function on epidermal keratinocytes. *J. Immunol.* **174**, 6137-6143 (2005).

Mirchandani,A.S. *et al.* Type 2 innate lymphoid cells drive CD4+ Th2 cell responses. *J. Immunol.* **192**, 2442-2448 (2014).

Mitjans,M. *et al.* Role of p38 MAPK in the selective release of IL-8 induced by chemical allergen in naive THp-1 cells. *Toxicol. In Vitro* **22**, 386-395 (2008).

Miyazaki,Y. *et al.* Glucocorticoids augment the chemically induced production and gene expression of interleukin-1alpha through NF-kappaB and AP-1 activation in murine epidermal cells. *J. Invest Dermatol.* **115**, 746-752 (2000).

Miyazawa,M. *et al.* Role of MAPK signaling pathway in the activation of dendritic type cell line, THP-1, induced by DNCB and NiSO4. *J. Toxicol. Sci.* **33**, 51-59 (2008).

Miyazawa,M. & Takashima,A. Development and validation of a new in vitro assay designed to measure contact allergen-triggered oxidative stress in dendritic cells. *J. Dermatol. Sci.* **68**, 73-81 (2012).

Mizuashi,M., Ohtani,T., Nakagawa,S., & Aiba,S. Redox imbalance induced by contact sensitizers triggers the maturation of dendritic cells. *J. Invest Dermatol.* **124**, 579-586 (2005).

Mizutani,H., Black,R., & Kupper,T.S. Human keratinocytes produce but do not process pro-interleukin-1 (IL-1) beta. Different strategies of IL-1 production and processing in monocytes and keratinocytes. *J. Clin. Invest* **87**, 1066-1071 (1991).

Mohamadzadeh,M. *et al.* Enhanced expression of IL-8 in normal human keratinocytes and human keratinocyte cell line HaCaT in vitro after stimulation with contact sensitizers, tolerogens and irritants. *Exp Dermatol* **3**, (1994).

Monks,C.R., Freiberg,B.A., Kupfer,H., Sciaky,N., & Kupfer,A. Three-dimensional segregation of supramolecular activation clusters in T cells. *Nature* **395**, 82-86 (1998).

Montagna,W. & Lobitz,W.C. *The epidermis*(New York, Academic Press,1964).

Montagna,W. & Parakkal,P.F. *The structure and function of skin*(New York : Academic Press,1974).

Monteiro-Riviere,N.A., Inman,A.O., Snider,T.H., Blank,J.A., & Hobson,D.W. Comparison of an in vitro skin model to normal human skin for dermatological research. *Microsc. Res. Tech.* **37**, 172-179 (1997).

Moore,K.W., de Waal,M.R., Coffman,R.L., & O'Garra,A. Interleukin-10 and the interleukin-10 receptor. *Annu. Rev. Immunol.* **19**, 683-765 (2001).

Morales,J. *et al.* CTACK, a skin-associated chemokine that preferentially attracts skin-homing memory T cells. *Proc. Natl. Acad. Sci. U. S. A* **96**, 14470-14475 (1999).

Morita,K. & Miyachi,Y. Tight junctions in the skin. *J. Dermatol. Sci.* **31**, 81-89 (2003).

Mosley,B. *et al.* The interleukin-1 receptor binds the human interleukin-1 alpha precursor but not the interleukin-1 beta precursor. *J. Biol. Chem.* **262**, 2941-2944 (1987).

Moussion,C., Ortega,N., & Girard,J.P. The IL-1-like cytokine IL-33 is constitutively expressed in the nucleus of endothelial cells and epithelial cells in vivo: a novel 'alarmin'? *PLoS. One.* **3**, e3331 (2008).

Muller,G. *et al.* Identification and induction of human keratinocyte-derived IL-12. *J. Clin. Invest* **94**, 1799-1805 (1994).

Naik,S.M. *et al.* Human keratinocytes constitutively express interleukin-18 and secrete biologically active interleukin-18 after treatment with pro-inflammatory mediators and dinitrochlorobenzene. *Journal of Investigative Dermatology* **113**, 766-772 (1999).

Natsch,A. *et al.* The intra- and inter-laboratory reproducibility and predictivity of the KeratinoSens assay to predict skin sensitizers in vitro: results of a ring-study in five laboratories. *Toxicol. In Vitro* **25**, 733-744 (2011).

Nestle,F.O., Di,M.P., Qin,J.Z., & Nickoloff,B.J. Skin immune sentinels in health and disease. *Nat. Rev. Immunol.* **9**, 679-691 (2009).

Newby,C.S., Barr,R.M., Greaves,M.W., & Mallet,A.I. Cytokine release and cytotoxicity in human keratinocytes and fibroblasts induced by phenols and sodium dodecyl sulfate. *J. Invest Dermatol.* **115**, 292-298 (2000).

Nickoloff,B.J., Fivenson,D.P., Kunkel,S.L., Strieter,R.M., & Turka,L.A. Keratinocyte interleukin-10 expression is upregulated in tape-stripped skin, poison ivy dermatitis, and Sezary syndrome, but not in psoriatic plaques. *Clin. Immunol. Immunopathol.* **73**, 63-68 (1994).

Nistico,G. & Marmo,E. Antagonism of Prostaglandin-E1 and Prostaglandin-E2 Fever by Catecholamines. *Research Communications in Chemical Pathology and Pharmacology* **23**, 89-95 (1979).

Nordberg,J., Zhong,L., Holmgren,A., & Arner,E.S. Mammalian thioredoxin reductase is irreversibly inhibited by dinitrohalobenzenes by alkylation of both the redox active selenocysteine and its neighboring cysteine residue. *J. Biol. Chem.* **273**, 10835-10842 (1998).

Noursadeghi,M. *et al.* Quantitative imaging assay for NF-kappaB nuclear translocation in primary human macrophages. *J. Immunol. Methods* **329**, 194-200 (2008).

Nukada,Y. *et al.* Production of IL-8 in THP-1 cells following contact allergen stimulation via mitogen-activated protein kinase activation or tumor necrosis factor-alpha production. *J. Toxicol. Sci.* **33**, 175-185 (2008).

Numazawa,S. *et al.* Regulation of ERK-mediated signal transduction by p38 MAP kinase in human monocytic THP-1 cells. *J. Biochem.* **133**, 599-605 (2003).

O'Neill,L.A. & Bowie,A.G. The family of five: TIR-domain-containing adaptors in Toll-like receptor signalling. *Nat. Rev. Immunol.* **7**, 353-364 (2007).

Odland,G.F. Structure of the skin in *Physiology, Biochemistry and Molecular Biology of the Skin* (ed. Goldsmith,L.A.) (Oxford University Press, New York, 1991).

Ohashi,K., Burkart,V., Flohe,S., & Kolb,H. Cutting edge: heat shock protein 60 is a putative endogenous ligand of the toll-like receptor-4 complex. *J. Immunol.* **164**, 558-561 (2000).

Ohl,L. *et al.* CCR7 governs skin dendritic cell migration under inflammatory and steady-state conditions. *Immunity.* **21**, 279-288 (2004).

Okamoto,I., Kohno,K., Tanimoto,T., Ikegami,H., & Kurimoto,M. Development of CD8+ effector T cells is differentially regulated by IL-18 and IL-12. *J. Immunol.* **162**, 3202-3211 (1999).

Okamura,H. *et al.* Cloning of a new cytokine that induces IFN-gamma production by T cells. *Nature* **378**, 88-91 (1995).

Okamura,Y. *et al.* The extra domain A of fibronectin activates Toll-like receptor 4. *J. Biol. Chem.* **276**, 10229-10233 (2001).

Okazaki,F. *et al.* Initial recruitment of interferon-gamma-producing CD8+ effector cells, followed by infiltration of CD4+ cells in 2,4,6-trinitro-1-chlorobenzene (TNCB)-induced murine contact hypersensitivity reactions. *Journal of Dermatology* **29**, 699-708 (2002).

Oliphant,C.J. *et al.* MHCII-mediated dialog between group 2 innate lymphoid cells and CD4(+) T cells potentiates type 2 immunity and promotes parasitic helminth expulsion. *Immunity.* **41**, 283-295 (2014).

Onami,K. *et al.* Nonmetal haptens induce ATP release from keratinocytes through opening of pannexin hemichannels by reactive oxygen species. *J. Invest Dermatol.* **134**, 1951-1960 (2014).

Ostrov,D.A. *et al.* Drug hypersensitivity caused by alteration of the MHC-presented self-peptide repertoire. *Proc. Natl. Acad. Sci. U. S. A* **109**, 9959-9964 (2012).

Ouwehand,K. *et al.* CXCL12 is essential for migration of activated Langerhans cells from epidermis to dermis. *European Journal of Immunology* **38**, 3050-3059 (2008).

Ouwehand,K. *et al.* Technical advance: Langerhans cells derived from a human cell line in a full-thickness skin equivalent undergo allergen-induced maturation and migration. *J. Leukoc. Biol.* **90**, 1027-1033 (2011).

Ozawa,H., Nakagawa,S., Tagami,H., & Aiba,S. Interleukin-1 beta and granulocyte macrophage colony-stimulating factor mediate langerhans cell maturation differently. *Journal of Investigative Dermatology* **106**, 441-445 (1996).

Palm,N.W. & Medzhitov,R. Pattern recognition receptors and control of adaptive immunity. *Immunological Reviews* **227**, 221-233 (2009).

Palm,N.W. & Medzhitov,R. Immunostimulatory activity of haptenated proteins. *Proc. Natl. Acad. Sci. U. S. A* **106**, 4782-4787 (2009).

Park,J.S. *et al.* Involvement of toll-like receptors 2 and 4 in cellular activation by high mobility group box 1 protein. *J. Biol. Chem.* **279**, 7370-7377 (2004).

Partridge,M., Chantry,D., Turner,M., & Feldmann,M. Production of interleukin-1 and interleukin-6 by human keratinocytes and squamous cell carcinoma cell lines. *J. Invest Dermatol.* **96**, 771-776 (1991).

Pasparakis,M. *et al.* TNF-mediated inflammatory skin disease in mice with epidermis-specific deletion of IKK2. *Nature* **417**, 861-866 (2002).

Pasparakis,M. Regulation of tissue homeostasis by NF-kappaB signalling: implications for inflammatory diseases. *Nat. Rev. Immunol.* **9**, 778-788 (2009).

Pastore,S. *et al.* Effects of contact sensitizers neomycin sulfate, benzocaine and 2,4-dinitrobenzene 1-sulfonate, sodium salt on viability, membrane integrity and IL-1 alpha mRNA expression of cultured normal human keratinocytes. *Food Chem. Toxicol.* **33**, 57-68 (1995).

Pastore,S. *et al.* Granulocyte macrophage colony-stimulating factor is overproduced by keratinocytes in atopic dermatitis. Implications for sustained dendritic cell activation in the skin. *J. Clin. Invest* **99**, 3009-3017 (1997).

Pastore,S., Corinti,S., La,P.M., Didona,B., & Girolomoni,G. Interferon-gamma promotes exaggerated cytokine production in keratinocytes cultured from patients with atopic dermatitis. *J. Allergy Clin. Immunol.* **101**, 538-544 (1998).

Pastore,S. *et al.* ERK1/2 regulates epidermal chemokine expression and skin inflammation. *J. Immunol.* **174**, 5047-5056 (2005).

Pennino,D. *et al.* IL-17 amplifies human contact hypersensitivity by licensing hapten nonspecific Th1 cells to kill autologous keratinocytes. *J. Immunol.* **184**, 4880-4888 (2010).

Percoco,G. *et al.* Antimicrobial peptides and pro-inflammatory cytokines are differentially regulated across epidermal layers following bacterial stimuli. *Exp. Dermatol.* **22**, 800-806 (2013).

Peterson,R.L., Wang,L.L., Albert,L., & Dorner,A.J. Subcutaneous or oral administration of rhIL-11 modulated the contact hypersensitivity response. *Cytokine* **12**, 1769-1777 (2000).

Peveri,P., Walz,A., Dewald,B., & Baggiolini,M. A Novel Neutrophil-Activating Factor Produced by Human Mononuclear Phagocytes. *Journal of Experimental Medicine* **167**, 1547-1559 (1988).

Phillips,W.G., Feldmann,M., Breathnach,S.M., & Brennan,F.M. Modulation of the IL-1 cytokine network in keratinocytes by intracellular IL-1 alpha and IL-1 receptor antagonist. *Clin. Exp. Immunol.* **101**, 177-182 (1995).

Pichler,W.J. The p-i Concept: Pharmacological Interaction of Drugs With Immune Receptors. *World Allergy Organ J.* **1**, 96-102 (2008).

Pickard,C. *et al.* The cutaneous biochemical redox barrier: a component of the innate immune defenses against sensitization by highly reactive environmental xenobiotics. *J. Immunol.* **183**, 7576-7584 (2009).

Piepkorn,M., Lo,C., & Plowman,G. Amphiregulin-Dependent Proliferation of Cultured Human Keratinocytes - Autocrine Growth, the Effects of Exogenous Recombinant Cytokine, and Apparent Requirement for Heparin-Like Glycosaminoglycans. *Journal of Cellular Physiology* **159**, 114-120 (1994).

Pierce,J.W. *et al.* Novel inhibitors of cytokine-induced IkappaBalpha phosphorylation and endothelial cell adhesion molecule expression show anti-inflammatory effects in vivo. *J. Biol. Chem.* **272**, 21096-21103 (1997).

Piguet,P.F., Grau,G.E., Hauser,C., & Vassalli,P. Tumor-Necrosis-Factor Is A Critical Mediator in Hapten-Induced Irritant and Contact Hypersensitivity Reactions. *Journal of Experimental Medicine* **173**, 673-679 (1991).

Piguet,P.F. Keratinocyte-derived tumor necrosis factor and the physiopathology of the skin. *Springer Semin. Immunopathol.* **13**, 345-354 (1992).

Pivarcsi,A. *et al.* CC chemokine ligand 18, an atopic dermatitis-associated and dendritic cell-derived chemokine, is regulated by staphylococcal products and allergen exposure. *J. Immunol.* **173**, 5810-5817 (2004).

Plowman,G.D. *et al.* Molecular-Cloning and Expression of An Additional Epidermal Growth-Factor Receptor-Related Gene. *Proceedings of the National Academy of Sciences of the United States of America* **87**, 4905-4909 (1990).

Ponec,M. Reconstruction of human epidermis on de-epidermized dermis: Expression of differentiation-specific protein markers and lipid composition. *Toxicol. In Vitro* **5**, 597-606 (1991).

Ponec,M. *et al.* Lipid and ultrastructural characterization of reconstructed skin models. *Int. J. Pharm.* **203**, 211-225 (2000).

Ponec,M., Boelsma,E., Gibbs,S., & Mommaas,M. Characterization of reconstructed skin models. *Skin Pharmacology and Applied Skin Physiology* **15**, 4-17 (2002).

Poumay,Y. *et al.* A simple reconstructed human epidermis: preparation of the culture model and utilization in in vitro studies. *Arch. Dermatol. Res.* **296**, 203-211 (2004).

Prens,E.P. *et al.* IFN-alpha enhances poly-IC responses in human keratinocytes by inducing expression of cytosolic innate RNA receptors: relevance for psoriasis. *J. Invest Dermatol.* **128**, 932-938 (2008).

Price,A.A., Cumberbatch,M., Kimber,I., & Ager,A. Alpha 6 integrins are required for Langerhans cell migration from the epidermis. *J. Exp. Med.* **186**, 1725-1735 (1997).

Python,F., Goebel,C., & Aeby,P. Assessment of the U937 cell line for the detection of contact allergens. *Toxicol. Appl. Pharmacol.* **220**, 113-124 (2007).

Python,F., Goebel,C., & Aeby,P. Comparative DNA microarray analysis of human monocyte derived dendritic cells and MUTZ-3 cells exposed to the moderate skin sensitizer cinnamaldehyde. *Toxicol. Appl. Pharmacol.* **239**, 273-283 (2009).

Qin,J.Z. *et al.* Role of NF-kappaB in the apoptotic-resistant phenotype of keratinocytes. *J. Biol. Chem.* **274**, 37957-37964 (1999).

Qiu,X.B., Shao,Y.M., Miao,S., & Wang,L. The diversity of the DnaJ/Hsp40 family, the crucial partners for Hsp70 chaperones. *Cell Mol. Life Sci.* **63**, 2560-2570 (2006).

Raghavan,B., Martin,S.F., Esser,P.R., Goebeler,M., & Schmidt,M. Metal allergens nickel and cobalt facilitate TLR4 homodimerization independently of MD2. *EMBO Rep.* **13**, 1109-1115 (2012).

Ratzinger,G. *et al.* Matrix metalloproteinases 9 and 2 are necessary for the migration of Langerhans cells and dermal dendritic cells from human and murine skin. *J. Immunol.* **168**, 4361-4371 (2002).

Rauschmayr,T., Groves,R.W., & Kupper,T.S. Keratinocyte expression of the type 2 interleukin 1 receptor mediates local and specific inhibition of interleukin 1-mediated inflammation. *Proc. Natl. Acad. Sci. U. S. A* **94**, 5814-5819 (1997).

Regnier,M., Caron,D., Reichert,U., & Schaefer,H. Barrier function of human skin and human reconstructed epidermis. *J. Pharm. Sci.* **82**, 404-407 (1993).

Reich,K. *et al.* Association of allergic contact dermatitis with a promoter polymorphism in the IL16 gene. *J. Allergy Clin. Immunol.* **112**, 1191-1194 (2003).

Reinholz,M. *et al.* HPV16 activates the AIM2 inflammasome in keratinocytes. *Arch. Dermatol. Res.* **305**, 723-732 (2013).

Reis e Sousa, Stahl,P.D., & Austyn,J.M. Phagocytosis of antigens by Langerhans cells in vitro. *The Journal of Experimental Medicine* **178**, 509-519 (1993).

Reiss,Y., Proudfoot,A.E., Power,C.A., Campbell,J.J., & Butcher,E.C. CC chemokine receptor (CCR)4 and the CCR10 ligand cutaneous T cell-attracting chemokine (CTACK) in lymphocyte trafficking to inflamed skin. *J. Exp. Med.* **194**, 1541-1547 (2001).

Reuter,H. *et al.* In vitro detection of contact allergens: development of an optimized protocol using human peripheral blood monocyte-derived dendritic cells. *Toxicol. In Vitro* **25**, 315-323 (2011).

Rice,R.H. & Green,H. Cornified Envelope of Terminally Differentiated Human Epidermal Keratinocytes Consists of Cross-Linked Protein. *Cell* **11**, 417-422 (1977).

Richter,A. *et al.* Human T cell priming assay (hTCPA) for the identification of contact allergens based on naive T cells and DC--IFN-gamma and TNF-alpha readout. *Toxicol. In Vitro* **27**, 1180-1185 (2013).

Ring,S., Schafer,S.C., Mahnke,K., Lehr,H.A., & Enk,A.H. CD4(+)CD25(+) regulatory T cells suppress contact hypersensitivity reactions by blocking influx of effector T cells into inflamed tissue. *European Journal of Immunology* **36**, 2981-2992 (2006).

Rivas,J.M. & Ullrich,S.E. Systemic suppression of delayed-type hypersensitivity by supernatants from UV-irradiated keratinocytes. An essential role for keratinocyte-derived IL-10. *J. Immunol.* **149**, 3865-3871 (1992).

Robinson,K.A. *et al.* Redox-sensitive protein phosphatase activity regulates the phosphorylation state of p38 protein kinase in primary astrocyte culture. *J. Neurosci. Res.* **55**, 724-732 (1999).

Roelofs,M.F. *et al.* Identification of small heat shock protein B8 (HSP22) as a novel TLR4 ligand and potential involvement in the pathogenesis of rheumatoid arthritis. *J. Immunol.* **176**, 7021-7027 (2006).

Rogers,M.A., Langbein,L., Praetzel-Wunder,S., Winter,H., & Schweizer,J. Human hair keratin-associated proteins (KAPs). *Int. Rev. Cytol.* **251**, 209-263 (2006).

Roman,E. & Moreno,C. Delayed-type hypersensitivity elicited by synthetic peptides complexed with Mycobacterium tuberculosis hsp 70. *Immunology* **90**, 52-56 (1997).

Roman,J., Ritzenthaler,J.D., Fenton,M.J., Roser,S., & Schuyler,W. Transcriptional regulation of the human interleukin 1beta gene by fibronectin: role of protein kinase C and activator protein 1 (AP-1). *Cytokine* **12** , 1581-1596 (2000).

Rosdy,M., Pisani,A., & Ortonne,J.P. Production of basement membrane components by a reconstructed epidermis cultured in the absence of serum and dermal factors. *Br. J. Dermatol.* **129**, 227-234 (1993).

Rovere,P. *et al.* Bystander apoptosis triggers dendritic cell maturation and antigen-presenting function. *J. Immunol.* **161**, 4467-4471 (1998).

Ryan,C.A. *et al.* Gene expression changes in peripheral blood-derived dendritic cells following exposure to a contact allergen. *Toxicol. Lett.* **150**, 301-316 (2004).

Saalbach,A. *et al.* Dermal fibroblasts promote the migration of dendritic cells. *J. Invest Dermatol.* **130**, 444-454 (2010).

Saeki,H., Moore,A.M., Brown,M.J., & Hwang,S.T. Cutting edge: Secondary lymphoid-tissue chemokine (SLC) and CC chemokine receptor 7 (CCR7) participate in the emigration pathway of mature dendritic cells from the skin to regional lymph nodes. *Journal of Immunology* **162**, 2472-2475 (1999).

Saito,K. *et al.* Development of a new in vitro skin sensitization assay (Epidermal Sensitization Assay; EpiSensA) using reconstructed human epidermis. *Toxicol. In Vitro* **27**, 2213-2224 (2013).

Saitoh,M. *et al.* Mammalian thioredoxin is a direct inhibitor of apoptosis signal-regulating kinase (ASK) 1. *EMBO J.* **17**, 2596-2606 (1998).

Sakaguchi,H. *et al.* Development of an in vitro skin sensitization test using human cell lines; human Cell Line Activation Test (h-CLAT). II. An inter-laboratory study of the h-CLAT. *Toxicol. In Vitro* **20**, 774-784 (2006).

Sakaguchi,H. *et al.* The relationship between CD86/CD54 expression and THP-1 cell viability in an in vitro skin sensitization test--human cell line activation test (h-CLAT). *Cell Biol. Toxicol.* **25**, 109-126 (2009).

Salimi,M. *et al.* A role for IL-25 and IL-33-driven type-2 innate lymphoid cells in atopic dermatitis. *J. Exp. Med.* **210**, 2939-2950 (2013).

Salimi,M. & Ogg,G. Innate lymphoid cells and the skin. *BMC. Dermatol.* **14**, 18 (2014).

Sallusto,F., Cella,M., Danieli,C., & Lanzavecchia,A. Dendritic Cells Use Macropinocytosis and the Mannose Receptor to Concentrate Macromolecules in the Major Histocompatibility Complex Class-Ii Compartment - Down-Regulation by Cytokines and Bacterial Products. *Journal of Experimental Medicine* **182**, 389-400 (1995).

Salmeen,A. & Barford,D. Functions and mechanisms of redox regulation of cysteine-based phosphatases. *Antioxid. Redox. Signal.* **7**, 560-577 (2005).

Sauter,B. *et al.* Consequences of cell death: Exposure to necrotic tumor cells, but not primary tissue cells or apoptotic cells, induces the maturation of immunostimulatory dendritic cells. *Journal of Experimental Medicine* **191**, 423-433 (2000).

Sayama,K. *et al.* Apoptosis signal-regulating kinase 1 (ASK1) is an intracellular inducer of keratinocyte differentiation. *J. Biol. Chem.* **276**, 999-1004 (2001).

Scheynius,A., Fischer,T., Forsum,U., & Klareskog,L. Phenotypic Characterization Insitu of Inflammatory Cells in Allergic and Irritant Contact-Dermatitis in Man. *Clinical and Experimental Immunology* **55**, 81-90 (1984).

Schiering,C. *et al.* The alarmin IL-33 promotes regulatory T-cell function in the intestine. *Nature*(2014).

Schmidt,M. *et al.* Crucial role for human Toll-like receptor 4 in the development of contact allergy to nickel. *Nat. Immunol.* **11**, 814-819 (2010).

Schmitz,J. *et al.* IL-33, an interleukin-1-like cytokine that signals via the IL-1 receptor-related protein ST2 and induces T helper type 2-associated cytokines. *Immunity.* **23**, 479-490 (2005).

Schnurr,M. *et al.* Extracellular ATP and TNF-alpha synergize in the activation and maturation of human dendritic cells. *J. Immunol.* **165**, 4704-4709 (2000).

Schoeters,E. *et al.* Microarray analyses in dendritic cells reveal potential biomarkers for chemical-induced skin sensitization. *Mol. Immunol.* **44**, 3222-3233 (2007).

Schraufstatter,I.U., Zhao,M., Khaldoyanidi,S.K., & Discipio,R.G. The chemokine CCL18 causes maturation of cultured monocytes to macrophages in the M2 spectrum. *Immunology* **135**, 287-298 (2012).

Schreiner,M. *et al.* A loose-fit coculture of activated keratinocytes and dendritic cell-related cells for prediction of sensitizing potential. *Allergy* **62**, 1419-1428 (2007).

Schreiner,M. *et al.* A new dendritic cell type suitable as sentinel of contact allergens. *Toxicology* **249**, 146-152 (2008).

Schuler,G. & Steinman,R.M. Murine Epidermal Langerhans Cells Mature Into Potent Immunostimulatory Dendritic Cells-Invitro. *Journal of Experimental Medicine* **161**, 526-546 (1985).

Schuster,C. *et al.* HLA-DR+ leukocytes acquire CD1 antigens in embryonic and fetal human skin and contain functional antigen-presenting cells. *J. Exp. Med.* **206**, 169-181 (2009).

Schuster,C. *et al.* Human embryonic epidermis contains a diverse Langerhans cell precursor pool. *Development* **141**, 807-815 (2014).

Schwarzenberger,K. & Udey,M.C. Contact allergens and epidermal proinflammatory cytokines modulate Langerhans cell E-cadherin expression in situ. *J. Invest Dermatol.* **106**, 553-558 (1996).

Seitz,C.S., Lin,Q., Deng,H., & Khavari,P.A. Alterations in NF-kappaB function in transgenic epithelial tissue demonstrate a growth inhibitory role for NF-kappaB. *Proc. Natl. Acad. Sci. U. S. A* **95**, 2307-2312 (1998).

Seitz,C.S., Freiberg,R.A., Hinata,K., & Khavari,P.A. NF-kappaB determines localization and features of cell death in epidermis. *J. Clin. Invest* **105**, 253-260 (2000).

Seneschal,J., Clark,R.A., Gehad,A., Baecher-Allan,C.M., & Kupper,T.S. Human epidermal Langerhans cells maintain immune homeostasis in skin by activating skin resident regulatory T cells. *Immunity.* **36**, 873-884 (2012).

Serada,S. *et al.* IL-6 blockade inhibits the induction of myelin antigen-specific Th17 cells and Th1 cells in experimental autoimmune encephalomyelitis. *Proc. Natl. Acad. Sci. U. S. A* **105**, 9041-9046 (2008).

Shao,Y. *et al.* Keratinocytes play a role in the immunity to Herpes simplex virus type 2 infection. *Acta Virol.* **54**, 261-267 (2010).

Shiraki,Y., Ishibashi,Y., Hiruma,M., Nishikawa,A., & Ikeda,S. Cytokine secretion profiles of human keratinocytes during Trichophyton tonsurans and Arthroderma benhamiae infections. *J. Med. Microbiol.* **55**, 1175-1185 (2006).

Shklovskaya,E. *et al.* Langerhans cells are precommitted to immune tolerance induction. *Proc. Natl. Acad. Sci. U. S. A* **108**, 18049-18054 (2011).

Shornick,L.P. *et al.* Mice deficient in IL-1 beta manifest impaired contact hypersensitivity to trinitrochlorobenzene. *Journal of Experimental Medicine* **183**, 1427-1436 (1996).

Shornick,L.P., Bisarya,A.K., & Chaplin,D.D. IL-1beta is essential for langerhans cell activation and antigen delivery to the lymph nodes during contact sensitization: evidence for a dermal source of IL-1beta. *Cell Immunol.* **211**, 105-112 (2001).

Silberberg,I., Baer,R.L., & Rosenthal,S.A. Role of Langerhans Cells in Allergic Contact Hypersensitivity - Review of Findings in Man and Guinea-Pigs. *Journal of Investigative Dermatology* **66**, 210-217 (1976).

Simonsson,C. *et al.* Caged fluorescent haptens reveal the generation of cryptic epitopes in allergic contact dermatitis. *J. Invest Dermatol.* **131**, 1486-1493 (2011).

Smiley,S.T., King,J.A., & Hancock,W.W. Fibrinogen stimulates macrophage chemokine secretion through toll-like receptor 4. *J. Immunol.* **167**, 2887-2894 (2001).

Smith,C.K. & Hotchkiss,S.A.M. Allergic Contact Dermatitis. 2001. Taylor and Francis.
Ref Type: Generic

Smith,K.J., Diwan,H., & Skelton,H. Death receptors and their role in dermatology, with particular focus on tumor necrosis factor-related apoptosis-inducing ligand receptors. *Int. J. Dermatol.* **42**, 3-17 (2003).

Song,P.I. *et al.* Human keratinocytes express functional CD14 and toll-like receptor 4. *J. Invest Dermatol.* **119**, 424-432 (2002).

Sorensen,O.E. *et al.* Injury-induced innate immune response in human skin mediated by transactivation of the epidermal growth factor receptor. *J. Clin. Invest* **116**, 1878-1885 (2006).

Spetz,A.L., Strominger,J., & Groh-Spies,V. T cell subsets in normal human epidermis. *Am. J. Pathol.* **149**, 665-674 (1996).

Spiekstra,S.W. *et al.* Induction of cytokine (interleukin-1 alpha and tumor necrosis factor-alpha) and chemokine (CCL20, CCL27, and CXCL8) alarm signals after allergen and irritant exposure. *Experimental Dermatology* **14**, 109-116 (2005).

Spiekstra,S.W., dos Santos,G.G., Scheper,R.J., & Gibbs,S. Potential method to determine irritant potency in vitro - Comparison of two reconstructed epidermal culture models with different barrier competency. *Toxicol. In Vitro* **23**, 349-355 (2009).

Spielmann,H. *et al.* The ECVAM international validation study on in vitro tests for acute skin irritation: report on the validity of the EPISKIN and EpiDerm assays and on the Skin Integrity Function Test. *Altern. Lab Anim* **35**, 559-601 (2007).

Steinman,R.M., Turley,S., Mellman,I., & Inaba,K. The induction of tolerance by dendritic cells that have captured apoptotic cells. *J. Exp. Med.* **191**, 411-416 (2000).

Stoll,S. *et al.* Production of IL-18 (IFN-gamma-inducing factor) messenger RNA and functional protein by murine keratinocytes. *J. Immunol.* **159**, 298-302 (1997).

Streilein,J.W. Antigen-Presenting Cells in the Induction of Contact Hypersensitivity in Mice - Evidence That Langerhans Cells Are Sufficient But Not Required. *Journal of Investigative Dermatology* **93**, 443-448 (1989).

Sugaya,M. *et al.* Human keratinocytes express fractalkine/CX3CL1. *J. Dermatol. Sci.* **31**, 179-187 (2003).

Sugaya,M. *et al.* Oncostatin M enhances CCL21 expression by microvascular endothelial cells and increases the efficiency of dendritic cell trafficking to lymph nodes. *J. Immunol.* **177**, 7665-7672 (2006).

Surasombatpattana,P. *et al.* Dengue virus replication in infected human keratinocytes leads to activation of antiviral innate immune responses. *Infect. Genet. Evol.* **11**, 1664-1673 (2011).

Sutterwala,F.S., Ogura,Y., Zamboni,D.S., Roy,C.R., & Flavell,R.A. NALP3: a key player in caspase-1 activation. *J. Endotoxin. Res.* **12**, 251-256 (2006).

Sutterwala,F.S. *et al.* Critical role for NALP3/CIAS1/Cryopyrin in innate and adaptive immunity through its regulation of caspase-1. *Immunity.* **24**, 317-327 (2006).

Suzuki,M., Hirota,M., Hagino,S., Itagaki,H., & Aiba,S. Evaluation of changes of cell-surface thiols as a new biomarker for in vitro sensitization test. *Toxicol. In Vitro* **23**, 687-696 (2009).

Szameit,S., Vierlinger,K., Farmer,L., Tuschl,H., & Noehammer,C. Gene expression studies in cultured dendritic cells: new indicators for the discrimination of skin sensitizers and irritants in vitro. *Clin. Exp. Allergy* **39**, 856-868 (2009).

Szolnoky,G. *et al.* A mannose-binding receptor is expressed on human keratinocytes and mediates killing of Candida albicans. *J. Invest Dermatol.* **117**, 205-213 (2001).

Takayama,K. *et al.* IL-4 inhibits the migration of human Langerhans cells through the downregulation of TNF receptor II expression. *J. Invest Dermatol.* **113**, 541-546 (1999).

Takekoshi,T. *et al.* CXCR4 negatively regulates keratinocyte proliferation in IL-23-mediated psoriasiform dermatitis. *J. Invest Dermatol.* **133**, 2530-2537 (2013).

Taniguchi,K. *et al.* Interleukin 33 is induced by tumor necrosis factor alpha and interferon gamma in keratinocytes and contributes to allergic contact dermatitis. *J. Investig. Allergol. Clin. Immunol.* **23**, 428-434 (2013).

Teng,C.H., Huang,W.N., & Meng,T.C. Several dual specificity phosphatases coordinate to control the magnitude and duration of JNK activation in signaling response to oxidative stress. *J. Biol. Chem.* **282**, 28395-28407 (2007).

Tensen,C.P. *et al.* Human IP-9: A keratinocyte-derived high affinity CXC-chemokine ligand for the IP-10/Mig receptor (CXCR3). *J. Invest Dermatol.* **112**, 716-722 (1999).

Termeer,C. *et al.* Oligosaccharides of Hyaluronan activate dendritic cells via toll-like receptor 4. *The Journal of Experimental Medicine* **195**, 99-111 (2002).

Terunuma,A., Aiba,S., & Tagami,H. Cytokine mRNA profiles in cultured human skin component cells exposed to various chemicals: a simulation model of epicutaneous stimuli induced by skin barrier perturbation in comparison with that due to exposure to haptens or irritant. *J. Dermatol. Sci.* **26**, 85-93 (2001).

Teunissen,M.B. *et al.* Composition of innate lymphoid cell subsets in the human skin: enrichment of NCR(+) ILC3 in lesional skin and blood of psoriasis patients. *J. Invest Dermatol.* **134** , 2351-2360 (2014).

Teunissen,M.B.M., Koomen,C.W., Malefyt,R.D., Wierenga,E.A., & Bos,J.D. Interleukin-17 and interferon-gamma synergize in the enhancement of proinflammatory cytokine production by human keratinocytes. *Journal of Investigative Dermatology* **111**, 645-649 (1998).

Thauland,T.J. & Parker,D.C. Diversity in immunological synapse structure. *Immunology* **131**, 466-472 (2010).

Thornberry,N.A. *et al.* A Novel Heterodimeric Cysteine Protease Is Required for Interleukin-1-Beta Processing in Monocytes. *Nature* **356**, 768-774 (1992).

Toebak,M.J. *et al.* CXCL8 secretion by dendritic cells predicts contact allergens from irritants. *Toxicol. In Vitro* **20**, 117-124 (2006).

Trautmann,A. *et al.* T cell-mediated Fas-induced keratinocyte apoptosis plays a key pathogenetic role in eczematous dermatitis. *Journal of Clinical Investigation* **106**, 25-35 (2000).

Trefzer,U. *et al.* 55-kd tumor necrosis factor receptor is expressed by human keratinocytes and plays a pivotal role in regulation of human keratinocyte ICAM-1 expression. *J. Invest Dermatol.* **97**, 911-916 (1991).

Trefzer,U. *et al.* The 55-Kd Tumor-Necrosis-Factor Receptor on Human Keratinocytes Is Regulated by Tumor-Necrosis-Factor-Alpha and by Ultraviolet-B Radiation. *Journal of Clinical Investigation* **92**, 462-470 (1993).

Trifari,S., Kaplan,C.D., Tran,E.H., Crellin,N.K., & Spits,H. Identification of a human helper T cell population that has abundant production of interleukin 22 and is distinct from T(H)-17, T(H)1 and T(H)2 cells. *Nat. Immunol.* **10**, 864-871 (2009).

Trompezinski,S., Berthier-Vergnes,O., Denis,A., Schmitt,D., & Viac,J. Comparative expression of vascular endothelial growth factor family members, VEGF-B, -C and -D, by normal human keratinocytes and fibroblasts. *Exp. Dermatol.* **13**, 98-105 (2004).

Trompezinski,S. *et al.* Characterization of early events involved in human dendritic cell maturation induced by sensitizers: cross talk between MAPK signalling pathways. *Toxicol. Appl. Pharmacol.* **230**, 397-406 (2008).

Troutman,J.A. *et al.* The incorporation of lysine into the peroxidase peptide reactivity assay for skin sensitization assessments. *Toxicol. Sci.* **122**, 422-436 (2011).

Tuschl,H., Kovac,R., & Weber,E. The expression of surface markers on dendritic cells as indicators for the sensitizing potential of chemicals. *Toxicol. In Vitro* **14**, 541-549 (2000).

Urmacher,C. Histology of normal skin. *Am. J. Surg. Pathol.* **14**, 671-686 (1990).

Vabulas,R.M. *et al.* The endoplasmic reticulum-resident heat shock protein Gp96 activates dendritic cells via the Toll-like receptor 2/4 pathway. *J. Biol. Chem.* **277**, 20847-20853 (2002).

Valk,E., Zahn,S., Knop,J., & Becker,D. JAK/STAT pathways are not involved in the direct activation of antigen-presenting cells by contact sensitizers. *Arch. Dermatol. Res.* **294**, 163-167 (2002).

van den Bogaard,E.H. *et al.* Crosstalk between keratinocytes and T cells in a 3D microenvironment: a model to study inflammatory skin diseases. *J. Invest Dermatol.* **134**, 719-727 (2014).

van der Aar,A.M. *et al.* Langerhans cells favor skin flora tolerance through limited presentation of bacterial antigens and induction of regulatory T cells. *J. Invest Dermatol.* **133**, 1240-1249 (2013).

Van Och,F.M.M., Van Loveren,H., Van Wolfswinkel,J.C., Machielsen,A.J.C., & Vandebriel,R.J. Assessment of potency of allergenic activity of low molecular weight compounds based on IL-1 alpha and IL-18 production by a murine and human keratinocyte cell line. *Toxicology* **210**, 95-109 (2005).

van Stipdonk,M.J., Lemmens,E.E., & Schoenberger,S.P. Naive CTLs require a single brief period of antigenic stimulation for clonal expansion and differentiation. *Nat. Immunol.* **2**, 423-429 (2001).

Van,D.J. *et al.* Identification of the human 26-kD protein, interferon beta 2 (IFN-beta 2), as a B cell hybridoma/plasmacytoma growth factor induced by interleukin 1 and tumor necrosis factor. *J. Exp. Med.* **165**, 914-919 (1987).

van,d., V, Pronk,T.E., van,L.H., & Ezendam,J. Applicability of a keratinocyte gene signature to predict skin sensitizing potential. *Toxicol. In Vitro* **27**, 314-322 (2013).

Vandebriel,R.J. *et al.* Keratinocyte gene expression profiles discriminate sensitizing and irritating compounds. *Toxicol. Sci.* **117**, 81-89 (2010).

Veldhoen,M., Hocking,R.J., Atkins,C.J., Locksley,R.M., & Stockinger,B. TGFbeta in the context of an inflammatory cytokine milieu supports de novo differentiation of IL-17-producing T cells. *Immunity.* **24**, 179-189 (2006).

Villanova,F. *et al.* Characterization of innate lymphoid cells in human skin and blood demonstrates increase of NKp44+ ILC3 in psoriasis. *J. Invest Dermatol.* **134**, 984-991 (2014).

Vocanson,M. *et al.* Human T cell priming assay: depletion of peripheral blood lymphocytes in CD25(+) cells improves the in vitro detection of weak allergen-specific T cells. *EXS* **104**, 89-100 (2014).

Voss,A., Bode,G., & Kerkhoff,C. Double-stranded RNA induces IL-8 and MCP-1 gene expression via TLR3 in HaCaT-keratinocytes. *Inflamm. Allergy Drug Targets.* **11**, 397-405 (2012).

Voss,E. *et al.* NOD2/CARD15 mediates induction of the antimicrobial peptide human beta-defensin-2. *J. Biol. Chem.* **281**, 2005-2011 (2006).

Walunas,T.L. *et al.* CTLA-4 can function as a negative regulator of T cell activation. *Immunity.* **1**, 405-413 (1994).

Wang,B. *et al.* Enhanced epidermal Langerhans cell migration in IL-10 knockout mice. *Journal of Immunology* **162**, 277-283 (1999).

Wang,B.H. *et al.* CD4(+) Th1 and CD8(+) type 1 cytotoxic T cells both play a crucial role in the full development of contact hypersensitivity. *Journal of Immunology* **165**, 6783-6790 (2000).

Wang,D. *et al.* Human keratinocytes release high levels of inducible heat shock protein 70 that enhances peptide uptake. *Exp. Dermatol.* **20**, 637-641 (2011).

Watanabe,H. *et al.* Activation of the IL-1beta-processing inflammasome in the skin mediates contact hypersensitivity. *Journal of Investigative Dermatology* **126**, 117 (2006).

Watanabe,H. *et al.* Danger signaling through the inflammasome acts as a master switch between tolerance and sensitization. *J. Immunol.* **180**, 5826-5832 (2008).

Watt,F.M. Stem cell fate and patterning in mammalian epidermis. *Current Opinion in Genetics & Development* **11**, 410-417 (2001).

Weber,F.C. *et al.* Lack of the purinergic receptor P2X(7) results in resistance to contact hypersensitivity. *J. Exp. Med.* **207**, 2609-2619 (2010).

Werman,A. *et al.* The precursor form of IL-1alpha is an intracrine proinflammatory activator of transcription. *Proc. Natl. Acad. Sci. U. S. A* **101**, 2434-2439 (2004).

Williams,I.R. & Kupper,T.S. Immunity at the surface: Homeostatic mechanisms of the skin immune system. *Life Sciences* **58**, 1485-1507 (1996).

Willis,C.M., Young,E., Brandon,D.R., & Wilkinson,J.D. Immunopathological and Ultrastructural Findings in Human Allergic and Irritant Contact-Dermatitis. *British Journal of Dermatology* **115**, 305-316 (1986).

Willis,C.M., Stephens,C.J., & Wilkinson,J.D. Differential effects of structurally unrelated chemical irritants on the density and morphology of epidermal CD1+ cells. *J Invest Dermatol* **95**, 711-716 (1990).

Willis,C.M., Stephens,C.J.M., & Wilkinson,J.D. Differential Patterns of Epidermal Leukocyte Infiltration in Patch Test Reactions to Structurally Unrelated Chemical Irritants. *J Investig Dermatol* **101**, 364-370 (1993).

Witmer-Pack,M.D., Olivier,W., Valinsky,J., Schuler,G., & Steinman,R.M. Granulocyte/macrophage colony-stimulating factor is essential for the viability and function of cultured murine epidermal Langerhans cells. *J. Exp. Med.* **166**, 1484-1498 (1987).

Wood,L.C. *et al.* Barrier disruption stimulates interleukin-1 alpha expression and release from a pre-formed pool in murine epidermis. *Journal of Investigative Dermatology* **106**, 397-403 (1996).

Xu,H., DiIulio,N.A., & Fairchild,R.L. T cell populations primed by hapten sensitization in contact sensitivity are distinguished by polarized patterns of cytokine production: Interferon gamma-producing (Tc1) effector CD8(+) T cells and interleukin (Il) 4/Il-10-producing (Th2) negative regulatory CD4(+) T cells. *Journal of Experimental Medicine* **183**, 1001-1012 (1996).

Yamaki,M., Sugiura,K., Muro,Y., Shimoyama,Y., & Tomita,Y. Epidermal growth factor receptor tyrosine kinase inhibitors induce CCL2 and CCL5 via reduction in IL-1R2 in keratinocytes. *Exp. Dermatol.* **19**, 730-735 (2010).

Yamazaki,S., Uchiumi,A., & Katagata,Y. Hsp40 regulates the amount of keratin proteins via ubiquitin-proteasome pathway in cultured human cells. *Int. J. Mol. Med.* **29**, 165-168 (2012).

Yasumura,S., Lin,W.C., Weidmann,E., Hebda,P., & Whiteside,T.L. Expression of interleukin 2 receptors on human carcinoma cell lines and tumor growth inhibition by interleukin 2. *Int. J. Cancer* **59**, 225-234 (1994).

Yawalkar,N., Limat,A., Brand,C.U., & Braathen,L.R. Constitutive expression of both subunits of interleukin-12 in human keratinocytes. *J. Invest Dermatol.* **106**, 80-83 (1996).

Yoshikawa,Y. *et al.* Upregulation of genes orchestrating keratinocyte differentiation, including the novel marker gene ID2, by contact sensitizers in human bulge-derived keratinocytes. *J. Biochem. Mol. Toxicol.* **24**, 10-20 (2010).

Yoshimoto,T. *et al.* Role of IL-16 in delayed-type hypersensitivity reaction. *Blood* **95**, 2869-2874 (2000).

Yu,M. *et al.* HMGB1 signals through toll-like receptor (TLR) 4 and TLR2. *Shock* **26**, 174-179 (2006).

Yun,W. & Li,C. JNK pathway is required for TNCB-induced IL-18 expression in murine keratinocytes. *Toxicol. In Vitro* **24**, 1064-1069 (2010).

Yusuf,N. *et al.* Heat shock proteins HSP27 and HSP70 are present in the skin and are important mediators of allergic contact hypersensitivity. *J. Immunol.* **182**, 675-683 (2009).

Zeitvogel,J., Werfel,T., & Wittmann,M. Keratinocytes enriched for epidermal stem cells differ in their response to IFN-gamma from other proliferative keratinocytes. *Exp. Dermatol.* **17**, 998-1003 (2008).

Zepter,K. *et al.* Induction of biologically active IL-1 beta-converting enzyme and mature IL-1 beta in human keratinocytes by inflammatory and immunologic stimuli. *J. Immunol.* **159**, 6203-6208 (1997).

Zhang,H., Shi,X., Hampong,M., Blanis,L., & Pelech,S. Stress-induced inhibition of ERK1 and ERK2 by direct interaction with p38 MAP kinase. *J. Biol. Chem.* **276**, 6905-6908 (2001).

Zhao,Y. *et al.* Th17/Tc17 infiltration and associated cytokine gene expression in elicitation phase of allergic contact dermatitis. *British Journal of Dermatology* **161**, 1301-1306 (2009).

Zheng,Y., Humphry,M., Maguire,J.J., Bennett,M.R., & Clarke,M.C. Intracellular interleukin-1 receptor 2 binding prevents cleavage and activity of interleukin-1alpha, controlling necrosis-induced sterile inflammation. *Immunity.* **38**, 285-295 (2013).

Zhou,L. *et al.* IL-6 programs T(H)-17 cell differentiation by promoting sequential engagement of the IL-21 and IL-23 pathways. *Nat. Immunol.* **8**, 967-974 (2007).

Zhou,R., Yazdi,A.S., Menu,P., & Tschopp,J. A role for mitochondria in NLRP3 inflammasome activation. *Nature* **469**, 221-225 (2011).